



<https://theses.gla.ac.uk/>

Theses Digitisation:

<https://www.gla.ac.uk/myglasgow/research/enlighten/theses/digitisation/>

This is a digitised version of the original print thesis.

Copyright and moral rights for this work are retained by the author

A copy can be downloaded for personal non-commercial research or study, without prior permission or charge

This work cannot be reproduced or quoted extensively from without first obtaining permission in writing from the author

The content must not be changed in any way or sold commercially in any format or medium without the formal permission of the author

When referring to this work, full bibliographic details including the author, title, awarding institution and date of the thesis must be given

Enlighten: Theses

<https://theses.gla.ac.uk/>
research-enlighten@glasgow.ac.uk

Cellular and molecular characterisation of porcine congenital splayleg and the involvement of *P311* and *SPARCL-1* as candidate genes

by

OOI PECK TOUNG D.V.M.

A thesis completed in partial fulfilment of the degree of Doctor of Philosophy,
Faculty of Veterinary Medicine, University of Glasgow

Division of Animal Production and Public Health
Faculty of Veterinary Medicine
University of Glasgow
Glasgow G61 1QH

February 2007

©Ooi Peck Young, 2007

ProQuest Number: 10396124

All rights reserved

INFORMATION TO ALL USERS

The quality of this reproduction is dependent upon the quality of the copy submitted.

In the unlikely event that the author did not send a complete manuscript and there are missing pages, these will be noted. Also, if material had to be removed, a note will indicate the deletion.



ProQuest 10396124

Published by ProQuest LLC (2017). Copyright of the Dissertation is held by the Author.

All rights reserved.

This work is protected against unauthorized copying under Title 17, United States Code
Microform Edition © ProQuest LLC.

ProQuest LLC.
789 East Eisenhower Parkway
P.O. Box 1346
Ann Arbor, MI 48106 – 1346

*For my beloved wife, Phang Wai San,
My dearest parent, Kelly Low and Ooi Leong Whye
and my sister, Ooi Peck Yin*

Summary

Porcine congenital splayleg (PCS) is the most important congenital condition of piglets, associated with lameness and immobility, of unknown aetiology and pathogenesis. The aim of this study is to investigate the cellular and molecular changes in skeletal muscles of PCS, thereby gaining new molecular insights into this clinical condition.

Based on immunohistochemistry and histological image analyses on 4 sets of 2-day-old splayleg piglets, each with a corresponding normal litter mate, a consistent discovery has been that PCS muscles [*semitendinosus* (ST), *longissimus dorsi* (LD) and *gastrocnemius* (G)] showed extensive fibre atrophy without apparent tissue damage. At present, it is not certain if PCS-associated fibre atrophy is accompanied by fibre hypoplasia. Both normal and PCS muscle fibres showed similar widespread distribution of lipid- and oxidative-positive fibres. Although there was no significant difference in fibre type composition, several structural myosin heavy chain (MyHC) genes were significantly down-regulated in PCS affected muscles. Interestingly, *MAFbx*, a major atrophy marker, was highly up-regulated in almost all PCS muscles, when compared with controls from normal litter mates. In contrast, *P311*, a novel 8-kDa protein, was relatively down-regulated in all PCS muscles examined.

To further investigate the functional role of *P311* in skeletal muscle, its full-length cDNA was sequenced (Accession. N^o. EF416570) and over-expressed in murine C2C12 muscle cells. *P311* over-expression enhanced cell proliferation and reduced myotube formation in C2C12 cells. The over-expression of calcineurin, a key intracellular calcium-dependent signalling factor of muscle differentiation, down-

regulated *P311* expression. Reduced *P311* expression in PCS piglets might contribute to atrophy through reduced myotube contribution.

To investigate the functional role of *SPARCL-1*, a matricellular secreted glycoprotein that belongs to SPARC family, its full-length cDNA was sequenced (Accession. N^o. EF416571) and over-expressed in murine C2C12 muscle cells. *SPARCL-1* over-expression led to reduced cell proliferation and down-regulation of MyHC genes during late differentiation. *SPARCL-1* might be associated as a negative regulator of skeletal muscle cell proliferation and cell differentiation. However, endogenous *SPARCL-1* expression was similar between PCS and normal muscles. Hence, although *SPARCL-1* could play a role in muscle development, it is unlikely to be a main factor in the development of PCS.

In summary, PCS is shown to be a condition characterised by extensive fibre atrophy and raised fibre density, and it is proposed that the combined differential expression of *MAFbx* and *P311* is of potential value in the diagnosis of sub-clinical PCS.

Table of contents

Summary	3
Table of contents	5
List of figures	9
List of tables	12
Acknowledgements	13
Declaration	14
Abbreviations	15
 Chapter 1 ~ Literature review	 17
1.1. Porcine congenital splayleg	19
1.1.1. Clinical signs	20
1.1.2. Prevalence and incidence	21
1.1.3. Pathogenesis of PCS	22
1.1.4. Histopathology of PCS	23
1.1.5. Control and treatment of PCS	25
1.2. An overview of muscle fibres	26
1.2.1. Muscle fibres types	28
1.2.2. Myosin heavy chain	30
1.2.3. Muscle fibre adaptation and transition	33
1.2.3.1. Neuromuscular activity	34
1.2.3.2. Mechanical loading and unloading	36
1.2.3.3. Hormones	38
1.2.3.4. Ageing	40
1.2.4. Muscle hypertrophy and atrophy	41
1.2.4.1. Hypertrophy and the PI3-K pathway	41
1.2.4.2. Atrophy and the ubiquitin-proteasome proteolysis pathway	42
1.2.5. Calcineurin	44
1.3. Candidate genes of PCS	45
1.3.1. SPARC	47
1.3.1.1. SPARC and related proteins	50
1.3.2. SPARCL-1	52
1.3.3. P311	53
1.4. Aims	55
1.4.1. Cellular and molecular characterisation of PCS	55
1.4.2. Functional studies of PCS candidate genes	55
 Chapter 2 ~ Materials and Methods	 57
2.1. Introduction	58
2.2. Porcine congenital splayleg	58
2.2.1. PCS piglets and muscle selection	58
2.2.2. Immunohistochemistry and histochemistry	59
2.2.3. Image analysis	62
2.3. Recombinant DNA techniques	65
2.3.1. Transformation of bacteria with plasmid DNA	65
2.3.1.1. Transformation of commercially available ultracompetent cells	65
2.3.1.2. Topo- TA cloning	66

2.3.2 Isolation of plasmid DNA	66
2.3.2.1. Small scale plasmid preparations	67
2.3.2.2. Large scale plasmid preparations	68
2.3.2.3. Determination of DNA concentration by spectrophotometry	69
2.3.3. Restriction endonuclease digestion	69
2.3.4. DNA electrophoresis	70
2.3.4.1. Agarose gel electrophoresis	70
2.3.4.2. Excision of DNA bands	71
2.3.5. DNA ligation	71
2.4. Polymerase chain reaction	72
2.4.1. PCR primer design	72
2.4.2. PCR conditions	73
2.5. DNA sequence analysis	73
2.5.1. Sequencing primer design	74
2.5.2. Reaction conditions for cycle sequencing	74
2.6. Cell culture	75
2.6.1. C2C12 cell culture	75
2.6.1.1. Cell passaging	76
2.6.1.2. Cell storage	76
2.6.1.3. Surface coating	77
2.6.2. AD293 cell culture	78
2.6.3. Lipofectin transfection	78
2.6.4. Recombinant adenovirus production	80
2.6.4.1. Adenovirus vector cloning	80
2.6.4.2. <i>Pac</i> I digestion of recombinant Adeno-X DNA for transfection	84
2.6.4.3. Transfecting AD293 cells with <i>Pac</i> I digested Adeno-X DNA	85
2.6.4.4. Purification of recombinant adenoviruses	86
2.6.5. Cell cytotoxicity assay	88
2.6.6. Cell proliferation assays	88
2.6.7. Fusion index assay	90
2.6.8. BrdU assay	93
2.6.9. Immunofluorescence	94
2.6.10. Protein extraction	95
2.6.11. Determination of protein concentration	95
2.7. Quantitative Real-Time RT-PCR	96
2.7.1. Total RNA extraction	97
2.7.1.1. Extraction of total RNA from cells	97
2.7.1.2. Extraction of total RNA from splayleg skeletal muscles	98
2.7.2. Total RNA quality and quantity determination	99
2.7.3. Reverse transcription	100
2.7.4. Real-time PCR primer and probe design	101
2.7.5. Taqman reaction conditions	101
2.7.6. Real-time PCR data analysis	102
2.8. Western blot analysis	103
2.8.1. Preparation of protein samples	104
2.8.2. Protein electrophoresis	104
2.8.3. Transfer onto PVDF membranes	106

2.8.4. Antibody binding	107
2.8.5. Use of ECL reporting	108
2.9. Statistical analyses	108
Chapter 3 ~ Cellular and molecular characterisation of PCS	112
3.1. Introduction	113
3.2. Materials and methods	114
3.2.1. Immunohistochemical and histochemical staining	114
3.2.2. Total muscle fibre number measurement in PCS	114
3.2.3. Quantitative real-time RT-PCR	115
3.3. Results	119
3.3.1. Muscle fibre atrophy in PCS muscles	119
3.3.2. Selective reduction of MyHC expression in PCS muscles	124
3.3.3. Relative expression of MyHC isoforms within muscles	128
3.3.4. Up-regulation of <i>MAFbx</i> and down-regulation of <i>P311</i> in PCS muscles	130
3.4. Discussion	135
3.4.1. PCS is associated with extensive muscle fibre atrophy	135
3.4.2. Widespread distribution of lipid and oxidative fibres in PCS muscles	137
3.4.3. PCS is associated with muscle wasting	137
3.4.4. Down-regulation of <i>P311</i> in PCS muscles	138
Chapter 4 ~ Functional studies of <i>P311</i>	139
4.1. Introduction	140
4.2. Materials and methods	141
4.2.1. <i>P311</i> cDNA cloning and sequencing	141
4.2.2. <i>P311</i> cell cultures, transfections and recombinant adenovirus production	144
4.2.3. <i>P311</i> immunofluorescence, cell cytotoxicity and Western blotting	145
4.2.4. <i>P311</i> cell proliferation, fusion index and BrdU assay	146
4.2.5. <i>P311</i> quantitative real-time RT-PCR	146
4.3. Results	149
4.3.1. <i>P311</i> cDNA cloning and sequencing	149
4.3.2. Recombinant <i>P311</i> adenovirus production	155
4.3.3. <i>P311</i> over-expression in C2C12 cells by adenovirus infection and by stable transfection	158
4.3.4. <i>P311</i> over-expression increased C2C12 cell proliferation and reduced differentiation	162
4.3.5. Muscle gene expression in <i>P311</i> - adenovirus infected C2C12 cells	162
4.4. Discussion	170
Chapter 5 ~ Functional studies of <i>SPARCL-1</i>	173
5.1. Introduction	174
5.2. Materials and methods	174
5.2.1. <i>SPARCL-1</i> cDNA cloning and sequencing	175
5.2.2. <i>SPARCL-1</i> cell cultures, transfections and recombinant adenovirus production	176
5.2.3. <i>SPARCL-1</i> cell cytotoxicity and Western blotting	177
5.2.4. <i>SPARCL-1</i> cell proliferation, fusion index and BrdU assay	177

5.2.5. <i>SPARCL-1</i> quantitative real-time RT-PCR	177
5.2.6. <i>SPARCL-1</i> expression in PCS muscle	178
5.3. Results	179
5.3.1. <i>SPARCL-1</i> cDNA cloning and sequencing	179
5.3.2. Recombinant <i>SPARCL-1</i> adenovirus production	186
5.3.3. <i>SPARCL-1</i> over-expression in C2C12 cells by adenovirus infection and by stable transfection	189
5.3.4. <i>SPARCL-1</i> over-expression decreased C2C12 cell proliferation but did not affect fusion	192
5.3.5. <i>SPARCL-1</i> over-expression depressed expression of muscle genes	192
5.3.6. <i>SPARCL-1</i> expression in PCS muscles, and interactions between <i>SPARCL-1</i> and <i>P311</i>	198
5.4. Discussion	201
Chapter 6 ~ General discussion	204
References	211
Appendix:	225
Published paper:	
Ooi PT, da Costa N, Edgar J, Chang KC (2006) Porcine congenital splayleg is characterised by muscle fibre atrophy associated with relative rise in MAFbx and fall in P311 expression. BMC Veterinary Research 2: 23.	
Poster Presentation	

List of figures

Figure 1.1. Porcine congenital splayleg.	21
Figure 1.2. Arrangement of filaments in a skeletal muscle myofibril that produces the striated banding pattern.	28
Figure 1.3. Myosin heavy chain dimer with bound myosin light chain.	31
Figure 1.4. Summary of the factors influencing MyHC expression and fibre type.	34
Figure 1.5. Modular structure of human SPARC.	48
Figure 1.6. SPARC and related proteins.	51
Figure 2.1. Image analysis.	63
Figure 2.2. Identification of MyHC fast and MyHC slow fibres.	64
Figure 2.3. Plasmid vector pDNR-CMV.	81
Figure 2.4. Overview of recombinant adenovirus production.	83
Figure 2.5. Overview of BD-Adeno-X virus purification protocol.	87
Figure 2.6. Neubauer haemocytometer.	89
Figure 2.7. Fusion index determination.	92
Figure 2.8. A RNA 6000 Nano labchips and a chip priming station with plunger.	100
Figure 2.9. Standard curve for real-time RT-PCR.	103
Figure 2.10. Gel Electrophoresis system.	105
Figure 2.11. The complete transferred unit assembled.	107
Figure 3.1. Total cross-sectional area measurement.	116
Figure 3.2. Morphological comparisons between muscles of PCS and normal piglets.	120
Figure 3.3. Mean fibre size and fibre density in four sets of 2-day-old PCS piglets, each with a corresponding normal litter mate.	121
Figure 3.4. Distribution of muscle fibre cross-sectional areas in four sets of 2-day-old PCS piglets, each with a corresponding normal litter mate.	122
Figure 3.5. Composition of slow and fast fibres in four sets of 2-day-old PCS piglets, each with a corresponding normal litter mate.	123
Figure 3.6. Widespread distribution of lipid positive fibres.	125
Figure 3.7. Widespread distribution of highly oxidative fibres.	126
Figure 3.8. Comparison of muscle gene expression between PCS affected and normal muscles.	127

Figure 3.9. Relative mRNA levels of <i>MyHC</i> isoforms within PCS affected and normal muscles.	129
Figure 3.10. Quantitative PCR performed for <i>MAFbx</i> and <i>P311</i> expression.	131
Figure 3.11. Developmental expression of <i>MAFbx</i> and <i>P311</i> .	134
Figure 4.1. Plasmid vector (A) pBK-CMV and (B) pBluescript II SK (+).	142
Figure 4.2. TOPO vector.	144
Figure 4.3. Restriction digestion of pBK-CMV-P311.	150
Figure 4.4. Sub-cloning of <i>P311</i> .	151
Figure 4.5. Full length nucleotide sequence of porcine <i>P311</i> cDNA.	153
Figure 4.6. Pile-up of <i>P311</i> deduced amino acid sequences for pig, human, mouse and chicken.	154
Figure 4.7. Comparison of PEST domains in <i>P311</i> deduced amino acid sequences for pig, human, mouse and chicken.	155
Figure 4.8. Cloning of <i>P311</i> into TOPO vector.	156
Figure 4.9. Cloning of <i>P311</i> into pDNR-CMV vector.	157
Figure 4.10. 3x FLAG and stop codon of <i>P311</i> in pDNR-CMV vector.	158
Figure 4.11. Over-expression of <i>P311</i> in C2C12 cells.	159
Figure 4.12. Over-expression of <i>P311</i> in C2C12 cells enhanced proliferation and reduced differentiation.	164
Figure 4.13. Muscle gene expression in <i>P311</i> -adenovirus infected C2C12 cells.	168
Figure 4.14. Effect of calcineurin over-expression on endogenous <i>P311</i> expression in C2C12 cells.	169
Figure 5.1. Restriction digestion of pBK-CMV-SPARCL-1.	180
Figure 5.2. Sub-cloning of <i>SPARCL-1</i> .	181
Figure 5.3. Full length nucleotide sequence of porcine <i>SPARCL-1</i> cDNA.	183
Figure 5.4. Pile-up of <i>SPARCL-1</i> deduced amino acid sequences for pig, human, mouse and rat.	185
Figure 5.5. Comparison of <i>SPARCL-1</i> domain deduced amino acid sequences for pig, human and mouse.	186
Figure 5.6. Cloning of <i>SPARCL-1</i> into TOPO vector.	187
Figure 5.7. Cloning of <i>SPARCL-1</i> into pDNR-CMV vector.	188
Figure 5.8. 3x FLAG and stop codon of <i>SPARCL-1</i> in pDNR-CMV vector.	189
Figure 5.9. Over-expression of <i>SPARCL-1</i> in C2C12 cells.	190
Figure 5.10. Over-expression of <i>SPARCL-1</i> reduced C2C12 cell proliferation.	193

Figure 5.11. Muscle gene expression in <i>SPARCL-1</i> -adenovirus infected C2C12 cells.	197
Figure 5.12. Quantitative PCR performed for <i>SPARCL-1</i> expression.	199
Figure 5.13. Expression interaction between <i>SPARCL-1</i> and <i>P311</i> .	200

List of tables

Table 1.1. The properties and metabolic profiles of MyHC fibre types.	32
Table 3.1. Sequences of porcine primers and TaqMan probes.	117
Table 3.2. Porcine RT-PCR primer concentration and value of standard curve.	118
Table 4.1. Sequences of primers and TaqMan probes.	147
Table 4.2. RT-PCR primer concentration and value of standard curve.	148
Table 5.1. Sequences of porcine <i>SPARCL-1</i> primers and TaqMan probes.	178
Table 5.2. Porcine <i>SPARCL-1</i> RT-PCR primer concentration and value of standard curve.	178

Acknowledgements

I would like to take this opportunity to express my deepest gratitude to my supervisor, Dr. Kin-Chow Chang. Without his teaching, advices and guidance, this work would not have succeeded.

I wish to extend my warm and sincere thanks to Mr. Nuno da Costa and Dr. Julia Edgar, Molecular Medicine Laboratory, who gave me important guidance and support during my research studies. Their patient teaching and ideas have had a remarkable influence on my research experiments. I am deeply grateful to Prof. David Taylor, Head of Animal Production and Public Health Division, for his detailed and constructive comments. I also thank Prof. Michael Stear, Immunogenetic Laboratory, for his valuable advice and friendly assistance with the statistical analyses.

I wish to thank Mr. Colin Nixon and Mrs. Lynn Stevenson, Veterinary Clinical Services Unit, for their marvellous assistance in immunohistochemistry and histochemistry staining. I would like to give thanks to all my colleagues in the Molecular Medicine Laboratory, past and present: Prof. Su Yuhong, Dr. Ronald Birrell and Miss Annette Reid for providing support and encouragement during this period. Last, but by no means least, I am grateful to the Ministry of Science, Technology and Innovation Malaysia (MOSTI), the University of Putra Malaysia (UPM), for my postgraduate scholarship.

Declaration

The studies described in this thesis were carried out in the Molecular Medicine Laboratory, Division of Animal Production and Public Health (APPH) at University of Glasgow Veterinary School between September 2003 and December 2006. The author was directly responsible for all the work described here. The exceptions are noted below:

The immunohistochemistry and histochemistry staining for PCS described in Chapter 3 were carried out by Mr. Colin Nixon and Mrs. Lynn Stevenson. The humane slaughter of the animals used in the studies was carried out by Richard Irvine in the post mortem room. In Chapter 3, the basic murine calcineurin A (Cn) construct used was kindly supplied by Dr. S. Williams, University of Texas. The prenatal cDNA muscle samples used in the study were kindly provided by Mr. Nuno da Costa, Molecular Medicine Laboratory. The design of primers and probes for real-time RT-PCR in Chapter 3-5 was carried out by Mr. Nuno da Costa. The statistical analyses with SAS software was carried out with the assistance of Prof. Michael Stear.

(PECK- TOUNG OOI)

02/03/2007.

Abbreviations

°C	degree Celsius
μl	microlitre(s)
μM	micromolar
APS	ammonium persulphate
ATP	adenosine triphosphate
bp	base pair
BCA	bicinchoninic acid
BrdU	5-bromo-2-deoxyuridine
cDNA	complementary deoxyribonucleic acid
Cn	calcineurin
CLFS	chronic low-frequency stimulation
CMV	cytomegalovirus
DM	differentiation medium
DMEM	Dulbecco's modified Eagle's medium
DMSO	dimethylsulphoxide
DNA	deoxyribonucleic acid
DTT	dithiothreitol
EC domain	extracellular calcium binding domain
EDTA	ethylene diamine tetra acetic acid
EMS	extramyofibrillar space
FCS	foetal calf serum
FG	fast-glycolytic
FOG	fast oxidative-glycolytic
FS domain	folistatin-like domain
G	<i>gastrocnemius</i>
GFP	green fluorescent protein
GH	growth hormone
HEK 293	human embryonic kidney 293
HMM	heavy meromyosin
HRP	horseradish peroxidase
Hz	hertz
IGF	insulin-like growth factor
IGF1R	type 1 IGF receptor
IGF2R	type 2 IGF receptor
IGFBP	IGF binding proteins
IRES	internal ribosome entry site
kDa	kilodalton
kg	kilogram(s)
L	litre(s)
LD	<i>longissimus dorsi</i>
LM	light meromyosin
M	molar
MAFbx	muscle atrophy F-box
MCS	multiple cloning site
MFH	myofibrillar hypoplasia
MGF	mechano growth factor

min	minute(s)
ml	milliliter(s)
mg	milligram(s)
MyHC	myosin heavy chain
MyLC	myosin light chain
mRNA	messenger RNA
MuRF1	muscle ring finger 1
NaOAc	sodium acetate
Norm	normal
ORF	open reading frame
PI3-K	phosphatidylinositol 3'-kinase
PAGE	polyacrylamide gel electrophoresis
PBS	phosphate buffered saline
PCR	polymerase chain reaction
PCS	porcine congenital splayleg
PM	proliferation medium
PSE	pale, soft and exudative
rpm	revolutions per minute
RT-PCR	reverse-transcriptase polymerase chain reaction
s	seconds
SacB	sucrase gene from <i>B.subtillis</i>
SB	sample buffer
SBB	sudan black B
SDH	succinate dehydrogenase
SDS	sodium dodecyl-sulphate
SPARC	secreted protein acidic and rich in cysteine
SPARCL-1	SPARC like 1 protein
ST	<i>semitendinosus</i>
SO	slow-oxidative
TbT	tris buffer Tween
TEMEID	tetramethyl-1-,2-diaminomethane
Tris	tris (hydroxymethyl) aminomethane
Tris Hcl	tris hydrochloride
TRITC	tetramethyl rhodamine iso-thiocyanate
TBS	tris buffer saline
Ub	ubiquitin
UV	ultraviolet

Chapter 1

Literature review

Prewaning mortality in piglets constitutes a major loss to the pig industry. The Meat and Livestock Commission, UK (2003) reported a preweaning mortality rate for liveborn piglets of 12.2% in indoor herds and 9.9% in outdoor herds (Cutler et al., 2006). Congenital abnormalities account for a small but significant proportion of preweaning losses (Partlow et al., 1993). They have been reported more frequently in pigs than in any other domestic animal species (Priester et al., 1970). A number of abnormalities may be seen in newborn piglets or shortly after birth. Briefly, congenital conditions can be categorised as: (1) spontaneous developmental abnormalities, such as cystic lymph nodes, (2) heritable abnormalities such as congenital meningoencephalocoele, atresia ani, arthrogryposis, porcine congenital splayleg, (3) infectious agents such as congenital tremor type AI (myoclonia congenita), (4) nutritional deficiency or poisoning such as mulberry heart disease and (5) unknown causes such as bleeding navel syndrome (Taylor, 2006).

Cystic lymph nodes can occur in ileal mesenteric lymph nodes, caecocolic lymph nodes and colonic lymph nodes and measure up to 2 cm in diameter. Congenital meningoencephalocoele, also known as cranioschisis is a heritable abnormality. Affected pigs have exposed meninges protruding through incomplete fusion of parietal or frontal bones and the mortality rate is high (Wijeratne et al., 1974). Atresia ani is a common condition in which the rectum fails to open to the exterior. A thin membrane or a band of fibrous tissue may be present at the anal opening. Male pigs usually have swollen abdomens and die within 3 weeks of birth, but in females the rectum may open into the vagina and the animals survive in 50% of cases. Arthrogryposis is a condition of joints and/or limbs being fused together, affected piglets normally die after birth. Arthrogryposis is caused by arthrogryposis multiplex

congenita (*amc*) recessive gene (Lomo, 1985). Porcine congenital splayleg is a clinical condition of newborn piglets, characterised by muscle weakness, resulting in inability to properly stand and walk (Thurley et al., 1967). Congenital tremor Type AI (myoclonia congenita) results from infection of the sow by classical swine fever (hog cholera) virus. Affected piglets show various degrees of muscular tremor, ataxia and inability to stand and suck (Harding et al., 1966). Mulberry heart disease is a syndrome related to vitamin E and selenium deficiency. Affected piglets have acute heart failure and sudden death may occur (Mortimer, 1983). The cause of bleeding navel syndrome is unknown. Affected piglets bleed to death as a result of failed closure of the umbilicus. Attendance at farrowings and ligation of the umbilical cord can reduce the mortality. Feeding of ascorbic acid to the sow also has been shown to prevent the syndrome (Sandholm et al., 1979).

1.1. Porcine congenital splayleg

Porcine congenital splayleg (PCS), also known as straddlers or myofibrillar hypoplasia (reduced numbers of myofibrils), is a clinical disease of newborn piglets. It is arguably the most important congenital defect of newborn piglets and causes significant economic impact to the industry. PCS is the inability of newborn pigs to stand and walk properly, often with their limbs extending forwards or sideways as a result of muscular weakness (Thurley et al., 1967).

In 1967, the clinical term was first reported by Thurley et al. (1967). Since then, reports from different countries regarding congenital splayleg were published (Dobson, 1968; Cunha, 1968; Olson and Prange, 1968; Bollwahn and Pfeiffer, 1969;

Lax, 1971; Svendsen and Andereasson, 1980). Reports on the prevalence vary considerably. In the United Kingdom, Ward and Bradley (1980) estimated that about 0.4% piglets were affected by splayleg, which caused an annual loss of £300,000 to the pig industry at that time. In another two studies by Dobson (1968, 1971), the overall average prevalence rates were reported at 11% and 13% respectively. A further study in Ontario indicated that PCS was the most common congenital defect with 0.87% piglets affected (Partlow et al., 1993).

1.1.1 Clinical signs

PCS can be found at or a few hours after birth. At birth, 2 to 3 piglets may be affected in each litter. It invariably affects the hindlimbs, but occasionally affects the forelimbs. Most of the affected piglets are unable to move around or stand, although some splayleg pigs may be able to move around with difficulty. The affected limbs are abducted, splayed forward or in sideways position. Often, an affected piglet is found seated on its hindquarters (Fig.1.1).

An affected piglet is often separate from its healthy litter mates. Its immobility means that it cannot gain sufficient nutrients from the sow, resulting in starvation and hypothermia. Affected neonatal pigs become emaciated, weak and dirty. Abrasions and ulceration develop on the body due to long periods of lying on the floor. Splayleg pigs are more predisposed to arthritis, polyarthritis, pododermatitis and osteomyelitis of the digits due to secondary bacterial infections. The mortality rate of splayleg piglets can reach around 50%. The cause of death is either starvation or crushing by

the sow. However, if supportive treatment and extra care can be provided, the affected piglet can recover after one week.



Figure 1.1. Porcine congenital splayleg. A 2-day-old piglet with PCS showing forward extension and abduction of hindlimbs as a consequence of muscle weakness.

1.1.2. Prevalence and incidence

The condition is particularly prevalent in Landrace and Large White breeds, which are heavily muscled (Dobson, 1968; Tomko, 1993; Vogt et al., 1984), although it is known to occur in virtually all commercial lines. Both male and female piglets are susceptible to PCS (Tomko, 1993; Thurley et al., 1967), however, some studies indicate that male offspring are more susceptible. In one of the studies, male progeny are 1.74 times more likely than females to succumb to PCS (Vogt et al., 1984). Another study showed that about twice as many males were affected as females (Van

Der Heyde et al., 1989). Presently, it is not clear whether PCS is related to birth weight or litter size. One study found that PCS occurs more frequently in large litters than in smaller ones (Van Der Heyde et al., 1989). However, another study suggested that the occurrence of splayleg was significantly higher in small litters (Tomko, 1993).

1.1.3. Pathogenesis of PCS

The aetiology and pathogenesis of PCS are not known. It is considered to be a multifactorial condition. The factors that are involved are thought to include genetic and environmental factors like sow management, administration of various drugs and mycotoxins.

Treatment of pregnant sows with glucocorticoids can induce a myopathy in the newborn which mimics PCS (Jirmanova, 1983). However, there were histological differences in muscle from glucocorticoid induced and naturally occurring PCS (Ducatelle et al., 1986). Dexamethasone is a synthetic glucocorticoid used primarily as an anti-inflammatory agent in various conditions, including allergic states. More recently, it was suggested that affected muscles have a reduced number of myofibrils and an increased accumulation of glycogen when compared with the muscles of normal piglets. The investigation had concentrated on the activity of glucose-6-phosphatase (G-6-Pase), a liver enzyme that breaks down glycogen reserves (Antalikova et al., 1996). Another study suggested that the slippery floor in farrowing crates could predispose newborns to PCS problems (Dobson, 1971). However, this environmental factor is not likely to be a causal factor of splayleg (Van Der Heyde et al., 1989). Choline is a vitamin like compound which is essential for acetylcholine

synthesis. Supplementation with 2.2 to 3.0 g of choline in the diet of pregnant sow until parturition was reported to reduce the incidence of PCS (Cunha, 1968). However, a subsequent study could not reproduce this finding (Dobson, 1971).

Consumption of *fusarium* F-2 toxin (zearalenone) contaminated grain by sows in late pregnancy, could lead to a higher incidence of PCS, a condition that can be experimentally reproduced by the administration of purified F-2 toxin to pregnant sows (Miller et al., 1973). Increased stillbirths and neonatal mortality were also recorded. However, F-2 induced PCS piglets did not show the typical histopathological lesions described by Thurley et al (1967).

Misuse of certain drugs in pregnant sows may lead to signs of PCS in newborn piglets. Administration of 3.6 mg/kg/day of pyrimethamine, an anthelmintic, to pregnant Goettingen minipigs raised the incidence of PCS to 74% of the newborn, while the control group had only an incidence of 5.6% (Ohnishi et al., 1989). Induction by prostaglandin before the 113th day of pregnancy could also lead to higher incidence of congenital myofibrillar hypoplasia (Boleskei et al., 1996).

1.1.4. Histopathology of PCS

A variety of lesions have been described as the underlying pathological changes in congenital splayleg. The most consistent change is the presence of so-called myofibrillar hypoplasia (MFH), interpreted as an immaturity of the muscle (Ducatelle et al., 1986; Thurley et al., 1967). Myofibrillar hypoplasia ranges from a slight reduction of myofibrillar content to severe myofibrillar deficiency, vacuolisation,

focal degeneration and necrosis. However, myofibrillar hypoplasia can also be found in clinically normal piglets. The term congenital myofibrillar hypoplasia may not therefore be the diagnostic description of PCS (Ducatelle et al., 1986).

As pointed out earlier, the morphological findings of dexamethasone treatment suggest that PCS might represent a congenital form of glucocorticoid myopathy (Ducatelle et al., 1986). Another study on muscle ultrastructure of PCS piglet, also showed reduced numbers of myofibrils and an increase in glycogen accumulation in comparison with muscle of normal piglets (Antalikova et al., 1996). Other studies found differences between PCS piglets and piglets with experimentally-induced glucocorticoid myopathy. Naturally occurring PCS had glycogen-filled extramyofibrillar space (EMS), whereas dexamethasone splayleg had only limited glycogen in the EMS (Ducatelle et al., 1986).

There were no significant qualitative differences between normal pigs and splayleg pigs aged from birth to 1 week, based on light microscopic and ultrastructural examinations (Bradley et al., 1980; Ward and Bradley, 1980). The progressive clinical improvement in splayleg during the first week of life was found to be accompanied by an increase in muscle cell size, a reduction in the number of nuclei, a reduction in the severity of MFH, a reduction in the size of the extra-myofibrillar space and an increase in intracellular lipid. However similar changes were also found in normal pigs. The results indicated that light microscopy or ultrastructural morphology were not useful to diagnose splayleg due to the failure to detect any significant differences (Ward and Bradley, 1980). However, both studies took the

form of visual subjective assessments. Quantitative measurements were not performed.

Generally, hypoplasia refers to underdevelopment of an organ because of a decrease in the numbers. In contrast, atrophy refers to a decrease in the size of an organ caused by disease or disuse. There are uncertainties about the histopathology of PCS. To date, it is not clear if clinical splayleg is involved reduction of fibre size (atrophy), number (hypoplasia) or both. In addition, few histochemical and/or biochemical parameters have been detected which are unequivocally associated with congenital splayleg. Therefore, further detailed study is required to accurately characterise the cellular features of PCS. With recent advances in imaging technology, morphological analysis of PCS can now be carried out with greater accuracy. This could add valuable information to our understanding of the pathogenesis of the disease.

1.1.5. Control and treatment of PCS

Given the uncertain aetiology and pathogenesis of PCS, it is difficult to reduce its incidence. From the husbandry viewpoint, a dry and non-slippery floor should be provided for farrowing. In addition, neonatal piglets should be protected from injury by the sow, and provided with adequate opportunities to suckle. These could reduce the incidence or the severity of PCS. Selection of breeding stock may help to control the disease. Good farm breeding records can help to identify individuals that are predisposed to the production of affected offspring. In addition, affected piglets that recover should not be used for breeding. With supportive care, adequate warmth and nutrition, affected piglets can recover from the condition. However, nursing is labour

consuming and may not be economical as a routine in herd health management. The common treatment method used is tying together the affected limbs, with a loose “figure of 8” just above the hock joint. It appears to help the piglet to recover and gain the ability to move around. Adhesive tape can be used to tie affected legs but care must be exercised to avoid occlusion of blood flow.

1.2. An overview of muscle fibres

PCS is a disease condition that is closely related to muscle weakness, which leads to lameness and immobility. Hence, it is essential to have some understanding of the basic biology of fibre types, their properties and distribution in skeletal muscle. In addition, to investigate PCS it is necessary to evaluate the condition in the context of molecular mechanisms, which could involve the processes of muscle hypertrophy or atrophy.

Each muscle fibre is formed by the fusion of a number of undifferentiated myoblasts into a single cylindrical, multinucleated cell. Both skeletal and cardiac muscles are striated muscles. The term striated muscle is derived from its feature of light and dark bands perpendicular to the long axis of the fibre when examined under light microscopy.

This banding pattern is derived from the overlap of thick and thin filaments into cylindrical bundles known as myofibrils. The thick and thin filaments are arranged in repeating patterns, one unit of this repeating pattern is known as a sarcomere (Fig.1.2). The thick filaments are located in the middle of each sarcomere, where their orderly

parallel arrangement produces a wide, dark band (A band). Each sarcomere contains two sets of thin filaments, one at each end anchored to a network of interconnecting protein known as the Z line. The thick filaments are principally composed of the contractile protein myosin, while the thin filaments contain the contractile protein actin. During contraction, cross-bridges are formed between these myosin and actin filaments in a cyclical, ATP-dependent manner. The thin filaments are drawn in over the thick filaments, resulting in a shortening of the sarcomere and the generation of force.

The thin filaments also contain troponin and tropomyosin proteins, which play important roles in regulating contraction. Tropomyosins are rod-shape molecules, which are arranged end to end to form a chain along the thin actin filament. It partially covers the myosin-binding site, thereby preventing cross-bridge formation. Each tropomyosin is held in this position by a troponin complex. When calcium binds to specific binding sites on troponin, tropomyosin is dragged away from the myosin binding site which allows cross-bridge formation to take place.

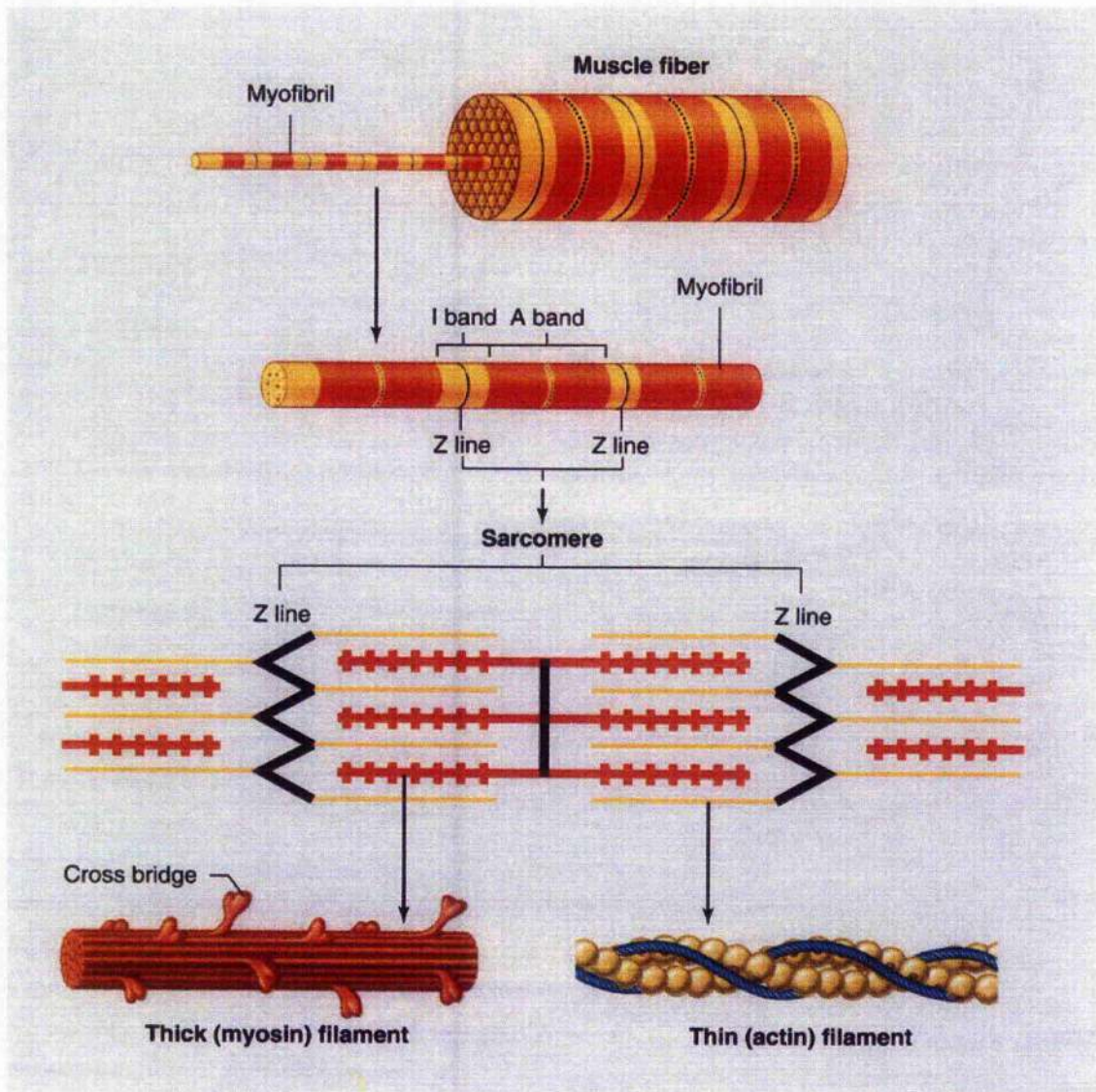


Figure 1.2. Arrangement of filaments in a skeletal muscle myofibril that produces the striated banding pattern. (Adapted from Vander et al, 2001, Human Physiology: the mechanism of body function, 8th edition)

1.2.1. Muscle fibres types

All skeletal muscle fibres do not have the same mechanical and metabolic characteristics (Pette and Staron, 1990). Generally, fibre types are identified based on two specific characters: (1) fast or slow fibre (2) oxidative or/and glycolytic fibre.

Fast and slow fibres are classified according to their ability to split adenosine triphosphate (ATP). Fast fibres possess myosin that hydrolyses ATP rapidly, and thus have a faster cross-link cycle and greater velocities and power output. The downside of this is in the increased demand for ATP and rapid onset of muscle fatigue. In contrast, slow fibres have a lower velocity of contraction and a lower power output but are fatigue resistant. As a result, it is more economical in ATP usage and capable of sustaining isometric force for a longer period of time.

Another way of determining skeletal muscle fibres is based on the type of enzymatic machinery available for synthesizing ATP. Oxidative fibres are characterised by their large lipid storage, numerous mitochondria and high oxidative enzyme content (Goldspink, 1996). Normally, oxidative fibres are surrounded by small blood vessels and contain large amounts of myoglobin. These features give the fibres a dark-red colour, and thus oxidative fibres are also known as red muscle fibres.

In contrast, glycolytic fibres contain high concentrations of glycolytic enzymes, relatively large storage of glycogen, few mitochondria, less myoglobin and low capillary density. These features impart a pale appearance to these fibres, which are also known as white muscle fibres. Oxidative metabolism is limited by the requirement for adequate perfusion of oxygen and nutrient from blood circulation. Glycolytic fibres generally have much large diameters than oxidative fibres, and generate greater strength. Oxidative metabolism is tailored for low intensity activity; it is less useful for high intensity exercise due to the limitation of oxygen and blood supply. Therefore, as the force requirement increases, glycolytic metabolism will be recruited for the generation of necessary strength and power (Goldspink, 1996).

Based on the characteristics of (1) fast or slow fibre, and (2) oxidative or/and glycolytic fibre, skeletal muscle fibres can be distinguished into three major types, which are slow-oxidative (SO), fast oxidative-glycolytic (FOG), and fast-glycolytic (FG) (Brooke and Kaiser, 1970; Handel and Stickland, 1987).

1.2.2. Myosin heavy chain

Myosin is both a structural and regulatory protein, comprising about 25% of the total protein pool in striated muscle cells (Pette and Staron, 2000). It forms the backbone of contractile machinery and serves as the motor that drives muscular activity (Baldwin and Haddad, 2002). Myosin is a hexameric protein composed of myosin heavy chain (MyHC) and myosin light chain (MyLC). It is the MyHC component that is of most interest when considering muscle fibre type, since these proteins mediate both the myosin motor function and filament formation. Each MyHC is made up of two functional domains, a globular head domain subfragment 1 (S1) proteolysis fraction, and a long helical rod domain subfragment 2 (S2) and light meromyosin (LMM) proteolysis fractions (Fig. 1.3). Both S1 and S2 are grouped as heavy meromyosin (HMM). The globular head S1 contains the actin binding domain and ATPase, while the rod domain is required for filament formation.

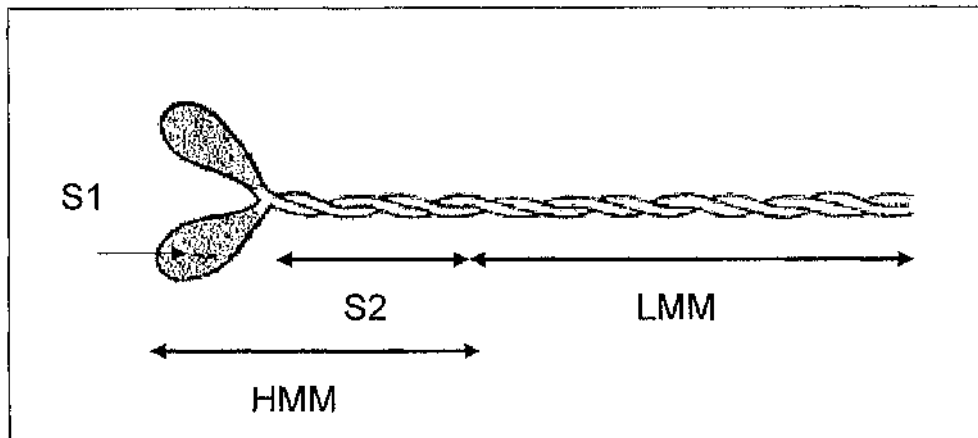


Figure 1.3. Myosin heavy chain dimer with bound myosin light chain. The HMM portion can be divided into the S1 and S2 fragment. The shaded S1 proteolytic fragment/myosin head domain contains the actin binding and ATPase sites. S2 and LMM proteolytic fragments both correspond to the alpha helical coiled rod domain. (Modified from Weiss and Leinwand, 1996). S1= subfragment 1; S2= subfragment 2; LMM= light meromyosin; HMM= heavy meromyosin.

MyHCs are encoded by a highly conserved multi-gene family. To date, there are eight known MyHC isoforms expressed in mammalian muscle. These are the (1) embryonic, (2) perinatal, (3) I/slow/ β , (4) 2a, (5) 2x, (6) 2b, (7) α , and (8) extra-ocular or mandibular or masticatory MyHCs (Baldwin and Haddad, 2001). The properties of actin binding, ATPase activity and the speed of filament cross-linking, are unique to each MyHC isoform. Recently, some researchers categorised MyHC 2x as MyHC 2c based on immunohistochemistry staining (Sutherland et al., 2006).

During the foetal and embryonic stage, the MyHC embryonic, MyHC perinatal and MyHC I/slow/ β are the three isoforms that predominantly expressed. Shortly after birth, the MyHC I/slow/ β , MyHC 2a and MyHC 2x isoforms are most important in post-natal skeletal muscle. MyHC 2b is expressed in the fast fibres of rodent and porcine muscles (Pette and Staron, 2000), but it is absent from many other mammalian species such as the cattle and horse (Chikuni et al., 2004a; Chikuni et al.,

2004b). The expression of MyHC 2b in humans is limited to extraocular and masseter muscles, with only mRNA detectable in the latter (Horton et al., 2001). The presence of MyHC 2b in porcine muscle makes the pig distinctive among large animals. It has been suggested that the high expression of the MyHC 2b isoform in porcine muscle is related to intensive breeding for leaner meat (Chang et al., 2003).

The extraocular MyHC isoform is confined mainly to the eye, laryngeal and mandibular muscles of carnivores (Baldwin and Haddad, 2001). Based on the MyHC classification approach, the post-natal muscle fibres in mammals can be divided according to metabolic, biochemical and biophysical characteristics (Schiaffino and Reggiani, 1996). A summary of MyHC properties differences are illustrated in Table 1.1.

MyHC	I/slow/ β	2a	2x	2b
Type	Slow-oxidative	Fast oxidative-glycolytic	Fast oxidative-glycolytic	Fast-glycolytic
Size	++	(++)	(++)	+++
Glycogen	(+)	(++)	(++)	+++
Lipids	+++	++	(+)	(+)
Fatigue	resistant	intermediate	intermediate	sensitive
PSE*	resistant	intermediate	intermediate	prone

Table 1.1. The properties and metabolic profiles of MyHC fibre types. * Pale, soft exudative meat quality, independent of ryanodine mutation. () indicates variable levels.

The MyHC I/slow/ β and MyHC 2b fibres, also known as slow oxidative (red) and fast glycolytic (white) respectively, represent 2 extreme metabolic profiles. The MyHC 2a and MyHC 2x fibres are intermediate fast oxidative-glycolytic fibres. Fast MyHC

2a fibres are more closely related to MyHC I/slow/ β fibres, and fast MyHC 2x are more similar to fast MyHC 2b fibres. Besides the single MyHC isoform (pure fibre type), it should be noted that mixed expression of two or more MyHC isoforms can occur (hybrid fibre type). The combinations of hybrid fibre may range from MyHC I/slow/ β with MyHC 2a, MyHC 2a with MyHC 2x to MyHC 2x with MyHC 2b isoforms (Schiaffino and Reggiani, 1994). The normal proportions of hybrid fibres in skeletal muscle are low, but their numbers may increase dramatically during MyHC fibre transition (Talmadge et al., 1999).

In general, each muscle is composed of different types of fibres. Fibre type distribution is largely dependant on their anatomical and functional roles. Postural muscles such as the *soleus* muscle, contain a high proportion of oxidative fibres and are activated continuously to produce slow and repetitive movements (Hnik et al., 1985). In contrast, the muscles used for intensive activities, like sprinting, are composed of FG or FOG fibres, with their greater capacity for force and strength generation, but lower resistance to fatigue.

1.2.3. Muscle fibre adaptation and transition

Muscle fibres are dynamic structures capable of altering their phenotype under various conditions, e.g. increasing or decreasing neuromuscular activity, mechanical loading or unloading, altering hormonal profiles (especially of thyroid hormones), and ageing (Pette and Staron, 2000). This allows muscles to adopt the most energy-efficient configuration for the demand at any given time. Fibre transition not only involves changes in MyHC expression, but includes alteration in the isoform profiles

of a multitude of sarcomeric proteins. Changes in MyHC isoforms tend to follow a general scheme of sequential and reversible transitions from fast-to-slow and slow-to-fast. A summary of these factors and their effects on fibre expression of MyHC isoforms is shown (Fig. 1.4).

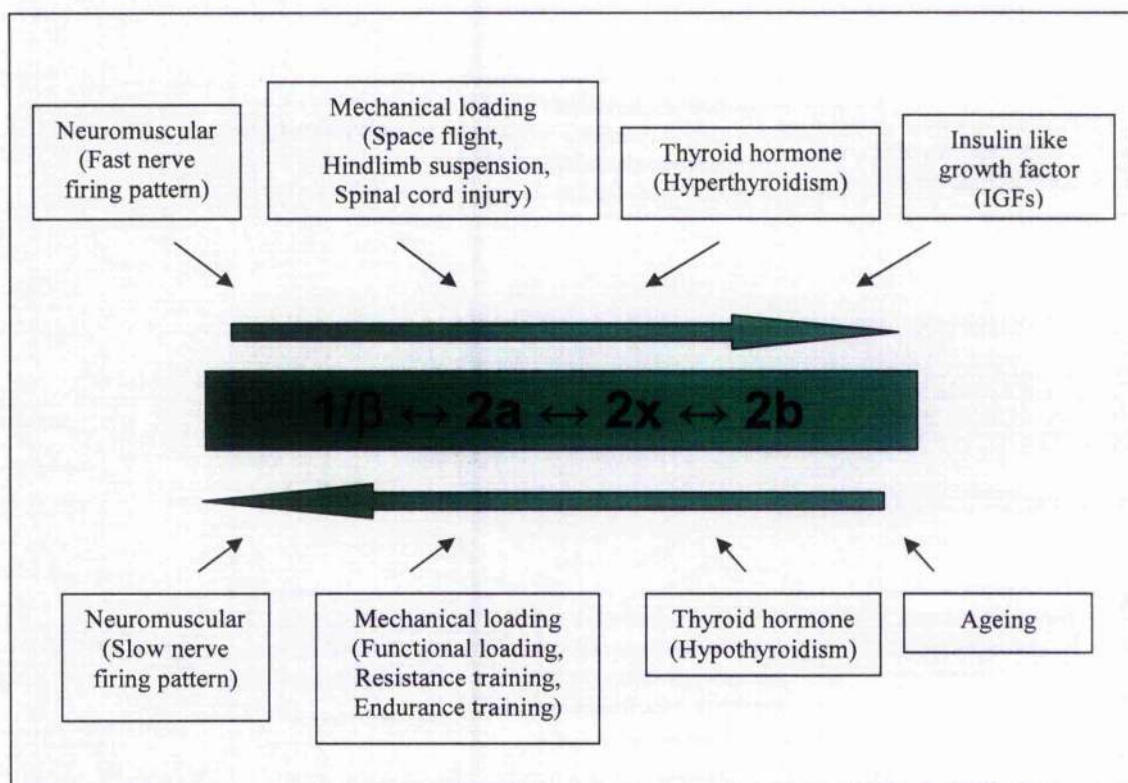


Figure 1.4. Summary of the factors influencing MyHC expression and fibre type. (Modified from Fluck and Hoppeler, 2003).

1.2.3.1. Neuromuscular activity

Neuromuscular activity is an important factor for specific muscle fibre phenotype development and its subsequent maintenance (Pette and Vrbova, 1985). Cross-reinnervation studies clearly demonstrated that neural activity could lead to switch in fibre phenotype (Buller, 1965). Reports from spinal cord injury and denervation

experiments, also suggested that in the absence of innervation, muscle will undergo atrophy and switch in fibre phenotype from slow to fast (Pette and Staron, 2000). Fast fibres will turn to slow type when reinnervated by a slow nerve and vice versa (Pette and Vrbova, 1985).

Electrical activity is the main mechanism by which the nervous system exerts control over fibre phenotype. Based on the slow and fast motoneuron-specific firing patterns, electrical stimulation can be classified into two protocols. The chronic low-frequency stimulation (CLFS), which mimics the tonic low-frequency (10-20 Hz) impulse pattern is normally delivered to a slow-twitch muscle (Salmons and Vrbova, 1969). On the other hand, the short burst (phasic) of high-frequency (100-150 Hz) stimulation mimics the pattern that is normally delivered to a fast-twitch muscle (Lomo et al., 1974). The use of CLFS as an experimental model to study neuromuscular activity has proved to be very fruitful (Pette and Vrbova, 1999).

Calcium (Ca^{2+}) is an essential element in muscle function. It is required for the activation of muscle contraction through the troponin-tropomyosin complex, and for secondary roles such as regulation of ATP provision. The different concentrations of Ca^{2+} in cytosol also serve as indicators for the electrical activation pattern in skeletal muscle. Slow-type signalling pattern results in a sustained intracellular Ca^{2+} concentration of 100 to 300 nM (Chin and Allen, 1996), while fast pattern results in short-lived Ca^{2+} elevations of up to 1 μM (Westerblad and Allen, 1991). Hence, the concentration of cytosolic calcium-ion is controlled by electrical stimulation, and is believed to be a major influence on MyHC isoform expression in muscle (Talmadge,

2000). Increasing intracellular Ca^{2+} levels in myotube cultures has been shown to enhance the expression of MyHC slow (Kubis et al., 1997).

1.2.3.2. Mechanical loading and unloading

When considering the role of mechanical loading, focus will be on: (1) functional overload, (2) resistance training and (3) endurance training. Conversely, to appreciate the effects of reduced weight bearing, focus will be on: (1) space flight, (2) hindlimb suspension and (3) spinal cord injury.

In events of functional overload, such as the surgical removal of targeted muscle synergists to induce functional overload, results indicate that in fast muscles such as *plantaris* muscle, the expression of MyHC 2x and MyHC 2b are decreased, whereas both MyHC I and MyHC 2a expression are raised (Baldwin and Haddad, 2001). Similar results were observed in resistance training. In rodents, the expression of MyHC 2b shifted to the MyHC 2x isoform. As previously mentioned, MyHC 2b is hardly detectable in human muscle, therefore the major finding was the decreased expression of MyHC 2x and concomitant increase in MyHC 2a expression in a human model (Carroll et al., 1998).

Unlike resistance training, endurance training appears to be both muscle specific and dose dependent. Only in mixed fast or fast muscles that undergo moderate to high endurance training, show a shift from MyHC 2b to MyHC 2x/MyHC 2a expression (Demirel et al., 1999). If the endurance training is extended to extreme, it is possible to induce MyHC I expression (Demirel et al., 1999). In human world-class marathon

runners, a strong bias towards the expression of up to 80-90% of the slow type MyHC isoform was found (Andersen et al., 1994).

On the other hand, when skeletal muscle is continuously unloaded, the opposite pattern of transformation occurs. The effects of mechanical unloading have been studied using various models. Neonatal rats in a microgravity spaceflight environment showed significant reduction in muscle growth with a resulting MyHC pool biased towards fast MyHC 2b and 2x expression (Adams et al., 2000). The findings indicated that weight bearing activity is essential for slow muscle isoform development and expression. In contrast, it is not essential for fast MyHC 2x and MyHC 2b development expression (Adams et al., 2000). Muscles of rats subjected to hindlimb suspension showed a transition from slow-to-fast fibre phenotype switch (Haddad et al., 1998).

Spinal cord injury in small animals (cats and rats) has been shown to cause transformation in MyHC expression that is qualitatively similar to those reported in spaceflight or hindlimb suspension experiments (Talmadge, 2000). There was a marked reduction in the expression of MyHC slow isoform, and an increase in the relative expression of all three fast MyHC isoforms (Talmadge, 2000). However, there is a difference between small animals and humans in response to spinal cord injury. In humans suffering from spinal cord injuries with lower extremity paralysis, there was considerable delay in the transformation of slow to fast MyHC profiles, unlike that seen in animal models (Talmadge, 2000; Andersen et al., 1996).

1.2.3.3. Hormones

Hormonal signalling has a major influence on skeletal muscle development and muscle fibre phenotype determination. Several notable hormones are involved in increasing muscle mass by promoting protein synthesis or by reducing protein degradation, such as anabolic hormones, which include growth hormone, insulin-like growth factors (IGFs) and testosterone. In contrast, catabolic hormones such as glucagon and glucocorticoids, increase protein metabolism and lead to reduced muscle mass. Among the hormones listed, thyroid hormone and IGFs also showed marked influence on the expression of specific MyHC isoforms.

Thyroid hormone consists of two iodine-containing amine hormones-thyroxine (T4) and triiodothyronine (T3). Of the two, T3 appears to have the greater effect on skeletal muscle fibre phenotype. In general, hypothyroidism causes fast-to-slow transition. The magnitude and specific isoform transition vary between different muscle types. The transition of MyHC 2a/2x to MyHC I was observed in slow muscle, whereas a shift from MyHC 2b/2x to MyHC 2a/I was detected in fast and mixed muscles (Caiozzo et al., 1998). In contrast, hyperthyroidism elicits a slow-to-fast transition. The transition involves repression of MyHC I expression and enhancement of fast MyHC 2x/2b isoform (Caiozzo et al., 1998). T3 with clenbuterol also greatly enhances the slow to fast fibre type switch (Awede et al., 2002). In addition to their impact on adult muscle fibre phenotype, thyroid hormone also plays an important role in muscle development and maturation. In a space flight study, results indicated that an intact thyroid gland was essential for down-regulation of neonatal isoform during muscle development (Adams et al., 2000).

IGFs (IGF-1 and IGF-2) are polypeptides with high sequence similarity to insulin. The IGFs stimulate both muscle cell proliferation and differentiation through interaction with the type 1 IGF receptor (IGF1R), insulin receptor exon 11- (IR-A) and insulin receptor exon11+ (IR-B), all of which are transmembrane tyrosine kinase receptors (Denley et al., 2005). The type 2 IGF receptor (IGF2R) (known also as mannose-6-phosphate receptor), has no intrinsic signalling transduction capability and serves to sequester IGF-2 from potential receptor interactions and to internalise and degrade IGF-2 (Denley et al., 2005). The action of the IGFs are modulated by a family of six high-affinity IGF binding proteins (IGFBP 1-6). The IGFBPs act as carrier proteins for the IGFs in the circulation, protecting them from degradation and transporting them to specific tissues (Florini et al., 1996). Both IGF hormones are secreted by the liver as a result of growth hormone (GH) stimulation. They are also synthesised locally in muscle tissues, acting in an autocrine/paracrine manner in response to damage, mechanical loading or stretching (Adams, 2002). Besides the major IGF-1 (IGF-1Ea), a spliced variant with a carboxyl terminus different from IGF-1Ea, named mechano growth factor (MGF), is rapidly inducible in skeletal muscle and appears to be an early trigger for satellite cell proliferation (Hill and Goldspink, 2003; Yang and Goldspink, 2002). The autocrine/paracrine muscle production of IGF-2 during muscle differentiation and regeneration was found to participate in a positive feedback loop to further enhance muscle differentiation (Erbay et al., 2003; Wilson et al., 2003) and regeneration (Kirk et al., 2003). IGF-1 has the additional effect of converting fibres to fast glycolytic, by raised expression of glycolytic enzymes in IGF-1-transfected C2C12 myotubes (Semsarian et al., 1999a), by a modest rise in fast 2b fibres in transgenic mice carrying muscle IGF-1 isoform driven by a rat myosin light chain (MyLC)-1/3 promoter (Musarò et al., 2001), and by

raised type 2a and 2b fibres at the expense of slow fibres in IGF-1-treated dystrophic mice (Lynch et al., 2001). The mechanism responsible for the slow to fast fibre type switch, however, remains elusive.

1.2.3.4. Ageing

Ageing is associated with structural and functional changes in skeletal muscle. Studies on slow and fast rat muscle indicated age-related changes in fibre type and MyHC isoform composition. It has been shown that ageing leads to fast-to-slow transition (Larsson and Ansved, 1995).

In fast muscles of rat, results showed decreases in the MyHC 2b/2x and increases in the slow myosin isoform with ageing (Skorjanc et al., 1998; Danieli-Betto et al., 1995). A similar transition was observed in slow muscle, in which MyHC 2a was gradually replaced with MyHC I isoform (Larsson and Ansved, 1995). However, increases of MyHC I expression in ageing muscle do not necessarily lead to increase in fatigue resistance, as in endurance training athletes. In endurance runners, slow type fibres are rich with mitochondria, but the mitochondrial content in ageing fibres is reduced.

In addition, an age-related decline in protein synthesis rate of MyHC has been demonstrated (Lexell et al., 1986; Balagopal et al., 2001). The reduction of MyHC, the key protein in contractile apparatus, is likely to contribute to muscle weakness and reduced locomotion. The reduction in MyHC and mitochondrial protein production could be caused by decreases in mitochondrial DNA and messenger RNA (Nair,

2005). To reduce the ageing effect, resistance training that could increase MyHC protein has shown to be beneficial (Balagopal et al., 1997).

1.2.4. Muscle hypertrophy and atrophy

Skeletal muscle hypertrophy is characterised by an expansion of fibre sizes, either through enlargement or elongation that will lead to increase in muscle mass. In contrast, muscle atrophy refers to reduction in fibre size or fibre loss as a consequence of disease, age or muscle inactivity (Glass, 2003; Glass, 2005).

1.2.4.1. Hypertrophy and the PI3-K pathway

The IGF-activated PI3-K signalling pathway is widely regarded as the primary route to skeletal muscle hypertrophy (Glass, 2003; Glass, 2005). Phosphatidylinositol 3'-kinase (PI3-K) consists of two sub-units, the SH2 domain containing regulatory unit (p85), and a catalytic sub-unit (p110) (Vivanco and Sawyers, 2002). PI3-K catalyses the phosphorylation of membrane-bound phosphatidylinositol (4,5)-biphosphate (PIP₂) to phosphatidylinositol (3,4,5)-trisphosphate (PIP₃). PIP₃ subsequently serves as a docking station for Akt1 (also known as protein kinase B) and phosphatidylinositol-dependent protein kinase 1 (PDK1). Akt1 is phosphorylated by PDK1, and once activated Akt1 phosphorylates a number of substrates that are responsible for a range of growth processes, which include protein synthesis, glycogen synthesis, muscle differentiation and cell proliferation. A key target of activated Akt1 is the phosphorylation of mTOR (mammalian target of rapamycin), a serine/threonine

kinase, which in turn activates a number of downstream effectors including ribosomal protein S6 kinase (p70S6K) and eIF-4E, both of which mediate translation initiation and appear to play important roles in muscle hypertrophy.

1.2.4.2. Atrophy and the ubiquitin-proteasome proteolysis pathway

It has been shown that protein degradation is elevated during muscle atrophy which leads to a reduction in muscle mass (DeMartino and Ordway, 1998). Among all MyHC isoforms in skeletal muscle, MyIIC I was the primary target for protein degradation as a consequence of mechanical unloading (Baldwin and Haddad, 2002). The pathways of protein degradation are poorly understood, but studies have implicated the involvement of the ubiquitin-proteasome proteolysis pathway, which degraded the contractile proteins that lead to muscle atrophy (Glass, 2005; Solomon and Goldberg, 1996; Solomon et al., 1998).

In this pathway, proteins are targeted for degradation by covalent ligation to ubiquitin (Ub), a 76-amino-acid residue protein. Ubiquitin protein ligation requires sequential action of three enzymes. Firstly, the ubiquitin is activated by an ubiquitin-activating enzyme (E1 family). Secondly the activated ubiquitin is conjugated to substrate proteins by an ubiquitin-conjugating enzyme (E2 family). Finally, degradation of the substrate proteins with ubiquitin protein ligase (E3 ligase family) (Hershko and Ciechanover, 1998). There is a single E1, but there are many species of E2s and multiple families of E3s or E3 multiprotein complexes. Specific E3s appear to be responsible mainly for the selectivity of ubiquitin-protein ligation and protein degradation (Hershko and Ciechanover, 1998).

Studies in different catabolic situations (fasting, diabetes, uraemia and tumour conditions) with cDNA microarrays, found that genes encoding the Ub-proteasome pathway (E2 and E3 family) were up-regulated (Lecker et al., 2004). Among the up-regulated genes, two E3 ligase family members were consistently highly up-regulated in all four conditions. There were the MuRF1 (muscle ring finger 1) and MAFbx (muscle atrophy F-box or atrogin-1), and were identified as mediators of muscle atrophy (Lecker et al., 2004). This result has strengthened the previous finding, in which genetically modified null mice that were deficient in either MuRF1 or MAFbx showed resistance toward atrophy (Bodine et al., 2001b). The same research group also demonstrated that these two genes were up-regulated in other atrophy conditions (denervation, immobilization or un-weighting) and over-expression of MAFbx lead to myotube atrophy in C2C12 cell culture (Bodine et al., 2001b).

MuRF1 comprises 3 domains: a RING-finger domain, required for ubiquitin activity, a B-box of unclear function, and a coil-coil domain, which may be required for the formation of heterodimer with a related protein MuRF2 (Glass, 2005). Over-expression of MuRF-1 has been shown to disrupt the titin subdomain (an important element for sarcomere formation) (McElhinny et al., 2002). On the other hand, MAFbx contains an F-box domain, a characteristic of E3 ubiquitin ligase family. F-box E3 ligases usually bind to a substrate that is post-translationally modified, for example by phosphorylation (Glass, 2005).

Decreased activity of the PI3-K/Akt1 signalling pathway can lead to muscle atrophy (Bodine et al., 2001a). Conversely, activation of Akt1 in rat muscle can prevent

denervation atrophy (Bodine et al., 2001a). Recent studies demonstrated that reduction the PI3-K/Akt1 signalling pathway in myotube atrophy condition, can lead to activation of FOXO transcription factors and MAFbx induction (Sandri et al., 2004). FOXO protein is a subgroup of the Forkhead family of transcription factors, it is one of the downstream targets of the PI3-K/Akt1 pathway that could mediate IGF-1. Mammalian cells contain three members of this family, which are FOXO 1 (FKHR), FOXO 3 (FKHRL1) and FOXO 4 (AFX). By inhibition of FOXO function through the use of a RNAi construct *in vivo* (fasting mouse) and dominant negative construct *in vitro* (cultured myotube treated with glucocorticoids), activation of MAFbx is prevented (Sandri et al., 2004). Moreover, over-expression of FOXO3 leads to a dramatic atrophy of myotube and muscle fibres. In contrast, the MAFbx mRNA level was reduced in FOXO3 over-expressed cells with IGF-1 added (Sandri et al., 2004). Therefore, inhibition of FOXO factors seems to prevent muscle atrophy.

1.2.5. Calcineurin

Calcineurin (Cn) is an enzyme complex that comprises three subunits: calcineurin A (CnA) catalytic subunit, calcineurin B (CnB) regulatory subunit and calcium-binding protein calmodulin (Schulz and Yutzey, 2004). There are three major isoforms of CnA (α , β and γ) and two gene isoforms of CnB (1 and 2). Only CnA α , CnA β (A α more abundant than A β) and CnB1 are expressed in skeletal muscle (Parsons et al., 2004). Cn is a calcium dependent serine-threonine phosphatase that is widely distributed throughout the body. It has been implicated in a wide variety of biological responses including T-lymphocyte activation, neuronal and cardiac development, and skeletal muscle development (Crabtree, 2001; Bassel-Duby and Olson, 2003). In

skeletal muscle, Cn is required for the muscle development process. It is involved in muscle differentiation and conversion of fast-to slow muscle phenotypes (Chin et al., 1998; Dunn et al., 1999). It has been shown that inhibition of Cn activity in primary cell culture can prevent cell differentiation, whereas over-expression of Cn has been shown to enhance differentiation (Delling et al., 2000; Friday et al., 2000).

It has been reported that activated calcineurin mediates the hypertrophic effect of IGF-1 (Musarò and Rosenthal, 1999; Semsarian et al., 1999b). However, there is compelling evidence, including transgenic and knock-out data, to indicate that Cn has no direct effect on muscle hypertrophy (Rommel et al., 2001; Pallafacchina et al., 2002; Parsons et al., 2003). In contrast, IGF-1-induced hypertrophy is mediated by the phosphatidylinositol-3 kinase PI3-K/Akt1 pathway as detailed earlier (Rommel et al., 2001; Pallafacchina et al., 2002; Parsons et al., 2003).

1.3. Candidate genes of PCS

PCS is a multifactorial disorder with intermediate heritability. It is a complex condition where pathogenesis is likely to be mediated by at least several genes, loosely termed as candidate genes. Candidate genes are genes that may be involved in the development or pathogenesis of a specific disease/condition. They may not necessarily be the cause of the disease.

Nine differentially expressed sequence tags (EST's) were isolated between the *biceps femoris* of normal and of splayleg piglets (Maak et al., 2001). EST is a unique stretch of DNA usually at the 3'end region of a gene that is useful for identifying full-length

genes and serves as a landmark for mapping. By homology comparison, nine porcine homologues to human genes were identified: (i) TATA box binding protein associated factor B (*TAF1B*), (ii) B-cell CLL/lymphoma 7B (*BCL7B*), (iii) pyruvate dehydrogenase kinase, isoenzyme 4 *PDK4*, (iv) SPARC-like 1 (*SPARCL-1*), (v) ribosomal protein S10 (*RPS10*), (vi) epithelial protein lost in neoplasm (*EPLIN*), (vii) N-myc downstream-regulated gene 2 (*NDRG2*), (viii) pleiomorphic adenoma gene like 2 (*PLAGL2*) and (ix) BCL-2 associated transcription factor short form (*BTFS*).

TAF1B has RNA polymerase I transcription factor activity, which could be involved in transcription from Pol I promoter and Pol II promoter (Comai et al., 2000). The function of *BCL7B* has not been determined, but it could be involved in cell differentiation and congenital Williams syndrome (a neuro developmental disorder) (Meng et al., 1998). *PDK4* expression is suppressed by insulin in porcine skeletal muscles (Kim et al., 2006). *SPARCL-1*, is down-regulated in many types of cancer cells and may serve as a negative regulator of cell growth and proliferation (Bendik et al., 1998). *EPLIN* is a cytoskeleton-associated protein that inhibits actin filament depolymerization (Chang et al., 1998). *NDRG2* is a cytoplasmic protein that may play a role in neurite outgrowth and may be involved in glioblastoma carcinogenesis (Deng et al., 2003). *PLAGL2* might induce the expression of a proapoptotic protein Nip3, leading to cellular apoptosis (Mizutani et al., 2002). Not much is known about *BTFS*.

In another recent differential display study, cyclin-dependent protein kinase inhibitor 3 (*CDKN3*) was identified as a potential candidate gene by differential display (Maak et al., 2003). *CDKN3* belongs to a family of dual-specificity protein phosphatases.

Over-expression of wild type *CDKN3* could delay cell cycle progression (Gyuris et al., 1993). However, the quantitative analysis of expression by real-time PCR showed no significant difference between normal and affected pigs (Maak et al., 2003).

Of the list of candidate genes for PCS highlighted (Maak et al., 2001; Maak et al., 2003), the association of *SPARCL-1* with PCS is particularly interesting to explore. The putative anti-proliferative property of *SPARCL-1* could play a role in PCS pathogenesis.

1.3.1. SPARC

SPARC (secreted protein acidic and rich in cysteine), also termed osteonectin, BM-40, is a 32-kDa protein. It was first identified as a major non-collagenous protein of bone matrix (Termine et al., 1981). It is a member of matricellular glycoprotein, a group of non homologous macromolecules that is involved in cell-matrix interactions which do not serve primarily structural roles (Lanc and Sage, 1994). Other members of this group of proteins include the thrombospondins (TSP) 1 and 2, osteopontin (OPN), tenascins (TN)-C and X (Brekken and Sage, 2000). Although their structures are different, they appear to perform related functions, e.g. they exhibit counter-adhesive effects that lead to cell rounding and changes in cell shape which result in the disruption of cell-matrix interactions. These proteins are also expressed when tissue undergoes changes in cell shape and motility, e.g. tissue renewal, tissue remodelling and embryonic development (Bornstein, 1995). Therefore, the matricellular proteins are different from the traditional adhesive proteins such as fibronectin, laminin,

fibrillar collagens and vitronectin, all of which contribute to the structural stability of the extracellular matrix.

SPARC contains modular domains that can function independently to bind cells and matrix components (Engel et al., 1987). Based on sequence analysis, four putative domains (Fig. 1.5), I to IV were distinguished in the protein sequence. Domain III and IV are also termed as Extracellular calcium binding domain (EC domain).

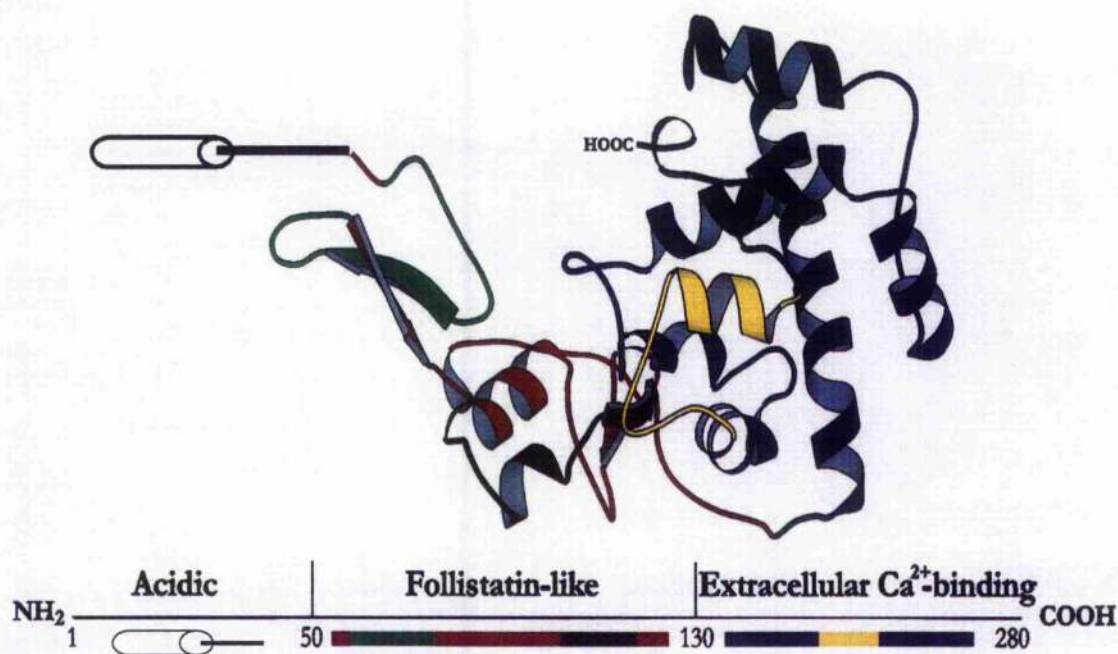


Figure 1.5. Modular structure of human SPARC. The ribbon diagram derived from crystallographic data indicates three structural modules. The follistatin-like domain, aa 53/137, is shown in red except for peptide 2.1, aa 55/74, and the K GHK angiogenic peptide, aa 114/130, which are shown in green and black, respectively. The EC-module aa 138/286 is shown in blue except for peptide 4.2, aa 255/274, which is shown in yellow. (Adapted from Hohenester et al. 1996 and the Brookhaven Protein database, accession number 1BM0)

The N-terminal domain I is highly acidic in character, it binds to several calcium ions with low affinity (Maurer et al., 1992). This N-terminal domain exhibits the most

divergent sequence among the family of SPARC-like proteins. Therefore, antibodies against a particular SPARC have not been found to cross react with other SPARC-like proteins (Yan et al., 1998). The second domain (Domain II) is the Cys-rich, follistatin-like (FS) domain, in which all the Cys residues are disulfide-bonded, and with an N-linked complex carbohydrate. Domain II is homologous to a follistatin (FS)-domain and Kazal type protease inhibitors (Maurer et al., 1995). Follistatin (FS) is an activin-binding protein, which inhibits the action of activin, and thereby inhibits the release of follicle stimulating hormone. Kazal inhibitors, which inhibit a number of serine proteases (such as trypsin and elastase), belong to the family of proteins that includes pancreatic secretory trypsin inhibitor; avian ovomucoid; acrosin inhibitor; and elastase inhibitor. Domain III (EC domain) is largely α -helical and is responsible for the binding site for collagen IV (Mayer et al., 1991). The C-terminal domain, Domain IV contains the EF-hand motif with a high-affinity calcium binding site (Pottgiesser et al., 1994). Domains III and IV were not independent but represent one domain (hence termed the EC domain) binding both calcium and collagens (Pottgiesser et al., 1994).

SPARC could: (a) disrupt cell adhesion through dissolution of the focal adhesion complex (Lane and Sage, 1994), (b) promote changes in cell shape, an effect of counter-adhesive function (Lane and Sage, 1994), (c) regulate cell differentiation in lens epithelial cells (Bassuk et al., 1999), (d) be anti-proliferative by inactivating cellular responses to certain growth factors induced by platelet-derived growth factor (PDGF), vascular endothelial growth factor (VEGF) and basic fibroblast growth factor (bFGF) (Yan and Sage, 1999), (e) be involved in angiogenesis and tumorigenesis via interaction with PDGF, VEGF and bFGF (Yan and Sage, 1999), (g)

promote wound healing, by influencing the activity of transforming growth factor-beta (TGF- β), a growth factor that associated with rapid remodelling of connective tissue (Yan and Sage, 1999).

The anti-proliferative property of SPARC has been verified on cells derived from SPARC-null mice. Fibroblast, mesangial cells, and smooth muscle cells isolated from SPARC-null mice exhibited a higher rate of proliferation relative to their wild-type counterparts. Null cells were also more sensitive to the inhibition of cell cycle progression induced by recombinant SPARC (Bradshaw et al., 1999).

SPARC also inhibits progression of cells from G1 to S phase or prolongs G1 phase of the cell cycle (Claeskens et al., 2000). If cell cycle progression is inhibited by SPARC, it is likely that SPARC functions in cell differentiation also. In fact, SPARC has exhibited prominent expression during the terminal differentiation of cultured human keratinocytes and in terminally differentiated retinal ganglion cells *in vivo* (Yan et al., 1998). Moreover, SPARC is believed to regulate terminal differentiation of lens epithelial cells, because disruption of the SPARC locus in mice resulted in the abnormal differentiation of lens fibres (Bassuk et al., 1999). *In vitro*, SPARC is secreted into the medium of a variety of cell types. In normal tissues, SPARC protein is detected intracellularly, except in bone matrix (Termine et al., 1981).

1.3.1.1. SPARC and related proteins

To date, four SPARC related proteins are known. They are: (a) quail retina protein QR1 (Guermah et al., 1991); (b) TSC-36/FPR, a TGF- β -induced, follistatin related

protein secreted by glioma cells (Shibanuma et al., 1993); (c) testican, a proteoglycan found in human testis (Alliel et al., 1993) and (d) SPARCL-1, a putative ECM glycoprotein which was found in rat brain (Johnston et al., 1990). All the members in this group have an EC domain (extracellular calcium binding domain), followed by a Follistatin (FS) like domain. However, the acidic Domain I exhibits considerably less identity within this group (Fig. 1.6).

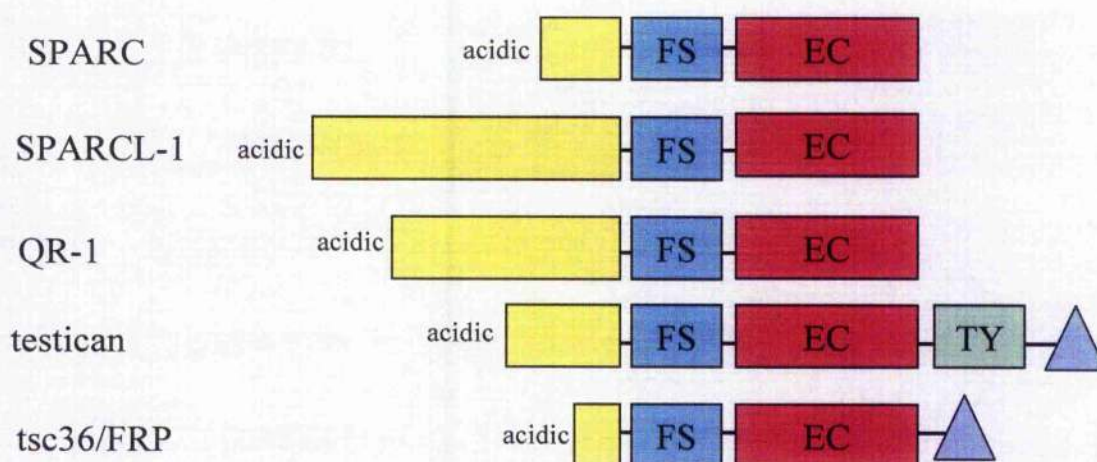


Figure 1.6. SPARC and related proteins. Three prominent modules are shown. The N-terminal domains I of each protein exhibit considerably reduced identity, although all are acidic. A follistatin-like, Cys-containing module (FS) is followed by the extracellular calcium-binding domain (EC). TY designates a thyroglobulin-like domain in testican. Triangles represent characterized modules in testican and tsc36/FRP. (Quote from Yan et al., 1999; Modified from Maurer et al., 1995.)

Among the related proteins, SPARCL-1 displays the highest amino acid similarity with SPARC, sharing 55.6% identity at FS domain and 61.4% identity at EC domain. The structure differences between SPARC and SPARCL-1 was at domain I, SPARCL-1 has a longer domain I sequence compare to SPARC. Although SPARCL-1 and SPARC share a similar pattern of tissue distribution, they are not found in the

same structures within organs (Soderling et al., 1997). SPARCL-1 was expressed in medium and large vessels of the kidney, whereas SPARC was expressed in glomeruli and vasculature of the kidney. However, another cell adhesion study has shown that these two proteins exhibit similar functions with respect to the inhibition of attachment and spreading of endothelial cells in culture (Girard and Springer, 1996).

1.3.2. SPARCL-1

The matricellular protein SPARC like-1 (SPARCL-1), also known as MAST9/hevin/SC1, is a member of the SPARC family. SPARCL-1 contains a follistatin-like domain (FS) and an extracellular calcium binding domain (ES), which are the hallmarks of the SPARC family.

SPARCL-1 (as SC1) was originally cloned from a rat brain expression library by screening with a polyclonal antibody raised against a synaptic junction glycoprotein (Johnston et al., 1990). Its mRNA was expressed widely throughout the brain and could be detected in many types of neurons (Johnston et al., 1990). MAST9, was identified in human non-small cell lung carcinomas (Schraml et al., 1994). Hevin, its human homologue, isolated from a specialised postcapillary vascular structure called high endothelial venules, was found in the tonsils (Girard and Springer, 1995). MAST9/Hevin gene encoded a glycoprotein, which exhibit 62% identity in its carboxy terminus to the extracellular matrix protein SPARC, therefore, MAST9/Hevin was renamed to SPARC-like 1 (SPARCL-1) (Isler et al., 2000).

SPARCL-1 mRNA is expressed in many normal human tissues including heart, kidney, prostate, ovary, small intestine, colon, and lymph nodes (Bendik et al., 1998). It has been shown to be a negative regulator of cell proliferation (Claeskens et al., 2000). It inhibits progression of cells from G1 to S phase or prolongs G1 phase (Claeskens et al., 2000). SPARCL-1 is down-regulated in many types of cancer cells and may serve as a negative regulator of cell growth and proliferation (Bendik et al., 1998).

PCS is suspected to be caused by a delayed maturation of limb muscles. SPARCL-1 was highlighted in PCS skeletal muscle and could be a candidate gene involved in the development of myofibrillar hypoplasia (Maak et al., 2001).

1.3.3. P311

P311 is another candidate gene identified for its possible association with PCS. *P311* was found to be highly expressed during dietary restriction in skeletal muscle of young pigs (da Costa et al., 2004). This finding suggests that *P311* could play an important role in the differentiation and growth of skeletal muscle. No direct evidence was obtained of its relationship with PCS. Down regulation of *P311* expression is hypothesised to be involved in the development of muscular weakness in PCS directly or indirectly.

P311, also referred as PTZ17 (pentylenetetrazol), is an 8-kDa intracytoplasmic protein originally found in the developing mouse brain (Studler et al., 1993). P311 is characterized by the presence of a conserved PEST domain (sequence rich in Pro, Glu,

Ser, and Thr). P311 has three PEST like domains, only the domain located at the N-terminus, shows similarity within human, mouse and chicken species. To date, little is known about the function of the PEST domain, and little is known about the suggested function of P311. PEST domains are: (a) putative targets for degradation by the ubiquitin/proteasome system, which degrades proteins by covalently linking ubiquitin to lysine residues of the protein, thereby allowing recognition and degradation of the protein by the proteasome. (Varshavsky, 1997); (b) candidate sites for protein-protein binding (Ghose et al., 2001); (c) targets for degradation by calpains (Noguchi et al., 1997) and (d) thought to be involved in phenotypic changes consistent with myofibroblast transformation (Pan et al., 2002). Myofibroblasts are cells with features intermediate between fibroblasts and smooth muscle cells that play a main role in tissue repair.

With the presence of PEST domain, P311 protein was subjected to extremely rapid degradation by the ubiquitin/proteasome system. To detect the presence of P311 protein, different approaches were used. The PEST domain was deleted during plasmid construction (Paliwal et al., 2004) or by adding proteasome inhibitor to reduce the degradation of P311 protein (Taylor et al., 2000). Lactacystin was selected but did not block decay of the protein effectively. In addition, pulse-chase experiments were performed in which cells were treated with lactacystin in combination with a series of protease inhibitors including o-phenanthroline, pepstatin, leupeptin, and aprotinin. Only the combination of lactacystin and the metalloprotease inhibitor, o-phenanthroline, was able to block degradation of *P311* (Taylor et al., 2000). The data suggested that *P311* was subject to rapid degradation by both the ubiquitin/proteasome system and an unknown metalloprotease.

1.4. Aims

PCS is a classic example of a multifactorial disorder with intermediate heritability. Histological examination of affected muscle reveals the presence of “myofibrillar hypoplasia”. However, the cellular changes, including biochemical and fibre type changes, associated with PCS remain poorly described. Hardly any information is available on the molecular changes that occur in the muscles in PCS. Therefore, the aims of this thesis are to undertake: (1) cellular and molecular characterisation of PCS and (2) functional studies of PCS candidate genes.

1.4.1. Cellular and molecular characterisation of PCS

The aim is to undertake a detailed cellular and molecular characterisation of the morphological, metabolic and fibre type changes in PCS affected muscles. The investigations will incorporate the use of immunohistochemistry and histochemistry coupled with detailed image analysis. TaqMan quantitative real-time RT-PCR will be used to investigate the expression of *MyHC* genes in PCS. Findings would aid in diagnosis and understanding of the pathogenesis of PCS.

1.4.2. Functional studies of PCS candidate genes

P311 and *SPARCL-1* are 2 novel genes identified from the literature as candidates for PCS investigation. To investigate the functional role of these candidate genes, their

full-length cDNAs will be over-expressed in murine C2C12 muscle cells by adenovirus infection and stable transfection. Quantitative changes in cell proliferation rate (BrdU), myotube formation (fusion index) and expression of *MyHC* genes (TaqMan quantitative real-time RT-PCR) will be determined.

Chapter 2

Materials and Methods

2.1. Introduction

The general materials and methods used throughout the project are described in this Chapter. More specialised protocols are listed in the relevant sections. Most of the general materials and methods described in this Chapter are derived from standard materials and methods that can be found in common laboratory manuals e.g. Maniatis, (1989).

2.2. Porcine congenital splayleg

2.2.1. PCS piglets and muscle selection

PCS is a condition in newborn piglets that show inability to stand and walk properly, the limbs extending forwards or sideways as a result of muscular weakness. In this study, 2-day-old PCS affected piglets with both hind limbs extended were selected, along with a normal litter mate. The selected normal litter mates were active and did not have lameness problems.

PCS is closely associated with muscle weakness. Among the muscles examined, the most seriously affected are the *semitendinosus* (ST) in the hindlimb, the *longissimus dorsi* (LD) in the lumbar region and the *triceps* in the forelimbs (Thurley et al., 1967). However, some researchers believed that the *adductor* and *sartorius* are more seriously affected because they are the major muscles concerned with upper hindlimb adduction (Bradley et al., 1980). In a more recent study, the LD muscle and *biceps femoris* were found to show less number of myofibrils (Antalikova et al., 1996). Thus, a wide range of muscles can be affected by PCS. In this study, the ST, LD and

gastrocnemius (G) muscles were selected for cellular and molecular analyses from those described above. The *gastrocnemius* muscle was selected in this study because it is a hindlimb muscle and might be involved in PCS. The selected muscles were removed from four 2-day-old splayleg male piglets, along with 4 corresponding normal litter mates (commercial hybrid stock, Large White × Landrace). Piglets were put down by captive bolt. The selected skeletal tissue samples were quickly dissected out, a complete cross section was taken from the mid-belly of the muscles. Two sets of selected muscle samples were prepared. The first set of muscle samples were rapidly frozen in isopentane cooled in liquid nitrogen. They were then wrapped in aluminium foil and stored in liquid nitrogen until required for immunohistochemistry and histochemistry (Section 2.2.2). The second set of muscle samples were placed in cryotubes and immediately snap-frozen in liquid nitrogen until required for total RNA extraction (Section 2.7.1.1).

2.2.2. Immunohistochemistry and histochemistry

A SLEE cryostat (CM3050, Leica) was used to section all muscle samples. Each muscle sample was transferred to a cryostat chuck, then tissue embedding compound (OCT compound, Sakura) and cryo spray agent (Cellpath) were applied until a mould was formed. The sample was then placed in the cryostat where it was left to warm to the cryostat temperature of -20°C before sectioning. The cryostat section thickness was set at 10 µm. Each tissue block was trimmed to a satisfactory muscle depth. Each section was picked up with pre-3-aminopropyltriethoxysilane (2 % in acetone) coated microscope slide, and held for few seconds to allow the section to melt onto the slide. Each slide was air dried for 30 min before storage in -70°C. The remaining

tissue was brushed in an upward direction, and the process was repeated to generate more sections. When the sectioning was completed, the muscle block was wrapped in cellophane and aluminium foil, and stored at -70°C.

Muscles were immunostained for: (a) β -dystroglycan at 1:200 dilution (VisionBiosystems) to outline individual muscle fibres, (b) slow myosin heavy chain (MyHC) at 1:50 dilution (cat. N^o. M8421, Sigma) for slow muscle fibres and (c) fast MyHC at 1:50 dilution (cat. N^o. M4276, Sigma) for fast muscle fibres. The slow MyHC antibody is a human monoclonal antibody that shows specificity only for slow fibres. The fast MyHC antibody is a rabbit monoclonal antibody that shows specificity to all three porcine fast MyHC fibres (2a, 2x and 2b) (Chang et al., 2003). Histochemical staining was performed with: (a) Sudan Black B (SBB) staining to detect the presence of lipids and (b) succinate dehydrogenase (SDH) staining as an indicator of muscle fibre oxidative capacity.

Upon commencing staining, slides were removed from the freezer and left at room temperature for 30 min. The sections were ringed using a 'pap' pen (DakoCytomation) and placed in 10 mM Tris Buffer Tween (TbT), pH 7.5, for 5 min. The sections were stained using the EnVision+ system, Peroxidase (DAB kit K4007, DakoCytomation) according to the manufacturer's instructions. Briefly, the sections were first removed from the wash buffer and laid out in a humidified chamber where the endogenous peroxidase activity was quenched by application of a peroxidase block for 5 min. Next, the slides were washed in TbT for 5 min before application of the primary antibody (β -dystroglycan, MyHC slow or MyHC fast antibody) in 10 mM Tris Buffer Saline (TBS), pH 7.5, for 1 hour at room temperature. After incubation,

the slides were washed in TbT for 5 min, and incubated with polymer-horseradish peroxidase (HRP) anti-mouse antibody for 30 min. Subsequently, the sections were rinsed in TbT for 5 min, followed by two 5 min rinses in deionised water. The staining was visualised with a 5 min incubation in 3, 3-diaminobenzidine (DAB)+ substrate-chromogen that resulted in brown coloured staining at the antigen site. Following the DAB staining, the slides were washed in deionised water. The sections were counterstained with Gill's haematoxylin (Sigma), a specially formulated high contrast stain solution used as a biological nuclear stain. Next, the slides were washed in tap water, dehydrated through an ethanol gradient and were cleared in Histo-clear solution (BDH, UK), a xylene substitute. DPX *mountant for microscopy* (BDH, UK) was used to mount the cover-slip before examination by light microscopy (Carl Zeiss Ltd).

Prior to histochemical staining, slides were left to dry at room temperature for 30 min. For SBB staining, the sections were ringed using a 'pap' pen and rinsed in 70% ethanol (Fisher Scientific, UK). The sections were stained using saturated SBB in 70% ethanol for 2 hours. After the incubation period, the slides were rinsed with 70% ethanol followed by deionised water. The sections were counterstained with Gill's haematoxylin, a specially formulated high contrast nuclear stain solution. For SDII (Nachlas et al., 1957), slides were incubated in 1M of sodium succinate with tetrazolium solution (nitro blue tetrazolium, 2M Tris-HCl and 1M $MgCl_2$) at 37°C for 1 hour. They were then incubated in formal saline [4% formaldehyde (Fisher Scientific, UK) in normal saline] for 10 min. After incubation, the slides were gently rinsed with deionised water for 2 min. Subsequently, the sections were counterstained with Meyer's carmalum (2g of carmine in 100 ml of 5% ammonium alum) for 5 min

to highlight muscle fibre membranes. For both stains, the same rinsing protocol was used. Slides were rinsed in tap water, dehydrated through an ethanol gradient and were cleared in Histo-clear solution (BDH, UK). Finally, DPX (BDH, UK) was used to mount the cover-slip.

2.2.3. Image analysis

Processed slides were examined under an image capturing light microscope (Carl Zeiss Ltd). For each muscle sample, 6 fields with at least 500 fibres each were randomly selected for morphometric analysis under magnification X200 using the KS300 image analysis software (Carl Zeiss Ltd). There are superficial and deep layers in *Semitendinosus* muscle (Handel and Stickland, 1987), the superficial layer was selected for study in this project. The parameters that were determined were fibre type, size and number (Figs. 2.1 and 2.2). Two technical problems encountered in the image analysis work. The first was connected to muscle fibre density. An adult muscle cross-section has an average of about 200-300 fibres within one field under a magnification of X100. However, in 2 day-old muscles there were about 800-1400 fibres per field under the same magnification. This number of fibres was too large to manage effectively. Hence a magnification of X200 was used. The use of this magnification resulted in the second technical problem. This concerned the usage of the in-house computer macro for the KS 300.3.0 software programme, which was for use at only X100. As a result, each mask prepared from a field viewed at X200, had to have each fibre outlined manually which was a time consuming process (2 hours/mask). In contrast, with the help of the software, each adult muscle only took 15 min to complete.

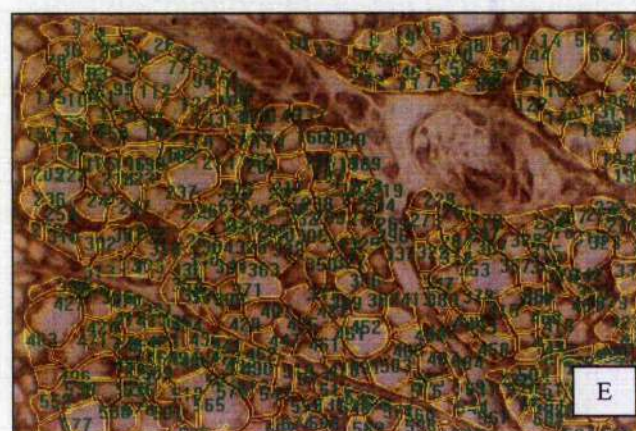
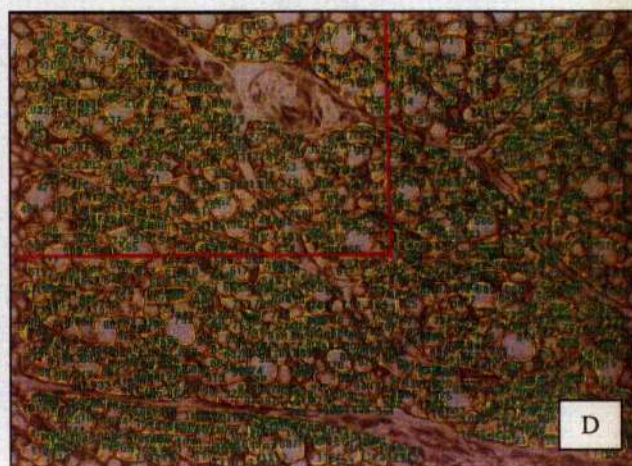
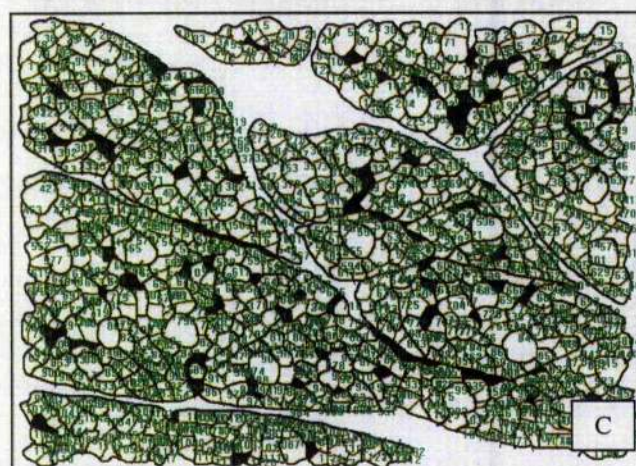
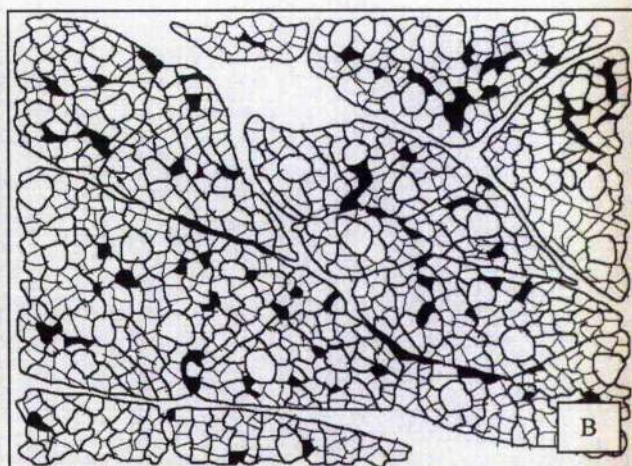
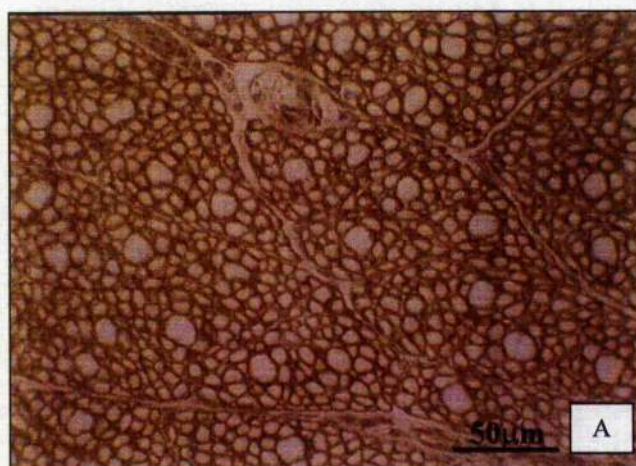


Figure 2.1. Image analysis. (A) Typical field of normal LD muscle immunostained for dystroglycan, captured under X200 magnification. (B) Manually drawn mask of image A. (C) Computer annotated fibres based on mask from B. (D) Overlay of images C and A. (E) Enlargement of part (red border) of image D.

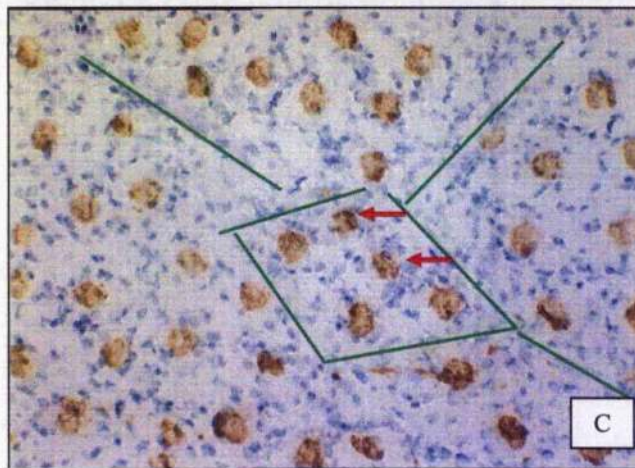
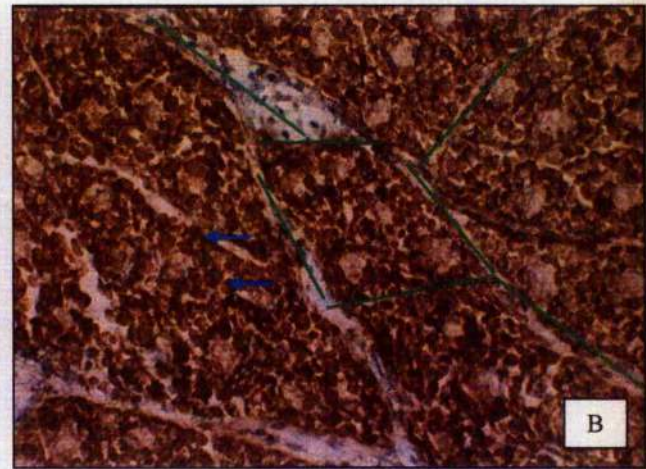
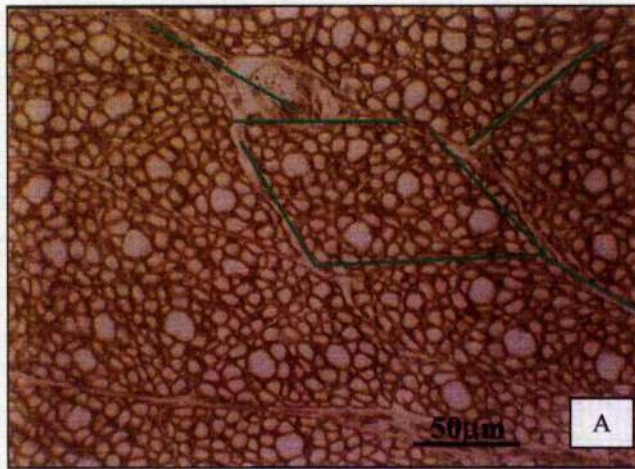


Figure 2.2. Identification of MyHC fast and MyHC slow fibres. (A) Typical field of normal LD muscle immunostained for dystroglycan, captured under X200 magnification. (B) and (C) are serial muscle cross-sections immunostained with MyHC fast and MyHC slow antibody, respectively. Both images were used to identify the numbers of fast and slow fibres located within the field. Blue arrows indicate positive MyHC fast fibres. Red arrows indicate positive MyHC slow fibres. Green lines are for orientation of the images.

2.3. Recombinant DNA techniques

2.3.1. Transformation of bacteria with plasmid DNA

2.3.1.1. Transformation of commercially available ultracompetent cells

Plasmids were maintained in *Escherichia coli* commercially available. XL2-Blue MRF⁺ and XL10-Gold ultracompetent cells supplied by Stratagene were used in most of the transformations. Plasmid DNA transformation was carried out following the manufacturer's guidelines, summarised as follows. Competent cells were thawed on ice, 4 µl of β-mercaptoethanol (Stratagene) was added to 100 µl of competent cell in a prechilled 15 ml Falcon 2059 polypropylene tubes (BD Biosciences), mixed gently and incubated on ice for 10 min. Plasmid DNA was then added to the cells, at a concentration of 0.1 to 50 ng of DNA per 100 µl of competent cells. The mixtures were incubated on ice for 30 min, then heat-shocked for 30 s at 42°C in a water bath, followed by incubation on ice for 2 min. At the same time, NZY broth (per litre, 5 g NaCl, 2 g MgSO₄ · 7H₂O, 5 g of yeast extract and 10 g of NZ amine) was pre-heated at 42°C and 900 µl of the pre-heated NZY broth was then added to the mixtures. Subsequently, the tube was incubated at 37°C for 1 hour in an orbital shaker (S150, Stuart) at 225-250 rpm. With a sterile spreader, 200 µl of the transformation reaction was plated on Luria-Bertani agar (LB agar per litre, 10 g of NaCl, 10 g of tryptone, 5 g of yeast extract and 20 g of agar) plates containing 1 units/ml kanamycin.

2.3.1.2. Topo- TA cloning

The TOPO-TA system is a specialised cloning kit (Invitrogen) specifically designed for the cloning of PCR products (Section 2.4), taking advantage of non-template terminal transferase activity of Taq polymerase that leaves a single deoxyadenosine residue overhang on PCR products. The linearised vector in the kit possesses a single deoxythymidine residue overhang, allowing any PCR product to be ligated into the vector.

The supplier's protocol was followed. Four μl of PCR product were added to 1 μl Topo-TA vector, mixed gently and left at room temperature for 5 min. Next, the mixture was added into the aliquot of "One-Shot" cells, mixed and incubated in ice for 30 min. The cells were heat-shocked for 30 s at 42°C in a water bath. The tube was immediately transferred back to ice and further incubated for another 2 min. Two hundred and fifty μl of SOC medium (per litre, 0.5 g of NaCl, 20 g of tryptone, 5 g of yeast extract and 20 mM glucose) at room temperature were added into the tube. Then, the cells were incubated at 37°C for 1 hour in an orbital shaker at 200 rpm. At the end of incubation, 50 μl of the transformed cells were plated onto LB agar supplemented with either ampicillin or kanamycin antibiotics, and incubated overnight at 37°C.

2.3.2 Isolation of plasmid DNA

Isolation of plasmid DNA was carried out in all instances by a modified version of the alkaline lysis technique (Birnboim and Doly, 1979).

2.3.2.1. Small scale plasmid preparations

Cells picked from single colonies were grown in 5 ml LB, overnight at 37°C in an orbital shaker. For each overnight culture, 1.5 ml of cells were spun down in a microcentrifuge tube at 10,000 x g for 1 min and the supernatant was discarded. Then, another 1.5 ml of culture were added to the pellet and the centrifugation step repeated, for a total of 3 ml of culture processed per overnight culture. The final pellet was spun again briefly, remove the remaining LB medium by pipette.

Plasmid DNA minipreps were prepared using the Spin Miniprep Kit (Qiagen). The supplier's protocol was used, briefly as follows. Each selected cell pellet was thoroughly resuspended in 250 µl Buffer P1 by pipetting. Cell suspensions were lysed by the addition of 250 µl Buffer P2, mixed by inversion. Three hundred and fifty µl Buffer N3 solution were added and mixed thoroughly to precipitate the protein. The resulting precipitate was centrifuged for 10 min at 10,000 × g, and then the supernatants were applied to Qiaprep spin columns. The columns were centrifuged at 10,000 × g for 1 min and the flow through was discarded. The DNA was bound to the column after it had been spun down. Each column was washed with 500 µl Buffer PB to remove trace nuclease activity. Each column was further washed by spinning with 750 µl Buffer PE. Centrifugation was repeated to remove any residual ethanol from the last washing step. Subsequently, the column was transferred to a clean 1.5 ml microcentrifuge tube, and plasmid DNA was eluted from the column by adding 50 µl of 10 mM Tris-Cl, pH 8.0. The columns were left to stand for 1 min, then centrifuged

at $10,000 \times g$ for 1min. The column was discarded and the plasmid DNA was stored at -20°C until required.

2.3.2.2. Large scale plasmid preparations

Cells picked from single colonies were grown in 5 ml LB, overnight at 37°C in an orbital shaker. Two ml of overnight culture were inoculated into 400 ml LB medium, supplemented with either ampicillin or kanamycin antibiotics in a one litre conical flask. The medium was cultured overnight in a shaking incubator. At this level of aeration, the cells were approximately mid-log phase when harvested the following morning. The bacterial broth was centrifuged at $6,000 \times g$ for 15 min at 4°C .

The Maxiprep Kit (Qiagen) was used to isolate the plasmid DNA. The manufacturer's protocol was used, re-stated briefly as follows. The cell pellets were each resuspended in 10 ml Buffer P1. The cells were then lysed with the addition of 10 ml Buffer P2 by mixing vigorously by inversion, followed by incubation at room temperature for 5 min. Ten ml of prechilled buffer P3 was added, mixed thoroughly and spun at $10,000 \times g$ for 40 min at 4°C . While waiting for the centrifugation, Qiagen maxiprep columns were equilibrated with 10 ml Buffer QBT. The supernatant from the centrifugation step was applied to the column by pouring through a $0.2 \mu\text{m}$ cell strainer (Qiagen) to remove residual particulate matter. Columns were washed twice, each time with 30 ml Buffer QC. All flow-through was discarded.

Plasmid DNA was eluted with 15 ml Buffer QF into a 30 ml clear centrifuge tube (BD Biosciences). 10.5 ml isopropanol (AnalaR[®], UK) was added and mixed by inversion to precipitate the DNA. The tube was centrifuged at $15,000 \times g$ for 30 min at 4°C. The supernatant was carefully discarded and the pellet was then carefully washed with 5 ml of 70% ethanol, prechilled to -20°C, and spun again at $15,000 \times g$ for 15 min at 4°C. Supernatant was removed and the pellet was left to air-dry. The plasmid DNA was resuspended in 200 µl 10 mM Tris Cl, pH 8.0 and stored at -20°C until required.

2.3.2.3. Determination of DNA concentration by spectrophotometry

The concentration of DNA preparations, principally from large scale plasmid preparations, was determined spectrophotometrically (DU-65 spectrophotometer, Beckman) with optical density measurements at 260 and 280 nm against a distilled-water blank. Each plasmid sample was diluted 1:200 in millipore-pure water (Millipore) to a total volume of 800 µl, and transferred to a quartz, optical cuvette (LCM, LA). An OD₂₆₀ measurement of 1.0 was taken to indicate a double-stranded, plasmid DNA concentration of 10 µg/µl. The OD ratio of 260/280 nm was used to estimate the purity of the DNA preparation, with a ratio approaching 1.8 as being the ideal (Hirschman and Felsenfeld, 1966).

2.3.3. Restriction endonuclease digestion

For most restriction digests, between 1 and 2 µg of DNA was digested in 20 µl of reaction mix containing 5 to 10 units of appropriate restriction enzyme, such as *EcoR*

I, *Xho* I, *Bam*H I, *Xba* I and others (Invitrogen), and the required enzyme buffer (Buffers A, B, L, M and H) (Invitrogen). Generally, all the reactions were incubated for a minimum of two hours at 37°C.

2.3.4. DNA electrophoresis

2.3.4.1. Agarose gel electrophoresis

The molecular weight of the DNA samples was determined in 0.8% agarose gels. Two grams of agarose powder (Biogene, UK) was added into 250 ml TAE buffer (40 mM Tris acetate, 1 mM EDTA) in a 1 litre conical flask. The agarose was melted in a microwave, and allowed to cool to around 55°C. Ethidium bromide (Fisher Scientific, UK) of 75 µg/ml concentration was then added, and the whole gel mix was poured into a casting plate (Pharmacia Biotech) with appropriate gel comb inserted. The casting comb was carefully removed once the gel had set. The gel was stored at 4°C until needed. DNA samples were prepared for loading by adding the appropriate volume of 10 x loading buffer [0.25% bromophenol blue (Sigma), 0.25% xylene cyanol FF (USB Corp, Ohio) and 30% glycerol (Fisher Scientific, UK) in water], together with a known molecular size standard DNA as a marker, typically a 1 kb DNA Ladder[®] (Invitrogen). After loading the samples, depending on DNA sizes, the gels were run for 60-90 minutes under 70 volts (GNA-200, Pharmacia Biotech). Examination of the gel was done under a UV transilluminator (UVP Inc), the molecular size of the DNA was determined by comparison with the standard marker.

2.3.4.2. Excision of DNA bands

Enzymatic digestion was performed as described in Section 2.3.3 to obtain DNA fragments of a particular size. The agarose containing DNA was visualized under a UV transilluminator and the desired band excised quickly from the gel using a scalpel. DNA was recovered from the gel slice using the QIAquick Gel Extraction Kit (Qiagen). The kit protocol is summarised as follows. Each gel slice was transferred to a 1.5 ml micro centrifuge tube and weighed. For each gel slice, three volumes of Buffer QG were added to every volume of gel sample. Samples were then heated for 10 min in a 50°C water bath. Once the gel slice was completely dissolved, one gel volume of absolute isopropanol was added. The mixture was transferred to a Qiaquick spin column/collection tube assembly. The column assembly was spun at $10,000 \times g$ for 1 min. Flow through was discarded and 750 μ l of PE buffer was added to the column. The column was spun again at $10,000 \times g$ for another 1 min, and the flow through discarded. To remove all traces of ethanol present, the centrifugation step was repeated. After that, the column was transferred to a clean 1.5 ml microcentrifuge tube. Thirty μ l of 10 mM Tris Cl, pH 8.5 were added to the column and left stand for 1 min. Finally, the column was spun again at $10,000 \times g$ for 1 min. The column was discarded and the eluted products stored at -20°C until required.

2.3.5. DNA ligation

T4 DNA ligase (Promega) was used for most of the cloning strategies. The multiple cloning site of the relevant plasmid vector was cut with the appropriate restriction enzymes (Section 2.3.3) and treated with calf alkaline phosphatase (Roche) for one hour at 37°C. Vector DNA (50-100 ng) was mixed with the target insert, at a molar ratio

of 1:5, together with an appropriate volume of ligation buffer and 4.5 units of T4 DNA ligase (Promega), to make up a final volume of 10-20 μ l. The reactions were left overnight at 14°C, before proceeding to the transformation step, described in Section 2.3.1.

2.4. Polymerase chain reaction

The polymerase chain reaction (PCR), a means of amplifying small amounts of specific DNA template from a complex mixture, is reviewed extensively by Innis and Gelfand, (1990). The general guideline of how the method was applied to DNA amplification throughout the project is described below. The details of more specific PCR experiments are provided in the relevant Chapters where necessary.

2.4.1. PCR primer design

Custom oligonucleotide syntheses were provided by MWG Biotech. Most of the oligonucleotide primers were between 20 to 30 deoxynucleotide residues in length, with a base composition of 50-60% guanine (G) or cytosine (C) where possible. Primer pairs with complementary sequences were avoided, and both primers were designed (Primer 3 software, US) so as to have matching annealing temperatures (T_m).

2.4.2. PCR conditions

PCR reagents were supplied by Promega. Amplification reactions were typically set up in a reaction mixture of the following: 200 μ M of dNTP, PCR buffer (50 mM KCl, 10 mM Tris-HCl, pH 9.0, 0.1% Triton[®] X-100 and 1.5 mM MgCl₂) and 2.5 units of *Taq* DNA polymerase. The appropriate amount of DNA or cDNA template varied between PCR reactions, but was generally between 10 to 100 ng. Thermal cycling was carried out on a thermocycler machine (Mastercycler[®] gradient, Eppendorf). For standard PCR, the template was denatured firstly for 3 min at 95°C, followed by 30 s at 95°C denaturing step, 30 s at 60°C annealing steps and 90 s at 72°C extension steps. The above process was repeated for 34 cycles, and a final 72°C for 2 min, before holding at 4°C. The PCR amplification products were stored at -20°C until needed. Amplification products were visualised by agarose gel electrophoresis, as mentioned in Section 2.3.4.1. Up to 10 μ l of the PCR reaction were loaded into each well for electrophoresis.

2.5. DNA sequence analysis

All sequence data were obtained using ABI sequencing kits (Applied Biosystems), based on the chain termination method (Sanger et al., 1977) with cycle sequencing modification as previously described (Innis et al., 1988). Version 3.0 ABI thermal cycle system (Applied Biosystems) was used in this project.

2.5.1. Sequencing primer design

Custom oligonucleotides for cycle sequencing were supplied by MWG Biotech. Most of the oligonucleotide primers were 20 to 25 oligonucleotides in length, with a base composition of 50-60% guanine (G) or cytosine (C) where possible. The last (3') bases of either adenosine (A) or thymidine (T) was avoided, with a 3' stretch of 4-5 guanine (G) or cytosine (C) residues preferred.

2.5.2. Reaction conditions for cycle sequencing

The majority of the templates used for sequencing in this project were plasmid DNA derived from small scale (Section 2.3.2.1) or large scale (Section 2.3.2.2) preparations. The supplier's guidelines (Applied Biosystems) were followed. Briefly, the cycle-sequencing reaction mixture consisted of ABI PRISM[®] Big Dye reagent mixture (Applied Biosystems) and appropriate sequencing buffer, together with 200 to 500 ng of DNA template and 1.6 pmol/ μ l of each sequencing primer, made up to 20 μ l with millipore-pure water. Cycle sequencing was carried out on a thermocycler machine (Mastercycler[®] gradient, Eppendorf), using the following programme. The template was denatured for 2 min at 96°C, followed by 10 s at 96°C (denaturing), 10 s at 50°C (annealing) and 4 min at 60°C (extension) . The last 3 steps of the above process were repeated for 24 cycles, with a final hold at 4°C. The cycle sequencing products were stored at -20°C until needed.

Performa[™] CTR gel filtration cartridges (Edge Biosystems) were used to clean the cycle-sequencing reaction product. The cartridge effectively removed dye terminators,

dNTPs, and other low molecular weight materials from sequencing reactions. The manufacturer's protocol for the cleaning process is summarised as follows. Firstly, the Performa Gel Filtration Cartridges were centrifuged for 3 min at $750 \times g$. Then, the cartridges were transferred to clean 1.5 ml microcentrifuge tubes. The sequencing products were added to the packed columns, and centrifuged for another 3 min at $750 \times g$. The eluted volume which contained the clean sequencing products was retained. These samples were then freeze-dried for 1 hour by vacuum desiccation (VR-1, Hetovac). The sequencing products were resuspended in 25 μ l Hi-Di formamide (Applied Biosystems). Twenty μ l of the resuspended samples were loaded into each of the 96-well-plate. Then, the plate was loaded in to the ABI PRISM[®] 3100 Genetic Analyzer (Applied Biosystems), a 16-capillary instrument. Data were analysed using Chromas version 2.2.3 software packages (Technelysium Pty Ltd, US). Sequence pileups and comparisons were carried out by Blast (NCBI) and AliBee Multiple Alignment (GeneBee).

2.6. Cell culture

2.6.1. C2C12 cell culture

Most of the cell culture work was performed with C2C12 cells (cat. N^o. CRL-1772, ATCC), a subclone of a mouse myoblast cell line. C2C12 cells differentiate readily to form contractile myotubes. C2C12 cells have several advantages over the usage of primary culture. Firstly, they are effectively a homogenous population of myoblasts without the other contaminating cell types. Secondly, C2C12 cells are robust and amenable to laboratory manipulation. All C2C12 cells were grown in proliferation

medium (PM) [10% foetal bovine serum (BioWest, France) in Dulbecco's modified Eagle medium (DMEM) (Gibco®) with 100 units/ml penicillin, 100 µg/ml streptomycin (Invitrogen) and 10 µg/ml ciproxine (Bayer)]. At 80% confluence, PM was replaced by differentiation medium (DM) [4% horse serum (BioWest, France) in DMEM with penicillin and streptomycin] to promote myotube formation.

2.6.1.1. Cell passaging

C2C12 cells were routinely passaged when they reached about 80% confluence. During passage, culture medium was carefully removed and discarded. The cells were washed twice with phosphate buffered saline (PBS) (Gibco®). Trypsin (0.05%) and EDTA (0.53 mM) (Invitrogen) were added to detach the cells and incubated at 37°C for 5 min. After the incubation, the flask was gently tapped to dislodge the cell monolayer. Five times the volume of serum containing medium was added to inactivate the enzyme, and the mixture was transferred to a 50 ml Falcon tube and centrifuged at $1200 \times g$ for 5 min. The supernatant was discarded and the cell pellet was resuspended in fresh PM.

2.6.1.2. Cell storage

Cells cannot be maintained indefinitely in culture and therefore must be stored in liquid nitrogen for long term usage. Cells that required storage were washed and trypsinised as mentioned in the above section. The cells were resuspended in 100% foetal calf serum with 10% DMSO (Ambion), and transferred into cryovials

(Invitrogen). Cryovials were pre-chilled in the ice. With help of an isopropanol-filled freezing container "Mr. Frosty" (cat. N^o. 5100, Nalgene[®]), the cryovials were frozen at a controlled rate (1°C/min) at -70°C freezer overnight. The following day, the vials were transferred to -196°C liquid nitrogen storage.

When removing cells from cryostorage, the vials were thawed quickly in a water bath at 37°C, without the tubes being submerged into the water bath. Ten ml of PM were added and the mixture was centrifuged at $1200 \times g$ for 5 min. The supernatant which contained cytotoxic DMSO was discarded. The cell pellet was resuspended in fresh cultured medium and transferred to a culture flask.

2.6.1.3. Surface coating

Some culture flasks, multi-well plates and chambered slides were coated with gelatin to modify the culture of C2C12 cells. Gelatin 2% stock solutions (Sigma) were preheated at 37°C for 30 min. Sterilised and millipore-pure water was used to prepare 0.1% gelatin solution. One day prior to plating, sufficient 0.1% gelatin was placed into each well or chamber, to cover the entire surface. After 15 min, the gelatine solution was aspirated away. Each well or chamber was then rinsed with water and left to air-dry. Coated culture dishes were kept at room temperature.

2.6.2. AD293 cell culture

AD293 cells (cat. N^o. 240085, Stratagene) were used for the production and amplification of recombinant adenoviruses. The AD293 cell line is a modified human embryonic kidney 293 (HEK293) cell line, with improved cell adherence and plaque formation properties. HEK293 cells are human embryonic kidney cells transformed by sheared adenovirus type 5 DNA. AD293 cells have similar properties to HEK293 cells, which produce the adenovirus E1 gene in *trans*, allowing the production of infectious virus particles when cells are transfected with E1-deleted adenovirus vectors. Standard HEK293 cells do not adhere well to tissue culture dishes.

AD293 cells were cultured in DMEM supplemented 10% FCS for growth purpose, together with standard antibiotics supplementation of 100 units/ml penicillin, 100 µg/ml streptomycin (Invitrogen) and 10 µg/ml ciproxine (Bayer). The passage and storage of the AD293 cells were similar to that of C2C12 cells as described previously in Sections 2.6.1.2 and 2.6.1.3.

2.6.3. Lipofectin transfection

The introduction of foreign DNA into mammalian cell culture was typically performed through liposome-mediated transfection, using Lipofectin (Life Technology[™]). The guidelines from the suppliers are briefly restated. Transfection in a 25 cm² culture flask was performed when cells were 40% confluent. Two solutions were prepared, solution A (60 µl of Lipofectin reagent with 900 µl of Optimum medium was allowed to stand at room temperature for 30-45 min) and solution B (10

μ l or 6.0 μ g of DNA with 900 μ l of Optimem medium). The two solutions were mixed and incubated at room temperature for 20 min to allow the formation of DNA-liposome complexes. At the same time, PM was removed from the cell culture, and it was rinsed twice with 5 ml Optimem solution. Four ml of serum-free PM were added into each tube containing the DNA-liposome mixture, and the whole solution was overlaid onto the cells. The cells were incubated for 5 to 6 hours at 37°C in a CO₂ incubator (Gallenkamp, UK). Following this, the DNA containing medium was replaced with 5ml of 10% DMEM and incubated for a further day.

In order to produce an enriched population of modified cells, a selection system must be used to remove untransfected cells. Geneticin (G418) (Gibco®) was used as a selectable marker. G418 is a type of aminoglycoside phosphotransferase which blocks protein synthesis by interfering ribosomal function. G418 (2000 μ g/ml) was used in stable selection for at least 7 days. To monitor the effectiveness of the selection process, a control population of untransfected cells was maintained in identical conditions. After 7 days, the surviving transfected cells were switched to 1000 μ g/ml of G418, to maintain the selection pressure.

To obtain larger populations of transfected cells, the transfection flasks were passaged from 25 cm² culture flasks to bigger 75 cm² culture flasks (Costar®, USA). Care was exercised to keep the passage number low. Cells were periodically stored in liquid nitrogen for future use. Cells derived from stable transfections were used for the proliferation assay and fusion index experiments, described in later sections. All subsequent experiments on stably transfected cells were conducted in the absence of G418.

2.6.4. Recombinant adenovirus production

As a complement to stable transfection, infectious recombinant adenoviruses were generated to carry the genes of interest. BD Adeno-XTM Expression System 2 (BD Biosciences) was used to produce recombinant adenoviruses. The protocol involved the transfer of the gene of interest from a BD Creator Donor Vector to a BD Adeno-X Acceptor Vector, by the use of cre recombinase. The manufacturer's protocol is summarised as follows.

2.6.4.1. Adenovirus vector cloning

The starting plasmid vector pDNR-CMV for the insertion of the gene of interest housed an expression cassette that was derived from the plasmid pAAV-IRES-hrGFP (Stratagene) which comprised a multiple cloning site for the creation of a 3'-end FLAG fusion gene and a GFP reporter gene, with an internal ribosomal entry site (IRES) between the two (Fig. 2.3).

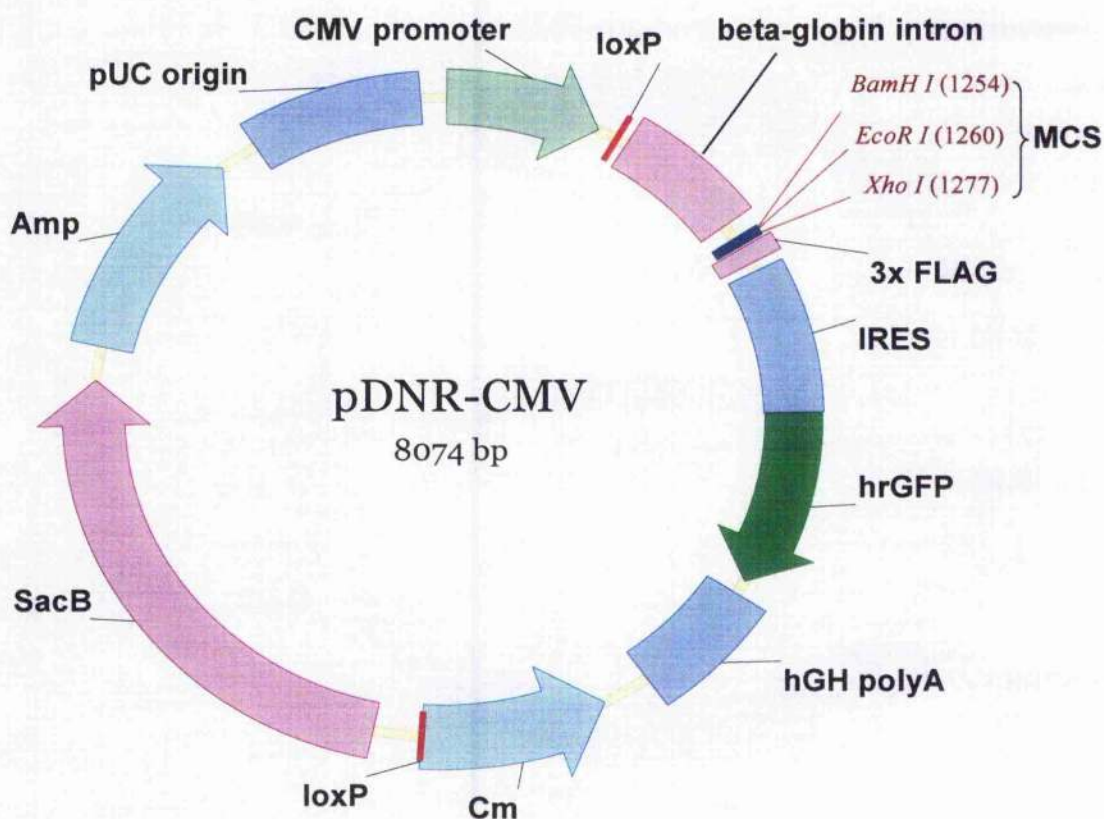


Figure 2.3. Plasmid vector pDNR-CMV. It comprises a multiple cloning site for the creation of a 3'-end FLAG fusion gene and a GFP reporter gene (which derived from pAAV-IRES-hrGFP vector). Amp= ampicillin resistance gene; Cm= chloramphenicol resistance gene; CMV= cytomegalovirus; IRES= internal ribosome entry site; MCS= multiple cloning site; SacB= sucrase gene from *B.subtilis*. *BamH* I, *EcoR* I & *Xho* I are vector restriction sites.

The following reagents were prepared for the creator reaction, which included: 1 μ l (200 ng) of recombinant donor vector, 1 μ l of Cre Recombinase and 18 μ l of reaction mix (pLP-Adeno-X-CMV acceptor vector, Cre reaction buffer and bovine serum albumin). The mixture was left at room temperature for 15 min. After incubation, the reaction was terminated at 70°C for 5 min. The recombinase enzyme binds to the *loxP* sites on both the donor vector and acceptor vector, and undertakes DNA cleaving

and ligation. As a result, the gene of interest was transferred in the appropriate orientation to the acceptor vector (Fig. 2.4).

Four μ l of reaction was withdrawn and added into to XL10-Gold ultracompetent cells (Stratagene). The procedure for ultracompetent cell transformation was described in Section 2.3.1.1. The next day, a minimum of 10 bacterial colonies were individually picked into 30 μ l of deionised H₂O. The colony was resuspended by gentle vortexing. Twenty μ l of bacterial suspension were transferred into 5 ml of LB broth containing 100 μ g/ml ampicillin and 30 μ g/ml chloramphenicol. The medium was cultured for 5-6 hour at 37°C in a shaking incubator (S150, Stuart). The remaining 10 μ l was analysed by PCR to identify positive clones. Each reaction was set up as follows. Ten μ l double-distilled water, 10 μ l of bacterial suspension, 2.5 μ l of 10X *Taq* PCR buffer, 1 μ l each of primer mix and dNTP mix, and 0.5 μ l of *Taq* polymerase. Thermal cycling was carried out on a thermocycler machine (Mastercycler[®] gradient, Eppendorf). The template was firstly denatured for 2 min at 95°C, followed by 15 s at 94°C, 30 s at 64°C and 30 s at 68°C. The last 3 steps of the above process were repeated for 20 cycles. Amplification products were visualised by agarose gel electrophoresis, as described in Section 2.3.4.1. The predicted band size for a successful recombination was 660 bp.

Once a positive clone was identified by PCR, the clone was amplified by maxiprep DNA preparation as described in Section 2.3.2.2 by using the previous 20 μ l of bacterial suspension inoculated into the 5 ml LB broth.

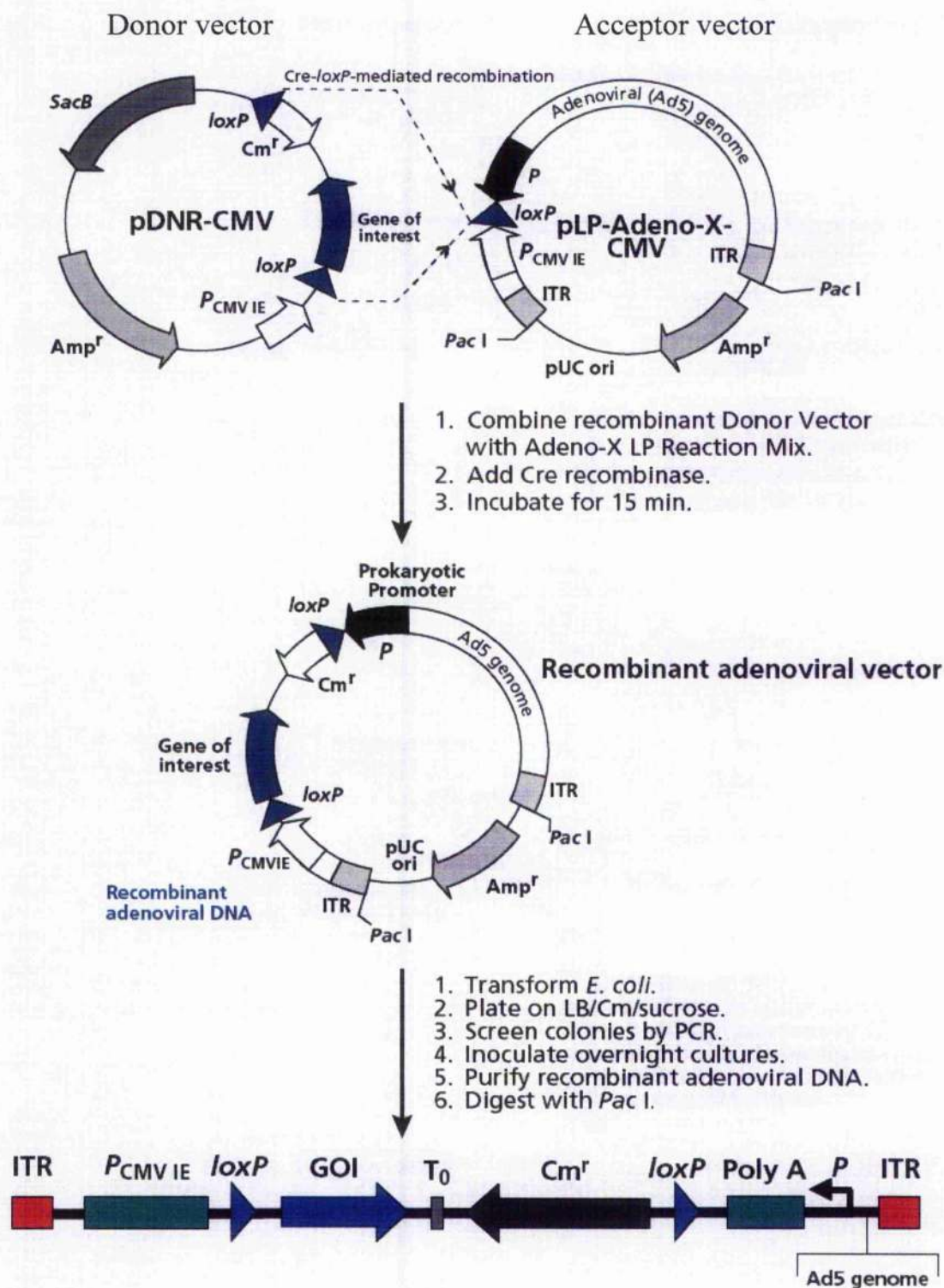


Figure 2.4. Overview of recombinant adenovirus production. (Diagram modified from BD-Adeno-X expression systems 2 User Manual, BD Bioscience)

2.6.4.2. *Pac* I digestion of recombinant Adeno-X DNA for transfection

Before the Adeno-X DNA could be packaged, the recombinant plasmid was linearised with *Pac* I to expose the inverted terminal repeats (ITRs) which were located at either end of the genome (Fig. 2.4). The ITRs contained the origins of adenovirus DNA replication and must be positioned at the terminal of the linear adenovirus DNA molecule to support the formation of the replication complex. A mixture of the following reagents were prepared in a sterile 1.5 ml microcentrifuge tube: 20 µl of deionised H₂O, 5 µg/µl of recombinant plasmid DNA from the above section, 4 µl of 10 X *Pac* I digestion buffer, 4 µl of 10 X BSA and 2 µl of *Pac* I restriction enzyme. The contents were incubated at 37°C for 2 hour. After the incubation period, 60 µl of 1X TE buffer (pH 8.0) and 100 µl of phenol: chloroform: isoamyl alcohol (25:24:1) (Sigma) were added to the reaction. The tube was mixed gently, and was spun at 10,000 × g for 5 min at 4°C to separate the phases.

The top aqueous layer was transferred to a clean sterile 1.5 ml microcentrifuge tube. Four hundred µl of 95% of ethanol and 1/10 volume of 3M sodium acetate (NaOAc) were added to the tube and was mixed gently. The mixture was spun at 10,000 × g at 4°C for 5 min, and the supernatant was discarded. Three hundred µl of 70% ethanol were added to wash the pellet and the tube was centrifuged again at 10,000 × g for 2 min. Subsequently, supernatant was removed and the pellet was left to air-dry at room temperature. The DNA was resuspended in 10 µl sterile 1X TE buffer pH 8.0 and used for transfection.

2.6.4.3. Transfecting AD293 cells with *Pac* I digested Adeno-X DNA

The transfection protocol was similar to lipofection transfection (Section 2.6.3). However, Lipofectamine (Life Technology™) was selected in this protocol instead of Lipofectin (Life Technology™), because of the need for higher transfection efficiency (Ciccarone et al., 1999). Transfection was performed in a 25 cm² culture flask.

Following transfection, AD293 cells were regularly checked for cytopathic effects (CPE), which were manifested as rounded and detached cells. It could take up to two weeks for full CPE to develop. Cells were transferred to a 50 ml tube. No trypsin was used. The cells were spun at 1,500 × g for 5 min at room temperature. The supernatant was removed and the pellet was resuspended in 500 µl of sterile PBS. Then, the cells were lysed with three consecutive freeze-thaw cycles. Each time the cells were frozen in dry ice for 5 min and thawed for 5 min in 37°C with vigorous mixing. After the third cycle, the cells were spun at 10,000 × g for 10 min. The lysate was transferred to a clean, sterile microcentrifuge tube and stored at -70°C.

For amplification of the recombinant adenovirus, the lysate from a 25 cm² culture flask was used to infect a larger 75 cm² culture flask. After CPE was fully established, cell lysate was harvested after 3 freeze-thaw cycles as before. To obtain a higher quantity of high-titre adenovirus, lysate from the first amplification was used to infect a series of 162 cm² culture flasks. Cell lysate and culture medium were pooled for virus purification.

2.6.4.4. Purification of recombinant adenoviruses

BD Adeno-X virus purification kits (BD Biosciences) were used to purify and concentrate adenoviruses (Fig. 2.5). All the procedures were performed in a Class II biosafety hood. Combined lysate and culture medium from the earlier steps described above were clarified with a filter disc in the filter unit bottle, connected to a vacuum source. Once the process was completed, the vacuum line was disconnected and the filtrate was transferred into a sterile filter bottle. Ten units of Benzonase nuclease (BD Biosciences) per ml were added to the filtrate to remove contaminating cellular DNA, and the mixture was incubated at 37°C for 30 min. An equal volume of 1X dilution Buffer was added to the filtrate.

Next, the tube assembly was placed in the virus containing filtrate. The supernatant was loaded into the syringe and the content pushed through the virus-affinity filter at ~20 ml/min. The inlet tubing was transferred to a holding vessel containing 1X wash buffer. Then, the wash buffer was pulled into the syringe through the tubing, and wash buffer was pushed through the filter at ~20 ml/min. Next, the filter was removed from the tubing assembly. To elute the adenovirus, the BD luer-lok tip syringe was filled with 3 ml of 1X elution buffer. It was attached to the filter cartridge and 1 ml of the elution buffer was pushed through the filter into a sterile 15 ml conical tube. The filter was incubated at room temperature for 5 min before pushing the remaining elution buffer through the filter. The purified adenovirus was aliquoted in sterile 1.5 ml microcentrifuge tubes and stored at -70°C.

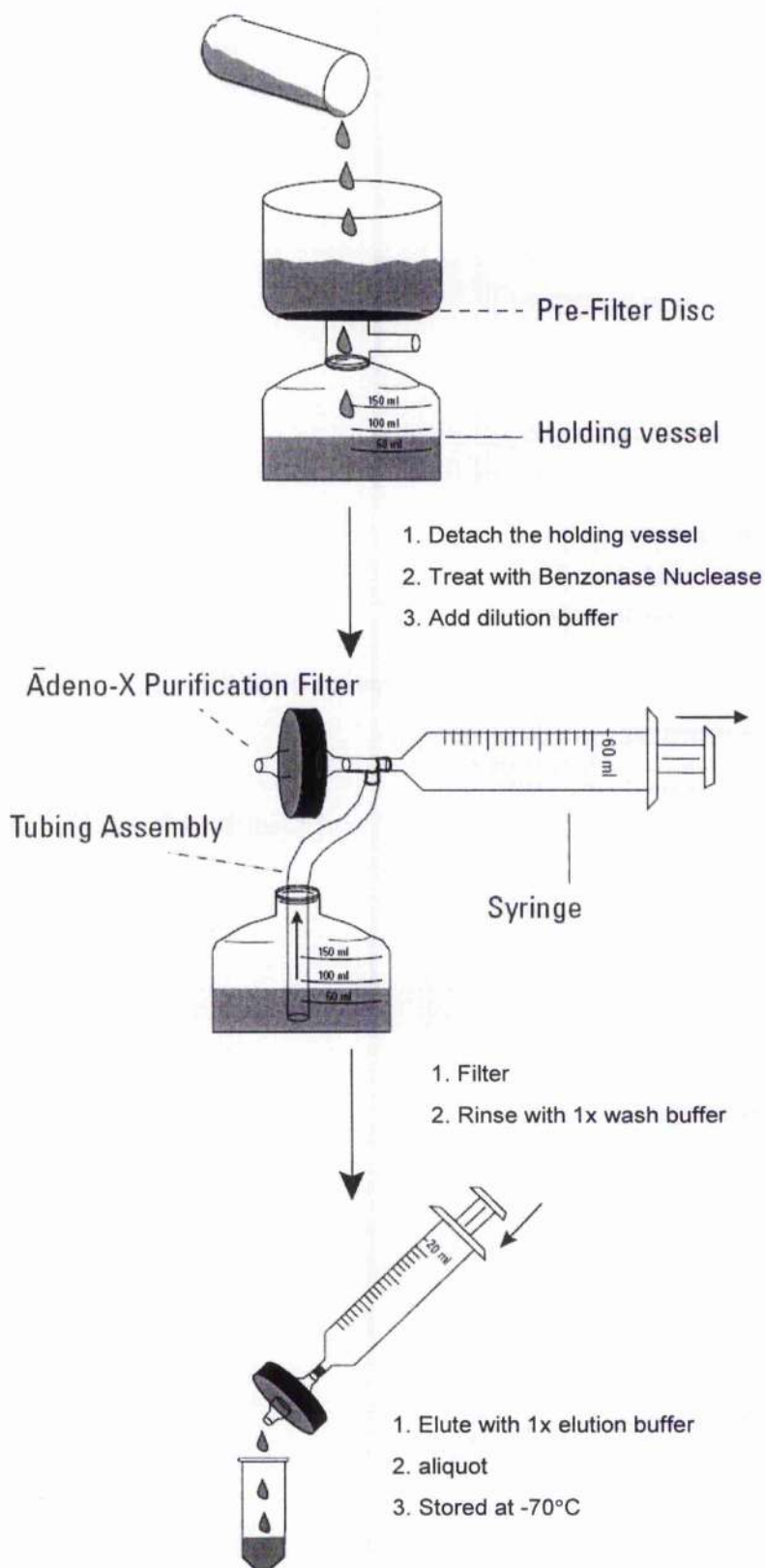


Figure 2.5. Overview of the BD-Adeno-X virus purification protocol. (Diagram modified from BD-Adeno-X Virus Purification User Manual, BD Bioscience)

2.6.5. Cell cytotoxicity assay

Cells cytotoxicity assay was performed with the Cell Titer-Blue kit (Promega), which uses the indicator dye resazurin to measure the metabolic capacity of cells as an indicator of cell viability. Viable cells retained the ability to reduce resazurin into resorufin, which is highly fluorescent. Non-viable cells do not reduce the indicator dye, and thus do not generate a fluorescent signal. Fifteen thousand C2C12 cells were plated into each well of a 96 well plate. For time course studies, infections with genes of interest were used at a multiplicity of infection (MOI) of 5. Cells were infected in PM for 3 days (3I), followed by 3 days in DM (3I 3D), or by 6 days in DM (3I 6D), or 10 days in DM (3I 10D). Stably transfected cells were grown in PM for 3 days (PM), followed by 3 days in DM (DM 3D), or 6 days in DM (DM 6D), or 10 days in DM (DM 10D). At the above selected time points, cells were incubated in 20 μ l of CellTiter-Blue Reagent at 37°C for 2 hours. The plate was then examined under fluorescence at 560 nm excitation and 590 nm emission wave lengths. The dye solution was removed and the wells were washed 3X with PBS. Cell lysate were harvested from the wells using the protocol described in Section 2.6.10. Fluorescence results were normalised to unit weight of protein (mg/ml).

2.6.6. Cell proliferation assays

Proliferation assays were performed in stably transfected C2C12 cells by quantifying cell number with a Neubauer haemocytometer. The haemocytometer is a thick glass slide with a ruled area etched on it, and the ruled square 3 mm by 3 mm. This square is further divided into nine squares, each 1 mm by 1 mm. The space between the top of the platform and the coverglass is 0.1 mm (Fig. 2.6). When the haemocytometer is

loaded properly, the volume of cell suspension that will occupy one primary square is 0.1 mm^3 ($1.0 \text{ mm}^2 \times 0.1 \text{ mm}$) or $1.0 \times 10^{-4} \text{ ml}$. All outside edges of the nine large squares of the haemocytometer are bounded by triple lines.

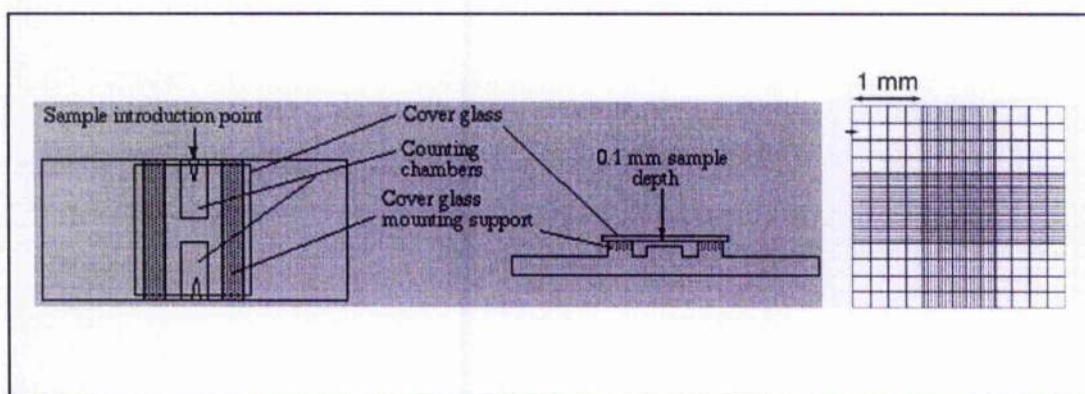


Figure 2.6. Neubauer haemocytometer. It contains nine squares, each 1 mm by 1 mm, and the space between the top of the platform and the cover-slip is 0.1 mm.

Thirty thousand cells were plated on each 25 cm^2 flask (three flasks each for individual DNA construct). The C2C12 cells were allowed to grow up to 5 days. The cells were trypsinized and spun down at $1200 \times g$ for 5 min. Cells were resuspended in 1 ml of fresh PM. Fifty μl of the resuspended cells were added to 50 μl of Trypan Blue, and mixed well. The cover-slip was gently placed on top of the haemocytometer and 15 μl of the mixture was carefully pipetted into each side of the haemocytometer.

With the X200 magnification of the microscope, all the cells that were located within the upper left corner of the primary square were counted, and counting was repeated for the other three corners. The same procedure was used to count the cells on the other side of the haemocytometer. Eight readings were obtained from the counting.

The cell concentration in the original suspension (in cells/ml) was determined by the formula:

$$\text{Cells/ml} = \text{total count} \times 1000 \times \text{dilution factor}$$

A dilution factor of two was used as 50 μ l of the resuspended cells had been mixed with an equal volume of Trypan Blue. The results were statistically analysed as detailed in Section 2.9.

2.6.7. Fusion index assay

Fusion index is defined as the number of nuclei within myotubes in a given field divided by the total number of nuclei in the same field. It was performed to determine whether different constructs in transfected cells conferred differences in fibre fusion. Thirty thousand C2C12 cells stably transfected with different DNA constructs were plated on 24 well plates in PM for 3 days, followed by DM for a further 9 days. During differentiation, DM was replaced every other day.

After 9 days in DM, cells were fixed in 50% methanol/50% acetone (Fisher Scientific, UK) for 15 min. The cells was washed 3X with PBS and permeabilized by PBS containing 0.25% Triton for 20 min. After washing, the cells were incubated for 1 hour in blocking buffer (0.1% Triton/5% sheep serum in PBS). Next, cells were incubated with a primary antibody [anti-desmin 1:200, (Dako), anti-MyHC slow or anti-MyHC fast 1:200, (Sigma)] at 4°C overnight. The next day, the cells were washed three times in PBS, and stained with a secondary FITC conjugated sheep anti-

mouse antibody at 1:200 dilution (Sigma). After washing, it was mounted using Vectashield[®] hard set mounting medium with DAPI (Vector). The stained cells were examined under an inverted fluorescence microscope (Leitz, Labovet). Images were captured by a CCD camera (C4742, Hamamatsu). Fusion rates were analysed using Adobe[®] photoshop software (Adobe[®]). Five fields were randomly chosen for counting captured at X200 magnification (Fig. 2.7). Three independent experiments were conducted. The collected data was statistically analysed as detailed in Section 2.9.

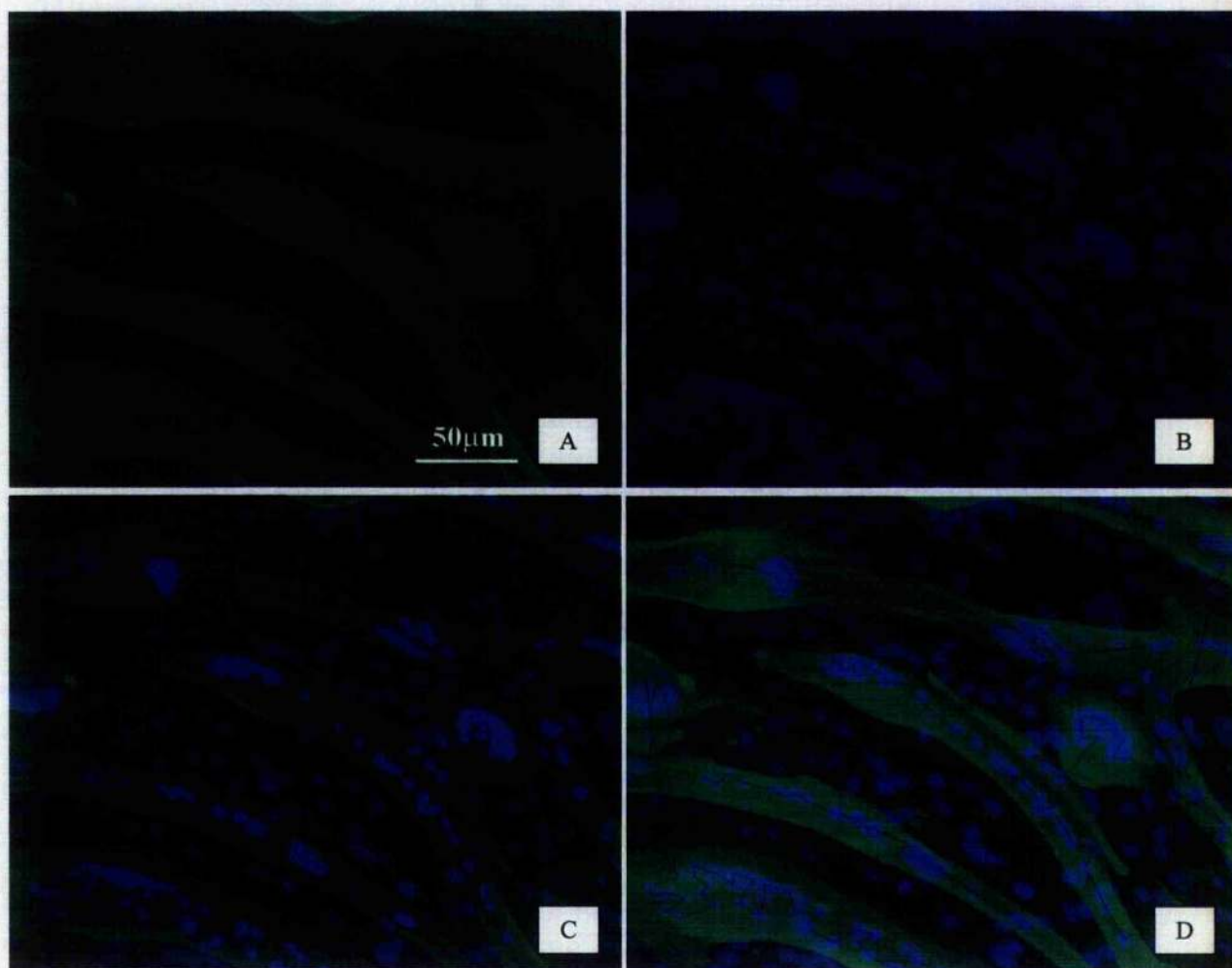


Figure 2.7. Fusion index determination. Stably transfected C2C12 myotubes (differentiated for 9 days) were immunostained for (A) desmin, along with (B) DAPI nuclei staining, captured under X200 magnification. (C) Overlaid image A and image B. (D) The number of nuclei within myotubes as well as the overall total number of nuclei were determined (fusion index). With the aid of Adobe® photoshop software, line dot was plotted on every nucleus within the myotubes.

2.6.8. BrdU assay

BrdU, also known as 5-bromo-2-deoxyuridine, is a common chemical used in the detection of proliferating cells. It works by substituting for thymidine during DNA replication (being a base analog of thymidine) and incorporating itself into the newly synthesized DNA. Antibodies specific for BrdU (linked to a fluorescent molecule) are used to detect the incorporated chemical. In this study, BrdU assay was used to measure the proliferation rate of recombinant adenovirus infected cells and stably transfected cells.

Fifteen thousand C2C12 cells were plated into each well of a 24 well plate. Cells were infected the following day with concentrated adenovirus. At day 3 of infection, cells were exposed to BrdU (40 µg/ml) for 2 hour prior to fixation. Five hundred µl of 100% pre-chilled methanol were added into each well for 10 min to fix and permeabilise cells. After a brief washing step with PBS, cells were fixed by 500 µl 0.2% paraformaldehyde for 1 min. The washing step was repeated, and cells were incubated with 500 µl 0.07 M NaOH for 10 min. This denatured the DNA to allow the antibody to access the BrdU molecules that had been incorporated into the replicating DNA. The washing step was repeated, cells were blocked with 5% sheep serum in 0.1% Triton X for 1 hour. Next, 200 µl anti-BrdU antibody at 1:300 (Sigma) in blocking buffer were incubated into the cells at 4°C overnight. The following day, the wells were rinsed, and secondary antibody (Texas Red conjugated goat anti-mouse IgG from Southern Biotech at 1:200) were applied for 1 hour. It was mounted using Vectashield® hard set mounting medium with DAPI (Vector). Images were captured by a CCD camera mounted on an inverted fluorescence microscope (Leitz, Labovert).

Images were analysed with Adobe® photoshop software. For each construct, 5 random fields were chosen under magnification X200. BrdU assay, was quantified as number of BrdU positive stained nuclei in a given field divided by the total number of nuclei (DAPI stained) in the same field. For each construct, three independent experiments were conducted. The data was statistically analysed as detailed in Section 2.9.

2.6.9. Immunofluorescence

Thirty thousand C2C12 cells, infected with the gene of interest or GFP control adenovirus, were grown for 3 days in PM, followed by 8 days in DM on each well of a 12 well plate. The procedures were similar to other immunofluorescence protocols (Section 2.6.8), the major differences being that the cells were fixed in 4% paraformaldehyde instead of methanol, and NP40 was used to permeabilise cells instead of Triton X.

Cells were incubated in blocking buffer [5% goat serum (BioWest, France) in PBS] for 1 hour. Subsequently, the cells were incubated with primary anti-FLAG M2 monoclonal antibody at 1: 2000 dilution (Sigma), overnight at 4°C. Next day, they were washed three times in PBS. A goat anti-mouse-TRITC (Tetramethyl Rhodamine Iso-Thiocyanate) at 1:200 dilution (Southern Biotech) was used as the secondary antibody in a 45 minute incubation at 37°C. The washing steps were repeated. Next, it was mounted using Vectashield® hard set mounting medium with DAPI (Vector). Images were captured by a CCD camera mounted on an inverted fluorescence microscope (Leitz, Labovet).

2.6.10. Protein extraction

Cells were grown at 37°C until they reached the required confluence level or differentiation state. First of all, cells were rinsed twice with PBS. Then, RIPA buffer (0.6 ml) (Santa Cruz Biotechnology) containing 6 µl of phenylmethylsulfonyl fluoride (PMSF), 6 µl of sodium orthovanadate and 6 µl of protease inhibitor were added into a 100 mm cell culture dish. The cells were incubated for 15 min at 4°C. After incubation, cells were scraped off with a cell scraper. The scrape lysate was transferred to a microcentrifuge tube. The dish was washed with a further 0.3 ml RIPA buffer to remove any remaining adherent cells. The solution was combined with the first lysate and, together incubated on ice for 30 min. The cells were spun at $10,000 \times g$ for 10 min at 4°C. The supernatant was transferred to a sterile microcentrifuge tube and stored at -20°C.

2.6.11. Determination of protein concentration

Spectrophotometry (DU-65 spectrophotometer, Beckman) at OD₅₆₂ was used to determine protein concentration. The BCA[™] protein Assay kit (Pierce) was used. It is a detergent-compatible formulation based on bicinchoninic acid (BCA) for the colorimetric detection and quantitation of total protein. The supplier's procedure is summarised below. A set of diluted albumin protein standards (0.05 mg/ml, 0.1 mg/ml, 0.2 mg/ml, 0.4 mg/ml, 0.6 mg/ml) was prepared. Fifty parts of reagent A with

1 part reagent B (50:1, Reagent A:B) were mixed together. For convenience, 20 ml of reagent A and 400 μ l of reagent B were prepared in bulk.

Each protein sample was diluted 1:10 in millipore-pure water to a total volume of 50 μ l. Fifty μ l of each standard and protein samples were loaded into microcentrifuge tubes. One ml of the mixture (reagent A and B) was added into each tube, and incubated at 37°C for 30 min. Next, each sample was transferred to an optical cuvette. Its optical density was determined at 562 nm. A standard curve was plotted with the albumin protein standards, and then used to determine the protein concentration of the sample.

2.7. Quantitative Real-Time RT-PCR

Quantitative real-time reverse-transcription polymerase chain reaction (real-time RT-PCR), was used to measure an accumulating PCR product in real time by using an internal fluorogenic TaqMan oligonucleotide probe that was activated by the endogenous 5'→3' nuclease activity of Taq polymerase (Freeman et al., 1999). Real-time RT-PCR is a combination of two separated techniques. The first technique involved is reverse transcription, the conversion of mRNA to cDNA. The second technique is the actual real-time PCR. The probes used in this study were based on TaqMan, or fluorogenic 5' nuclease, chemistry (Roche). In this method, the probe was labelled with a 5' fluorochrome and 3' quencher. As the DNA polymerase encountered the annealed probe, its 5' nuclease activity cleaved it and separated fluorochrome from quencher. This resulted in an increase in fluorescence that serves

as an indicator of the PCR reaction progress. The reaction was characterised by the point at which the level of fluorescence, and hence the PCR amplification, crossed a set threshold. The higher the target's copy number, the sooner this threshold would be reached. The samples were quantified relative to an endogenous control, typically a house-keeping gene. In this project work, β -actin was selected as the house-keeping for normalisation.

2.7.1. Total RNA extraction

2.7.1.1. Extraction of total RNA from cells

The RNeasy[®] Mini kit (Qiagen) was used to extract total RNA from cultured cells. The manufacturer's protocol was used, re-stated briefly as follows. Ten μ l of 14.3 M β -mercaptoethanol (PhioBio, UK) were added to 1 ml of Buffer RLT. Buffer RLT was added to disrupt the cells, approximately 600 μ l of Buffer RLT was used for each cell pellet containing 5×10^6 to 1×10^7 numbers. With a rotor-stator homogenizer (Ultra-Turrax[®] T8, IKA), each samples was homogenised for 30 s. Next, 600 μ l of 70% ethanol was added to the homogenized lysate and mixed well. The mixture was added to an RNeasy mini column placed in a 2 ml collection tube, and centrifuged for 15 s at $8,000 \times g$. The flow-through was discarded, 700 μ l Buffer RW1 were added and centrifuged for 15 s at $8,000 \times g$. The RNeasy column was transferred to a new 2 ml collection tube and 500 μ l Buffer RPE were added into the RNeasy column. The tube was closed gently, and centrifuged for 15 s at $8,000 \times g$. Another 500 μ l Buffer RPE were added, and centrifuged at $8,000 \times g$ for 2 min to dry the RNeasy silica-gel membrane. The tube was spun again at $10,000 \times g$ for 1 min. Next, the column was

transferred to a clean 1.5 ml collection tube, and 40 µl of double-distilled water were added directly onto the silica-gel membrane. The column was spun for the last time at $8,000 \times g$ for 1 min. The column was discarded and the total RNA was stored at -20°C .

2.7.1.2. Extraction of total RNA from splayleg skeletal muscles

Promptly after the piglets were put down by captive bolt, the selected skeletal tissues were dissected out. These tissue samples were placed in cryotubes and immediately snap-frozen in liquid nitrogen.

RNeasy[®] Mini kit (Qiagen) was used to extract total RNA from splayleg piglets. The supplier's protocol was used, summarised as follows. Tissues were removed from liquid nitrogen storage and kept on dry ice. Thirty mg of tissue were ground using a mortar and pestle, pre-chilled with liquid nitrogen. The muscle fragments were collected into a microcentrifuge tube with a fine spatula, and 300 µl of Buffer RLT with β -mercaptoethanol (PhioBio, UK) were added to the tube. With a rotor-stator homogenizer (Ultra-Turrax[®] T8, IKA), the samples were homogenised for 30 s. Next, 590 µl of double-distilled water were added to the homogenate, followed by 10 µl of 20 mg/ml Proteinase K solution (cat. N^o.19131, QIAGEN). The mixture was incubated at 55°C for 10 min. After incubation, the tube was spun at $10,000 \times g$ for 3 min. The supernatant was pipetted into a new tube, and 450 µl of 100% ethanol were added to the cleared lysate. The mixture was added to an RNeasy mini column placed in a 2 ml collection tube, and centrifuged for 15 s at $8,000 \times g$. Three hundred and fifty µl Buffer RW1 were added to the RNeasy column and centrifuged for 15 s at

8,000 × g. DNase I mixture (70 µl of Buffer RDD with 10 µl DNase I stock solution) (Qiagen) were added directly onto the RNeasy silica-gel membrane, and incubated for 15 min. Next, another 350 µl Buffer RW1 were added into the column, and centrifuged for 15 s at 8,000 × g. The remaining RNA extraction steps are identical to those described in the previous Section 2.7.1.1.

2.7.2. Total RNA quality and quantity determination

RNA 6000 Nano Labchip[®] kit (Agilent Technologies) was used to measure the quality and quantity of the total RNA extracted. The manufacturer's protocol is summarised below. RNA 6000 Nano gel matrix was filtered in advance before use. One µl of dye was added to 65 µl aliquot of filtered gel, vortexed and spun down at 10,000 × g for 10 min. At the same time, the chip priming station was set up (Fig 2.8). A RNA Nano chip was placed on the station, and 9.0 µl of the gel-dye mix were pipetted into the well marked "G". The plunger on the station was set at 1 ml. The station was closed and the plunger was pressed until held in place by the syringe clip. The plunger was released after 30 s and pulled back to the 1 ml position after 5 s. After the station was open, 9.0 µl of gel-dye mix were added to further two wells marked with "G"s. For all other wells on the chip, 5.0 µl of RNA 6000 Nano marker were added. Samples and the RNA 6000 ladder were preheated for 2 min at 70°C to minimise secondary structure. One µl of each sample was loaded into each of the 12 sample wells. Another 1 µl of ladder was loaded into the well marked with a ladder. Subsequently, the chip was vortexed for 1 min in an adapter vortex mixer (MS2-S8,

IKA) at 2400 rpm. The chip with samples was read in an Agilent 2100 bioanalyser (Agilent Technologies).

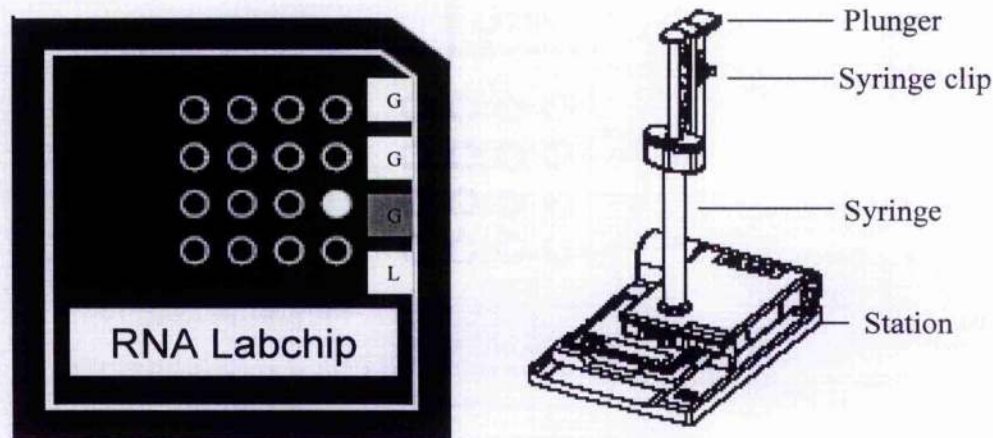


Figure 2.8. A RNA 6000 Nano labchips and a chip priming station with plunger. The well marked "G" is highlighted.

2.7.3. Reverse transcription

The Reverse Transcription System kit (Promega) was used to synthesise cDNA from total RNA template. The supplier's procedure is summarised below. The extracted total RNA was incubated at 70°C for 10 min in a water bath. The following reagents were prepared for a 1 µg of RNA sample: 4µl of 25 mM MgCl₂, 2 µl of 10 X reaction buffer (100 mM Tris-HCl, pH 9.0, 500 mM KCl, 1% Triton[®] X-100), 2 µl of 10 mM dNTP mixture, 0.5 µl of recombinant RNasin[®] ribonuclease inhibitor, 15 u/µl or 0.63 µl of AMV reverse transcriptase and 0.5 µg or 1 µl of random primer. One µg of total RNA and double-distilled water were added to make up to a final volume of 20 µl in each tube.

The mixture was incubated for 10 min at room temperature to allow primer extension. Then, the tube was transferred to a water bath for an hour at 42°C. Subsequently, the tube was placed at 99°C for 5 min in a heating block to inactivate the reverse transcriptase. Samples were stored at -20°C until needed. All the cDNA samples were diluted 100 fold in advance of real-time RT-PCR experiments.

2.7.4. Real-time PCR primer and probe design

Probe and primer sequences were designed using the Primer Express v 2.0 software (Applied Biosystems). Typically the probe and primer sequences were between 20 to 30 deoxynucleotide residues in length, with a base composition of 50-60% guanine (G) or cytosine (C) where possible and the repeats of long nucleotides were avoided. The annealing temperature (T_m) was typically around 70°C for probes and 60°C for primers. Probes designed were based on TaqMan chemistry (fluorogenic 5' nuclease chemistry, Roche).

2.7.5. Taqman reaction conditions

Reactions were set up in 96 well optical plates (Applied Biosystems), with the following reaction mixture in each sample well: 1 x Universal Master Mix (AmpliTaq Gold DNA polymerase, dNTP mix and $MgCl_2$, Applied Biosystems), 100 fold diluted cDNA template with the appropriate concentration of primers and probe, that made up to 25 μ l per well. Triplicate analysis of each target gene was performed on the 96

well optical plates. The ABI PRISM[®] 7700 sequence Detection System with software version 1.6 (Applied Biosystems) was used to quantify the cDNA samples. The real-time RT-PCR cycles were as below. The template was firstly denatured for 2 min at 50°C, followed by a 10 min denature step at 95°C, 15 s at 95°C annealing steps and 1 min at 60°C extension steps. The processes were repeated for 39 cycles.

2.7.6. Real-time PCR data analysis

The data obtained from ABI PRISM[®] 7700 sequencer was normalised against the endogenous reference, β -actin, to account for variation between cDNA samples, caused by differences in the efficiency of the total RNA extraction, in reverse transcription or in sample loading.

For each sample, an amplification plot was generated. An increase in the reporter dye fluorescence with each PCR cycle was displayed. From it, a threshold cycle (C_T) value was calculated, which was the PCR cycle number at which fluorescence was detected above threshold, based on the variability of baseline data in the first 15 cycles. Each C_T value was determined from the mean of three separate real-time PCR reactions. The relative standard curve for each gene was plotted as C_T (y-axis) vs log [cDNA diluted 10-fold sequentially] (x-axis). The slope (m) of the standard curve describes the efficiency of PCR, and is defined by the equation

$$C_T = m (\log Q) + C$$

Where C_T is the threshold cycle, Q is the initial amount, and c is the intercept on the y-axis. When PCR amplification is maximally efficient and resulting in a doubling of product in every cycle, the slope will be -3.3 (Medhurst et al., 2000). For example, the relative standard curve for porcine *SPARCL-1* cDNA was plotted based on a series of 10 fold dilution (Fig. 2.9). The slope is -3.255 and the Y-intercept is 14.19.

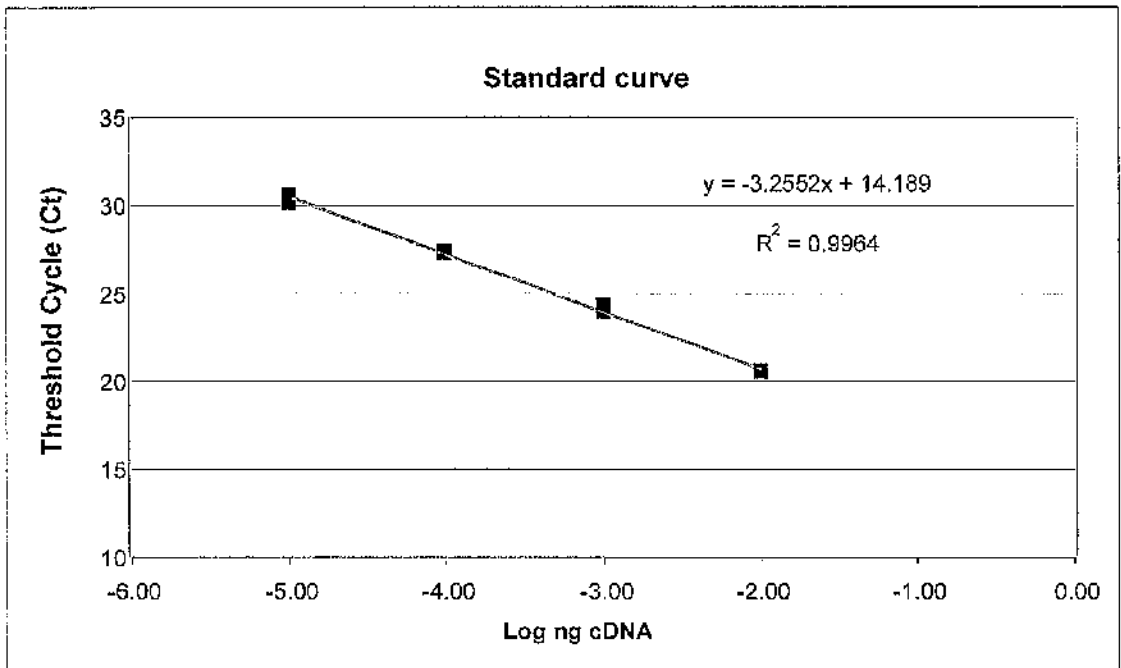


Figure 2.9. Standard curve for real-time RT-PCR.

2.8. Western blot analysis

Western blot is an electro-blotting method in which proteins are transferred from a gel to a membrane and detected by binding of labelled antibody. It can be divided into 5 steps: sample preparation, gel electrophoresis, nitrocellulose transfer, antibody binding, visualising results.

2.8.1. Preparation of protein samples

Two hundred and forty μ l of 3x sample buffer [0.1875 M Tris-HCl, pH 6.8, 6% sodium dodecyl-sulphate (SDS) (USB Corp, Ohio), 30% glycerol, 0.03% bromophenol blue] were added to 30 μ l 1M dithiothreitol (DTT) (Invitrogen) (in 0.5 ml tube) and vortexed thoroughly to mix, to prepare a SB/DTT master mix. Appropriate volumes of water and protein were added to a 1.5 ml microcentrifuge tube, followed by 6 μ l SB/DTT, to make up a final volume of 18 μ l. The samples were vortexed and spun briefly at $6,000 \times g$ for 8 s, incubated at 90°C for 4 min, and stored at -20°C until needed.

2.8.2. Protein electrophoresis

Sodium dodecyl sulphate-polyacrylamide gel electrophoresis (SDS-PAGE) was used to separate denatured proteins according to their molecular weight (Laemmli, 1970). Model mini-V8-10 Vertical Gel electrophoresis System (Life TechnologyTM) was used (Fig. 2.10). The gel plates, comb and spacer were assembled, and a distance of 1 cm below base of comb was marked. The following reagents were used for a 10% resolving gel: 0.1 ml of 10% ammonium persulphate (APS) (Sigma), 4 ml millipore-pure water, 2.5 ml Resolving Buffer (1.5 M Tris-HCl, pH 8.8), 3.3 ml acrylamide (Sigma) [29% (w/v) acrylamide, 1% (w/v) bisacrylamide in millipore-pure water], 0.1 ml of 10% SDS and 0.01 ml of tetramethyl-1-, 2-diaminomethane (TEMED) (Aldrich). The solution was gently syringed between the glass plates to a level just above that marked, the plates was tapped on bench to release any trapped air bubbles.

The resolving gel was overlaid with approximately 0.5 ml of 0.1% SDS, to ensure a smooth, flat, bubble free surface. The 0.1 % SDS was washed with millipore-pure water, and the loading comb placed between the glass plates. The stacking gel mix of 2.5 ml Stacking Buffer (0.5 M Tris-HCl, pH 6.8), 1.3 ml acrylamide [29% (w/v) acrylamide, 1% (w/v) bisacrylamide in millipore-pure water], 0.1 ml of 10% APS, 0.1 ml of 10% SDS, 0.01 ml TEMED and 6 ml millipore-pure water, was applied over the resolving gel, and left for 20 min to polymerise. The comb was removed and the wells were flushed with Running Buffer (0.25 M Tris Base, 1.92 M glycine, 1% SDS).

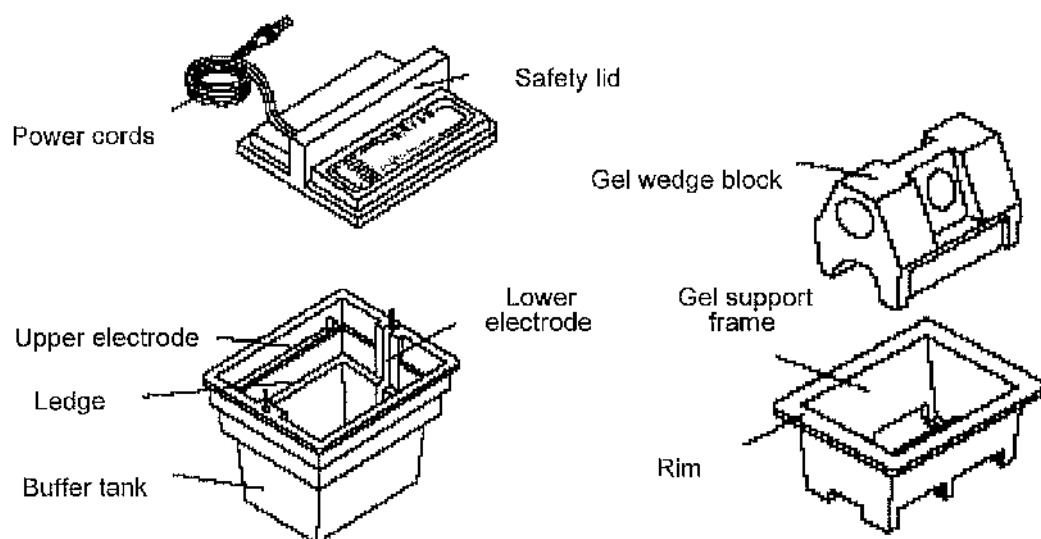


Figure 2.10. Gel Electrophoresis system. A mini-V8-10 Vertical model, which contains buffer tank, gel support frame, gel wedge block and safety lid. Two long and short glass plates with gel holder are not illustrated here.

Six hundred ml running buffer were poured into the running tank, polymerised gel was removed from its blue moulds and place in the running tank. Samples prepared by the method described in the previous Section 2.8.1 were warmed at 55°C to ensure that the SDS went into solution before being loaded into the gel. A colour protein

ladder marker (SeeBlue® Plus2 Pre-Stained standard, Invitrogen) was loaded along with the protein samples. Gels were run at 200 volts for approximately 1 hour or until the dye front reached the bottom of the glass plate.

2.8.3. Transfer onto PVDF membranes

At this stage, the protein in the gel was transferred onto a membrane made of polyvinylidene difluoride (PVDF). The membrane binds proteins non-specifically. Binding is based on hydrophobic interactions as well as charges between the membrane and protein. One sheet of filter paper (3MM, Whatman®) was soaked in anode buffer I [0.3 M Tris pH 10.4, 10% (v/v) methanol], two in anode buffer II [25 mM Tris, pH 10.4, 10% (v/v) methanol] and three in cathode buffer [25 mM Tris pH 10.4, 40 mM glycine, 10% (v/v) methanol]. PVDF membrane was rehydrated in methanol for 10 seconds, followed by water for 5 min, and then in Anode Buffer II until required. After gel electrophoresis, the gel was immersed in cathode buffer for 5 min. Three sheets of filter paper (one from anode buffer I and two from anode buffer II) were placed on the base of the transfer unit. Next, the PVDF was placed on top, followed by the gel onto the membrane. Three sets of cathode buffer pre-soaked filter papers were placed on top of the gel (Fig. 2.11). When the transfer unit was assembled, it was run at a constant current of 1.3 mA/cm² for 1 hour. After one hour, the power supply was switched off, and with the PVDF membrane still in place, a pencil was used to label the membrane. To assess the transferred proteins, the membrane was immersed in Ponceau S [0.5 g Ponceau S (Sigma), 25 ml acetic acid] for 1 min and washed with millipore-pure water. After visual assessment, the

membrane was washed with TBS/S [0.5 M Tris pH 7.4, 1.5 M NaCl, 0.1% tween (Invitrogen)] before antibody binding.

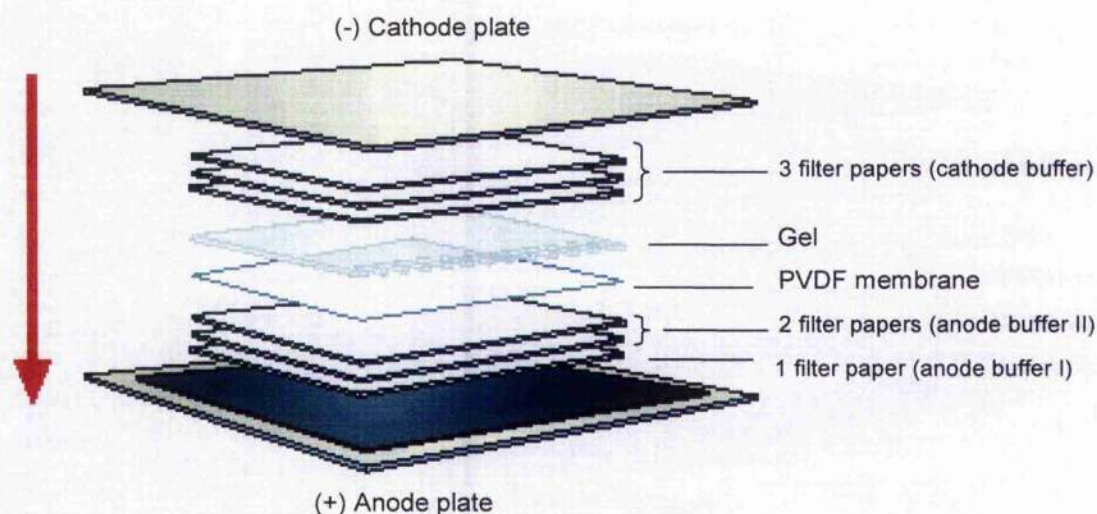


Figure 2.11. The complete transfer unit assembled. The gel and PVDF were sandwiched with three filter papers on either side. The current path from cathode to anode transferred the protein from the gel to the PVDF membrane.

2.8.4. Antibody binding

After transfer, the PVDF membrane was incubated in blocking buffer [5% skimmed milk (Marvel) in TBS/T] for 45 min on a rocker. Next, the membrane was incubated overnight with primary antibody in blocking buffer at 4°C. The membrane was washed three times in TBS/T, 30 min each. Subsequently, peroxidase conjugated secondary antibody (anti-mouse IgG, Dako) 1:5000 was applied to the blocking buffer and left to incubate for 1 hour. The washing step was repeated as before.

2.8.5. Use of ECL reporting

The presence of conjugated secondary antibody was detected by enhanced chemiluminescence (ECL Amersham, GE Healthcare). A secondary antibody conjugated with horseradish peroxidase (HRP), catalysed the oxidation of luminol by hydrogen peroxide in a light-emitting manner. Chemiluminescence was increased by a chemical enhancer, to the point where it was detectable by autoradiography through blue-light sensitive film. Its use was as described in the manufacturer's protocol. One ml each of ECL solutions A and B was mixed in a small, shallow dish. PVDF membrane was coated evenly in the mixture for one min, dried with filter paper and wrapped in cling film. The membrane was transferred into an X-ray cassette. A range of exposure time (seconds to min) was used. Finally, the film was processed in an X-ray processor (Compact X4, Xograph imaging system), and protein molecular weights were marked on the film.

2.9. Statistical analyses

SAS software (SAS Mixed Procedure, SAS Institute) was used to analyse most of the data.

Mean fibre size data were analyzed by mixed model variance analysis (SAS Mixed Procedure, SAS Institute) using muscle types (ST, LD, G), disease status (normal, splayleg) as fixed effects, experiments and replicates as random effects. The standard error of the difference between sample means was calculated using the error mean

square from the ANOVA. Differences between pair-wise combinations of the least square means were tested for significance ($P<0.05$).

Fibre density data were analyzed by mixed model variance analysis (SAS Mixed Procedure, SAS Institute) using muscle types (ST, LD, G), disease status (normal, splayleg) as fixed effects, experiments and replicates as random effects. The standard error of the difference between sample means was calculated using the error mean square from the ANOVA. Differences between pair-wise combinations of the least square means were tested for significance ($P<0.05$).

Percentage of slow and fast data were analyzed by mixed model variance analysis (SAS Mixed Procedure, SAS Institute) using muscle types (ST, LD, G), disease status (normal, splayleg) as fixed effects, experiments and replicates as random effects. The standard error of the difference between sample means was calculated using the error mean square from the ANOVA. Differences between pair-wise combinations of the least square means were tested for significance ($P<0.05$).

Proliferation assay data were analyzed by mixed model variance analysis (SAS Mixed Procedure, SAS Institute) using treatments (*SPARCL-1*, *P311*, *vector*) and experiments as fixed effects. In contrast, flasks (3 flasks from each treatment) and replicates (4 counts from each flask) were used as random effects. As the data were not normally distributed, log₁₀ transformation was used. The standard error of the difference between sample means was calculated using the error mean square from the ANOVA. Differences between pair-wise combinations of the least square means were tested for significance ($P<0.05$).

BrDU assay results were analyzed by mixed model variance analysis (SAS Mixed Procedure, SAS Institute) using treatments (*SPARCL-1*, *P311*, *vector*) and experiments as fixed effects. In contrast, wells (2 well from each treatment), replicates (4 counts from each well) were used as random effects. The standard error of the difference between sample means was calculated using the error mean square from the ANOVA. Differences between pair-wise combinations of the least square means were tested for significance ($P<0.05$).

Fusion index assay data were analyzed by mixed model variance analysis (SAS Mixed Procedure, SAS Institute) using treatments (*SPARCL-1*, *P311*, *vector*), immuno-stainings (desmin, MyHC fast, MyHC slow) as fixed effects and experiments as a random effect. The standard error of the difference between sample means was calculated using the error mean square from the ANOVA. Differences between pair-wise combinations of the least square means were tested for significance ($P<0.05$).

Real time PCR data for PCS muscle were analyzed by mixed model variance analysis (SAS Mixed Procedure, SAS Institute) using muscle types (ST, LD, G), disease status (normal, splayleg) as fixed effects, litters and replicates as random effects. The standard error of the difference between sample means was calculated using the error mean square from the ANOVA. Differences between pair-wise combinations of the least square means were tested for significance ($P<0.05$).

Unless specifically stated, quantitative real-time RT-PCR data for gene over-expression studies were expressed as mean \pm standard deviation from triplicate samples within the same experiment.

Chapter 3

Cellular and molecular characterisation of PCS

3.1. Introduction

Porcine congenital splayleg (PCS) is a clinical condition of newborn piglets, characterised by muscle weakness, resulting in the inability to properly stand and walk, with affected limbs extended sideways or forwards (Thurley et al., 1967). It is arguably the most important congenital defect of commercial piglets and causes significant economic loss to pig farmers (Partlow et al., 1993). The prevalence of PCS can range from less than 1% in most farms to over 8% in some establishments (Ward and Bradley, 1980).

A range of pathological lesions has been described for PCS, the most common feature being the presence of myofibrillar hypoplasia, often interpreted as an immaturity of the muscle (Thurley et al., 1967; Ducatelle et al., 1986). However, myofibrillar hypoplasia is not exclusive to PCS as the condition is also found in clinically normal piglets. The descriptive finding of myofibrillar hypoplasia is therefore not diagnostic of PCS (Ducatelle et al., 1986). In this study, the condition of myofibre hypoplasia (reduced numbers of myofibres) in PCS was examined. In general, hypoplasia refers to underdevelopment of an organ because of a decrease in numbers. If the description is correct, there would be fewer fibres in affected piglets compared with normal piglets. To date, no such quantitative measurements have been performed to verify the described term. It is possible that clinical splayleg is due to a reduction of fibre size (atrophy), number (hypoplasia) or both.

With recent advances in imaging technology and quantitative PCR, morphological analysis and relative muscle gene expression can now be conducted with greater precision. The aim of this Chapter is to investigate the cellular and molecular

pathology of PCS, which included the results obtained by immunohistochemistry, histochemistry and the relative muscle gene expression levels of PCS.

3.2. Materials and methods

3.2.1. Immunohistochemical and histochemical staining

The procedures of muscle selection, immunohistochemical and histochemical staining followed by image analysis were previously described in the Materials and Methods Chapter (Section 2.2).

3.2.2. Total muscle fibre number measurement in PCS

Selected *semitendinosus* (ST), *longissimus dorsi* (LD) and *gastrocnemius* (G) muscles were removed from four 2-day-old splayleg male piglets, along with 4 corresponding normal litter mates. Besides the determination of mean fibre size and fibre density as described in Section 2.2., attempts were made to measure the total muscle fibre number of each muscle.

To obtain such measurements, images were captured under an image capturing light microscope (Carl Zeiss Ltd) at a magnification of X12.5. Firstly, the total cross-sectional area of the muscle was measured and analysed using KS300 image software (Carl Zeiss Ltd), as described in Figure. 3.1. Secondly, several random fields were selected for measurements as described in Section 2.2.3. The number of fibres counted represented at least 3-5% of the total number present. Then, estimations of

total muscle fibre number were calculated, based on the following mathematical equation:

$$\text{Total muscle fibre number} = \frac{\text{fibre number in selected field} \times \text{total cross-sectional area}}{\text{area of selected field}}$$

3.2.3. Quantitative real-time RT-PCR

Total RNA was isolated from porcine muscles as described in the Section 2.7.1.2. Two µg of total RNA were used for each cDNA conversion. Four sets of cDNA samples from PCS and normal piglets were prepared (litters 1 to litters 4). For pre-natal muscles, LD was pooled from 3 Pietrain-based pig foetuses from gestation stage of 35, 49, 63, 77 and 91 days (da Costa et al., 2003). Additionally, pooled whole 14-day embryos and 21-day embryos derived from the same uterine horn were used (da Costa et al., 2003). The pre-natal and embryo samples were used to assess the developmental expression of *MAFbx* and *P311*.

TaqMan quantitative real-time RT-PCR (Applied Biosystems) was performed on a number of porcine genes: *MyHC slow*, *MyHC 2a*, *MyHC 2x*, *MyHC 2b*, *Myf5*, *MyHC embryonic*, *MyHC perinatal*, *α-actin*, *β-actin*, *MAFbx*, *P311* and *SPARCL-1*. All the primers and probes sequences are shown in Table 3.1. The design of *MAFbx*, *P311* and *SPARCL-1* primers and probes will be discussed in Chapters 4 and 5. A relative standard curve method, normalised to β-actin as described in Section 2.7.6 was used in the quantification of expression. The primer concentration and the value for the standard curve are shown in Table 3.2.

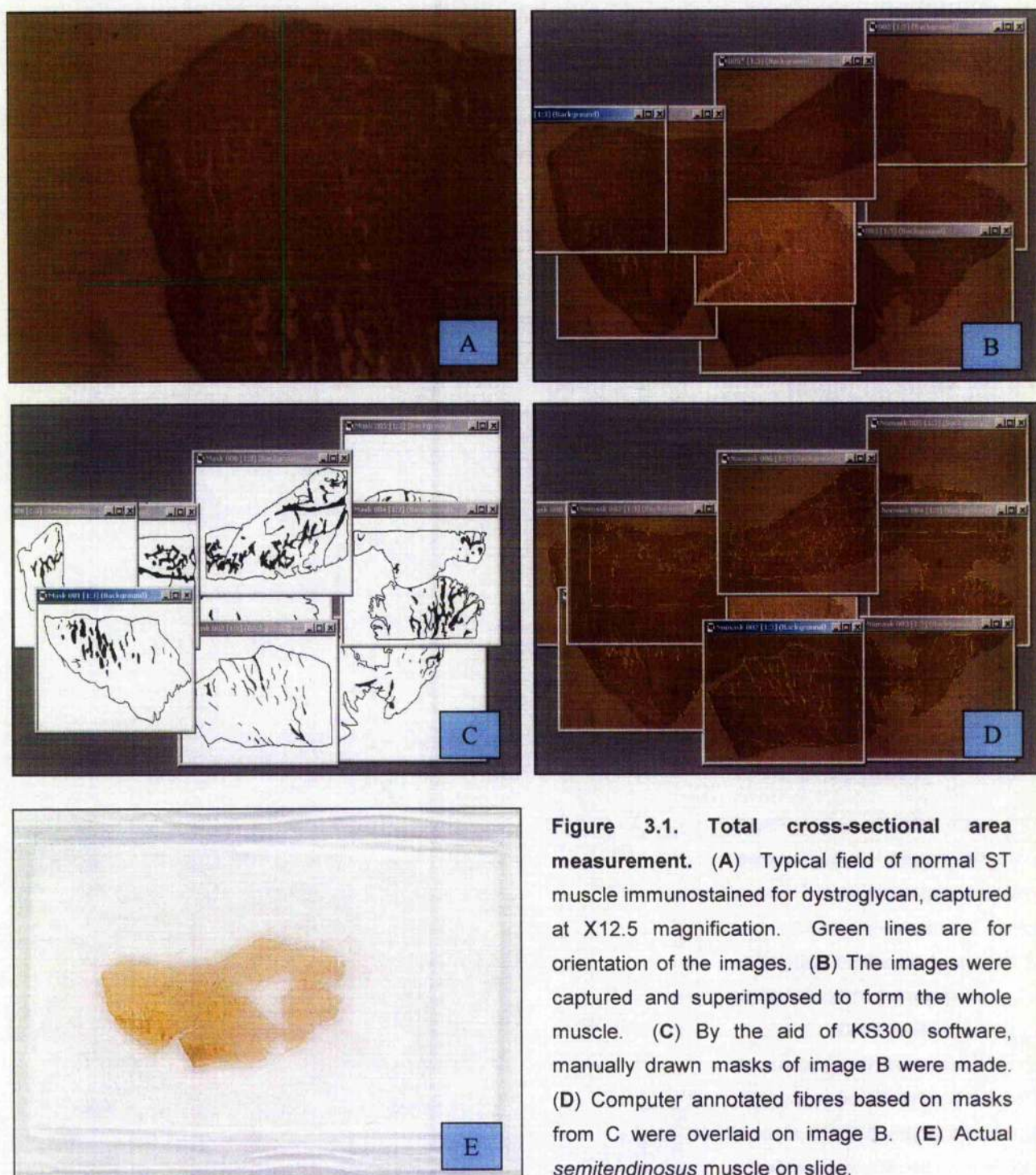


Figure 3.1. Total cross-sectional area measurement. (A) Typical field of normal ST muscle immunostained for dystroglycan, captured at X12.5 magnification. Green lines are for orientation of the images. (B) The images were captured and superimposed to form the whole muscle. (C) By the aid of KS300 software, manually drawn masks of image B were made. (D) Computer annotated fibres based on masks from C were overlaid on image B. (E) Actual *semitendinosus* muscle on slide.

Table 3.1. Sequences of porcine primers and TaqMan probes.

Gene	Primer	Sequence 5'→3'
MyHC slow	S	GGC CCC TTC CAG CTT GA
	A	TGG CTG CGC CTT GGT TT
	P	CCT CTT TCT TCT CCC AGG GAC ATT CGA
MyHC 2a	S	TTA AAA AGC TCC AAG AAC TGT TTC A
	A	CCA TTT CCT GGT CGG AAC TC
	P	TTC CAG GCT GCA TCT TCT CAC TTG CTA AG
MyHC 2x	S	AGC TTC AAG TTC TGC CCC ACT
	A	GGC TGC GGG TTA TTG ATG G
	P	AGC CCA GTC AAA GAC CCT TTG AGA TGC A
MyHC 2b	S	CAC TTT AAG TAG TTG TCT GCC TTG AG
	A	GGC AGC AGG GCA CTA GAT GT
	P	TGC CAC CGT CTT CAT CTG GTA ACA TAA GAG G
MyHC embryonic	S	CCC GGC TTT GGT CTG ATT T
	A	GGT GTC GGC TGA GAG TCA
	P	TGC TGC TGT CTG CTG TCC TCT GCG
MyHC perinatal	S	CGA GCC CTC CTG CTT TAT CTC
	A	TGC CAG ATG AAA ATG CAG GTT
	P	CCA AGA GCC CAG AGT GTT AGG CAC TTC C
skeletal α -actin	S	CCA GCA CCA TGA AGA TCA AGA TC
	A	ACA TCT GCT GGA AGG TGG ACA
	P	CCC CGC CGG AGC GCA AGT
β -actin	S	CTC CTT CCT GGG CAT GGA G
	A	CGC ACT TCA TGA TCG AGT TGA
	P	CCT GCG GCA TCC ACG AGA CCA C
MAFbx	S	AAG CGC TTC CTG GAT GAG AA
	A	GGC CGC AAC ATC ATA GTT CA
	P	AGC GAC CTC AGC AGT TAC TGC AAC AAG G

S, sense; A, antisense; P, TaqMan probe. All probes were 5' labelled with 6-carboxyfluorescein (FAM), and 3' labelled with 6-carboxytetramethylrhodamine (TAMRA).

Table 3.2. Porcine RT-PCR primer concentration and value of standard curve.

Gene	Primer concentration of 5':3'(pmol/ μ l)	Standard curve value
MyHC slow	900:900	T: 0.027
		S: -3.912
		Y: 13.934
MyHC 2a	900:900	T: 0.013
		S: -3.780
		Y: 12.190
MyHC 2x	50:50	T: 0.007
		S: -3.720
		Y: 13.889
MyHC 2b	50:50	T: 0.017
		S: -3.988
		Y: 9.624
MyHC embryonic	900:900	T: 0.012
		S: -3.645
		Y: 14.885
MyHC perinatal	900:900	T: 0.014
		S: -3.410
		Y: 10.311
skeletal α -actin	900:900	T: 0.031
		S: -3.675
		Y: 14.434
β -actin	300:300	T: 0.011
		S: -3.673
		Y: 13.201
MAFbx	900:900	T: 0.011
		S: -3.867
		Y: 14.636

T, threshold; S, slope; Y, y-intercept.

Besides the relative standard curve methods, comparative C_T method was used in *MyHC* composition profile in Section 3.3.4. This method makes use of the arithmetic formula $2^{-\Delta\Delta C_T}$ to quantify a target gene, where $\Delta C_T = C_T$ of the target less C_T of the reference, and where $\Delta\Delta C_T = \Delta C_T$ of the target gene less ΔC_T of the calibrator (ABI Prism 7700 Sequence Detection System User Bulletin #2).

3.3. Results

3.3.1. Muscle fibre atrophy in PCS muscles

Morphological and fibre type analyses were conducted on 4 sets of muscles from 4 separate litters of pigs (3 muscles per pig: ST, LD and G); each set comprised one 2-day-old affected PCS piglet and a normal litter mate. Histological examination of all PCS muscles showed no evidence of apparent inflammatory change. PCS fibres were clearly smaller than those in the normal counterpart. These features were more prominent in ST and LD muscles (Fig. 3.2). Based on results from image analysis, the average fibre cross-sectional area of affected PCS piglets was consistently significantly smaller than their normal counterparts in all 3 muscles (Fig. 3.3). Consequently, fibre density (fibre number per unit area) from affected individuals was higher in the 3 muscles (Fig. 3.3).

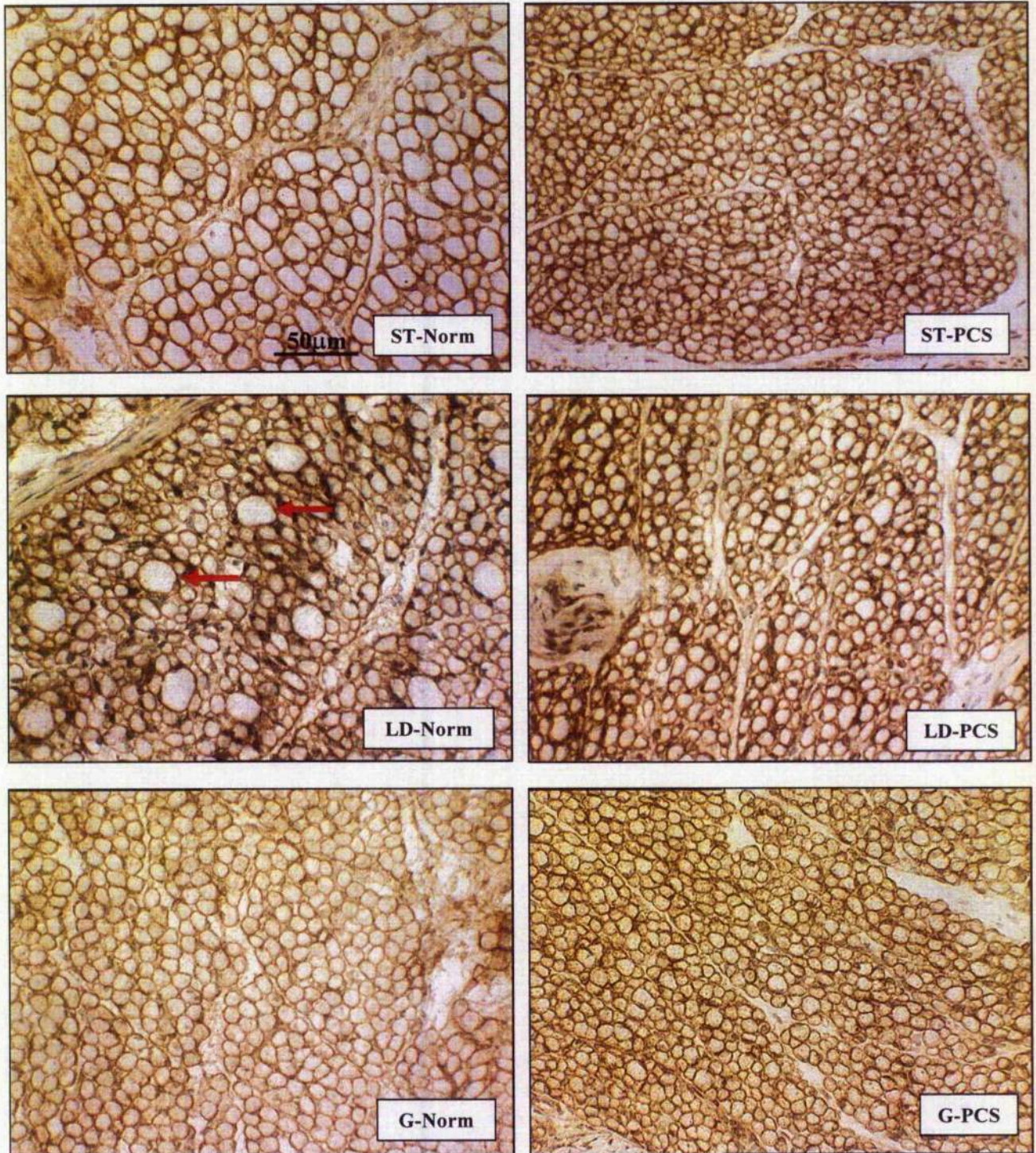


Figure 3.2. Morphological comparisons between muscles of PCS and normal piglets. (A) Typical muscle fields of normal and PCS (ST, LD and G muscles) were immunostained for dystroglycan to outline individual muscle fibres, captured at X200 magnification. PCS fibres were clearly smaller than those in the normal counterpart. Red arrows highlight relatively large slow muscle fibres. ST= *semitendinosus*; LD= *longissimus dorsi*; G= *gastrocnemius*; Norm= normal; PCS= porcine congenital splayleg.

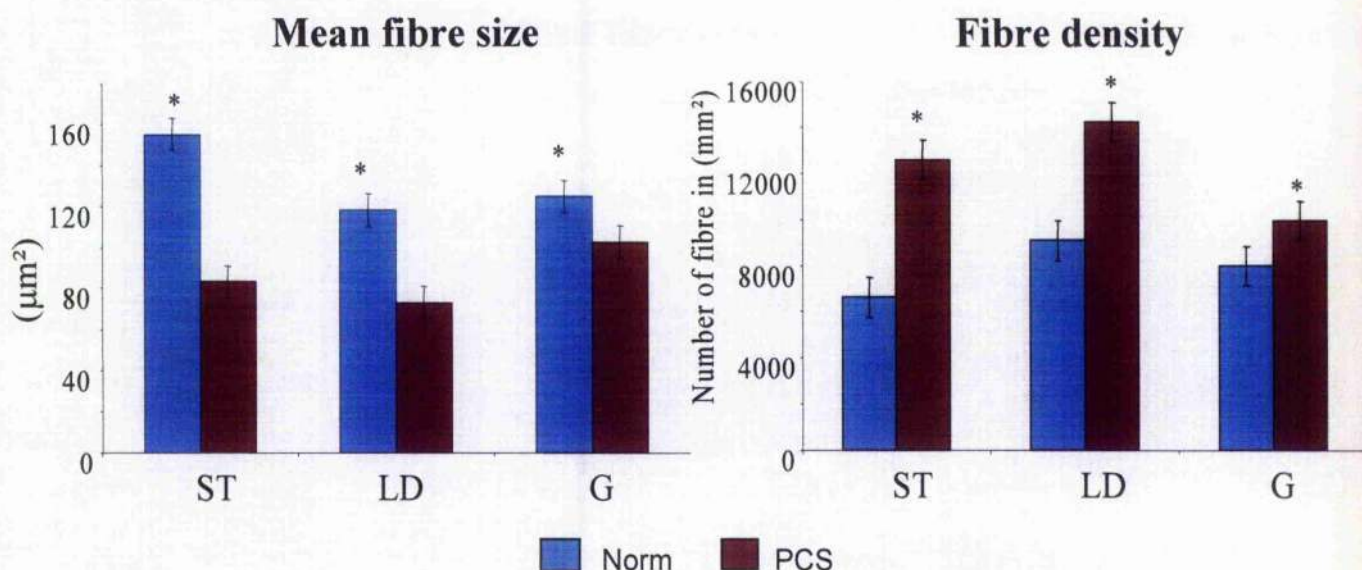


Figure 3.3. Mean fibre size and fibre density of four sets of 2-day-old PCS piglets and corresponding normal litter mates. Fibre cross-sectional area was determined in PCS and normal muscles. PCS piglets showed smaller fibre size and higher fibre density in all three muscles. Differences between pair-wise combinations of the least square means were tested for significance (* $p < 0.05$). Asterisks indicated statistical significance between normal and PCS muscle. The error bars indicate standard error. Norm= normal; PCS= porcine congenital splayleg.

PCS piglets also showed higher distribution of fibre number in the smaller fibre range than normal piglets (Fig. 3.4). The contrast in fibre size distribution was particularly evident in the ST and LD of PCS piglets, which showed a narrow and steep distribution pattern of smaller fibres (Fig. 3.4). In ST muscles, more than 50% of PCS fibres were less than $100 \mu\text{m}^2$, compared with normal fibres where only 35% were less than $100 \mu\text{m}^2$. In LD muscles, more than 50% of PCS fibres were less than $75 \mu\text{m}^2$; compared with normal fibres only about 35% were less than $75 \mu\text{m}^2$. The degree of atrophy may vary between the muscles, with the ST and LD muscles more severely affected than the G muscle. Hence fibre atrophy was a feature of PCS muscles.

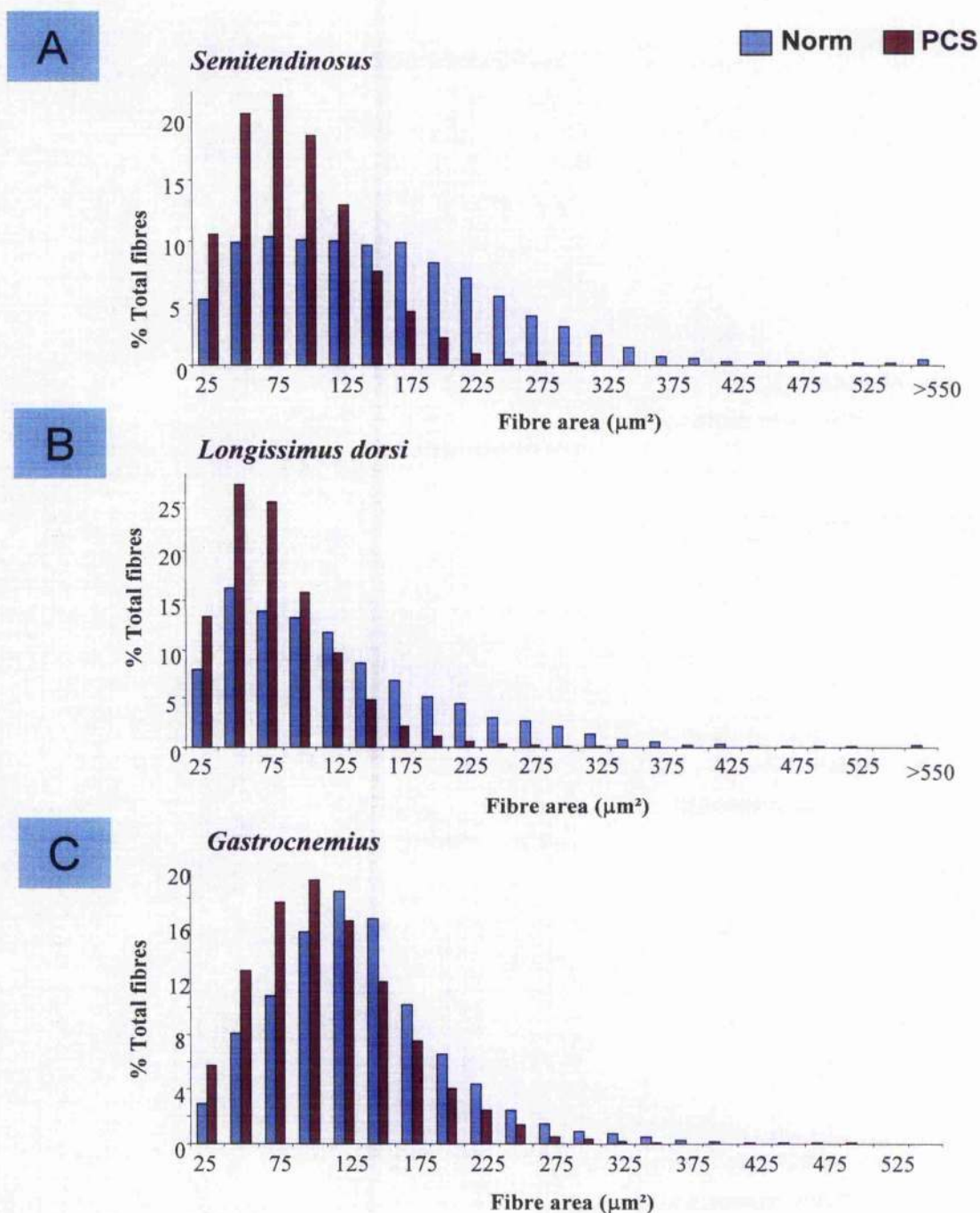


Figure 3.4. Distribution of muscle fibre cross-sectional areas of four sets of 2-day-old PCS piglets and corresponding normal litter mates. At least 10,000 fibres were measured per muscle section and grouped by size in $25 \mu\text{m}^2$ increments. ST and LD muscles of PCS piglets showed a narrow and steep pattern of distribution. G muscles of PCS piglets showed a similar but smaller fibre size distribution than their normal litter mates.

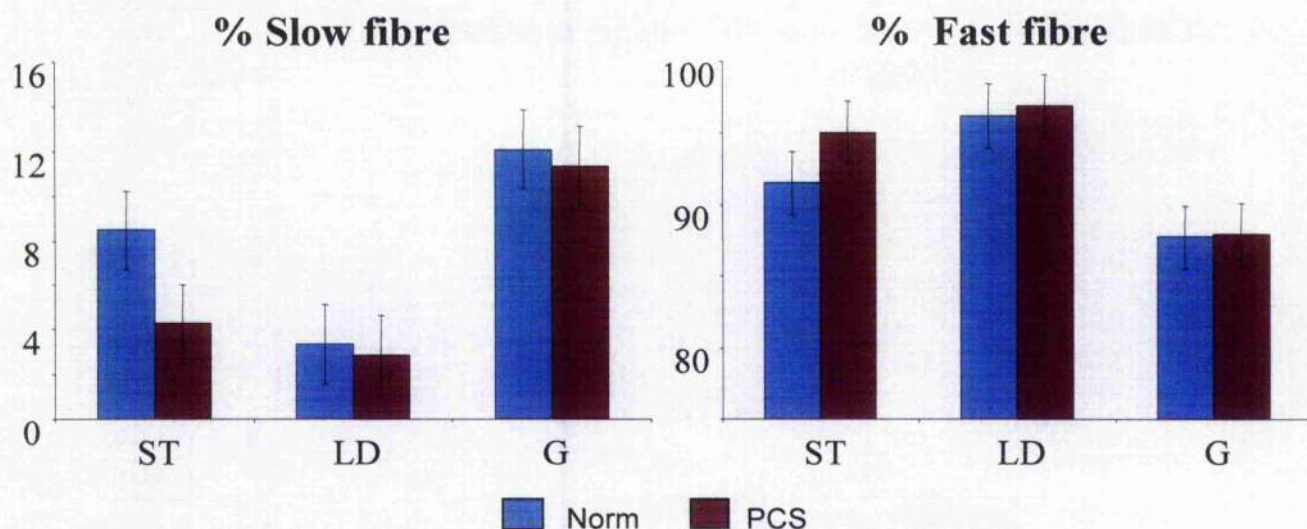


Figure 3.5. Composition of slow and fast fibres of four sets of 2-day-old PCS piglets and corresponding normal litter mates. No significant difference in slow or fast fibre types was found between normal and affected muscles. Differences between pair-wise combinations of the least square means were tested for significance (* $p < 0.05$). Asterisks indicated statistical significance between normal and PCS muscle. The error bars indicate standard error. Norm= normal; PCS= porcine congenital splayleg.

Based on immunostaining for MyHC slow and MyHC fast fibres, no significant difference was found in fibre type composition between normal and affected muscles (Fig. 3.5). Previously, Hanzlikova (1980) has showed higher number of slow muscle fibre in normal muscles compare to PCS muscles. The failure of detection significant differences in fibre type composition may be due to limitation of sample numbers and/or the level of P value tested.

Histochemical staining with Sudan Black B (SBB) and succinate dehydrogenase (SDH) are shown in Figures 3.6 and 3.7. The staining protocols were described in Section 2.2.2. SBB staining was used to detect the presence of lipids and SDH staining is an indicator of oxidative fibre capacity. Attempts were made to analyse the percentage of SBB and SDH positive in PCS affected and normal muscles. Widespread distributions of lipid positive fibres were found in PCS affected and normal muscles. Similarly, both PCS affected and normal muscles showed

widespread distribution of highly oxidative fibres. There was little difference in the distribution of lipid positive and oxidative fibre between PCS affected and normal piglets (Figs. 3.6 and 3.7).

Total muscle fibre number measurement could not be reliably determined, due to technical difficulty in obtaining complete cryostat cross-sections representative of total muscle areas. As such, it is not certain if PCS-associated fibre atrophy is also accompanied by fibre hypoplasia.

3.3.2. Selective reduction of MyHC expression in PCS muscles

Assessment of the phenotypic differences between muscles of normal and PCS piglets by TaqMan quantitative real-time PCR was performed on the muscles from the 4 sets of litter mates to determine the relative mRNA expression levels of *MyHC embryonic*, *MyHC perinatal*, *MyHC slow*, *MyHC 2a*, *MyHC 2x*, *MyHC 2b* and α -actin. No significant difference was found between normal and PCS piglets for *MyHC embryonic*, *MyHC perinatal*, *MyHC 2a* and α -actin (Fig. 3.8). PCS piglets, however, showed significantly lower expression of *MyHC slow* in LD and G muscles (Fig. 3.8). Expression of *MyHC 2x* and *MyHC 2b* in ST muscle was also statistically lower in PCS piglets (Fig. 3.8).

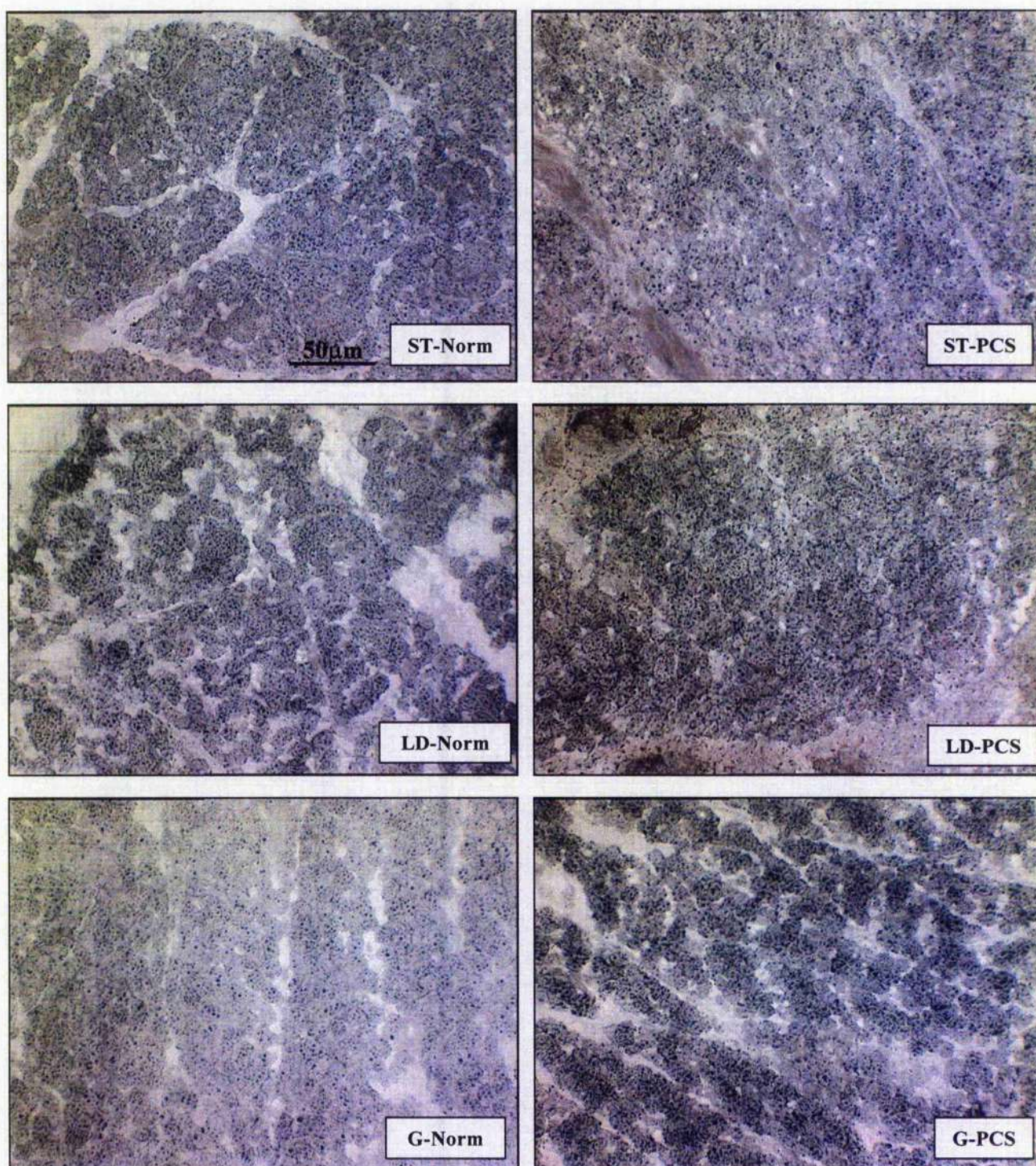


Figure 3.6. Widespread distribution of lipid positive fibres (stained as black pigments). Typical muscle fields of normal and PCS (ST, LD and G muscles) were immunostained for SBB, captured at X200 magnification. Both PCS affected and normal muscles were rich in intra fibre lipids. ST= *semitendinosus*; LD= *longissimus dorsi*; G= *gastrocnemius*; Norm= normal; PCS= porcine congenital splayleg.

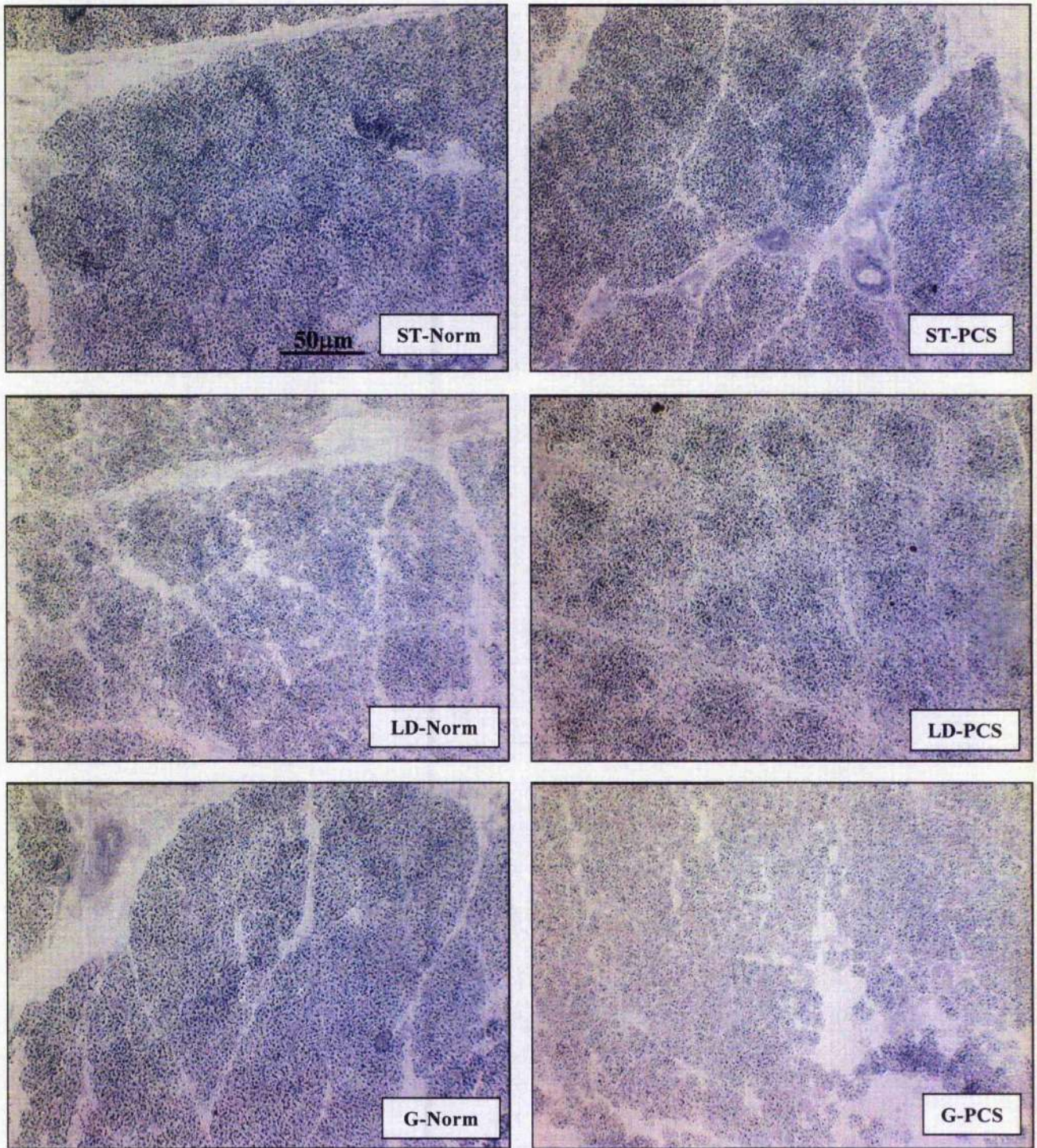


Figure 3.7. Widespread distribution of oxidative fibres (stained as dark purple pigment). (A) Typical muscle fields of normal and PCS (ST, LD and G muscles) were immunostained for SDH, captured at X200 magnification. Both PCS affected and normal muscles were highly oxidative. ST= *semitendinosus*; LD= *longissimus dorsi*; G= *gastrocnemius*; Norm= normal; PCS= porcine congenital splayleg.

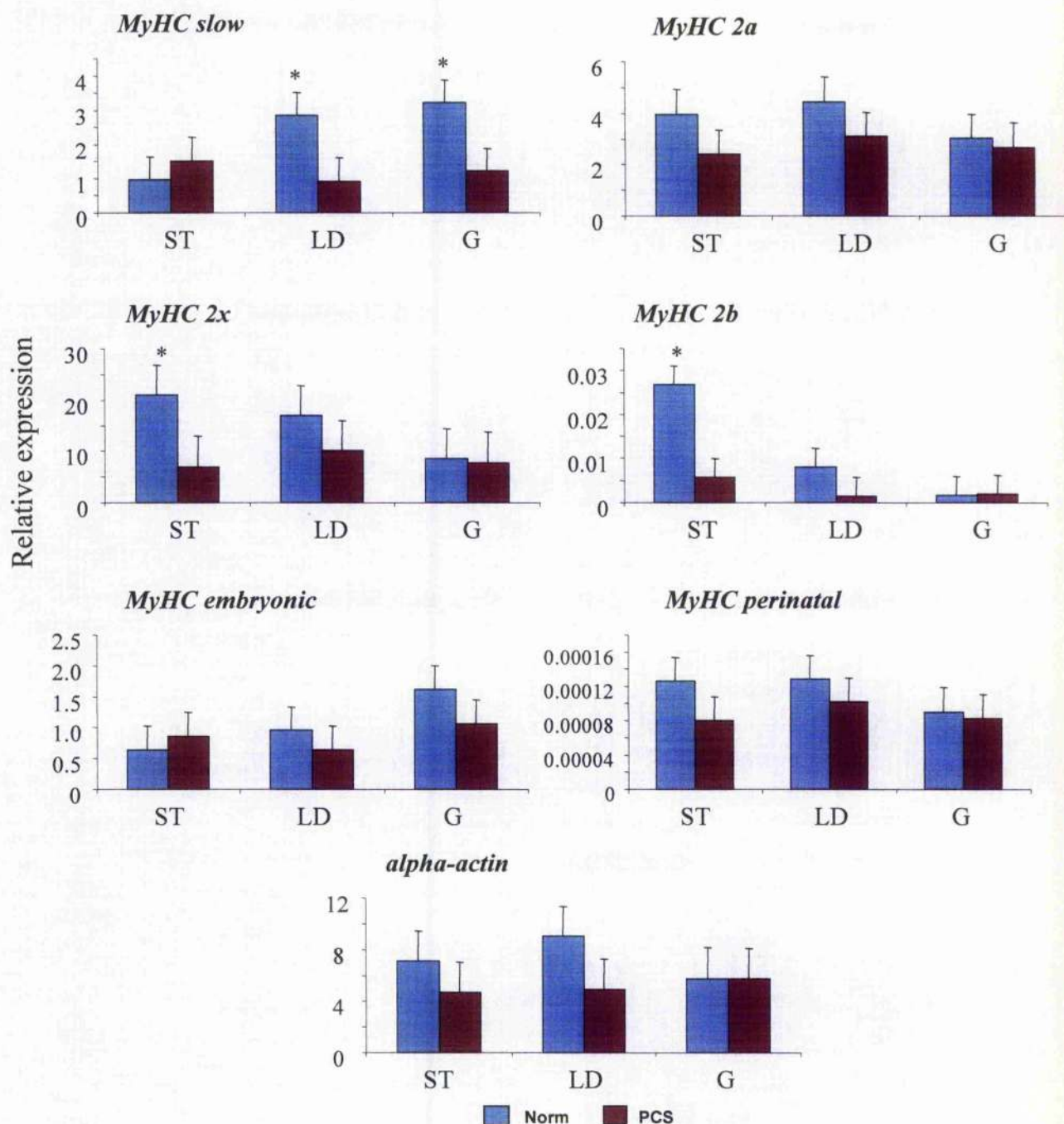


Figure 3.8. Comparison of muscle gene expression between PCS affected and normal muscles. Quantitative expression of *MyHC isoforms* and α -actin in ST, LD and G muscles, presented as combined results of 4 sets of 2-day-old PCS piglets. Differences between pair-wise combinations of the least square means were tested for significance (* $p < 0.05$). PCS piglets showed significantly lower expression of *MyHC slow* in LD and G muscles, and lower expression of *MyHC 2x* and *MyHC 2b* in ST muscles. Asterisks indicate statistical significance between normal and PCS muscles. Error bars indicate standard error. Norm= normal; PCS= porcine congenital splayleg.

3.3.3. Relative expression of MyHC isoforms within muscles

In general, ST, LD and G muscles selected in this study are considered as fast type muscles. More than 85% fibres were fast fibre type based on immunohistochemistry (Fig. 3.5). A comparative Ct method, described in Section 3.2.3, was used to profile the relative expressions within each muscle of the different *MyHC* isoforms. There were no significant differences in the relative expression of *MyHC* isoforms expression between PCS affected and normal muscles (Fig. 3.9). The *MyHC 2x* was the most abundant isoform in all muscles, followed by *MyHC 2a*, *MyHC slow*, *MyHC embryonic* and *MyHC 2b* (Fig. 3.9). The relative abundance of the three fast post-natal *MyHC* isoforms was in the order of $2x > 2a > 2b$.

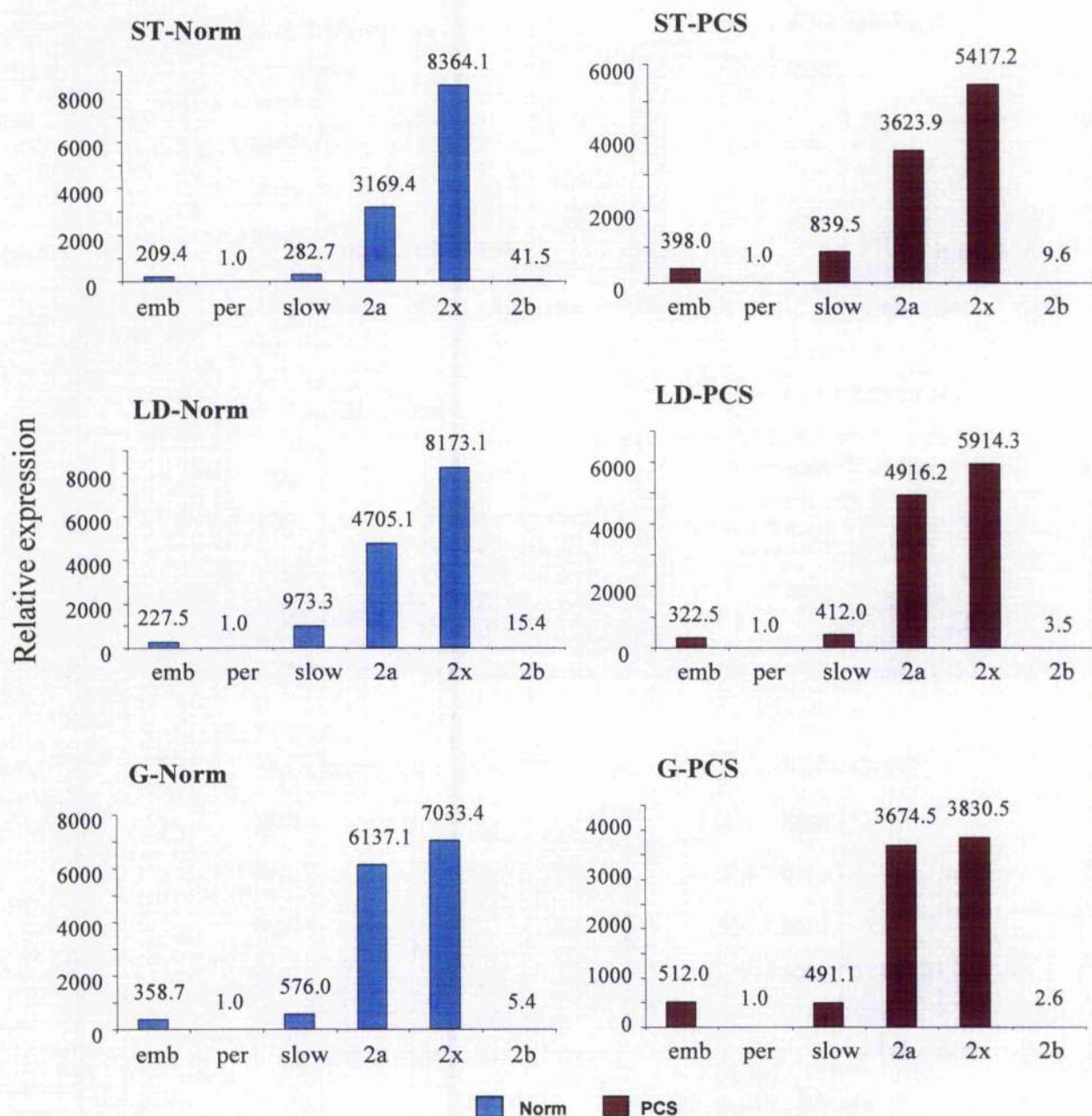


Figure 3.9. Relative mRNA levels of *MyHC* isoforms within PCS affected and normal muscles. There were no significant differences in patterns of *MyHC* isoforms expression within PCS affected and normal muscles. *MyHC* 2x mRNA was most abundant in all muscles, followed by *MyHC* 2a. The relative abundance of the three fast post natal *MyHC* isoforms were in the order of 2x>2a>2b. Expression levels are relative to the lowest expressing isoform within each muscle which is the *MyHC* perinatal. ST= semitendinosus; LD= longissimus dorsi; G= gastrocnemius; emb= embryonic; per= perinatal; Norm= normal; PCS= porcine congenital splayleg.

3.3.4. Up-regulation of *MAFbx* and down-regulation of *P311* in PCS muscles

The ubiquitin-proteasome proteolysis pathway is a principal route of muscle atrophy in which *MAFbx*, an E3 ubiquitin ligase, was found to be consistently up-regulated in a variety of muscle atrophic conditions (Bodine et al., 2001b; Lecker et al., 2004). Because of the close association of *MAFbx* expression with muscle atrophy, the relative expression of porcine *MAFbx* in normal and PCS muscles was determined (Fig. 3.10.A). In almost all muscle samples examined, with the exception of ST muscle in litter 2, *MAFbx* expression was clearly found up-regulated in PCS piglets (Fig. 3.10.A). Another growth-related gene associated with muscle atrophy, *P311*, is a novel gene reported to be down-regulated in a number of muscle atrophic conditions (Lecker et al., 2004) but up-regulated under moderate dietary restriction (da Costa et al., 2004). In contrast to *MAFbx*, *P311* expression in PCS muscles was consistently down-regulated in comparison with normal controls (Fig. 3.10.B). It is worthy to note that the significant differences in *MAFbx* and *P311* expression between normal and affected muscles of litter 2 were not as great as in the other 3 litters, which might be a reflection of differing gradation of the disease process (Fig. 3.10). Moreover, the wide variation in expression levels of *MAFbx* and *P311* between litters, were not entirely surprising. Endogenous gene expression is known to vary widely between individual pigs of the same genetic background and age, reared under identical husbandry conditions (Chang et al., 2003).

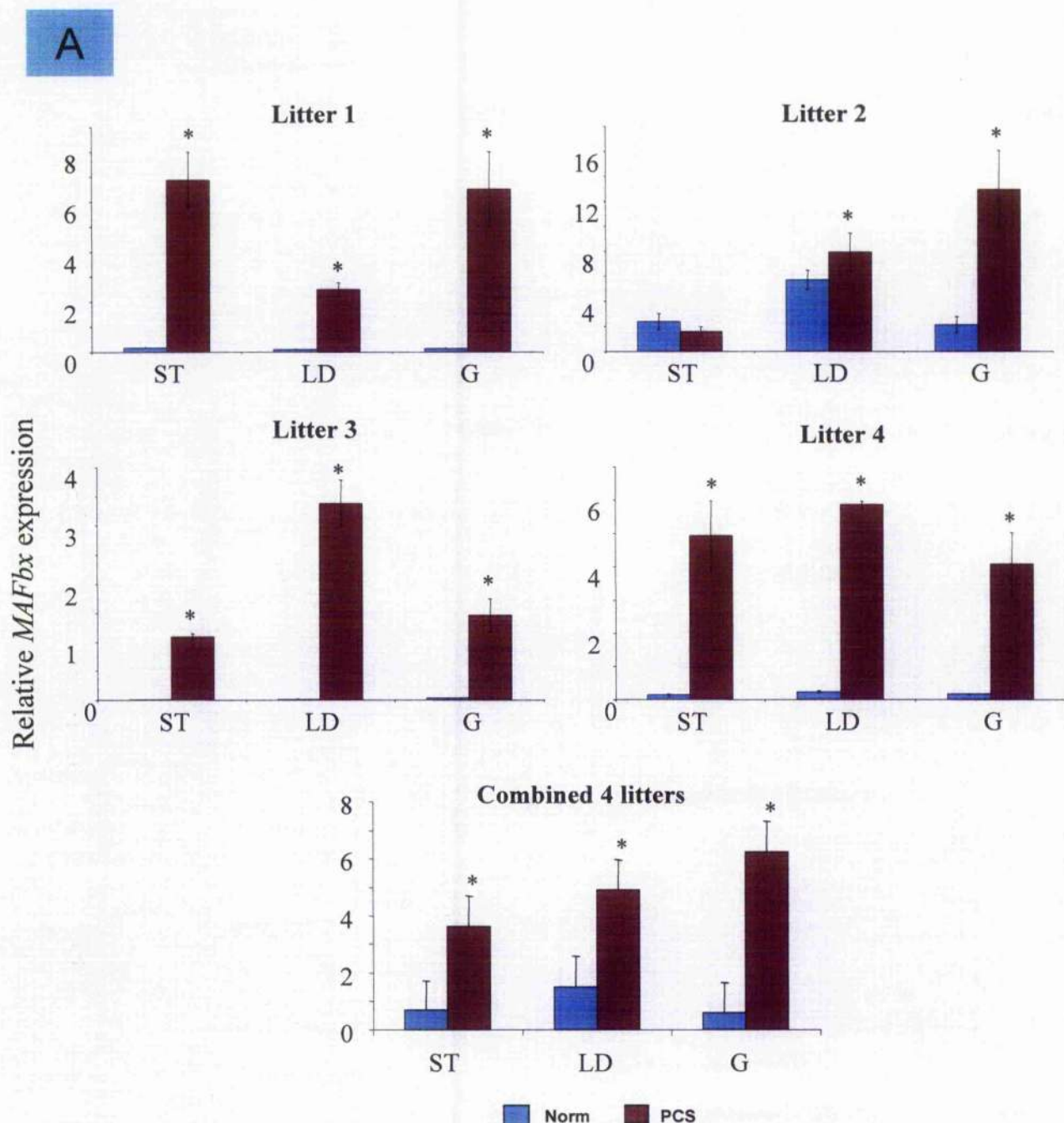


Figure 3.10. (A) Quantitative PCR performed for *MAFbx* expression. With the exception of ST muscles in litter 2, *MAFbx* was more highly expressed in all PCS muscle samples compared with the corresponding normal muscles. Results of each litter are expressed as mean \pm standard deviation from triplicate samples within the same experiment. Combined results of 4 sets of PCS piglets also tested for significance ($*p < 0.05$) in differences between pair-wise combinations of the least square means. Norm=normal; PCS= porcine congenital splayleg.

B

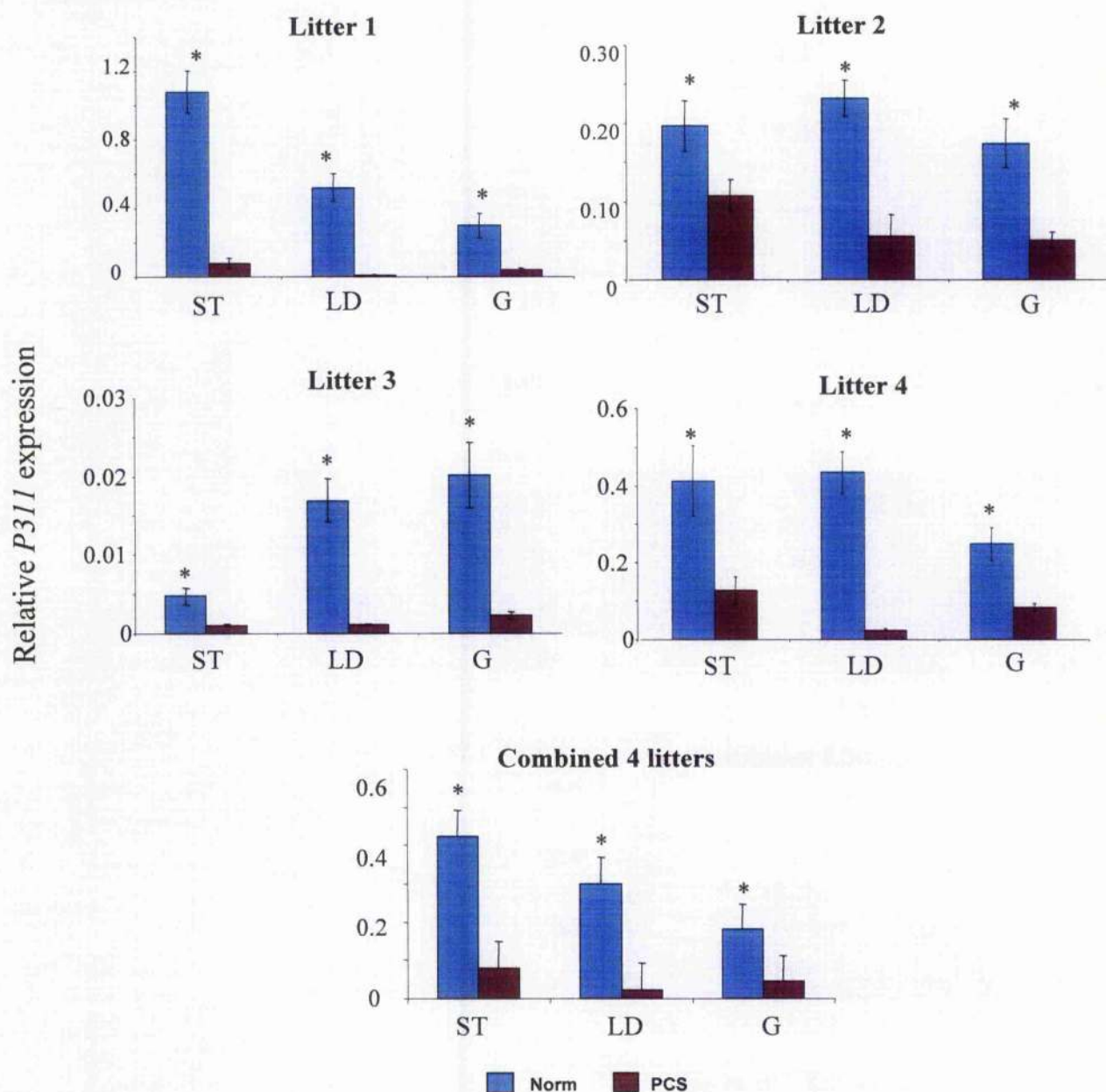
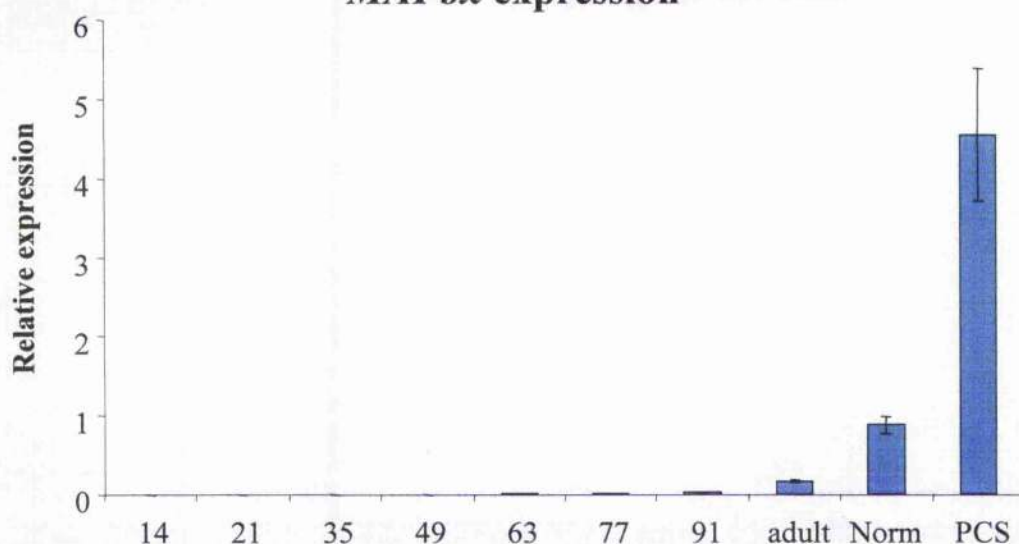


Figure 3.10. (B) Quantitative PCR performed for *P311* expression. In contrast to *MAFbx*, *P311* expression was down-regulated in all PCS muscle samples. Results of each litter are expressed as mean \pm standard deviation from triplicate samples within the same experiment. Combined results of 4 sets of PCS piglets also tested for significance ($*p < 0.05$) in differences between pair-wise combinations of the least square means. Norm= normal; PCS= porcine congenital splayleg.

As little is known about the normal developmental expression pattern of *MAFbx* and *P311*, their embryonic and muscle foetal expression at different stages of gestation, and their expression in adult muscle was examined (Fig. 3.11). Real-time PCR results showed that *MAFbx* expression remained at basal levels throughout gestation and in adult muscle (Fig. 3.11.A). In relation to normal muscles, *MAFbx* expression in PCS LD muscles was significantly elevated (Fig. 3.11.A). Real-time PCR results showed that *P311* expression in normal animals increased with gestation and remained raised in newborn and adult muscles. However, the expression of *P311* in 2-day-old PCS piglets was considerably down-regulated (Fig. 3.11.B).

A

MAFbx expression

B

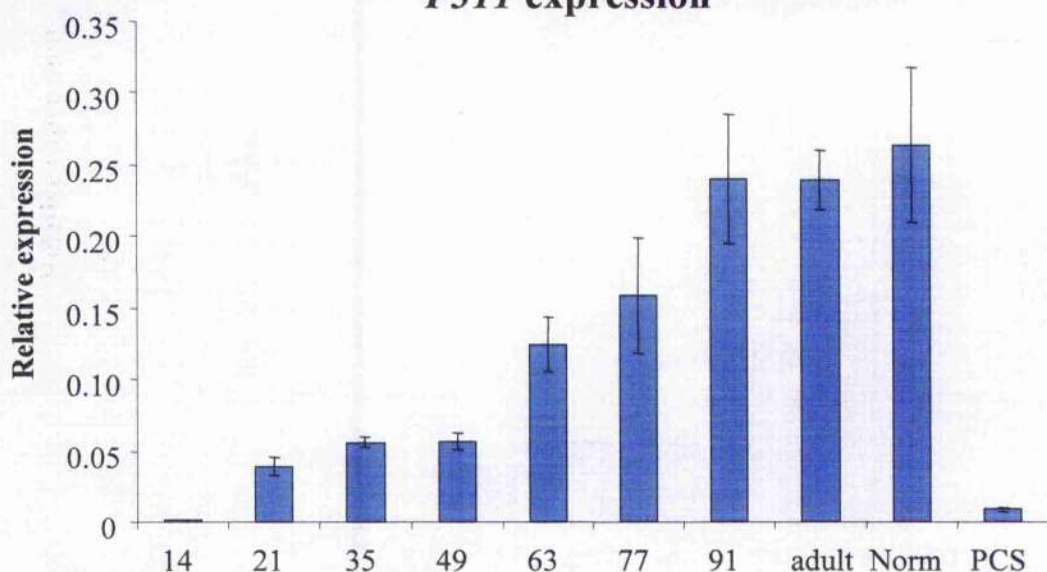
P311 expression

Figure 3.11. Developmental expression of *MAFbx* and *P311*. Expression of (A) *MAFbx* and (B) *P311* at different stages of embryonic/foetal development (14, 21, 35, 49, 63, 77 and 91 days of gestation), in 24-week-old (adult) pigs, in 2-day-old PCS piglets and corresponding normal litter mates (Norm) were determined. Embryonic/foetal and adult cDNAs were pooled samples from 3 individuals. PCS and Norm cDNAs were pooled from the LD muscles of the 4 sets of litter mates. Expression of *MAFbx* was detected at basal levels throughout gestation and into adulthood but was elevated in PCS muscles. *P311* expression showed rising levels throughout development. However, its expression in PCS piglets was much reduced. Results expressed as mean \pm standard deviation from triplicate samples within the same experiment. Norm= normal; PCS= porcine congenital splayleg.

3.4. Discussion

3.4.1. PCS is associated with extensive muscle fibre atrophy

PCS is a well-recognised, commercially important clinical congenital condition of piglets. However, woefully little is known about its aetiology, pathogenesis or pathology. In this study, fibre atrophy with concomitant increase in fibre density was consistently found in PCS muscles (LD, ST and G) (Figs. 3.2 and 3.3). It appears that PCS is an extensive muscle condition that affects several muscle groups. Indeed, previous work has shown that PCS affects different muscles (Thurley et al., 1967; Bradley et al., 1980). ST and LD muscles were more severely affected than the G muscle (Fig. 3.4). PCS associated atrophy was not accompanied by significant changes in fibre type composition (Fig. 3.5), but some affected muscles showed significant reduction in the expression of *MyHC slow*, *MyHC 2x* and *MyHC 2b* genes (Fig. 3.8). Hence PCS is a condition associated with muscle fibre atrophy ostensibly connected to reduced protein accretion, and is associated with reduction in the expression of structural muscle genes. At present, it is unclear if the atrophic fibre change observed in PCS muscles is a primary pathology of the condition or is a secondary outcome of disuse atrophy.

In the present work, due to technical difficulty in obtaining complete cryostat cross-sections representative of total muscle areas, the total muscle fibre number of each muscle could not be reliably determined. At present, it is not certain if PCS-associated fibre atrophy is also accompanied by fibre hypoplasia. For future work, to overcome this technical difficulty, accurate determination of the mid-belly circumference of each muscle is essential (Wigmore and Stickland, 1983; Rehfeldt et

al., 2001). The standard protocol for total muscle fibre number measurement is summarised as follows (Wigmore and Stickland, 1983; Stickland and Handel, 1986; Dwyer et al., 1994). Firstly, the total cross-sectional muscle area was determined from circumference measurement. Secondly, mean number of fibres per unit area was measured using a Seescan image analysis system. Finally, total muscle fibre number was estimated by the mean number of fibres per unit area and total cross-sectional area. Up to 3-5% of the total muscle fibre number in randomly selected areas was counted.

Owing to the manner in which PCS piglets were sourced, the weight of every animal in a litter was not obtained. Although body weight measurement was not taken, all PCS piglets appeared smaller in size compared with its normal counterparts. It had been shown that the smallest littermates developed fewer muscle fibres in their muscle compared with the largest littermate (Wigmore and Stickland, 1983; Stickland and Handel, 1986). PCS piglets through immobility could fail to gain sufficient nutrient from the sow, resulting in starvation and hypothermia. Post-mortem on PCS affected piglets revealed empty stomachs. In this study, the body weight differences observed in the 2-day-old PCS piglets might be the result of starvation. Equally, PCS associated with muscle fibre atrophy could contribute to the reduced body weight and immobility. Although only fibre atrophy has been demonstrated in this study, PCS could be caused by atrophy and hypoplasia. It has been suggested that muscle fibre number is an important determinant of postnatal growth such that pig littermates with a high fibre number tend to grow faster and more efficiently than littermate with a lower fibre number (Dwyer et al., 1993).

3.4.2. Widespread distribution of lipid and oxidative fibres in PCS muscles

SBB and SDH staining showed widespread distribution of lipid and oxidative positive fibres in PCS affected and normal muscles. The pattern of distribution was similar between PCS affected and normal muscles (Figs. 3.6 and 3.7). Relative expression of *MyHC* isoforms within muscles showed that *MyHC 2x* and *MyHC 2a* were the two most abundant isoforms in all muscles (Fig. 3.9). Both *MyHC 2a* and *MyHC 2x* are characterised as fast oxidative-glycolytic fibres, which are highly oxidative with corresponding lipid content.

3.4.3. PCS is associated with muscle wasting

MAFbx, an E3 ubiquitin ligase enzyme, was identified as an early marker of atrophy through differential expression screening studies in multiple models of skeletal muscle atrophy (Lecker et al., 2004; Bodine et al., 2001b). E3 ubiquitin ligase is one of three enzymatic components of the ubiquitin-proteasome pathway (Hershko and Ciechanover, 1998), a major protein degradation route known to be responsible for skeletal muscle atrophy (Mitch and Goldberg, 1996). High levels of *MAFbx* mRNA in all 4 atrophic PCS piglets from 4 litters were demonstrated (presented as individual and combined litters) (Fig. 3.10.A), in contrast with basal levels found in normal muscles pre- and post-natally (Fig. 3.11.A). The elevated expression of *MAFbx* would suggest that the PCS muscles were subjected to a process of muscle wasting, possibly as a consequence of disuse atrophy. It remains possible that PCS is primary condition of gestational muscle under development.

MAFbx atrophy marker was used in this study to exemplify atrophy in PCS. Besides *MAFbx*, muscle ring finger 1 (*MuRF1*) also is another well-known atrophy marker (Bodine et al., 2001b). Only *MAFbx* atrophy marker could be used to assess the condition because of the limited availability of porcine gene sequences.

3.4.4. Down-regulation of P311 in PCS muscles

Rising levels of *P311* expression were found throughout gestation, and this rise was maintained in post-natal normal muscles (Fig. 3.11 B). By contrast, in PCS muscles, *P311* was detected at much reduced levels (Figs. 3.10.B and 3.11.B). Expression of *P311* was previously reported to be down-regulated in atrophic murine muscles (Lecker et al., 2004). In conditions of muscle wasting, arising from denervation or disuse, the process of protein degradation exceeds the rate of protein synthesis, resulting in net protein loss (Lecker et al., 2004). In PCS muscles, reduced *P311* expression could be a consequence of net protein loss. On the other hand, given that *P311* promoted cell proliferation (Figs. 4.12.A and B), it may have an active role in promoting muscle growth through raised myoblast number.

Chapter 4

Functional studies of *P311*

4.1. Introduction

P311, first identified in murine embryonic neurons (Studler et al., 1993), is a small 8-kDa 68-amino acid protein with a short half-life of around 5 minutes (Taylor et al., 2000). It is characterised by the presence of a conserved PEST domain (sequences rich in proline, glutamic acid, serine and threonine), a target site for degradation by the ubiquitin-proteasome system (Paliwal et al., 2004).

The results obtained and discussed in Chapter 3, *P311* expression was much reduced in PCS muscle. P311 has been reported to be down-regulated in atrophic conditions (Lecker et al., 2004). P311 does not belong to any known family of proteins, and its cellular function remains largely unclear. There are several reports about the cellular effects of *P311* on different cell types. Elevated expression of *P311* was found to associate with smooth muscle differentiation, and transformation of fibroblasts into myofibroblasts (Pan et al., 2002; Taylor et al., 2000). *P311* was reported to be involved in glioblastoma cell migration and fibroblast cell proliferation (Pan et al., 2002; Mariani et al., 2001; Taylor et al., 2000). In addition, differentiation of neural cells was related to loss of *P311* expression (Taylor et al., 2000). To investigate the function of *P311* in skeletal muscle, it would be necessary to study its effects on muscle cell proliferation, differentiation and phenotype determination. The aims of this study were to first characterise the full-length *P311* cDNA clone, and then to apply it to over-expression functional studies.

4.2. Materials and methods

All the commonly used techniques in this section have been previously described in the Materials and Methods Chapter (Sections 2.3, 2.4, 2.5 and 2.6).

4.2.1. *P311* cDNA cloning and sequencing

The cDNA of porcine *P311* gene was previously isolated in the Molecular Medicine Laboratory, Faculty of Veterinary Medicine, University of Glasgow. The *P311* cDNA was housed in a pBK-CMV vector (Stratagene) (Fig. 4.1.A). A series of restriction digestions (Section 2.3.3), followed by DNA electrophoresis (Section 2.2.4) were performed to determine the insert size of *P311*. After restriction mapping, the *P311* cDNA insert was sub-cloned as 2 fragments and sequenced (Section 4.3.1. for details). pBK-CMV vector (Stratagene) and pBluescript II SK(+) vector (Stratagene) (Fig. 4.1.B) were used for the sub-cloning. Sequencing was performed on *P311* cDNA with primers T3 (5' ATT AAC CCT CAC TAA AG 3') and T7 (5' TAA TAC GAC TCA CTA TAG GG 3') as described in Section 2.5.

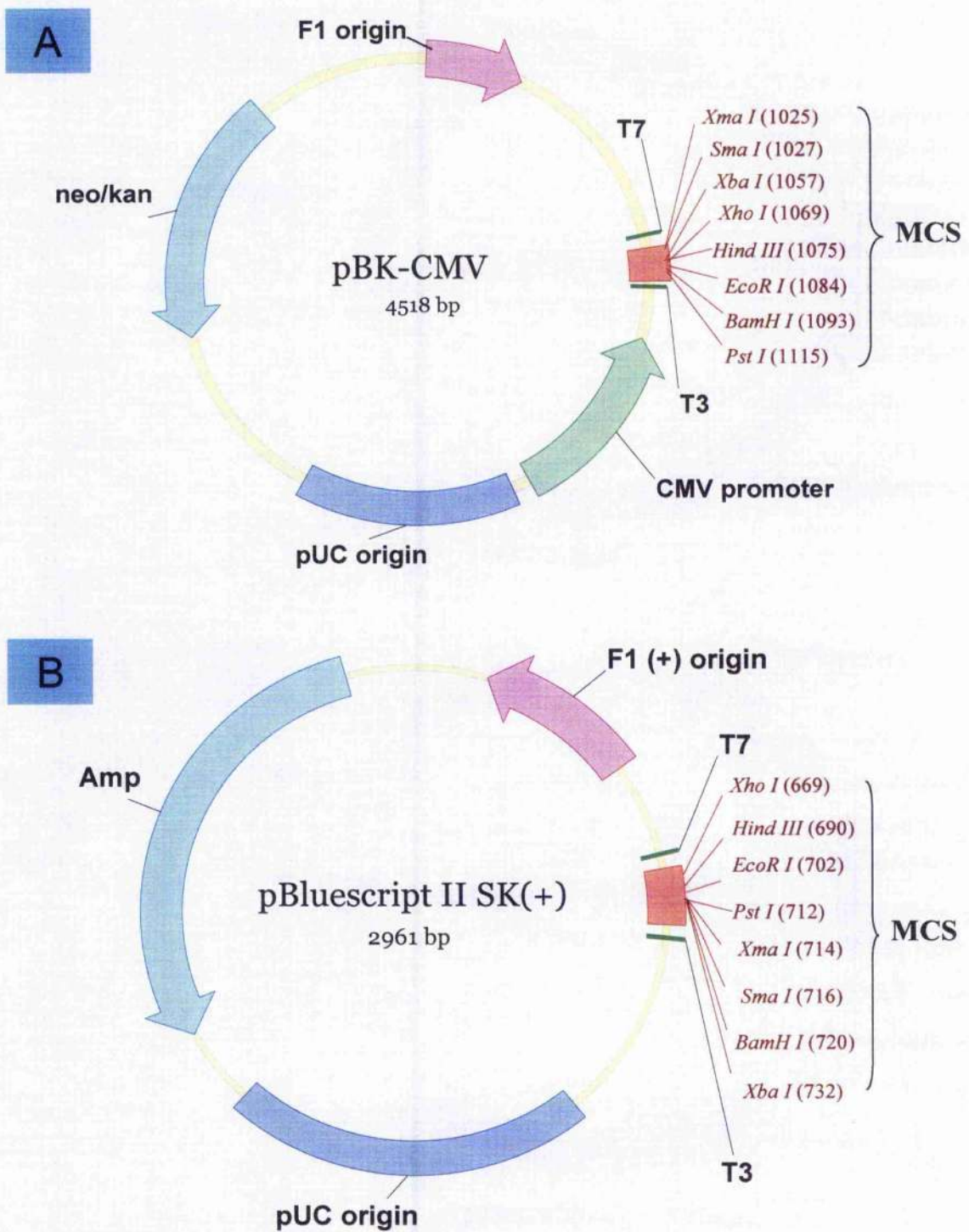


Figure 4.1. Plasmid vector (A) pBK-CMV and (B) pBluescript II SK (+). Both of the vectors comprise a multiple cloning sites and T3/T7 polymerase promoters. neo/kan = neomycin/kanamycin resistance; Amp = ampicillin resistance gene; CMV = cytomegalovirus; MCS = multiple cloning site.

Open reading frame finder (ORF finder, NCBI) was used to locate the possible starting codon and stop codon within *P311*. To amplify the coding region of *P311* without the stop codon, the following set of *P311* PCR primers was used. An *EcoR* I and a *Xho* I restriction digestion site were engineered into the 5' and 3' primers respectively. The primers are shown below, with the highlighted restriction digestion sites.

P311 PCR 5' (sense primer)

5' AA **GAA TTC** CCC AAC ACT TCA CGC TGA G 3'
EcoR I

P311 PCR 3' (anti-sense primer)

5' AA **CTC GAG** AAA AGA GCG GAG GTA ACT GAT 3'
Xho I

Amplification of the ORF was carried out as in Section 2.4. Next, the PCR products were cloned into TOPO- TA cloning vector (Invitrogen) (Fig.4.2) as in Section 2.3.1.2. The resulting colonies were selected for DNA miniprep preparation as described in Section 2.3.2.1. The insert size of *P311* was confirmed by digestion with *EcoR* I and *Xho* I. The correct DNA band was excised and directionally cloned into pDNR-CMV for recombinant adenovirus production as described in Section 2.6.4.

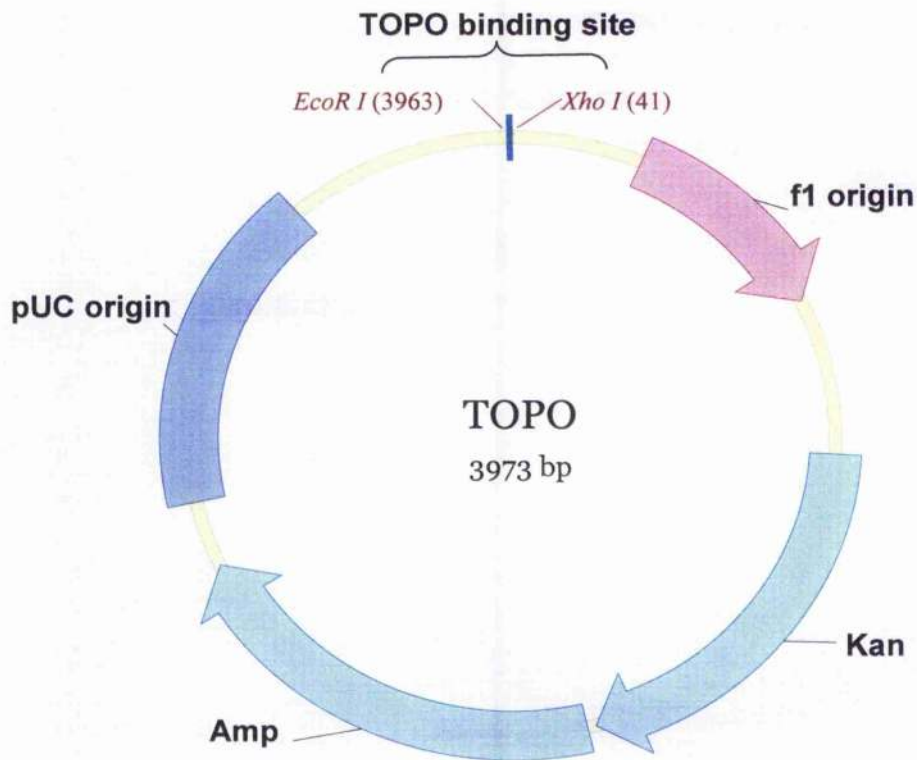


Figure 4.2. TOPO vector. It is designed to receive RT-PCR products. The PCR II-TOPO vector is 4.0 kb in size. Kan= kanamycin resistance; Amp= ampicillin resistance gene; MCS= multiple cloning site.

4.2.2. *P311* cell cultures, transfections and recombinant adenovirus production

C2C12 cells were grown in PM, and replaced by DM when cells reached 80% confluence. The C2C12 cell culture methods were described in Section 2.6.1. For stable transfections, C2C12 cells at 40% confluence in T25 culture flasks were transfected with 6.0 μ g *P311* pBK-CMV plasmid, by the use of lipofectamine and Opti-MEM, according to manufacturer's instructions (Invitrogen) as detailed in Section 2.6.3. Coding region of porcine *P311* cDNA and a constitutively active murine calcineurin A (Cn) (kindly supplied by Dr. S. Williams, University of Texas) were separately cloned into an adenovirus vector, using the Adeno-X Expression

System 2 (BD Biosciences) as described in Section 2.6.4. Both *P311* and Cn adenovirus constructs were cloned as fusion protein, which comprised a FLAG epitope at the carboxyl-end (Section 2.6.4.1). For time course studies, infection with *P311* and Cn-adenovirus constructs were used at a multiplicity of infection (MOI) of 5. Cells were infected in PM for 3 days (3I), followed by 3 days in DM (3I 3D), or by 6 days in DM (3I 6D). Stably transfected cells were grown in PM for 3 days (PM), followed by 3 days in DM (DM 3D), or 6 days in DM (DM 6D).

4.2.3. *P311* immunofluorescence, cell cytotoxicity and Western blotting

C2C12 cells upon infection with *P311* or GFP control adenovirus, were grown for 3 days in PM, followed by 8 days in DM. To improve *P311* stability, o-phenanthroline (cat. N^o. P9375, Sigma) and lactacystin (cat. N^o. L6785, Sigma) were added to the DM, at final concentrations of 1.26 mM and 10 mM respectively, 2 hours prior to fixation. The combination of proteasome inhibitor, lactacystin and the metalloprotease inhibitor, o-phenanthroline, was able to block degradation of *P311* (Taylor et al., 2000). The immunofluorescence procedure was described in Section 2.6.9. For cell cytotoxicity assay, a resazurin-based reduction assay that measures the metabolic capacity of cells, was performed according to manufacturer's protocol as in Section 2.6.5. Western blotting was performed as in Section 2.8 with the use of primary anti-FLAG M2 monoclonal antibody (Sigma).

4.2.4. *P311* cell proliferation, fusion index and BrdU assay

Thirty thousand C2C12 cells were plated on each 25 cm² flask (three flasks for each *P311*-pBK-CMV plasmid and pBK-CMV empty plasmid as control), and were grown for up to 5 days in PM. The cell proliferation assay was based on stably transfected cells as described in Section 2.6.6. For fusion index assays, after 9 days in DM, transfected cells were fixed and stained as detailed in Section 2.6.7. BrdU assays on C2C12 cells, infected with *P311*-adenovirus and stably transfected with *P311* plasmid construct, were performed as previously described (Section 2.6.8).

4.2.5. *P311* quantitative real-time RT-PCR

TaqMan quantitative real-time RT-PCR (Applied Biosystems) was performed on a number of murine genes: *MyHC slow*, *MyHC 2a*, *MyHC 2x*, *MyHC 2b*, *Myf5*, *MyHC embryonic*, *MyHC perinatal*, α -actin, β -actin, and *P311*. All the primer and probe sequences are shown in Table 4.1. A relative standard curve method, normalised to β -actin, was used in the quantification of expression. The primer concentration used and the values of the standard curve calculations are shown in Table 4.2.

Table 4.1. Sequences of primers and TaqMan probes.

Gene	Primer	Sequence 5'→3'
Porcine P311	S	GAG GGA AGG CCT AAG GG
	A	CGG TCT CGC CAT CCT TCT T
	P	ACT TCC CAT CCC AAA GGA AGT GAA CCG
Murine MyHC slow	S	GCC TGG GCT TAC CTC TCT ATC AC
	A	CTT CTC AGA CTT CCG CAG GAA
	P	CGT TTG AGA ATC CAA GGC TCA
Murine MyHC 2a	S	CAG CTG CAC CTT CTC GTT TG
	A	CCC GAA AAC GGC CAT CT
	P	TGA GTT CAG CAG TCA TGA G
Murine MyHC 2x	S	GGA CCC ACG GTC GAA GTT G
	A	GGC TGC GGG CTA TTG GTT
	P	CTA AAG GCA GGC TCT CTC ACT GGG CTG
Murine MyHC 2b	S	CAA TCA GGA ACC TTC GGA ACA C
	A	GTC CTG GCC TCT GAG AGC AT
	P	TGC TGA AGG ACA CAC AGC TGC ACC T
Murine Myf5	S	CAG CCC CAC CTC CAA CTG
	A	GCA GCA CAT GCA TTT GAT ACA TC
	P	TGT CTG GTC CCG AAA GAA CAG CAG CTT
Murine MyHC embryonic	S	TCC GAC AAC GCC TAC CAG TT
	A	CCC GGA TTC TCC GGT GAT
	P	ATG CTG ACT GAT CGT GAG AAC CAG TCT ATC CT
Murine MyHC perinatal	S	GGA GGC CAG GGT ACG TGA A
	A	GAG CAC ATT CTT GCG GTC TTC
	P	AGG AAC TTA CCT ACC AGA CTG
Murine skeletal α -actin	S	GAG CGT GGC TAT TCC TTC GT
	A	CAC ATA GCA CAG CTT CTC TTT GAT
	P	CGC GCA CAA TCT CAC GTT CAG CTG
Murine β -actin	S	CGT GAA AAG ATG ACC CAG ATC A
	A	CAC AGC CTG GAT GGC TAC GT
	P	TTG AGA CCT TCA ACA CCC CAG CCA TG
Murine P311	S	CAG CCA AGA ACC GTT TGC AT
	A	CAC TTC CTT AGG CAC GGG AA
	P	TTC CCT TAA TAA GAC CTC CCT CCA TTT CCT TG

S, sense; A, antisense; P, TaqMan probe. All probes were 5' labelled with 6-carboxyfluorescein (FAM), and 3' labelled with 6-carboxytetramethylrhodamine (TAMRA). Murine MyHC 2a was also labelled with Minor Groove Binder (MGB) to increase stability.

Table 4.2. RT-PCR primer concentration and values of standard curve.

Gene	Primer concentration of 5':3'($\mu\text{mol}/\mu\text{l}$)	Standard curve value
Porcine P311	900:900	T: 0.026
		S: -3.357
		Y: 12.360
Murine MyHC slow	900:900	T: 0.009
		S: -4.241
		Y: 13.583
Murine MyHC 2a	900:900	T: 0.006
		S: -3.993
		Y: 16.785
Murine MyHC 2x	900:900	T: 0.014
		S: -3.831
		Y: 13.018
Murine MyHC 2b	900:900	T: 0.012
		S: -3.943
		Y: 9.928
Murine Myf5	900:900	T: 0.011
		S: -3.495
		Y: 17.831
Murine MyHC embryonic	900:900	T: 0.011
		S: -3.900
		Y: 12.229
Murine MyHC perinatal	900:900	T: 0.007
		S: -3.600
		Y: 16.063
Murine skeletal α -actin	300:50	T: 0.017
		S: -4.335
		Y: 7.98
Murine β -actin	300:900	T: 0.017
		S: -3.859
		Y: 13.563
Murine P311	900:900	T: 0.023
		S: -3.023
		Y: 20.895

T, threshold; S, slope; Y, y-intercept.

4.3. Results

4.3.1. *P311* cDNA cloning and sequencing

The cDNA of porcine *P311* was previously isolated in the Molecular Medicine Laboratory. In vector pBK-CMV, a series of multiple restriction digestions, followed by DNA electrophoresis were performed to determine the insert size of the *P311* cDNA (Fig. 4.3). The construct was digested with 8 different combinations of enzymes. (1) *EcoR* I, (2) *Xho* I, (3) *Xho* I + *EcoR* I, (4) *Pst* I, (5) *Bam*HI I, (6) *Hind* III, (7) *Xba* I and (8) *Sma* I (Fig.4.3.A). Digestion results show that the *P311* fragment was 2.2 kb, with an internal *Xba* I restriction site (Fig.4.3.B). *Xba* I restriction enzyme was used to digest the pBK-CMV-*P311* into 2 fragments, which were 1.0 kb and 5.7 kb in size. The smaller insert (1.0 kb) fragment was cloned into pBluescript II SK⁽⁻⁾ (Stratagene), and the remaining fragment, housing the remaining 1.2 kb of *P311* insert was self-ligated (Fig. 4.4).

The full-length of a *P311* cDNA was sequenced with primers T3 and T7 (ABI Prism 3100 Genetic analyzer). The full-length of *P311* cDNA was 2.2 kb and the deduced coding sequence was 0.3 kb in length. The full DNA sequence result is shown in Figure 4.5. Basic nucleotide alignment search tool (BLAST) showed that porcine *P311* was 85% homologous to human *P311*. The deduced amino acid sequence of porcine *P311* is shown in Figure 4.6. It was 87% homologous to human *P311*. Besides *Homo sapiens*, comparisons with other species were also made. The deduced amino acid sequence of porcine *P311* was 73.4% homologous to mouse *P311* and 52.7% homologous to chicken *P311*.

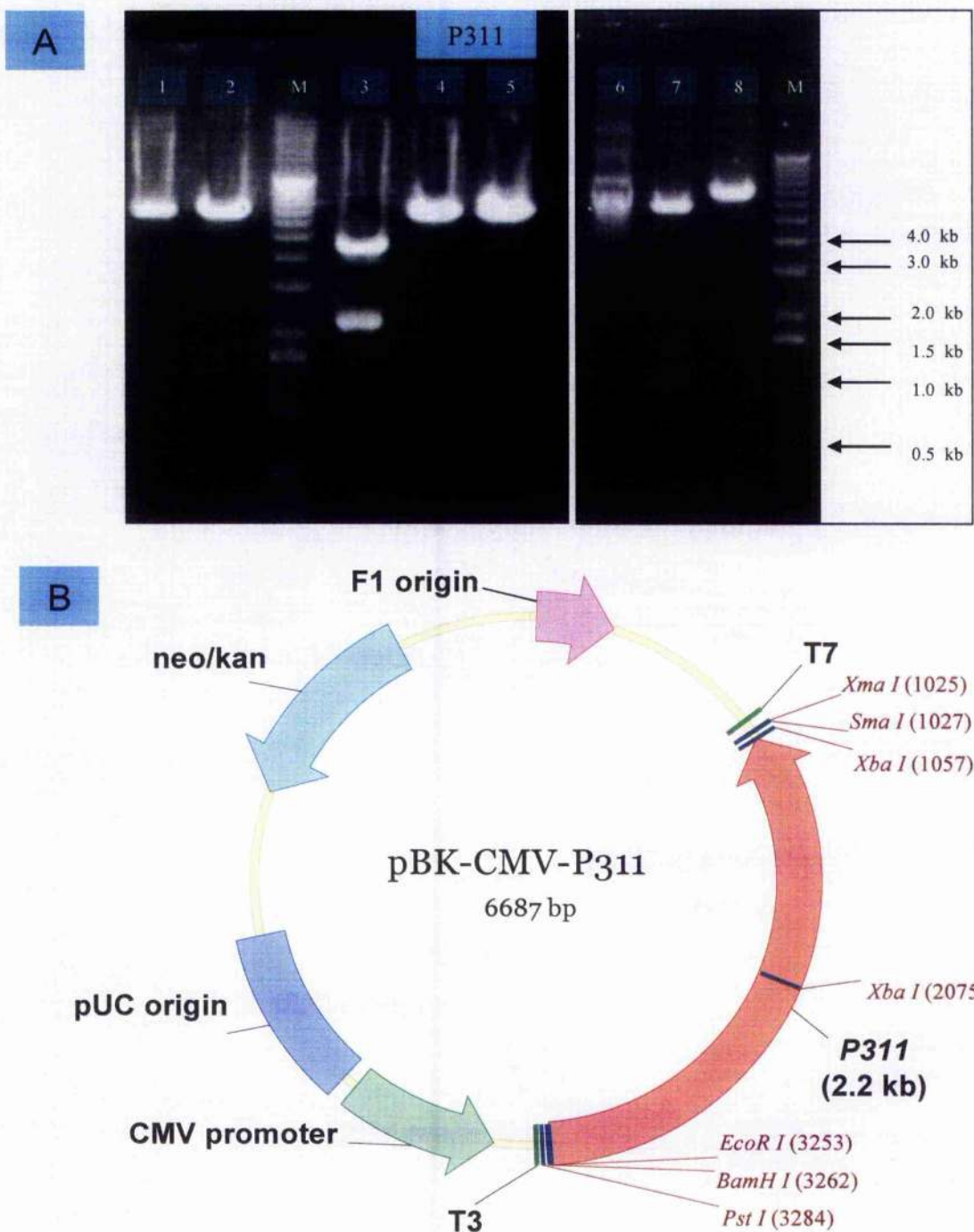


Figure 4.3. Restriction digestion of pBK-CMV-P311. (A) Gel electrophoresis of P311 plasmid in pBK-CMV vector after 2 hours of enzyme digestion. The constructs were digested with 8 different combinations of enzymes. (1) *EcoR* I (2) *Xho* I (3) *Xho* I + *EcoR* I (4) *Pst* I (5) *BamH* I (6) *Hind* III (7) *Xba* I and (8) *Sma* I. M=marker ladder. (B) The pBK-CMV with P311 insert is 6.7 kb. The P311 cDNA was 2.2 kb with an internal *Xba* I restriction site.

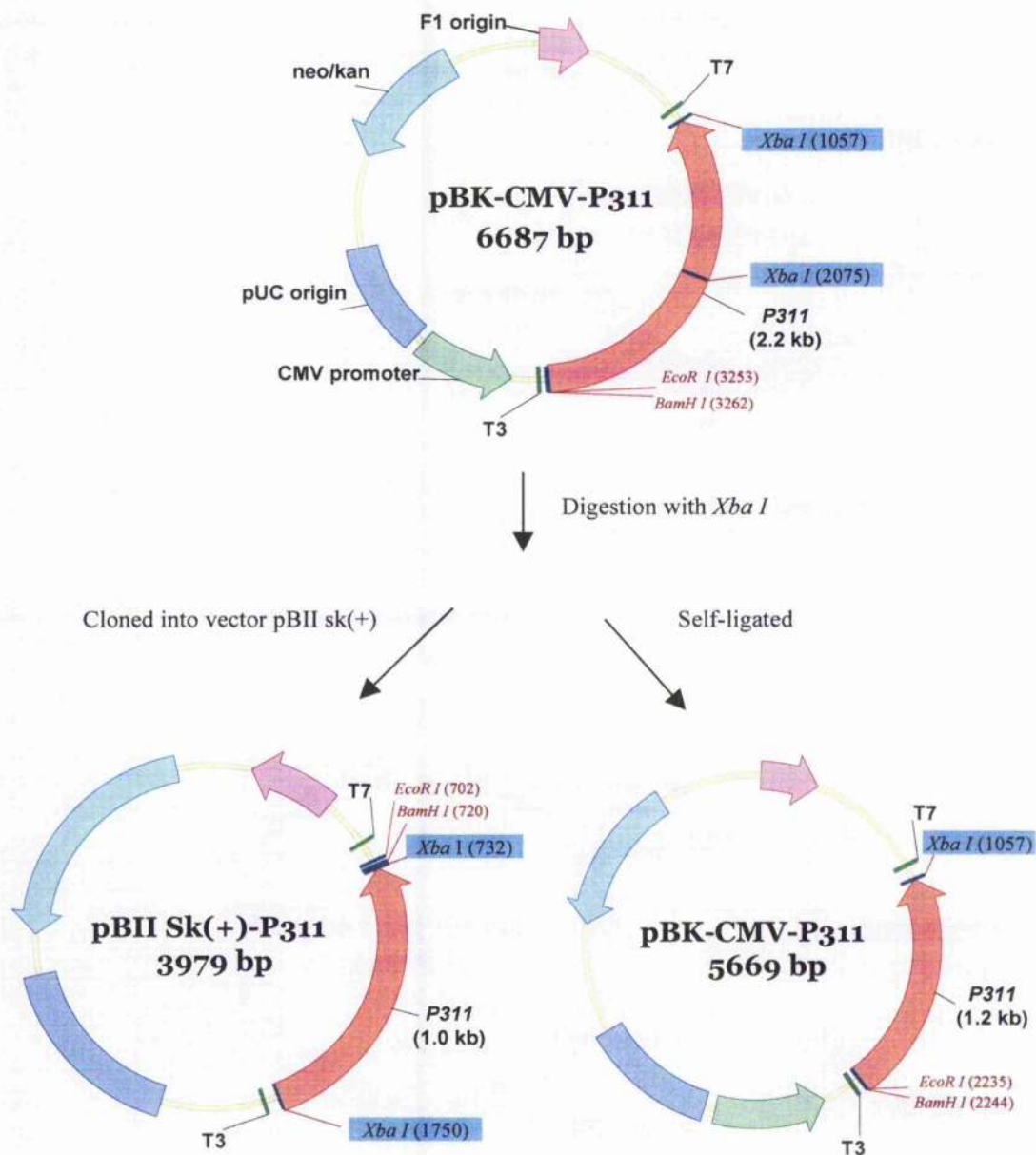


Figure 4.4. Sub-cloning of P311. A *Xba* I restriction enzyme was used to digest the pBK-CMV-P311 into 2 fragments, which were 1.0 kb and 5.7 kb in size. The smaller fragment was cloned into pBluescript II SK(+) (Stratagene), and the remaining fragment was self-ligated. *Xba* I restriction site highlighted in blue.

GAATTCGGCACGACG**CCCAACACTTCACGCTGAG**CTGACCCGGAGCCCTTGCTCCCCTGG 60

ATGGATGGTTTGGGAGGAGAGCTGCTTGGGTGGGCTGGTGGGCGGGGTCCAGGGAGGCA 120

CAGGTCCTTTTCCCAGCCCTTCTGCCAAAGAAGCAGCACCTGCCCTGGGTCTCCTCTG 180

CGACCTGTGCTGCATGAGCTGGCGTGGTCTGAGTGTGTCTGCGGGGCTTTTGTCTGTT 240

GCTTGGTCTCCCTGGACTGAAGAGAGGGAGGGTACAAGGCCAAGACTGTTAAGGATTCTC 300

AAA**ATG**GTTTATTACCCAGAGCTTTCTGTCTGGGTCAAGAACCATTTCCAAACAAG 360

GAAATG**AGGGAAGGCTTCCTAAGGAAG****ACTTCCCATCCCAAGGAAGTGAACCG****CAAG** 420
 *******TTC**

AGGATGGCAGACCGAGGCTGCCTCCCTGACTCCACTCGGCAGCAATGAAATGAATC 480
TTCCTACCGCTCTGGC*****

CACTCCCAGGA**ATCAGTTACCTCCGCTCTTTT****TA**TCACCTCCATTGTATTACATATG 540

GTGTATGGGTATTGATGAGGTCATGGTATCATATATGGGATTTTTTCTGTGTAATCAT 600

CAAGTATAAGAAGAACTATGGGACTCTGAGCCTTGCTTTAGAGAATTTACAGTGGACAA 660

ATAGGTATCATCAAACAGTTTTTAATCATTCTGACTCAAGTGAACGCTCAGAAATTC 720

ACACTGTGAATCCACGTTTACAACCCCTTACAGGTGGGCCTTCAGGCCTGGTTCGTACGA 780

CGATGTCTTCCACAACCTCAAACCCCAACTGCTCTCACACAACCGGTCCACTTCTGCCTT 840

TTCACTCACACAGCTCCCGACTGCTCCTGCGAGGCTGAGAGTCCCATTTTTTTTTTT 900

TTTTCATTTAGATGTAACAAGCCTAGTAGTTTATGTTCAATTTGTCTGTATATCTCTA 960

TATTTTATCCATGTA


```

GTTTTTAATAAATGCCCTCTGGAAAAAAAAAAAAAAAAAATCCAAAACTGACGTCTCCGTA 1560
*****

GGAACATGAAAATTACACCTTTCCCAAAATAAGGTTGAAAAATGTCTTGACAAAATTC 1620
*****

AAAAAAAAAAAAAAAAAAGGCAGAGCACTCTTTTTTGGTAGTTCTGATAAGCAAGGTG 1680
*****

TAGATTTTACATTTTGTCTTGTCTCCAATGAAATGGATAAACAAAAATACAATCAGAC 1740
*****

AATACCATCTACTCATGGAATGTTGTTGTGTAGCCAGTCTGAAAGCCACCTTAATTTT 1800
*****

TATATACTGTCTTTTAGCTCTTCCTTTGACAGGGCAGGCTTCGTTCTGAACTGTTCCGC 1860
*****

TTCTGACTTAACACATCGACGACGCATGCGCTGCACTTCTTCGTTCTCTTCTTGCTCCCC 1920
*****

CATTGGCCTGAGTTTCTTGTGCATCCCCGCCCTCCTTTGTTAGAATAGGTATATCCGC 1980
*****

TGTGTAAATAGAGCAAGAAAACAGTATTCTGCATCTGTGGCATTACGTAGAGTTGCAGT 2040
*****



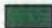


TGTGTACTGCTGAATATGCAGGCTTTTGTAACAATGTGATCTTTACCGATGCACTCACGA 2100
*****

CAAGTACCCAATGTATTTTAGCTATTTTAGTAGTATTGTTCATAAATATGCAAGCTGT 2160
*****

ATGGTAAAAAAGAAAAAATACTCGAGAGTACTTCTAGA 2202
*****

```

Figure 4.5. Full length nucleotide sequence of porcine *P311* cDNA.

-  P311 PCR 5' and 3' primers
-  Start / stop codon
-  P311 real-time RT-PCR 5 and 3' primers
-  P311 real-time RT-PCR probe
-  P311 internal detection 5 and 3' primers


```

          ****+***.*****+*+.+***.+.*+***+*****+.**+.***+
pig      ( +4.85) MVYYPELSVWVSQEFPNKEGRLPKGRLPIKENVNRKKDGETEAAS
human    ( +0.50) MVYYPELFWVVSQEFPNKMEGRLPKGRLPVPKEVNRKKNDETNAAS
mouse    ( +0.64) MVYYPELLVWVSQEFPAYKEMEGGLIKGRLPVPKEVNRKKMEETGAAS
chicken  ( -6.16) MIYQPRQTIWVSQKVFTSQDGGFLKGCLPISKEVNRKKESEVEGAC

          ***.***+.***+.***+.***+.***+.***+.***+.***+.***+.***+
pig      LTPLGSNeneLHSPGISYLRSF
human    LTPLGSSE--LRSPRISYLHFF
mouse    LTPPGSRE--FTSPATSYLHPF
chicken  WAPVNGDG--HHFTKINYLYTF

```

(**RED** ~the possible PEST region in porcine P311)
(Blue~ comparison of possible PEST region among other species)

* = homologous; + = limited homologous; . = not homologous.

Figure 4.7. Comparison of PEST domains in *P311* deduced amino acid sequences for pig, human, mouse and chicken.

4.3.2. Recombinant *P311* adenovirus production

The *P311* PCR 5' and 3' primers were used to amplify the coding sequence of *P311* in PCR. Gel electrophoresis of the 0.5 kb RT-PCR products is shown in Figure 4.8.A. TOPO-*P311* vector was digested with *EcoR* I and *Xho* I restriction enzymes to ascertain the *P311* insert (Figs. 4.8.B and C). The required DNA insert was excised and cloned into pDNR-CMV for recombinant adenovirus production. pDNR-CMV-*P311* vector was digested with *EcoR* I and *Xho* I restriction enzymes to ascertain the clones containing the appropriate *P311* insert (Figs. 4.9.A and B).

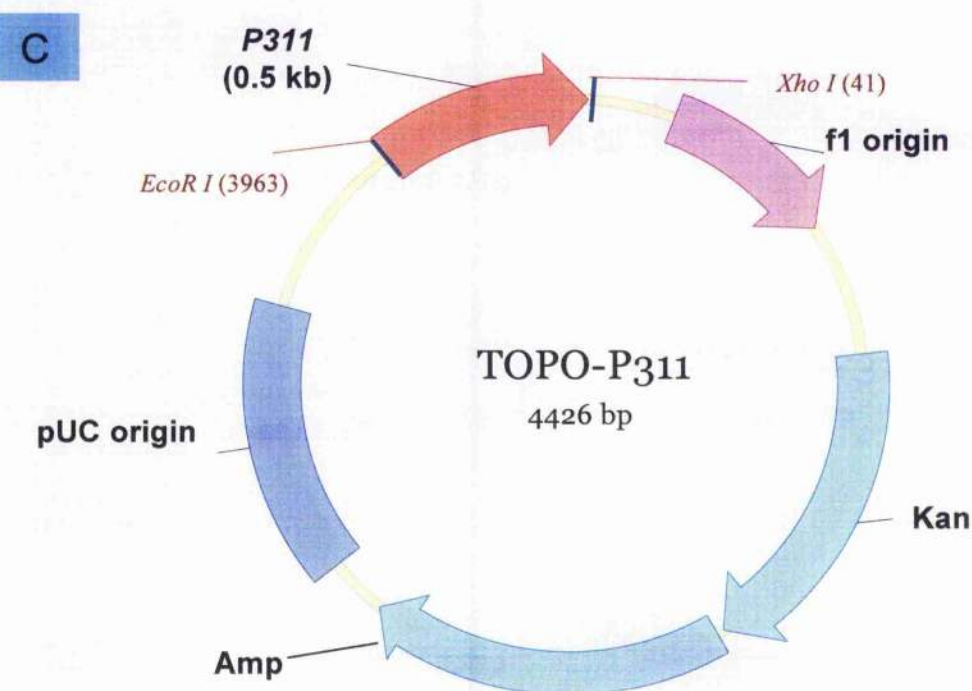
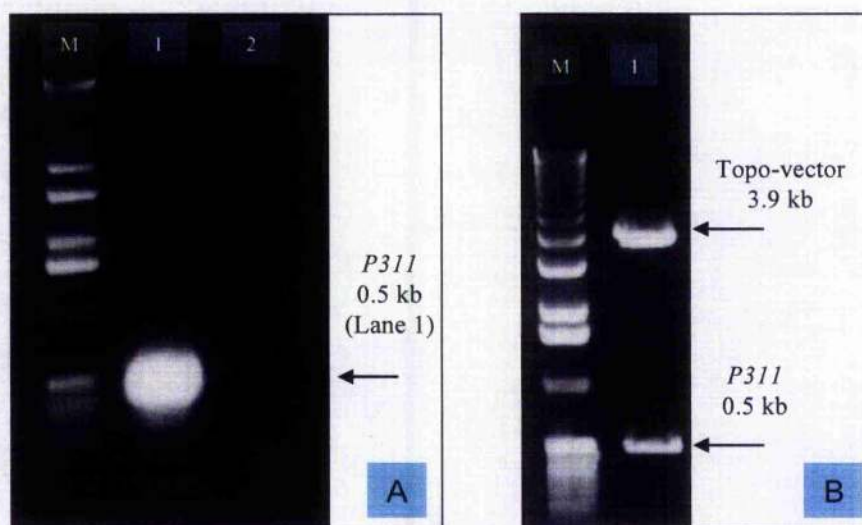


Figure 4.8. Cloning of *P311* into TOPO vector. (A) Gel electrophoresis of the 0.5 kb RT-PCR products with the use of sense and anti-sense primers (Lane 1). Sense primer with template DNA in alone Lane 2 as control; no band was detected. (B) Gel electrophoresis after digestion of TOPO-P₃₁₁ with *Xho*I and *EcoR*I; *P311* segment (0.5 kb) and topo vector (3.9 kb) are shown. (C) TOPO vector with *P311* insert. The *P311* insert is about 0.5 kb with *EcoR*I restriction in 5' and *Xba*I restriction site in 3' ends.

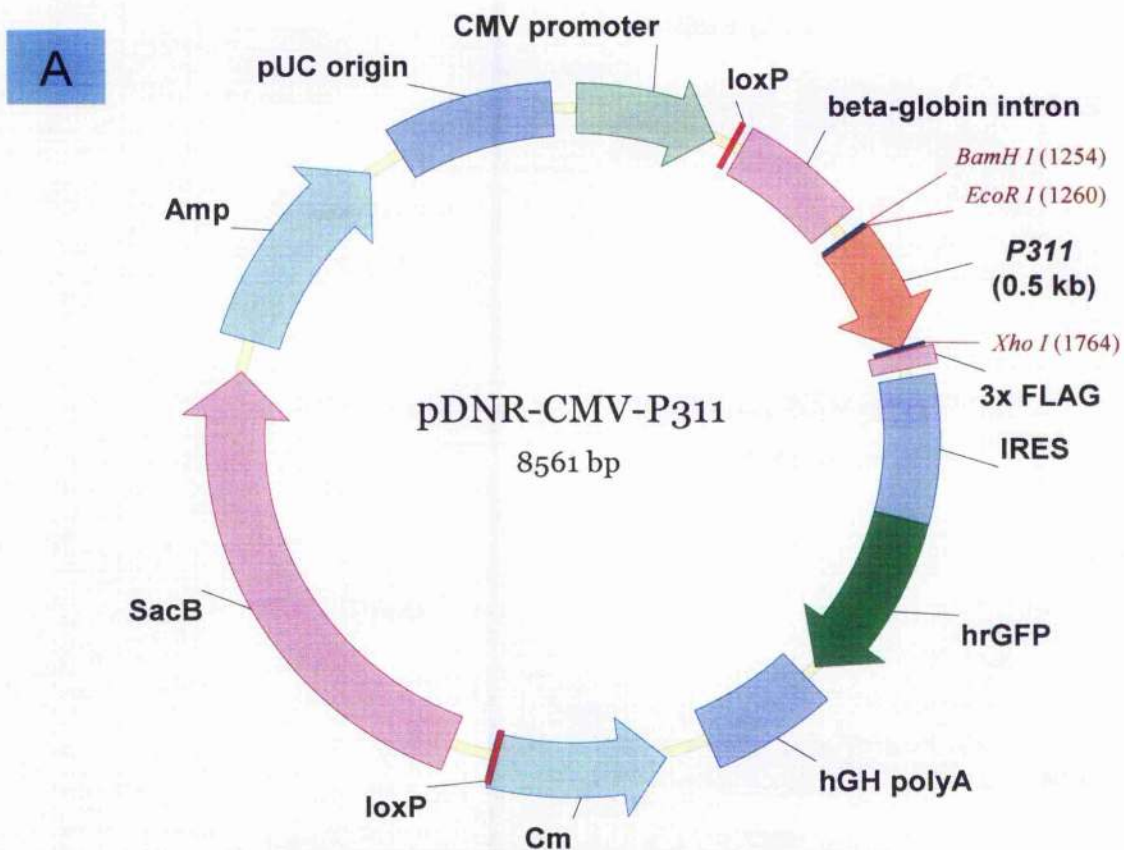


Figure 4.9. Cloning of *P311* into pDNR-CMV vector. (A) The pDNR-CMV with *P311* cDNA insert is 8.6 kb. The *P311* fragment is 0.5 kb with *Eco*R I restriction in 5' and *Xho* I restriction site in 3' ends. (B) Digestion of pDNR-CMV-*P311* with *Xho* I and *Eco*R I. Lanes 3-5 are clones with the appropriate cloned 0.5 kb insert.

After the correct pDNR-CMV-P311 clones were identified by restriction mapping, gene sequencing was performed to confirm an intact start codon at the 5' end and a FLAG epitope was cloned in frame at the 3' end. *P311* internal 5' primer (5' CGG TCT CGC CAT CCT TCT T 3') was used to detect the start codon at the 5' end. Another *P311* internal 3' primer (5' GAG GGA AGG CCT AAG GG 3') was used to detect FLAG epitope at the 3' end. The primers used are highlighted in grey in Figure 4.5. Sequencing results confirmed that both the start codon and FLAG epitope are correctly cloned. The sequence of the FLAG epitope at the 3' end is shown (Fig. 4.10).

Nucleotide sequence

TACCTCCGCTCTTTT CTC GAG **GAC TAC AAG GAT GAC GAT GAC AAG** **GAT TAC AAA**
GAC GAC GAT GAT AAG **GAC TAT AAG GAT GAT GAC GAC AAA** **TAA TAG**
 CAATTCTCGACGACTGCATAGGG

Deduced amino acid sequence

Y L R S F L E **DYKDDDDK** **DYKDDDDK** **DYKDDDDK** **Stop Stop**
 Q F L D D C I G

Figure 4.10. 3x FLAG and stop codon of *P311* in pDNR-CMV vector. The 3X FLAG sequence is highlighted in blue, while the stop codon is highlighted in red.

4.3.3. *P311* over-expression in C2C12 cells by adenovirus infection and by stable transfection

To assess the function of *P311* in muscle cells, *P311* was over-expressed in C2C12 muscle cells by stable transfection with pBK-CMV-*P311* plasmid (Fig. 4.3.B) as well as by infection with a *P311*-adenovirus construct (Fig. 4.11). Expression of both

constructs could be demonstrated by *P311* mRNA detection (Fig. 4.11.A), and by *P311*-FLAG fusion protein detection by immunofluorescence (Fig. 4.11.B). Cell cytotoxicity assays that measured metabolic capacity showed no significant difference between infected/transfected cells, and control cells over an extended period of 10 days differentiation, which indicated similar cell viability (Fig. 4.11.C). This finding also indicates that over-expression of *P311* is not detrimental to C2C12 cells. Western blot was performed to detect *P311* proteins. *P311* is reported to be highly labile, with a short half-life (Taylor et al., 2000). O-phenanthroline and lactacystin were added to improve *P311* stability. No prominent *P311* band sizes were detected in Western blotting. The instability of *P311* might account for the failure of its detection.

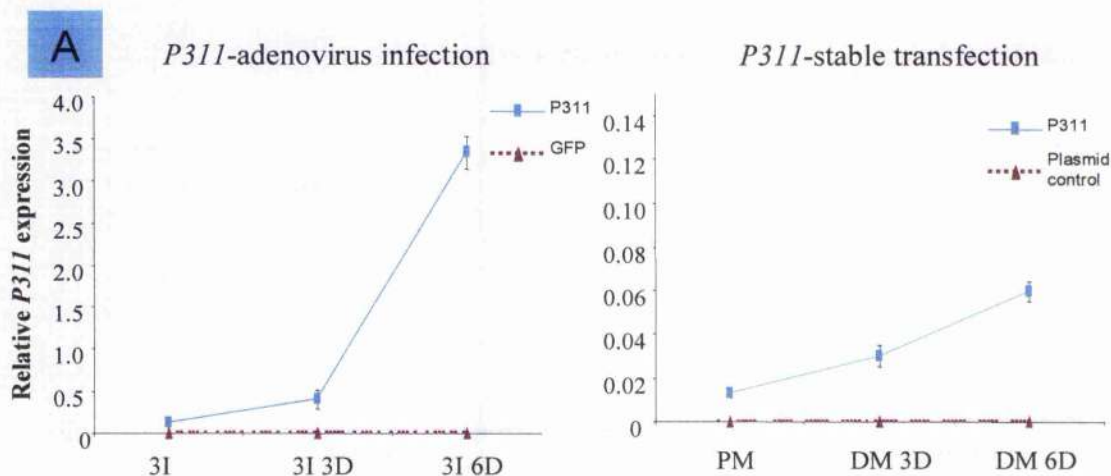


Figure 4.11. (A) Over-expression of *P311* in C2C12 cells. *P311* expression, through infection with an adenovirus construct and through stable transfection with an expression plasmid (Fig. 4.3.B), was determined over a time course. Proliferating cells were infected for 3 days in proliferation medium [PM] (3I), followed by 3 days in differentiation medium [DM] (3I 3D) or 6 days in DM (3I 6D). Stably transfected cells were incubated for 3days in PM (PM), followed by 3 days in DM (DM 3D) or 6 days in DM (DM 6D). Results expressed as mean \pm standard deviation from triplicate samples within the same experiment.

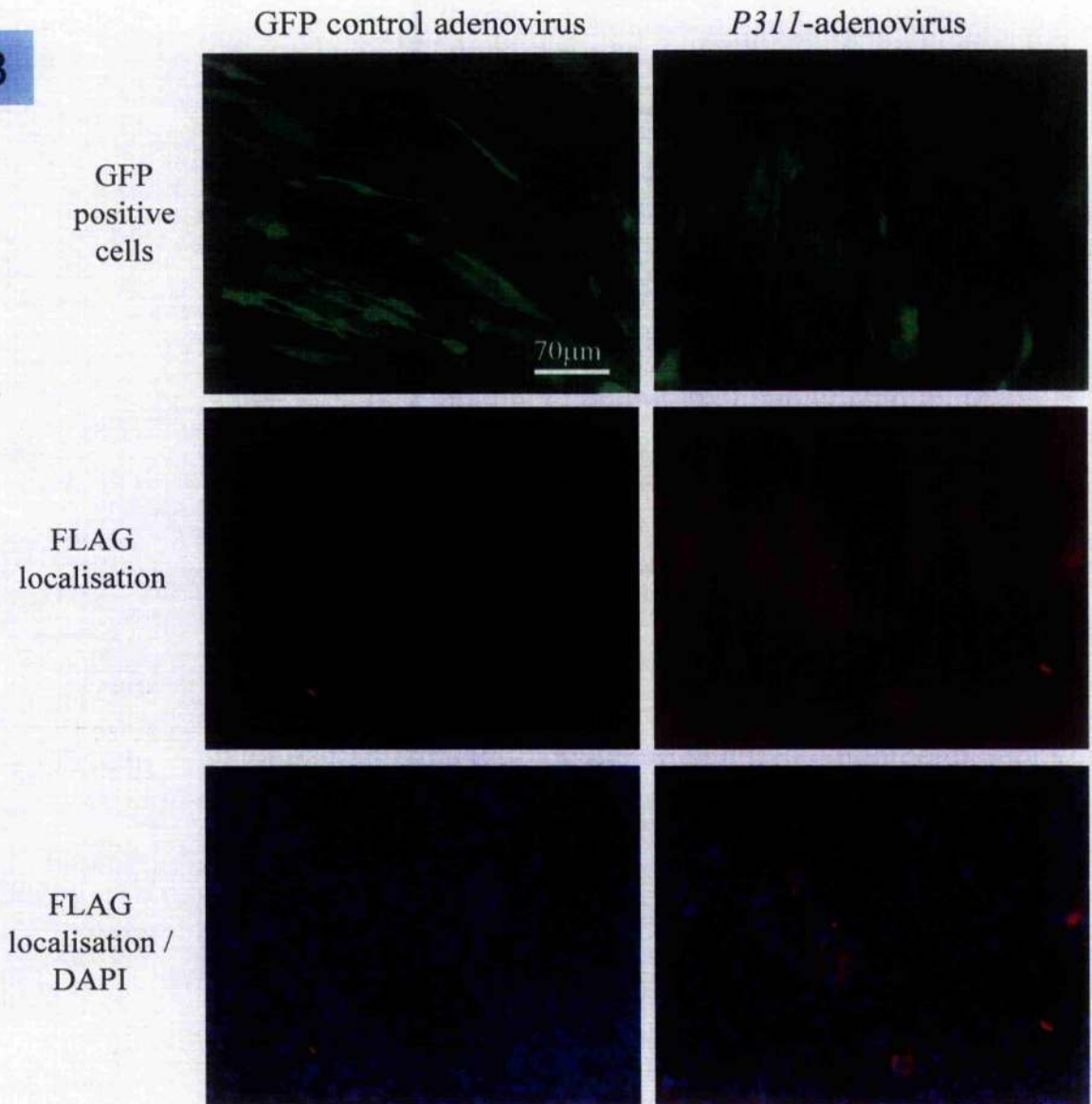
B

Figure 4.11. (B) P311-FLAG fusion protein detection by immunofluorescence. Adenovirus-mediated (MOI of 5) expression of *P311* in C2C12 cells (infected for 3 days during proliferation followed by 6 days of differentiation), viewed under fluorescence for GFP and immunostained for FLAG. *P311*-infected cells showed co-localisation of both proteins.

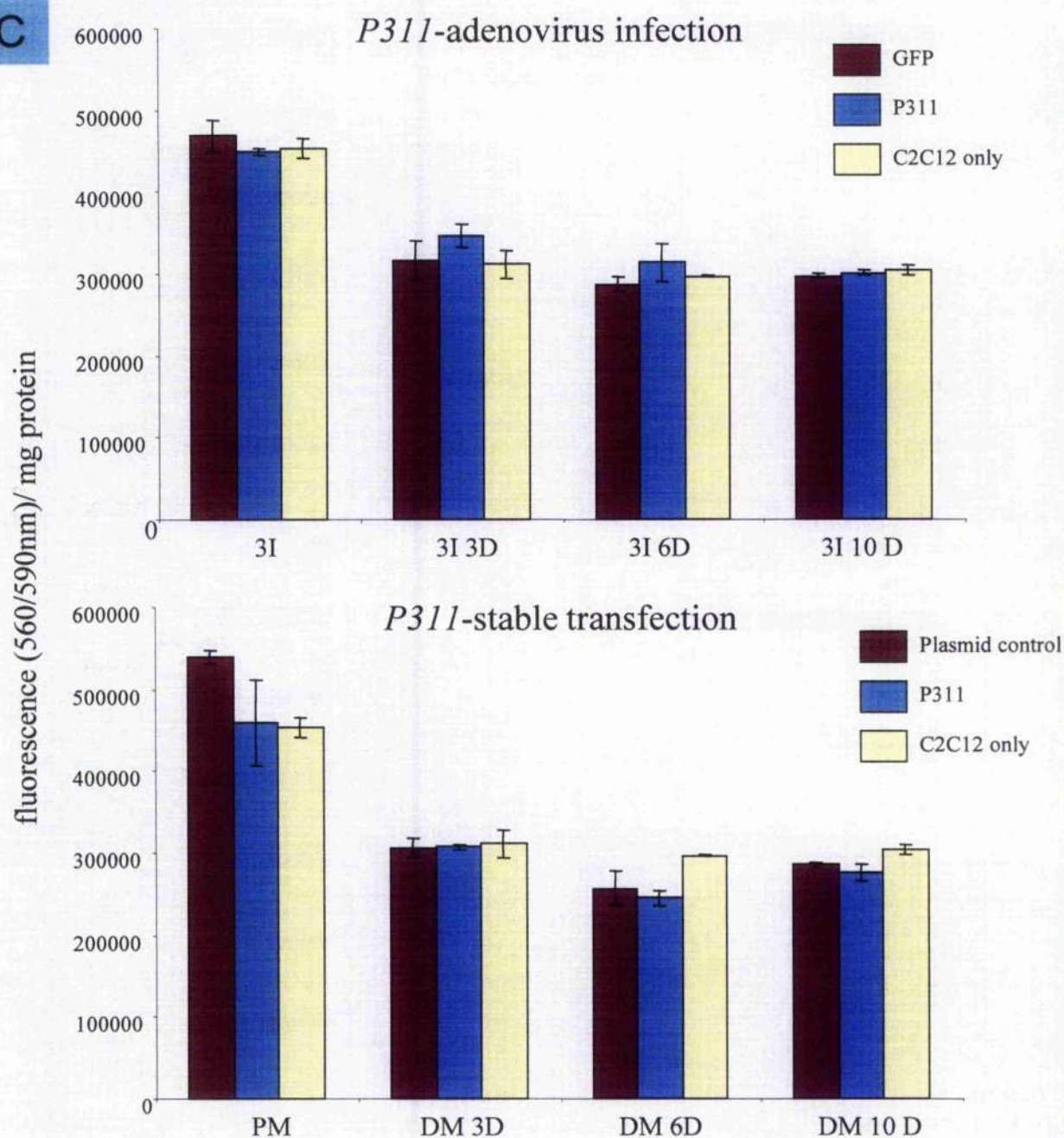
C

Figure 4.11. (C) Cell viability assay of *P311*-infected and *P311*-stably transfected C2C12 cells. The viability of *P311*-infected and *P311*-transfected C2C12 cells was similar to control cells over an extended culture period, as demonstrated by cell cytotoxicity assay (CellTiter-Blue kit, Promega). Results expressed as mean \pm standard deviation from triplicate samples within the same experiment.

4.3.4. *P311* over-expression increased C2C12 cell proliferation and reduced differentiation

Proliferation assays were performed in stably transfected C2C12 cells by quantifying cell number with a Neubauer haemocytometer. *P311* over-expressed C2C12 cells showed significant increase in cell proliferation compared with plasmid control cells (Fig. 4.12.A). In addition, 5'-bromo-2'-deoxyuridine (BrdU) assays were performed on *P311*-adenovirus infected and stably transfected C2C12 cells. Both constructs promoted proliferation compared with control GFP cells (Fig. 4.12.B). C2C12 cells stably transfected with *P311* also appeared to give rise to less myotubes as visualised by immunostaining for desmin, MyHC fast and MyHC slow proteins (Fig. 4.12.C). This observation could be further appreciated quantitatively by determining the fusion index of the transfected myotubes, which showed that *P311* over-expression produced fewer myotubes than control (Fig. 4.12.D).

4.3.5. Muscle gene expression in *P311*- adenovirus infected C2C12 cells

No obvious differences in *MyHC* expression were detected between *P311*-infected and control C2C12 cells during the early stages (3I and 3I 3D) of development (Fig 4.13.). However, at the later stage of differentiation (3I 6D), there was the suggestion of reduced expression of *MyHC embryonic*, *MyHC 2b*, *Myf-5* and α -actin in *P311*-infected C2C12 myotubes (Fig. 4.13), with the notable exception of *MyHC slow* which showed raised expression. The overall results of extended *P311* over-expression indicated a trend towards reduction in the expression of a number regulatory and structural muscle genes, which was consistent with reduced muscle

differentiation. *P311* appeared to associate with increased proliferation (Fig. 4.12.A), and reduced differentiation and myotube formation (Figs. 4.12.C and D to 4.13). *P311* was also examined to see if it could be down-regulated by the over-expression of constitutively active calcineurin (Cn), a key mediator of skeletal muscle differentiation (Bassel-Duby and Olson, 2003; Michel et al., 2004). Indeed, endogenous expression of *P311* was down-regulated a few days after Cn infection, regardless of the developmental stage of the C2C12 cells (Fig. 4.14). Hence, in the promotion of muscle differentiation, Cn down-regulated *P311* expression.

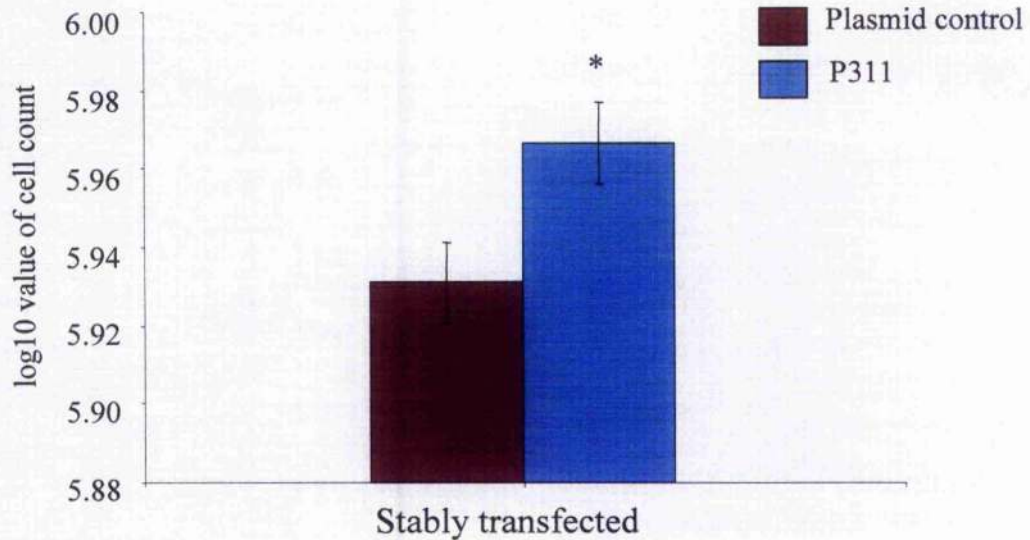
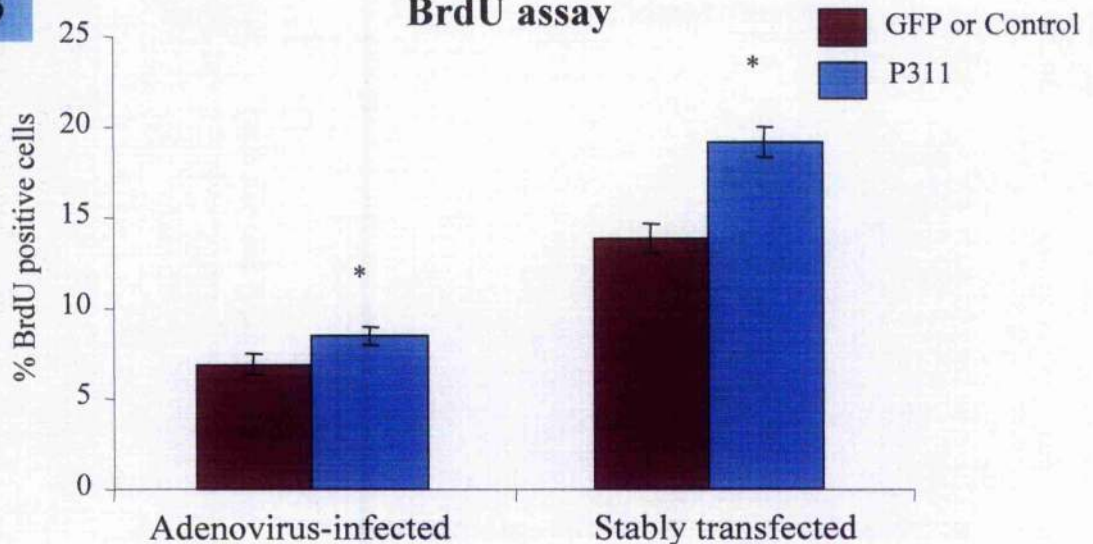
A**Proliferation assay (Haemocytometer based)****B****BrdU assay**

Figure 4.12. Over-expression of *P311* enhanced C2C12 cell proliferation. (A) *P311* over-express C2C12 cells showed significant increased in cell proliferation compared with plasmid control cells. (B) BrdU assay was performed on *P311*-infected and adenovirus-GFP control cells, as well as *P311*-stably transfected and vector only-transfected cells. For both approaches, *P311* over-expression significantly increased cell proliferation. Results were analysed with SAS software, differences between pair-wise combinations of the least square means were tested for significance (* $p < 0.05$). Error bars were standard error, $n=3$ replicates from 3 independent experiments.

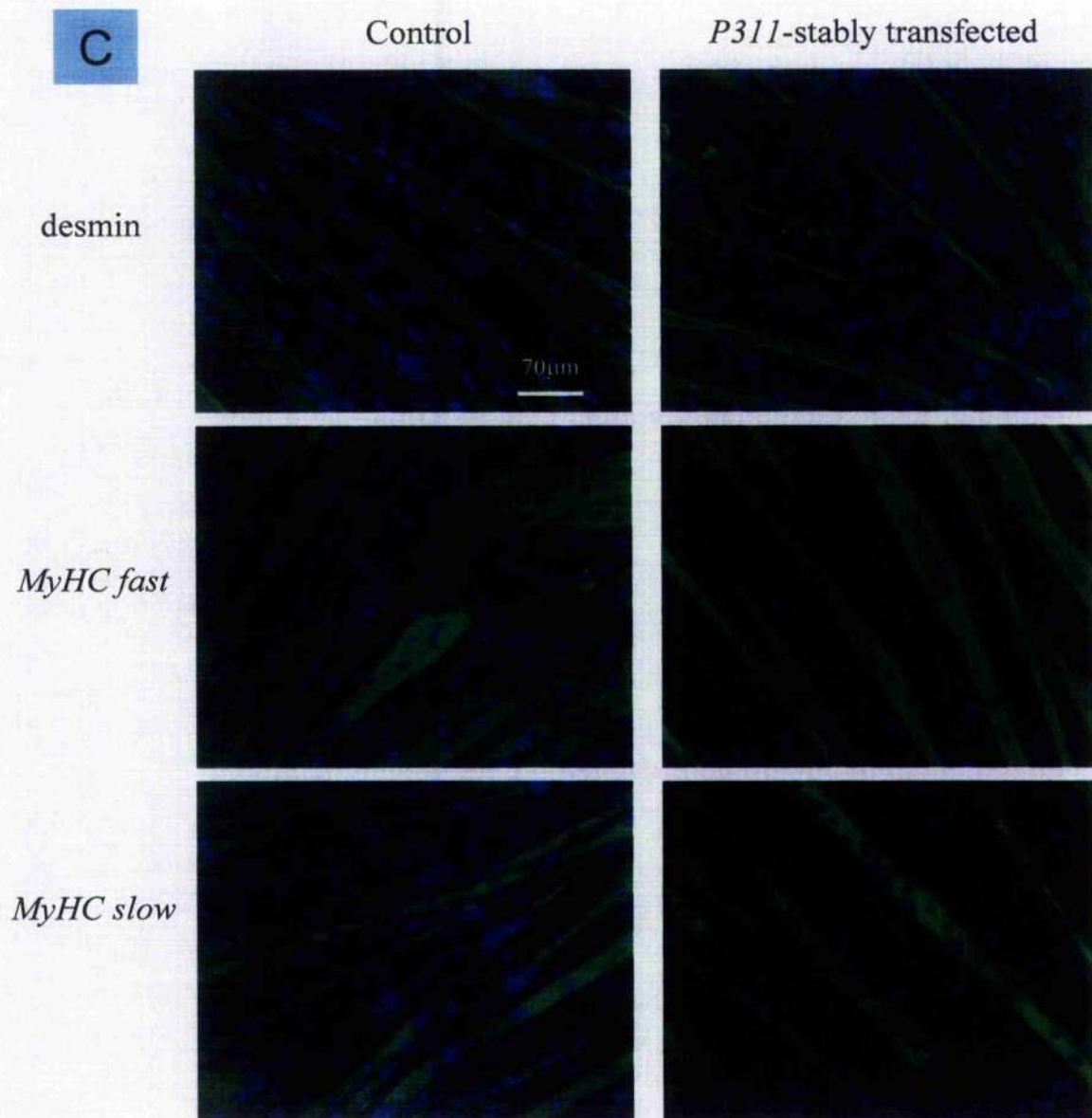


Figure 4.12. (C) Immunostaining of *P311*-stably transfected C2C12 cells. *P311*-stably transfected C2C12 myotubes (differentiated for 9 days) were separately immunostained for desmin, *MyHC fast* and *MyHC slow*, along with DAPI nuclei staining. Under immunofluorescence, myotubes appeared less abundant in *P311*-transfected cells.

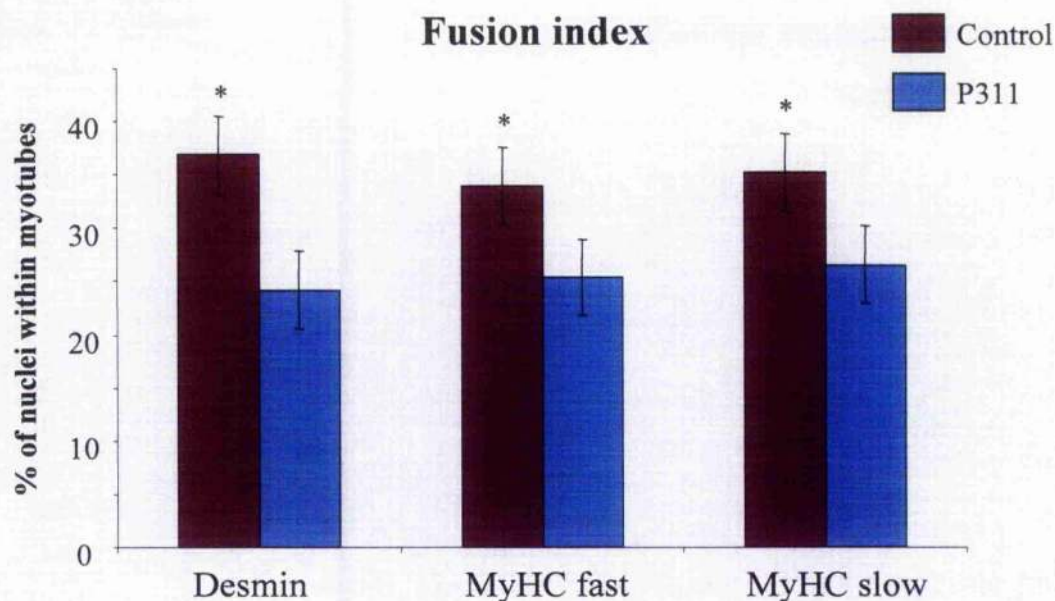
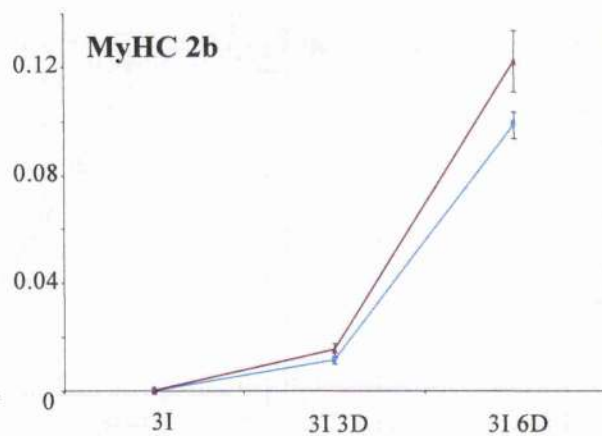
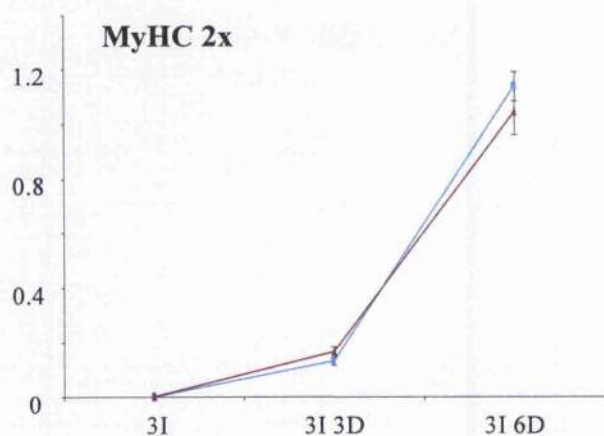
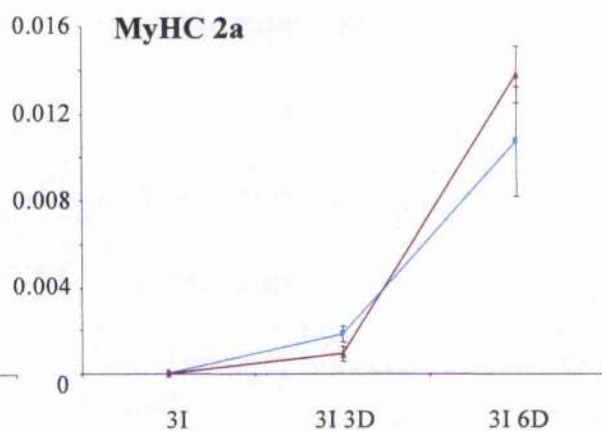
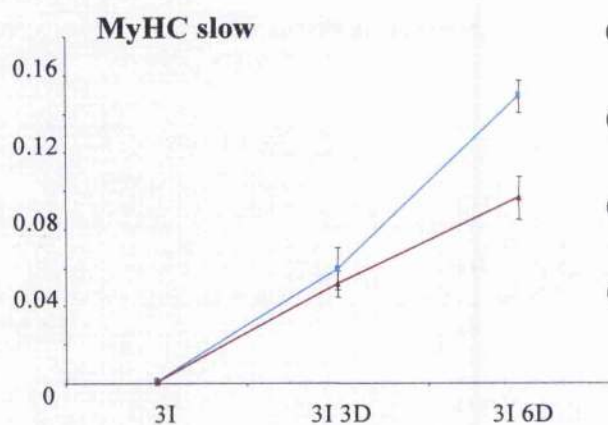
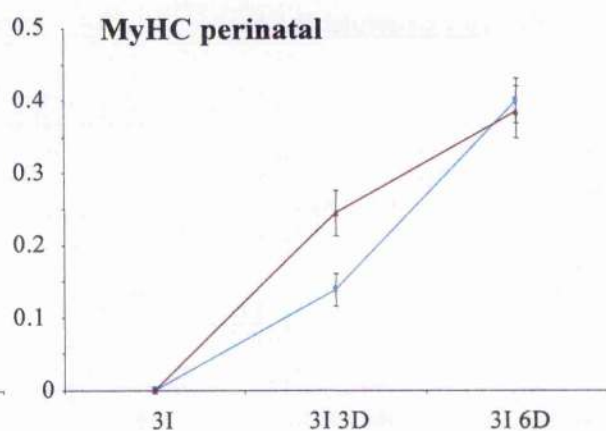
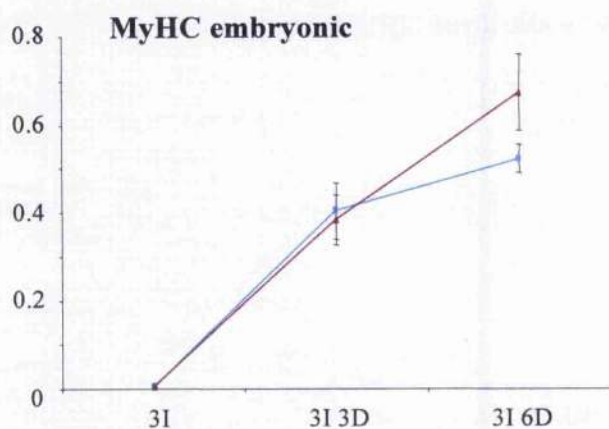
D

Figure 4.12. (D) Over-expression of *P311* reduced C2C12 cell differentiation. Fusion index quantification on immunostained images showed that *P311*-transfected cells resulted in less myotubes formation than control cells. Results were analysed with SAS software, differences between pair-wise combinations of the least square means were tested for significance (* $p < 0.05$). Asterisks indicate statistical significance. Error bars were standard error, $n=3$ replicates from 3 independent experiments.



—■— P311
—▲— GFP

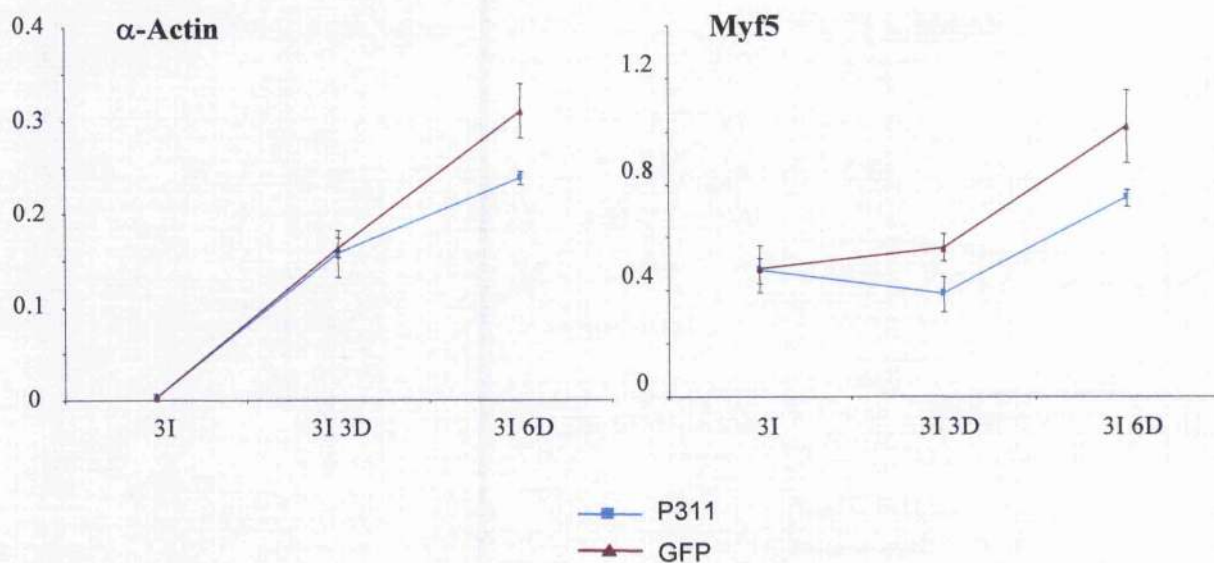
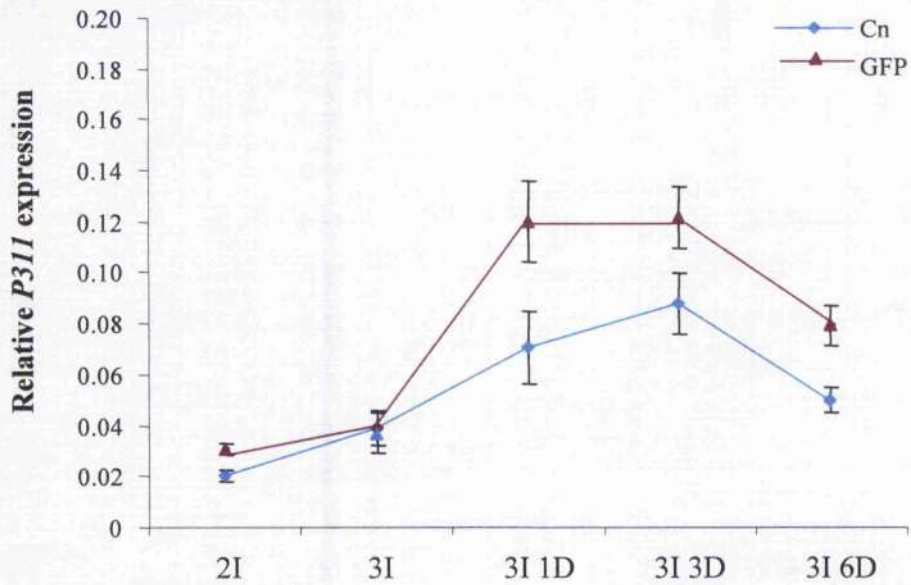


Figure 4.13. Muscle gene expression in P311-adenovirus infected C2C12 cells. Real-time PCR was performed on cDNAs derived from infected cells over a time course as detailed in Fig. 4.11. No dramatic difference in *MyHC* expression between P311-infected and control C2C12 cells was seen during the early infection time points (3I and 3I 3D). Reduction in expression of *MyHC embryonic*, *MyHC 2b*, *Myf-5* and *α-actin* in P311-infected C2C12 myotubes was noticeable at the last time point (3I 6D). Results expressed as mean \pm standard deviation from triplicate samples within the same experiment.

A



B

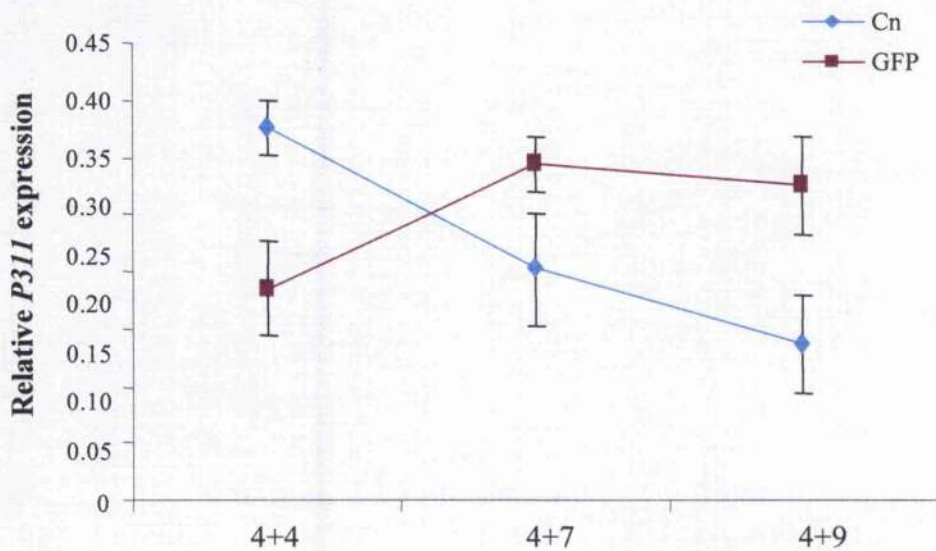


Figure 4.14. Effect of calcineurin over-expression on endogenous *P311* expression in C2C12 cells. (A) Cells were infected with a constitutively active calcineurin (Cn) or GFP-control adenoviral construct in PM for 2 days (2I), or for 3 days (3I), followed by 1 day DM (3I 1D), or 3 days in DM (3I 3D), or 6 days in DM (3I 6D). (B) Cells were also infected as myotubes (at 4 days in DM) for 2 days, followed by a further 2 days in DM (4+4), or 5 days in DM (4+7), or 7 days in DM (4+9). In both series (A and B), extended expression of Cn led to a reduction of *P311* expression. Results expressed as mean \pm standard deviation from triplicate samples within the same experiment.

4.4. Discussion

A full-length porcine *P311* cDNA clone was sequenced and molecularly characterised (Accession. N^o. EF416570). The full-length porcine *P311* cDNA was 2.2 kb and the coding sequence was 0.3 kb in length. The deduced amino acid sequence of porcine P311 is 87% homologous to human P311. P311 does not belong to any known family of proteins, and its cellular function remains largely unclear. To investigate the function of *P311* in skeletal muscle, it is necessary to ascertain its effects in muscle in the context of cell proliferation, differentiation and phenotype determination. In this study, *P311* over-expression led to raised C2C12 cell proliferation and reduced myotube formation (Figs. 4.12.B and C). Consistent with reduced myotube formation, expression of several muscle genes (*MyHC embryonic*, *MyHC 2b*, *α -actin* and *myf-5*) was down-regulated in late differentiation of *P311*-over-expressed C2C12 cells (Fig. 4.13.). *Myf-5*, like *MyoD*, is transcriptionally active in proliferating myoblasts; its exogenous expression can cause non-myogenic cells to differentiate and fuse into myotubes (Ishibashi et al., 2005). No P311 protein was detected with Western blotting because of its highly lability and short half life. However, P311-FLAG fusion protein was detected by immunofluorescence with o-phenanthroline and lactacystin added. To improve P311 protein detection, immunoprecipitation with rabbit polyclonal anti-P311 raised against the synthetic peptide might be useful (Pan et al., 2002).

At present, it is not certain if PCS-associated fibre atrophy is also accompanied by fibre hypoplasia. Given that *P311* expression was down-regulated in PCS muscles (Fig. 3.10.B) and *P311* promoted cell proliferation (Figs. 4.12.A and B), it may have an active role in promoting muscle growth through raised myoblast number. The

aetiology and pathogenesis of PCS remain unknown, but it seems likely that the development of clinical PCS is a function of fibre size and, possibly, fibre number at birth, such that below a certain fibre threshold, the newborn would no longer be able to properly support its own weight. However, there are wide variations in muscle fibre numbers between piglets (Stickland and Handel, 1986).

Previously, *P311* was shown to be involved in glioblastoma cell migration and fibroblast cell proliferation (Mariani et al., 2001; Pan et al., 2002). Moreover, differentiation of neural cells was related to loss of *P311* expression (Taylor et al., 2000). Hence, *P311* may play an active part in the determination of muscle mass through the promotion of myoblast proliferation. The endogenous expression of *P311* was suppressed by Cn over-expression (Fig. 4.14). As Cn is a key mediator of muscle differentiation (Bassel-Duby and Olson, 2003; Michel et al., 2004) it would suggest that *P311* could also have an effect of limiting muscle differentiation.

Recently, expression of *P311* was found to be down-regulated in human lung samples with emphysema and impaired alveolar formation. *P311* was suggested to be involved in protection against injury or it might play a role in the repair or regeneration of damaged lungs (Zhao et al., 2006). Consistently, *P311* expression was found to be down-regulated in almost all PCS muscles (Fig. 3.10). *P311* might be essential for protection, repair or regeneration of damaged skeletal muscles. On the other hand, the reduced *P311* expression could be consequence of muscle atrophy. Clearly, more work is needed to evaluate the *P311* potential in regeneration or repair. In future, to investigate the *P311* potential in regeneration or repair, it will be interesting to study the expression of *MAFbx*, a major atrophy marker, in *P311* over-

expressed cells. Synthetic glucocorticoid dexamethasone could be used to induce atrophy in C2C12 muscle cells (Thompson et al., 1999). The expression of murine *MAFbx* in *P311* over-expressed cells under atrophic condition over a time-course study could then be determined.

Chapter 5

Functional studies of *SPARCL-1*

5.1. Introduction

SPARC like-1 (*SPARCL-1*), also known as MAST9/hevin/SC1, is a matricellular secreted glycoprotein that belongs to the SPARC family. *SPARCL-1* was originally cloned from a rat brain expression library by screening with a polyclonal antibody raised against a synaptic junction glycoprotein (Johnston et al., 1990). *SPARCL-1* contains a follistatin-like domain (FS) and an extracellular calcium binding domain (ES), which are the hallmarks of the SPARC family.

SPARCL-1 was highlighted in PCS skeletal muscle and could be a candidate gene involved in PCS pathogenesis (Maak et al., 2001). It has shown to be a negative regulator of cell proliferation (Claeskens et al., 2000), and down-regulated in many types of cancer cells (Bendik et al., 1998). To investigate the function of *SPARCL-1* in skeletal muscle, it would be necessary to study its effects on muscle cell proliferation, differentiation and phenotype determination. The aims of this study were to first characterise the full-length *SPARCL-1* cDNA clone, and then to apply it on over-expression functional studies.

5.2. Materials and methods

All the commonly used techniques in this section have been previously described in the Materials and Methods Chapter (Sections 2.3, 2.4, 2.5 and 2.6).

5.2.1. *SPARCL-1* cDNA cloning and sequencing

The cDNA of porcine *SPARCL-1* gene was previously isolated in the Molecular Medicine Laboratory, Faculty of Veterinary Medicine, University of Glasgow. The *SPARCL-1* cDNA was housed in a pBK-CMV vector (Stratagene). A series of restriction digestions (Section 2.3.3), followed by DNA electrophoresis (Section 2.3.4) was performed to determine the insert size of *SPARCL-1*. After restriction mapping, *SPARCL-1* cDNA insert was sub-cloned as 2 fragments and sequenced (Section 5.3.1. for details). pBK-CMV vector (Stratagene) and pBluescript II SK(+) vector (Stratagene) were used for the sub-cloning. The sequencing was performed on the *SPARCL-1* cDNA insert with the T3 and T7 primers promoters (as described in Section 2.5).

Open reading frame finder (ORF finder, NCBI) was used to locate the possible starting codon and stop codon within *SPARCL-1*. To amplify the coding region of *SPARCL-1* without the stop codon, the following set of *SPARCL-1* PCR primers was used. An *EcoR* I and a *Xho* I restriction digestion site were engineered into the 5' and 3' primers respectively. The primers are shown below, with the highlighted restriction digestion sites.

SPARCL-1 PCR 5' (sense primer)

5' AA **GAA TTC** GTT GAC AGA GCA GCA GAA TTT 3'

EcoR I

SPARCL-1 PCR 3' (anti-sense primer)

5' AA **CTC GAG** AAA CAG GAG ATT TTC ATC TAT GT 3'

Xho I

Amplification of the ORF was carried out as in Section 2.4. Next, the PCR products were cloned into TOPO- TA cloning vector (Invitrogen) as in Section 2.3.1.2. The resulting colonies were selected for DNA miniprep preparation as described in Section 2.3.2.1. The insert size of *SPARCL-1* was confirmed by digestion with *EcoR* I and *Xho* I. The correct DNA band was excised and directionally cloned into pDNR-CMV for recombinant adenovirus production as described in Section 2.6.4.

5.2.2. *SPARCL-1* cell cultures, transfections and recombinant adenovirus production

C2C12 cells were grown in PM, and replaced by DM when cells reached 80% confluence. The C2C12 cell culture methods are described in Section 2.6.1. For stable transfections, C2C12 cells at 40% confluence in T25 culture flasks were transfected with 6.0 µg *SPARCL-1* pBK-CMV plasmid, by the use of lipofectamine and Opti-MEM, according to manufacturer's instructions (Invitrogen) as detailed in Section 2.6.3. Coding region porcine *SPARCL-1* cDNA was cloned into an adenovirus vector, using the Adeno-X Expression System 2 (BD Biosciences) as described in Section 2.6.4. The *SPARCL-1* construct was cloned as a fusion protein, which comprised a FLAG epitope at the carboxyl-end (Section 2.6.4.1). For time course studies, infection with *SPARCL-1* constructs was used at a multiplicity of infection (MOI) of 5. Cells were infected in PM for 3 days (3I), followed by 3 days in DM (3I 3D), or by 6 days in DM (3I 6D), or 10 days in DM (3I 10D). Stably transfected cells were grown in PM for 3 days (PM), followed by 3 days in DM (DM 3D), or 6 days in DM (DM 6D).

5.2.3. *SPARCL-1* cell cytotoxicity and Western blotting

For cell cytotoxicity assay, a resazurin-based reduction assay that measured the metabolic capacity of cells, was performed according to the manufacturer's protocol (Section 2.6.5). Western blotting was performed as in Section 2.8 with the use of primary anti-FLAG M2 monoclonal antibody (Sigma).

5.2.4. *SPARCL-1* cell proliferation, fusion index and BrdU assay

Thirty thousand C2C12 cells were plated on each 25 cm² flask (three flasks for each *SPARCL-1* pBK-CMV plasmid and pBK-CMV empty plasmid as control), and were grown for up to 5 days in PM. The cell proliferation assay was based on stably transfected cells as described in Section 2.6.6. For fusion index assays, after 9 days in DM, transfected cells were fixed and stained as detailed in Section 2.6.7. BrdU assays on C2C12 cells, infected with *SPARCL-1*-adenovirus and stably transfected with *SPARCL-1* plasmid construct, were performed as previously described (Section 2.6.8).

5.2.5. *SPARCL-1* quantitative real-time RT-PCR

TaqMan quantitative real-time RT-PCR (Applied Biosystems) was performed on a number of murine genes: *MyHC slow*, *MyHC 2a*, *MyHC 2x*, *MyHC 2b*, *Myf5*, *MyHC embryonic*, *MyHC perinatal*, α -actin, β -actin, and porcine *SPARCL-1*. The TaqMan

real-time PCR primer and probe set for *SPARCL-1* were designed using Primer Express v 2.0 software (Applied Biosystems) as in Section 2.7.4. The primers and probe sequences are shown (Table 4.1 and Table 5.1). A relative standard curve method, normalised to β -actin, was used in the quantification of expression. The primer concentration used and the values of the standard curve calculations are shown (Table 4.2 and Table 5.2).

Table 5.1. Sequences of porcine *SPARCL-1* primers and TaqMan probe.

Primer	Sequence 5'→3'
S	TGG GTC CAG CCA CCT ACC T
A	TCT GCA GTT GAA AGC CTG GTT T
P	AAG GTA TTC AAG GTC ACC CCG GAG GA

S, sense; A, antisense; P, TaqMan probe. All probes were 5' labelled with 6-carboxyfluorescein (FAM), and 3' labelled with 6-carboxytetramethylrhodamine (TAMRA).

Table 5.2. Porcine *SPARCL-1* RT-PCR primer concentration and values of standard curve.

Primer concentration of 5':3'(pmol/ μ l)	Standard curve value
300:300	T: 0.018
	S: -3.255
	Y: 14.190

T, threshold; S, slope; Y, y-intercept.

5.2.6. *SPARCL-1* expression in PCS muscle

Muscle collection and TaqMan quantitative real-time RT-PCR (Applied Biosystems) were performed as described in Section 3.2.3.

5.3. Results

5.3.1. *SPARCL-1* cDNA cloning and sequencing

The cDNA of *SPARCL-1* was previously isolated in the Molecular Medicine Laboratory. In vector pBK-CMV, a series of multiple restriction digestions, followed by DNA electrophoresis were performed to determine the insert size of the *SPARCL-1* cDNA (Fig. 5.1). The construct was digested with 8 different combinations of enzymes. (1) *EcoR* I, (2) *Xho* I, (3) *Xho* I + *EcoR* I, (4) *Pst* I, (5) *BamH* I, (6) *BamH* I + *Xho* I, (7) *EcoR* I + *BamH* I and (8) *Xho* I + *EcoR* I (Fig.5.1.A). Digestion results show that the *SPARCL-1* fragment was 2.8 kb, with an internal *BamH* I restriction site (Fig.5.1.B). A *BamH* I restriction enzyme was used to digest the pBK-CMV-*SPARCL-1* into 2 fragments, which were 1.0 kb and 6.3 kb in size. The smaller insert (1.0 kb) fragment was cloned into pBluescript II SK(+) (Stratagene), and the remaining fragment, housing the remaining 1.8 kb of *SPARCL-1* insert was self-ligated (Fig. 5.2).

The full-length of *SPARCL-1* cDNA was sequenced with primers T3 and T7 (ABI Prism 3100 Genetic analyzer). The full-length *SPARCL-1* cDNA was 2.8 kb and the deduced coding sequence was 2.0 kb in length. The full DNA sequence result is shown in Figure 5.3. Basic nucleotide alignment search tool (BLAST) had shown that porcine *SPARCL-1* was 75.2% homologous to human *SPARCL-1*. The deduced amino acid sequence of porcine *SPARCL-1* is shown in Figure 5.4. It was 76% homologous to human *SPARCL-1*. Besides *Homo sapiens*, comparisons with other species were also made. The deduced amino acid sequence of porcine *SPARCL-1* was 66% homologous to mouse *SPARCL-1* and 68% homologous to rat *SPARCL-1*.

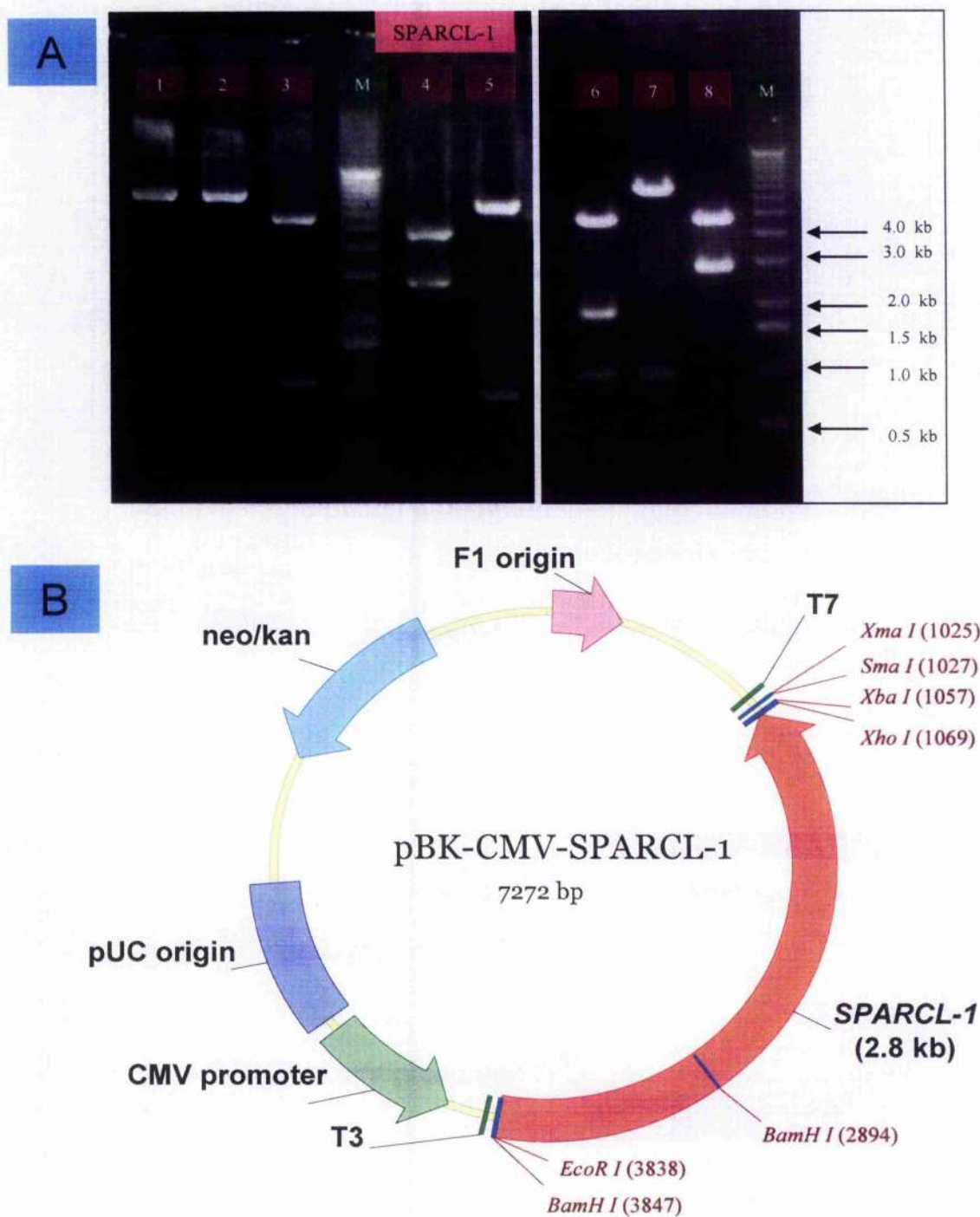


Figure 5.1. Restriction digestion of pBK-CMV-SPARCL-1. (A) Gel electrophoresis of *SPARCL-1* plasmid in pBK-CMV vector after 2 hours of enzyme digestion. The constructs were digested with 8 different combinations of enzymes. (1) *EcoR* I (2) *Xho* I (3) *Xho* I + *EcoR* I (4) *Pst* I (5) *BamH* I (6) *BamH* I + *Xho* I. (7) *EcoR* I + *BamH* I and (8) *Xho* I + *EcoR* I M=marker ladder. (B) The pBK-CMV with *SPARCL-1* insert, 7.3 kb. The *SPARCL-1* cDNA was 2.8 kb with an internal *BamH* I restriction site within.

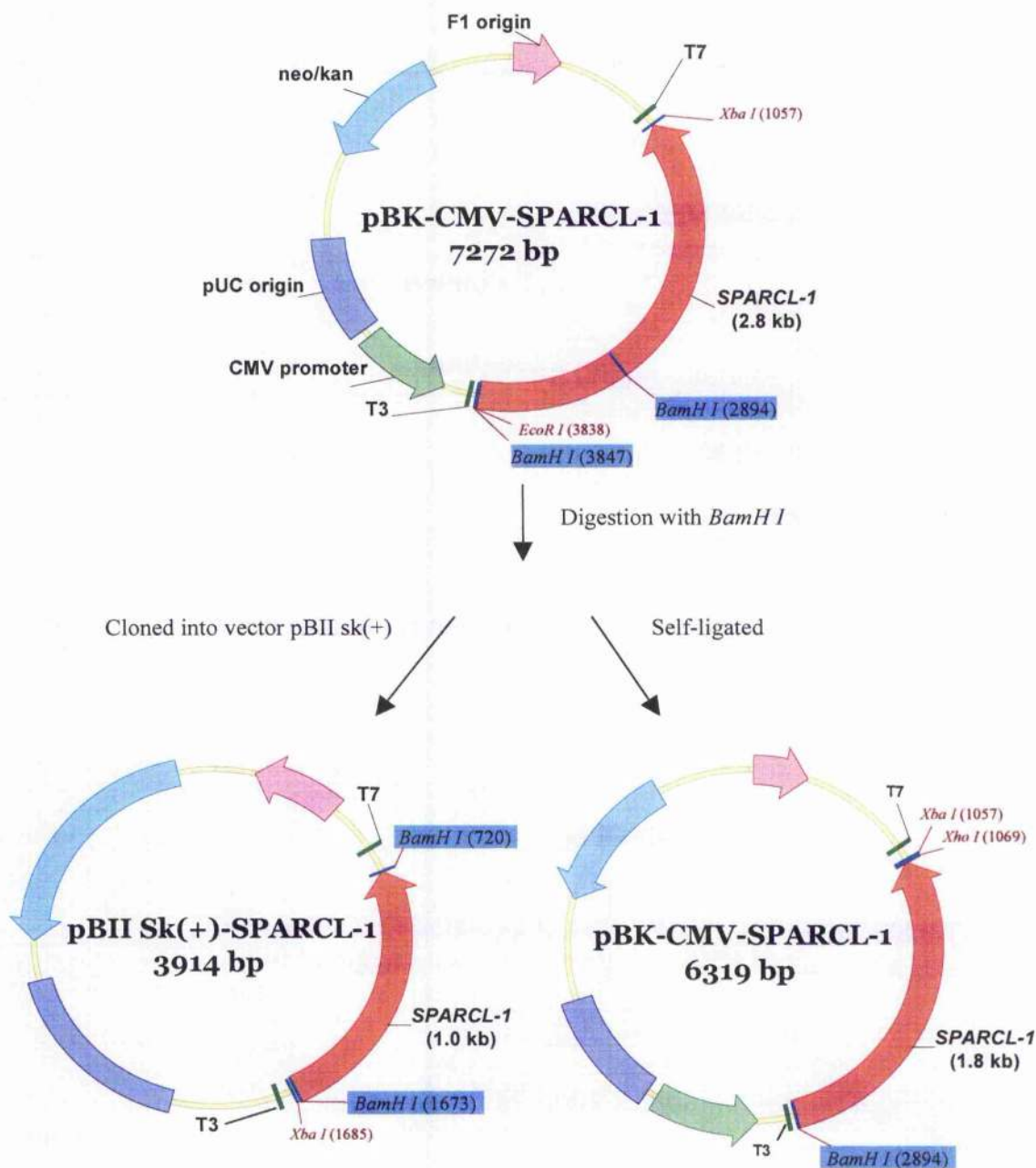


Figure 5.2. Sub-cloning of SPARCL-1. A *Bam* H I restriction enzyme was used to digest the pBK-CMV-SPARCL-1 into 2 fragments, which were 1.0 kb and 6.3 kb in size. The smaller fragment was cloned into pBluescript II SK(+) (Stratagene), and the remaining fragment was self-ligated. *Bam* H I restriction sites highlighted in blue.

GTGATCCAAAGAATTTCGGCACGAGACAGCCTGAAATACGTCCCAGTGCCAACTCCAAAT 60

 TCATCTGTACCTCAGACCCTGACTAGTTGACAGAGCAGCAGAATTCAACTCCAATAGA 120

 CCTGAATGTGTTTCTGGGCAAAGAAGCAGAGCTAACGAGGAAAGAGATATATAGAGTATT 180

 GGGTATTTGTCAAACCTTTATTTCTGGCTGTGTGCAAAGAGAAGATTCAACTTCAATT 240

 CCTGCCAAGGCTCTGGGTCGCGCCACTACGAAGGTATTCAGGTCACCCCGGAGGAG 300

 AAAACCAGGCTTTCAACTGCAGATGGATGCTGCGGATACTACAACCAGGAGGGGTAGAAA 360
 *TTGCTCGCAAAAGTTCAGCT*****
 GATTAAGACTCTGCTTTTCTCCTGTACATTTGGGAACGGCAGCTGCAGTCCCGACACA 420

 AGCCAGGTTCCCATCTGATCATTCCAACCCAACTGCTGCTTCCTTAAGTTCCTTCCAGCA 480

 GGCTGAAACGTTGGTAACAGCGGAGCAGACTGCAACCCCACTGGAAGGGTTGAAGATGC 540

 AGAAAGGAAAAGGAACAGCAGTGTCCTTAGAAGAGCATCCTATCATAAGGCTGAAAA 600

 ATCTTCAGTACTAAAGTCAAAGCAGGAAGACCATGAAGAGTCAGCAGACCAGGACCAGAG 660

 CTACAGCCAAAACCTGGGATCACAGGAACATGAGAAAAGTGAAAGAGACTTAATTGAGAA 720

 CTCCGAGTATATGCCAACTGAAGGTACATTGGACCTAAAAGAAGATGACTGAACCTCA 780

 AAAGGAAAAATCCCAGAGAGCATTGATTCCTTGGTCATGATGACAGTTCCATTGTAGA 840

 TTCTAACCAACAAGAAAGTATCAGAAAAGCAGAGGAAAACCAAGACTCACATCCTCAACT 900

 GAACGGGAGCAGTAAACATAGCCAGATCTAAGTGACCGAGGAAACCAAGGGCAGGATCC 960

 AGATAGTCCAACCTGGAGAAGAGGAAGGGGAAAAAGGCCACATGAAGTTGATACCTCTT 1020

 CGACAACCAAGAAGAGGAGAGAGAAGTGTCCAGGAGCAGTCTAACAGCGAGCAGGAAGA 1080

 AGACAGTACCCGATCAGATGACATCTTGAAGAGTCTTACCAACCAACTCAAGCAAGCAA 1140

 GATGCAGAAAGATGAATTTGAGCAGGGTAATCAAGGACGAGAAGAGGAAAACGCCAATGC 1200

 AGAAACAGAAGAGGAAACTGCCTCAAAAATCACTAAGCCCAATCAAGAAAGAGAATGGCA 1260

 GAGCCCAAGAGGAAAGCCTGGCCTTGAAGTTATCAGCAACCACGAGGAGATGGATAAAAA 1320

 GACCCTTGCTAAGCCTTTGTTGGTGGAGCCTACTGATGATGATAACGTCATGCCAGAAA 1380

 TCACGGGGCCGATGATGACAGTGATGATGATGATGAACACAACGCAAGTGAGGACGCCTT 1440

 CAACCCAGTGAGGCTTATCTGGAGCGTGAAAGAGCTCCATCCAATTACTACCACACCAA 1500

```

ATACGAGGAGCAAAGAGAAAAAGCACATGAGGGTGAGAATGTAGATACCAGCGAAGCTGC 1560
*****

AGAAAACCAAGGGGCCAAGAAAGCAGAGGGGCTACCAAATGAAGATGACAGTTCAACTGA 1620
*****

AGGCACCACGAGGGGGCACAGTGTGATTCTTGCATGAGCTTCCAGTGTAAGAGGACA 1680
*****

CATCTGCAAGGCTGATCAACAGGGAACCCCACTGTGTTGCCAAGACCCAGTGACATG 1740
*****

TCCTCCTACAAACTCCTTGACCAAGTTTGTGGCACTGACAATCAGACCTATGCCAGCTC 1800
*****

CTGTCTATCTCTTTGCTACCAAGTGCAGACTGGAGGGGACGAAAAGGGGCACCAACTGCA 1860
*****

GCTGGATTACTTTGGAGCCTGCAAATCTATTCTGCTGTACGGACTTTGAAGTGACCCA 1920
*****

GTTTCCTCTAAGGATGAGAGACTGGCTCAAGAATATCCTCATGCAGCTTTATGAGCCTAA 1980
*****

CCCTGAACATGCTGGATATCTAAATGAGAAGCAGAGAAATAAAGTCAAGAAAATTTACCT 2040
*****

GGATGAAAAGAGGCTCTTGGCTGGGGACCATTCCATCGACCTTCTCTTAAGGGACTTTAA 2100
*****

GAAAAACTACCACATGTATGTGTATCCCGTGCAGTGGCAGTTCAGTGAGCTTGACCAACA 2160
*****

TCCGCGGGACAGAGTCTTGACCCACTCTGAGCTCGCTCCTTTGCGAGCATCGCTGGTGCC 2220
*****

CATGGAACACTGCATAACACGCTTCTTTGGAGAGTGTGACCCCAACAAGGATAAGCACAT 2280
*****

CACCTGAAGGAGTGGGGCCGTGCTTTGAAATTAAAGAAGAAGACATAGATGAAATCT 2340
*****

CCTGTTTTGAATTAAGATTGAAAGAACTCAAACCTTTCTGCATCCTCCTGTTTGTATCA 2400
*****

CTTCTCAAGCATATGCAACGTGATACTTATAGATTTATATTAGCAAAATGCTTGATGT 2460
*****

CTAAGACAATGAGAGTAAGTGCCTTGATAACAGTATGTACACCAGGCATTTAACATTAAGT 2520
*****

TTGGAATACAACGTTTAAATTAAGTAAAGTCAGTATTGCAAAATACTATACACTGTGA 2580
*****

ACAGTTTAAGTCTCACTCCCTGCACCCATTACAAAATACTTAGATTATAACATCCCCC 2640
*****






CCAAAAAATACATTCTTTGTCCATTATCATGTGCACTTCAAAAAAGTGAATAAT 2700
*****

GTCCTTGTGCTGATGTGTTTCAATATCTTAATATTCTAATAAAATCTATAAAATCT 2760
*****

AAAAAAAAAAAAAAAAATCTCGAG 2785
*****

```

Figure 5.3. Full length nucleotide sequence of porcine *SPARCL-1* cDNA.

 SPARCL-1 PCR 5' and 3' primers
 Start / stop codon
 SPARCL-1 real-time RT-PCR 5 and 3' primers
 SPARCL-1 real-time RT-PCR probe
 SPARCL-1 internal detection 5 and 3' primers

pig (1) MKTLLFLLYILGTAAAVPTQARFSPDHSNPTAAslssfqgaeTLVTAEQTATPTGRVEDA
 human 76.0% (1) MKTGPFFLCLLGTAAPITNARLLSDHKSPTAE-----T-VAPDNTAIPSLWAEAE
 mouse 66.0% (1) MKAVLLLLCALGTAVAIPTSTRFLFDHSNPTTA-----TLVTPEDATVPIAGVEAT
 rat 68.0% (1) MKAVLLLLLYALGIAAAVPT--TFLSDHSNPTSA-----TLPTLEDATVPTVPAEAA

pig (61) EKEKEPAVSLEEHPYHKA EKSSVLKSKQEDHEESADQDQSYSONLGSQEHEKSERDLIEN
 human (51) ENEKETAVSTEDDSHHKA EKSSVLKSKEESHEQSAEQGKSSSQELGLKDQEDSDGHLNVN
 mouse (52) A-----DIENHPNDKA EKPSALNSEEEETHEQSTEQDKTYSFEVDLKDDEEDGDGDL---
 rat (50) A-----DIEKHPNHKA EKPSALNSEEEAHEQSTEQDKTYSFEVDLKDDEEDGDGDL---

pig (121) SEYMPTEG--TLDLKEDMTEPQKEKFPESIDSLGHDDSSIVDSNQGESITKAEENQD---
 human (111) LEYAPTEG--TLDIKEDMIEPQEKLSSENTDFLAPGVSSFTDSNQGESITKREENQEOPR
 mouse (102) SVD-PTEGtLTLDLQEGTSEPQQKSLPENGDFPATVSTSYVDPNQRANITKGKESQEOPV
 rat (100) SVD-PTER--TLDLQEGTSEPQQKRLPENADFPATVSTPFVDSQDPANITKGEESQEOPV

pig (176) --SHPQLNGSSKHSPDLSDRGNQGQDPDSPT-----GEEEGEKEPHEVDTLFDNQEE
 human (169) NYSHHQINRSSKHSSQGLRDQGNQEOPNIN-----GEEEEKEPGEVGTHTNDNQER
 mouse (161) SDSHQPNESKQTQDLKAESQTQDPDIPNeeeeeeedEEEEEEEPEDIGAPSDNQEE
 rat (157) SDSHQQDESQKQTQDSMTEESHKQDPGIPN-----EEKEEEEDPEDVGAPSDNQEE

pig (226) EREVLQEQQSNSEQEDSTRSDDILEESYQPTQASKMQKDEFEQGNQGrEEENANAETEEE
 human (221) KTELPREHANSKQEDNTQSDDILEESDQPTQVSKMQEDEFDQGNQE-QEDNSNAEMEEE
 mouse (221) GKEPLEEQPTSKWEGNREQSDDTLEESSQPTQISKTEKHQSEQGNQG-QESDSEAEGEDK
 rat (209) EKEPPEEQPTSKWEGNGDQSEDILQESSQPTQISKT-KNDFEQGSQG-QEGDSNAEGEDK

pig (286) TASKITKPNQEREWQSPEGKPGLEVISNHEEMD-KKTLAKPLLVPTDDDNVMPRNHGA-
 human (280) NASNVNKHIEQTEWQSQEGKTGLEAISNHKETE-EKTVSEALLMEPTDDGNTTPRNHGVd
 mouse (280) AAGS-KEHIPHTEQQDQEGKAGLEAIGNQKDTD-EKAVS----TEPTDAA-VVPRSHGG-
 rat (267) AAGS-KEHLPHTEWQQEGRAGLDAIGNRKDTDeKAVS----TEPTDAA-VVPRNHGA-

pig (344) ---DDSDDD---DD-EHNASDAFNPSEAYLERERAPSNNYYHTKY--EEQREKAHEGENV
 human (339) dDGDGDDGDDggtDGpRHSASDDYFIPSQAFLEAERAQSIAYHLKI--EEQREKVHENENI
 mouse (332) -AGDNGGGD---DS-KHGAGDDYFIPSQEFLEAERMHSLSYLYKYggGEET-TTGESEN-
 rat (320) --SDNGGGD---DS-KHGASDDYFIPSQEFLEAERMHSLSYLYKY--GEET--PDESEN-


```

      . . . * + + * * * | * * * * * + * . * . + + . * * + . * . * + + * * * + * * * * * + * * + * - + * * * * *
pig      (395) DTSEAAENQGAKKAEGSPNEDUSSTEGITRGHSVDSCMSFQCKRGHICKADQQGKPHVCV
human    (397) GTTEPGEHQEAKKAENSSNEEETSSEGNMRVHAVDSCMSFQCKRGHICKADQQGKPHVCV
mouse    (395) -RREAADNQEAKKAESSPNAEPSD-EGNSREHSAGSCTNFQCKRGHICKTDPQGKPHVCV
rat      (369) -RSEAGDNQGAKKAESSPNAEPSD-EGNSRGHSADSCMNFQCKRGHTCKTDQUGKPHVCV

      * * * . * * * * * + * . * * * + * * * * * + * * * * * + * * * * * + * * * * * + * * * * * + * * * * * + * * * * *
pig      (455) QDPVTCPPPTKLLDQVCGTDNQTYASSCHLFATKCRLEGTKKGHQLQLDYFGACKSIPACT
human    (457) QDPVTCPPPTKLLDQVCGTDNQTYASSCHLFATKCRLEGTKKGHQLQLDYFGACKSIPACT
mouse    (443) QDPVTCPPPAKILDQACGTDNQTYASSCHLFATKCRLEGTKKGHQLQLDYFGACKSIPACT
rat      (427) QDPVTCPPPAKILDQACGTDNQTYASSCHLFATKCMLEGTKKGHQLQLDYFGACKSIPACT

      * * * . * * * * * + * * * * * + * * * * * + * * * * * + * * * * * + * * * * * + * * * * * + * * * * * + * * * * *
pig      (515) DFEVTQFFPLMRDWLKNILMQLYEPNPEHAGYLNEKQRNKVKKIYLDEKRLLAGDHSIDL
human    (517) DFEVTQFFPLMRDWLKNILMQLYEANSEHAGYLNEKQRNKVKKIYLDEKRLLAGDHPIDL
mouse    (503) DFEVAQFFPLMRDWLKNILMQLYEPNPKHGGYLNEKQSKVKKIYLDEKRLLAGDHPIEL
rat      (487) DFEVAQFFPLMRDWLKNILMQLYEPNPKHGGYLNEKQSKVKKIYLDEKRLJAGDHPIEL

      * * * * * + * * * * * + * * * * * + * * * * * + * * * * * + * * * * * + * * * * * + * * * * * + * * * * *
pig      (575) LLRDFKKNYHMYVYPVHWQFSELDQHPDRVLTHSELAPLRASLVPMEHCITRFFEECDP
human    (577) LLRDFKKNYHMYVYPVHWQFSELDQHPMDRVLTHSELAPLRASLVPMEHCITRFFEECDP
mouse    (563) LLRDFKKNYHMYVYPVHWQFSELDQHPADRILTHSELAPLRASLVPMEHCITRFFEECDP
rat      (547) LLRDFKKNYHMYVYPVHWQFSELDQHPADRILTHSELAPLRASLVPMEHCITRFFEECDP

      * * * * * + * * * * * + * * * * * + * * * * * + * * * * * + * * * * * + * * * * * + * * * * * + * * * * *
pig      (635) NKDKHITLKEWGRCFEIKEEDIDENLLF
human    (637) NKDKHITLKEWGHCFGIKEEDIDENLLF
mouse    (623) NKDKHITLKEWGHCFGIKEEDIDENLLF
rat      (607) NKDKHITLKEWGHCFGIKEEDIDENLLF

```

* = homologous; + = limited homologous; . = not homologous.

Figure 5.4. Pile-up of SPARCL-1 deduced amino acid sequences for pig, human, mouse and rat.

Only 76% homology amino acid sequence was found between porcine and human *SPARCL-1*. However, when compared the FS domain and EC domain, it shows 100% and 98.6% similarity between the 2 species (Fig. 5.5). Moreover, porcine and mouse *SPARCL-1* also has shown 99.8% and 98.6% similarity for FS domain and EC domain. The differences between the species were mainly at Domain I.

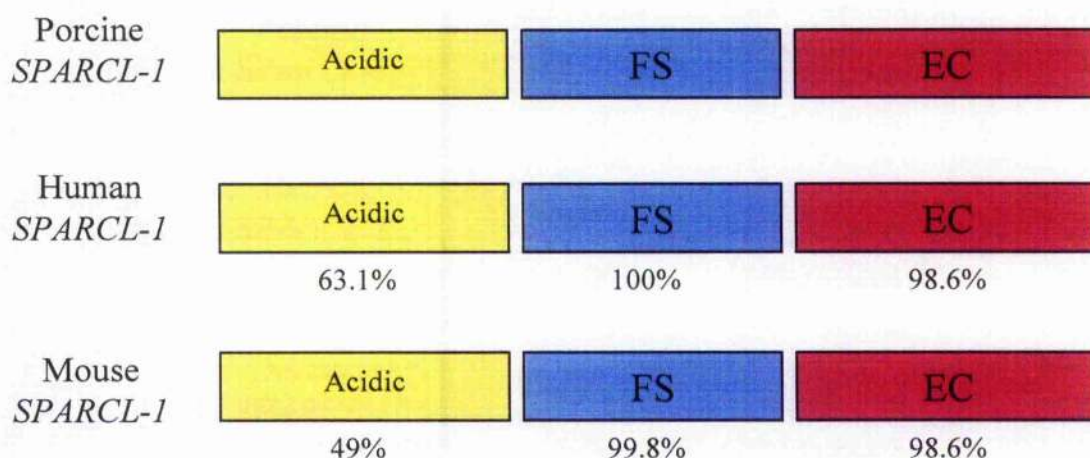


Figure 5.5. Comparison of *SPARCL-1* domain deduced amino acid sequences for pig, human and mouse.

5.3.2. Recombinant *SPARCL-1* adenovirus production

The *SPARCL-1* PCR 5' and 3' primers were used to amplify the coding sequence of *SPARCL-1* in PCR. Gel electrophoresis of the 2.2 kb RT-PCR products is shown in Figure 5.6.A. TOPO-*SPARCL-1* vector was digested with *EcoR* I and *Xho* I restriction enzymes to ascertain the *SPARCL-1* insert (Figs. 5.6.B and C). The required DNA insert was excised and cloned into pDNR-CMV for recombinant adenovirus production. pDNR-CMV-*SPARCL-1* vector was digested with *EcoR* I and *Xho* I restriction enzymes to ascertain the clones containing the appropriate *SPARCL-1* insert (Figs. 5.7.A and B).

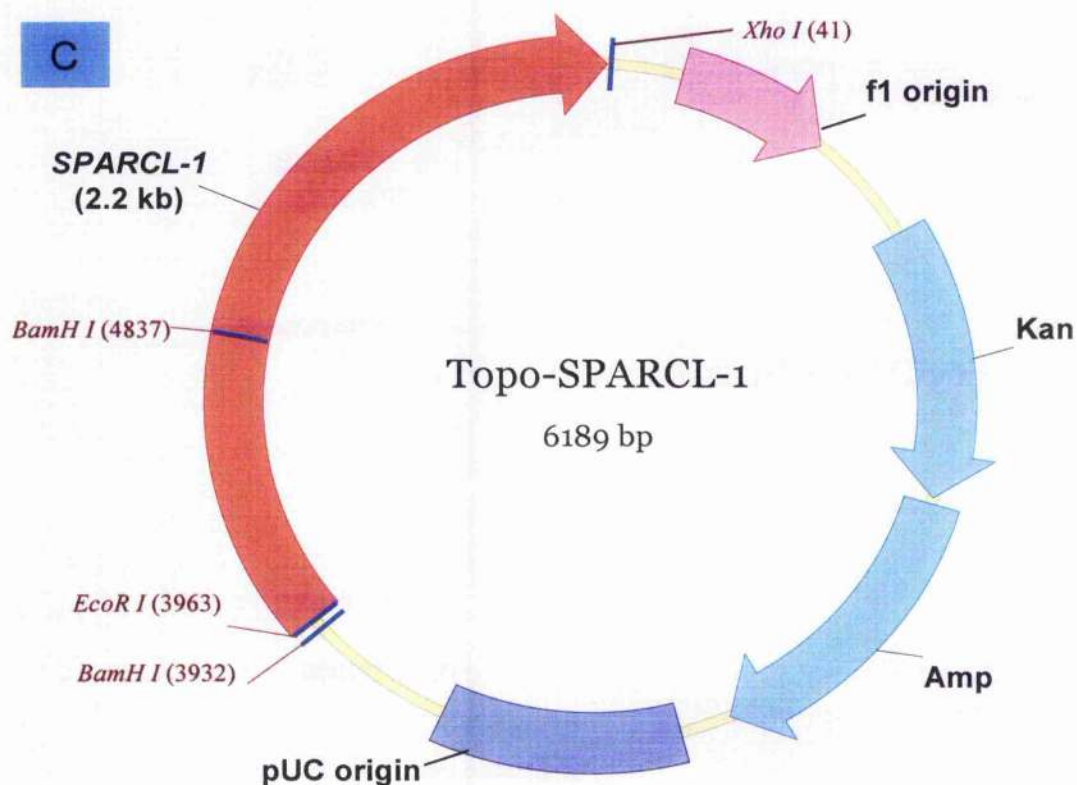
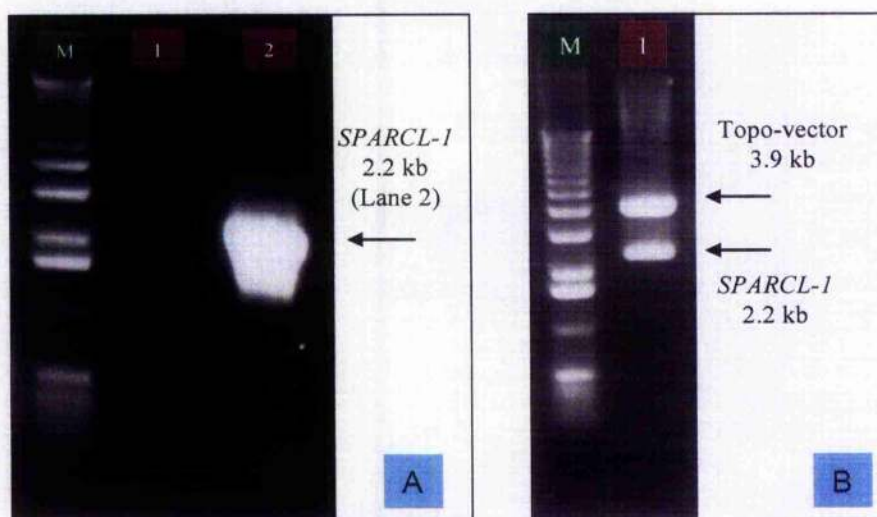


Figure 5.6. Cloning of *SPARCL-1* into TOPO vector. (A) Gel electrophoresis of the 2.2 kb RT-PCR with the use of sense and anti-sense primers (Lane 2). Sense primer with template DNA alone in Lane 1 as control; no band was detected. (B) Gel electrophoresis after digestion of TOPO-SPARCL-1 with *Xho I* and *EcoR I*; *SPARCL-1* segment (2.2 kb) and topo vector (3.9 kb) were shown. (C) TOPO vector with *SPARCL-1* insert. The *SPARCL-1* insert is about 2.2 kb with *EcoR I* restriction in 5' and *Xba I* restriction site in 3' ends.

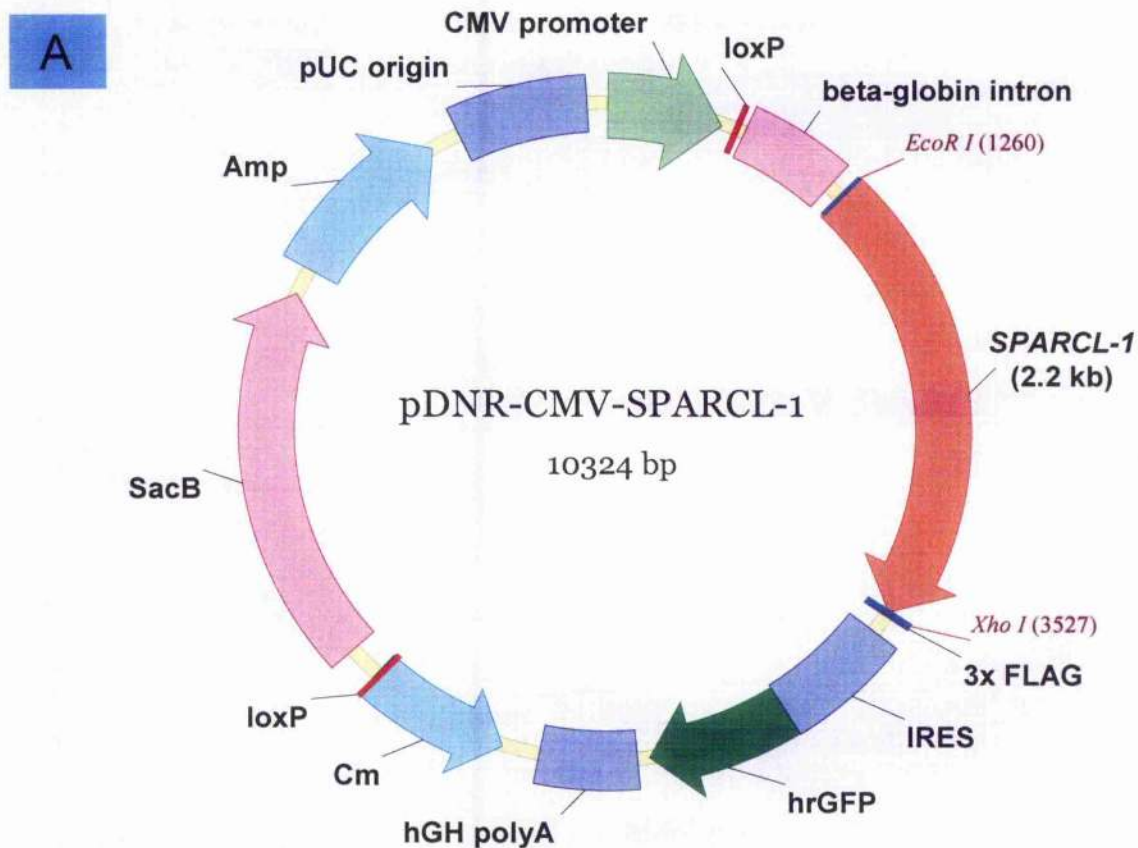


Figure 5.7. Cloning of *SPARCL-1* into pDNR-CMV vector. (A) The pDNR-CMV with *SPARCL-1* cDNA insert is 10.3 kb. The *SPARCL-1* fragment is 2.2 kb with *EcoR I* restriction in 5' and *Xho I* restriction site in 3' ends. (B) Digestion of pDNR-CMV-*SPARCL-1* with *Xho I* and *EcoR I*. Lanes 1-5 are clones with the appropriate cloned 2.2 kb insert.

After the correct pDNR-CMV-SPARCL-1 clones were identified by restriction mapping, gene sequencing was performed to confirm an intact start codon at the 5' end and a FLAG epitope was cloned in frame at the 3' end. *SPARCL-1* internal 5' primer (5' TGG GTC CAG CCA CCT ACC T 3') was used to detect the start codon at the 5' end. Another *SPARCL-1* internal 3' primer (5' CAC TCT GAG CTC GCT CCT TTG 3') was used to detect FLAG epitope at the 3' end. These primers used are highlighted in grey in Figure 5.3. Sequencing results confirmed that both the start codon and the FLAG epitope are correctly cloned. The sequence of the FLAG epitope at the 3' end is shown (Fig. 5.8).

Nucleotide sequence

GAAAATCTCCTGTTT CTC GAG GAC TAC AAG GAT GAC GAT GAC AAG GAT TAC AAA
 GAC GAC GAT GAT AAG GAC TAT AAG GAT GAT GAC GAC AAA TAA TAG
 CAATTCCTCGACGACTGCATAGGG

Deduced amino acid sequence

ENLLFLE DYKDDDDK DYKDDDDK DYKDDDDK Stop Stop
 QFLDDCIG

Figure 5.8. 3x FLAG and stop codon of *SPARCL-1* in pDNR-CMV vector. The 3X FLAG sequence is highlighted in blue, while the stop codon is highlighted in red.

5.3.3. *SPARCL-1* over-expression in C2C12 cells by adenovirus infection and by stable transfection

To assess the function of *SPARCL-1* in muscle cells, *SPARCL-1* was over-expressed in C2C12 muscle cells by stable transfection with pBK-CMV-*SPARCL-1* plasmid (Fig. 5.7.A) as well as by infection with a *SPARCL-1*-adenovirus construct (Fig. 5.9).

Expression of both constructs could be demonstrated by SPARCL-1 mRNA detection (Fig. 5.9.A). Cell cytotoxicity assays that measured metabolic capacity showed no significant difference between infected/transfected cells, and control cells over an extended period of 10 days differentiation, which indicated similar cell viability (Fig. 5.9.B). This finding also indicates that over-expression of *SPARCL-1* is not detrimental to C2C12 cells. Western blot was performed to detect SPARCL-1 proteins. SPARCL-1 is a secreted matricellular protein. However, no prominent SPARCL-1 bands were detected with anti-FLAG primary antibody (Sigma) (data not shown). The secretion of SPARCL-1 might account for the failure of its detection by conventional Western analysis.

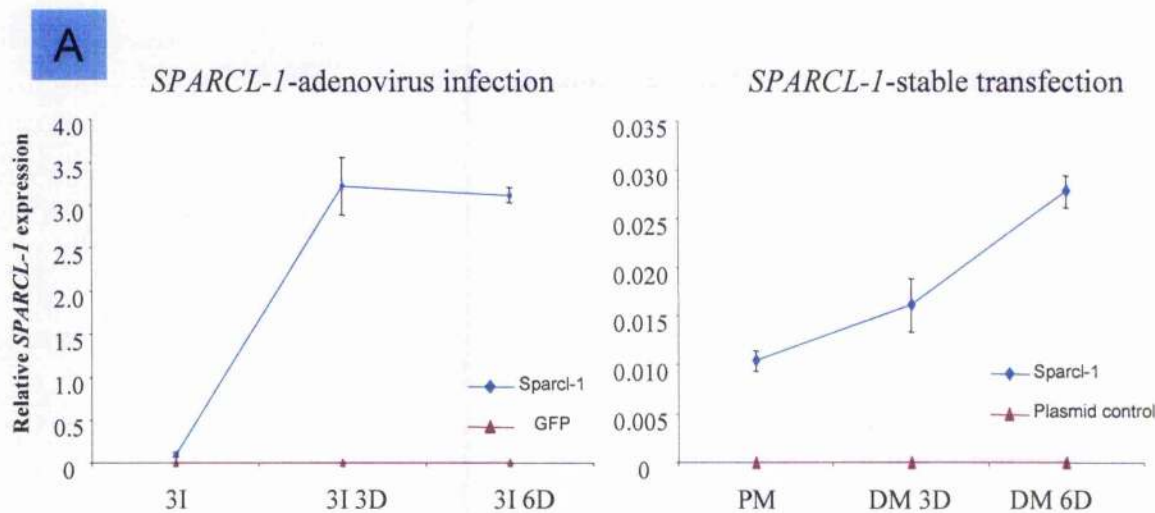


Figure 5.9. (A) Over-expression of *SPARCL-1* in C2C12 cells. *SPARCL-1* expression, through infection with an adenovirus construct and through stable transfection with an expression plasmid (Fig.5.1.B), was determined over a time course. Proliferating cells were infected for 3 days in proliferation medium [PM] (3I), followed by 3 days in differentiation medium [DM] (3I 3D) or 6 days in DM (3I 6D). Stably transfected cells were incubated for 3 days in PM (PM), followed by 3 days in DM (DM 3D) or 6 days in DM (DM 6D). Results expressed as mean \pm standard deviation from triplicate samples within the same experiment.

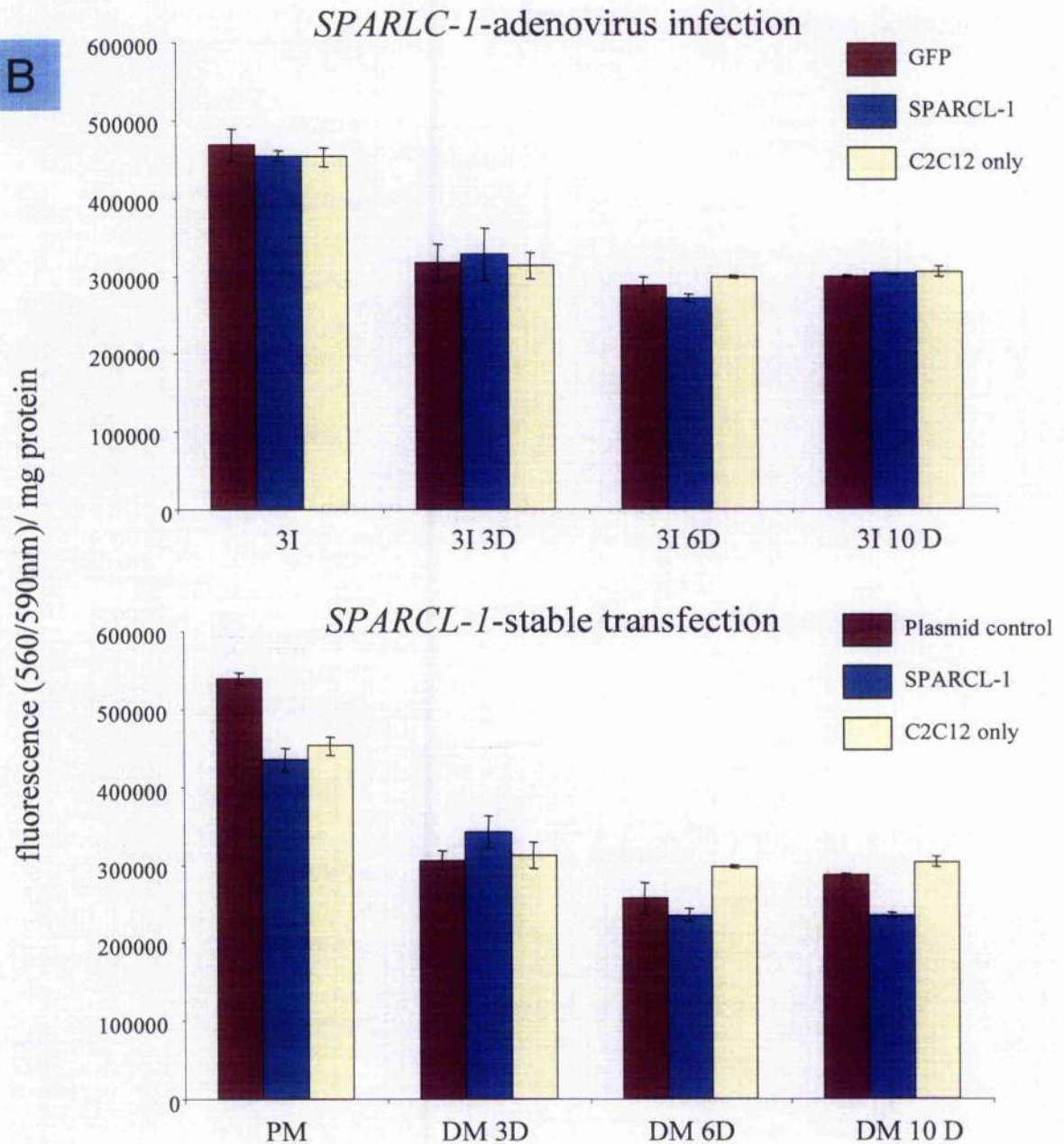


Figure 5.9. (B) Cell viability assay of *SPARCL-1*-infected and *SPARCL-1*-stably transfected C2C12 cells. The viability of *SPARCL-1*-infected and *SPARCL-1*-transfected C2C12 cells was similar to control cells over an extended culture period, as demonstrated by cell cytotoxicity assay (CellTiter-Blue kit, Promega). Results expressed as mean \pm standard deviation from triplicate samples within the same experiment.

5.3.4. *SPARCL-1* over-expression decreased C2C12 cell proliferation but did not affect fusion

Proliferation assays were performed in stably transfected C2C12 cells by quantifying cell number with a Neubauer haemocytometer. *SPARCL-1* over-expressed C2C12 cells showed significant decreases in cell proliferation compared with plasmid control cells (Fig. 5.10.A). In addition, BrdU assays were performed on *SPARCL-1* adenovirus infected and stably transfected C2C12 cells. Both constructs showed a decrease in proliferation compared with control GFP cells (Fig. 5.10.B). *SPARCL-1*-stably transfected C2C12 myotubes (differentiated for 9 days) were separately immunostained for desmin, MyHC fast and MyHC slow, along with DAPI nuclei staining (Fig. 5.10.C). Fusion index quantification on immunostained images showed no significant difference between *SPARCL-1*-transfected and control cells (Fig. 5.10.D).

5.3.5. *SPARCL-1*- over-expression depressed expression of muscle genes

No obvious differences in *MyHC* expression were detected between *SPARCL-1*-infected and control C2C12 cells at the early infection time point (3I) (Fig. 5.11). However, reductions in the expression of all skeletal *MyHC* isoforms, *Myf-5* and α -*actin* in *SPARCL-1*-infected C2C12 myotubes were noticeable at the later stages of differentiation (3I 3D and 3I 6D). The overall results of extended *SPARCL-1* over-expression indicated a reduction in the expression of regulatory and structural muscle genes.

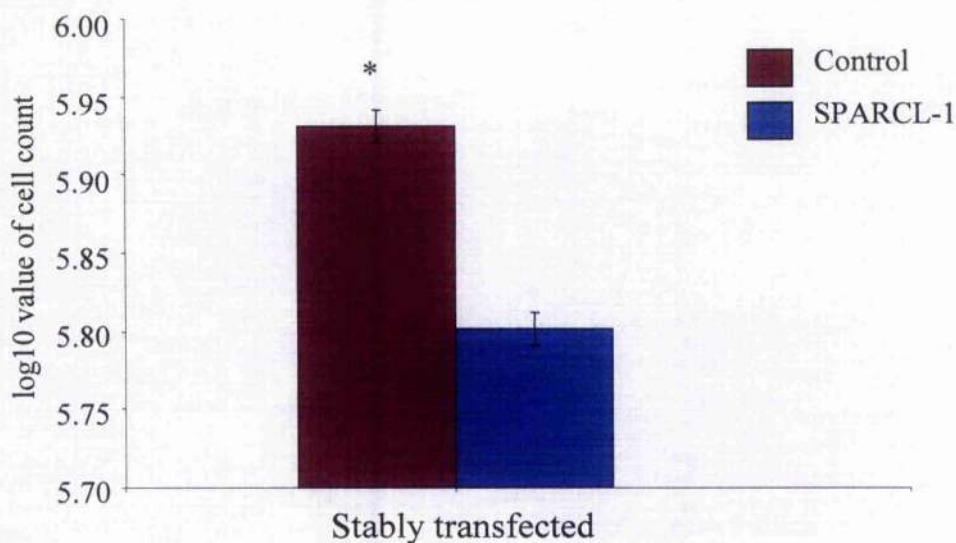
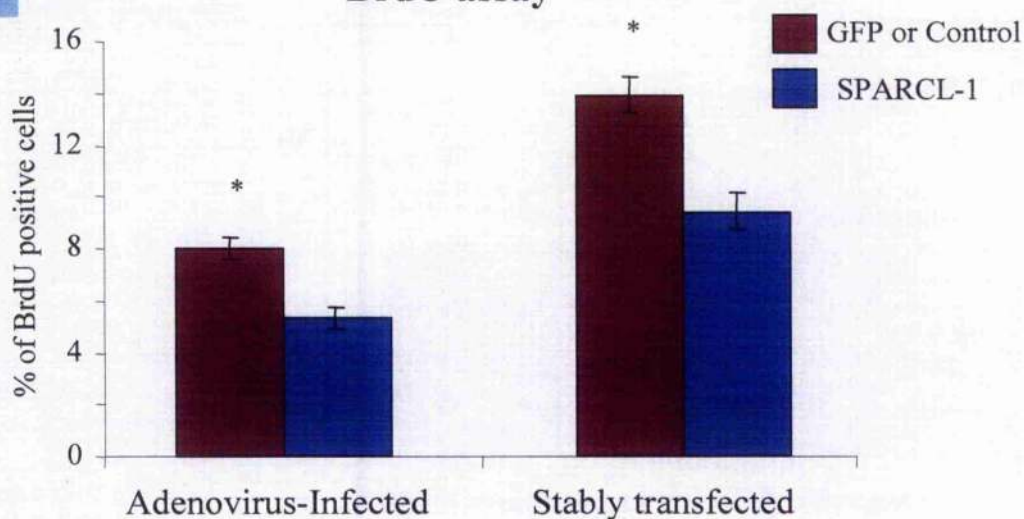
A**Proliferation Assay (haemocytometer based)****B****BrdU assay**

Figure 5.10. Over-expression of *SPARCL-1* reduced C2C12 cell proliferation. (A) *SPARCL-1* over-express C2C12 cells showed significant reduce in cell proliferation compared with plasmid control cells. (B) BrdU assay was performed on *SPARCL-1*-infected and adenovirus-GFP control cells, as well as *SPARCL-1*-transfected and vector only-transfected cells. For both approaches, *SPARCL-1* over-expression significantly reduced cell proliferation. Results were analysed with SAS software, differences between pair-wise combinations of the least square means were tested for significance (* $p < 0.05$). Error bars were standard error, $n=3$ replicates from 3 independent experiments.

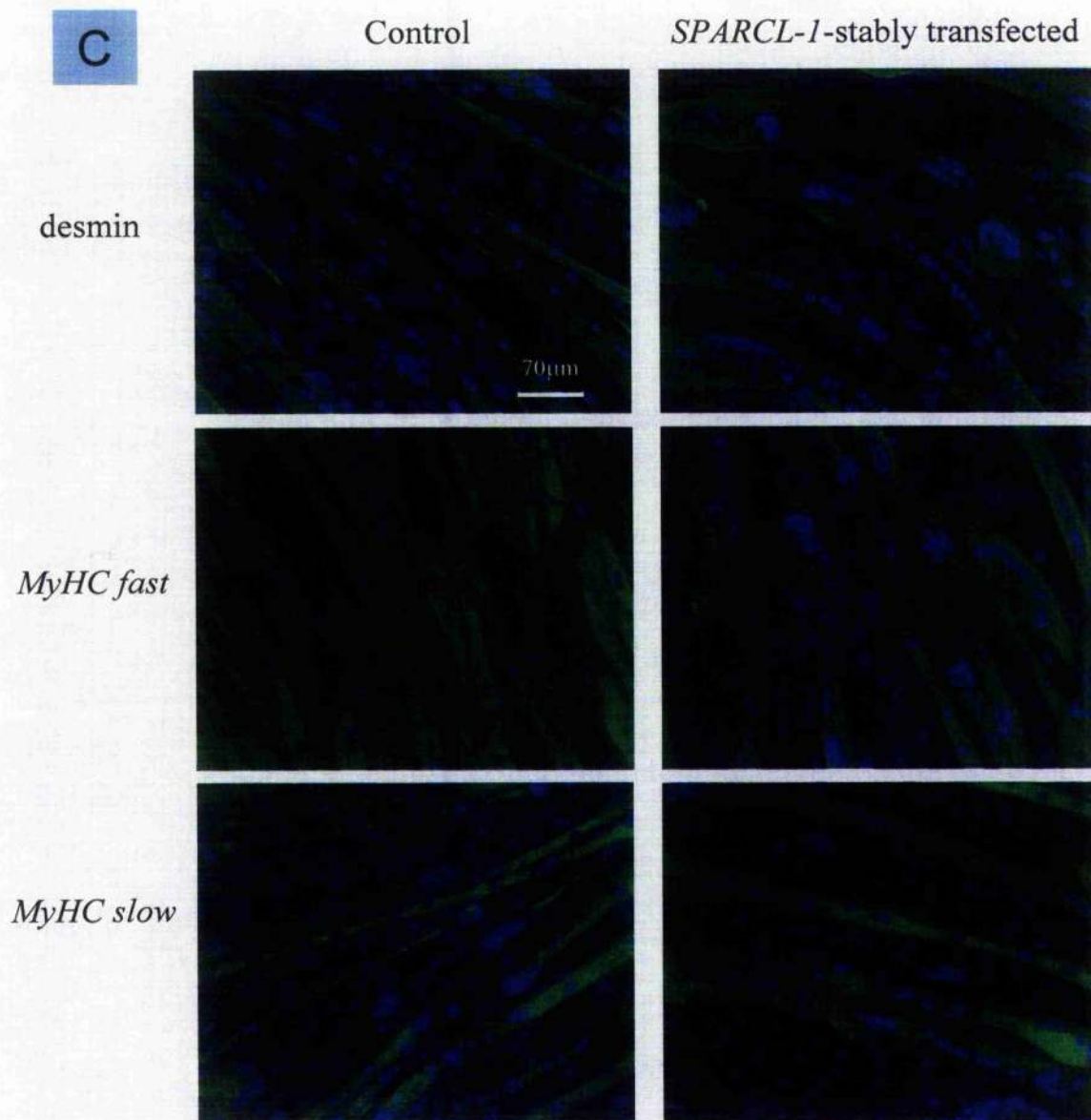


Figure 5.10. (C) Immunostaining of *SPARCL-1*-stably transfected C2C12 cells. *SPARCL-1*-stably transfected C2C12 myotubes (differentiated for 9 days) were separately immunostained for desmin, *MyHC fast* and *MyHC slow*, along with DAPI nuclei staining.

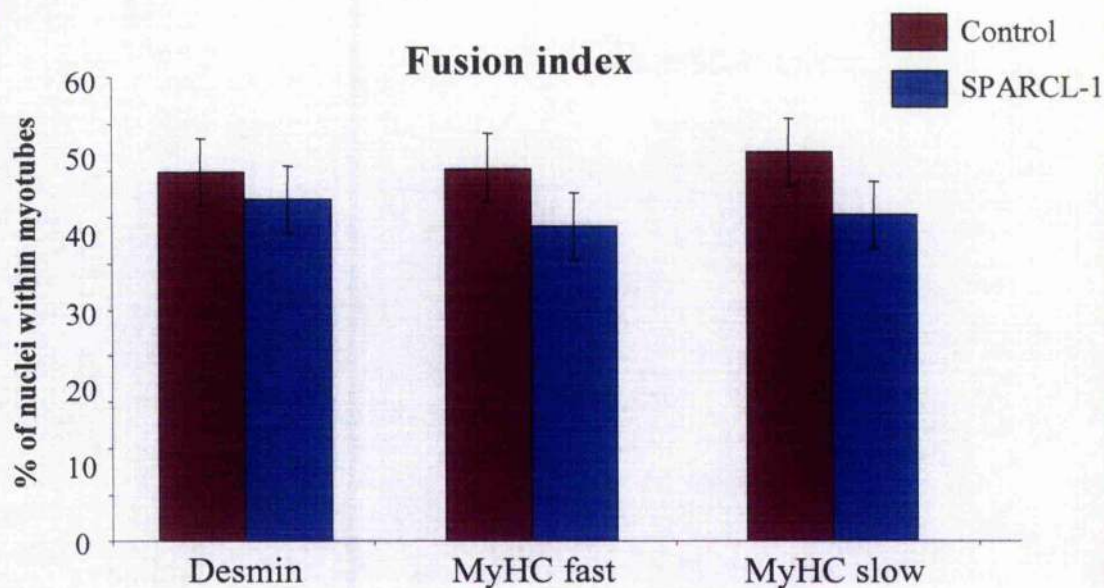
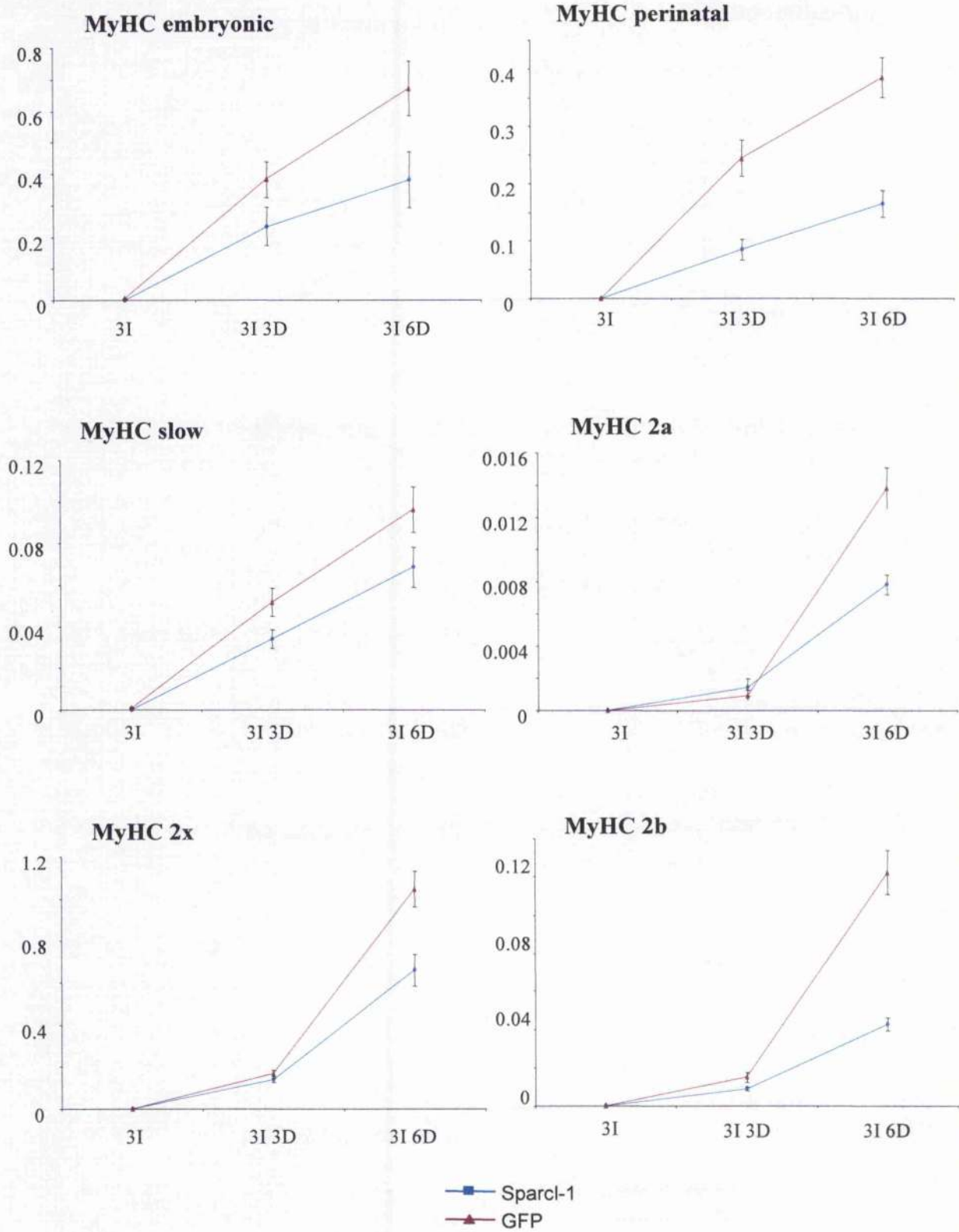
D

Figure 5.10. (D) Over-expression of SPARCL-1 on C2C12 cell differentiation. Results showed no significant difference between SPARCL-1-transfected and control cells. Results were analysed with SAS software, differences between pair-wise combinations of the least square means were tested for significance ($*p<0.05$). Asterisks indicate statistical significance. Error bars were standard error, $n=3$ replicates from 3 independent experiments.



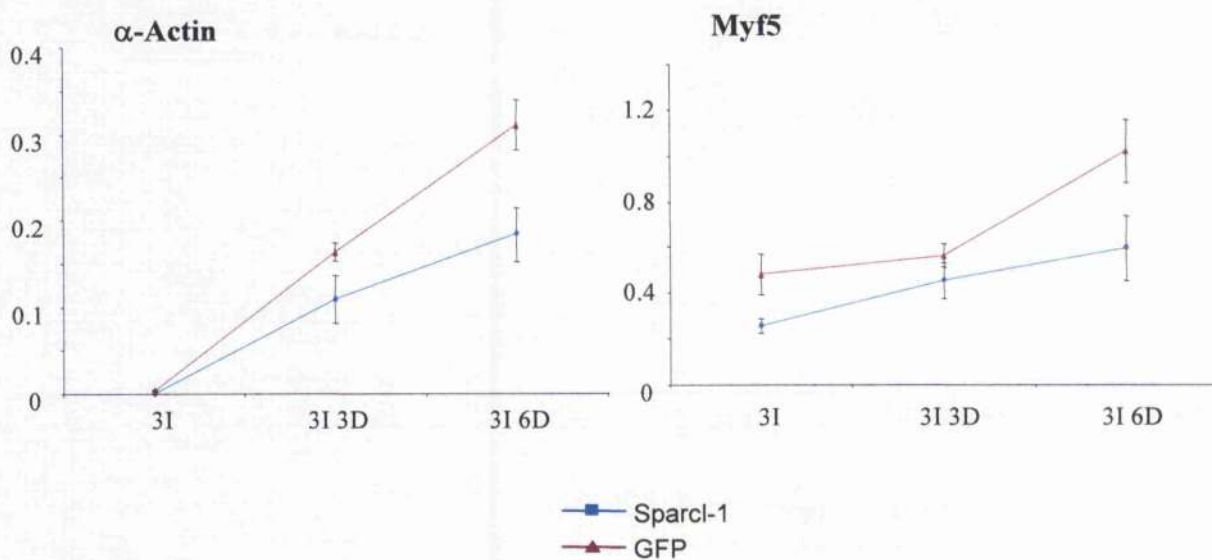


Figure 5.11. Muscle gene expression in *SPARCL-1*-adenovirus infected C2C12 cells. Real-time PCR was performed on cDNAs derived from infected cells over a time course as detailed in Fig. 5.9. No dramatic difference in *MyHC* expression between *SPARCL-1*-infected and control C2C12 cells was seen during the early infection (3I). However in the later time point (3I3D and 3I6D), reductions in expression of all *MyHC* isoforms, *Myf-5* and *α-actin* in *SPARCL-1*-infected C2C12 myotubes were noticeable. Results expressed as mean \pm standard deviation from triplicate samples within the same experiment.

5.3.6. *SPARCL-1* expression in PCS muscles, and interactions between *SPARCL-1* and *P311*

SPARCL-1 was previously suggested as differentially expressed in PCS (Maak et al., 2001). The relative expression of porcine *SPARCL-1* in affected and normal muscles was determined. No significant difference in *SPARCL-1* expression was found between affected and normal piglets, which suggest that *SPARCL-1* is not associated with PCS (Fig. 5.12).

To assess the interaction of *SPARCL-1* with *P311*, C2C12 cells were infected with *SPARCL-1*-adenovirus construct as described in Section 5.2.2 over a time course. No difference of *P311* endogenous expression in *SPARCL-1* over-expressed cells was detected (Fig. 5.13). These results indicate that over-expression of *SPARCL-1* has no apparent effect on endogenous expression of *P311*.

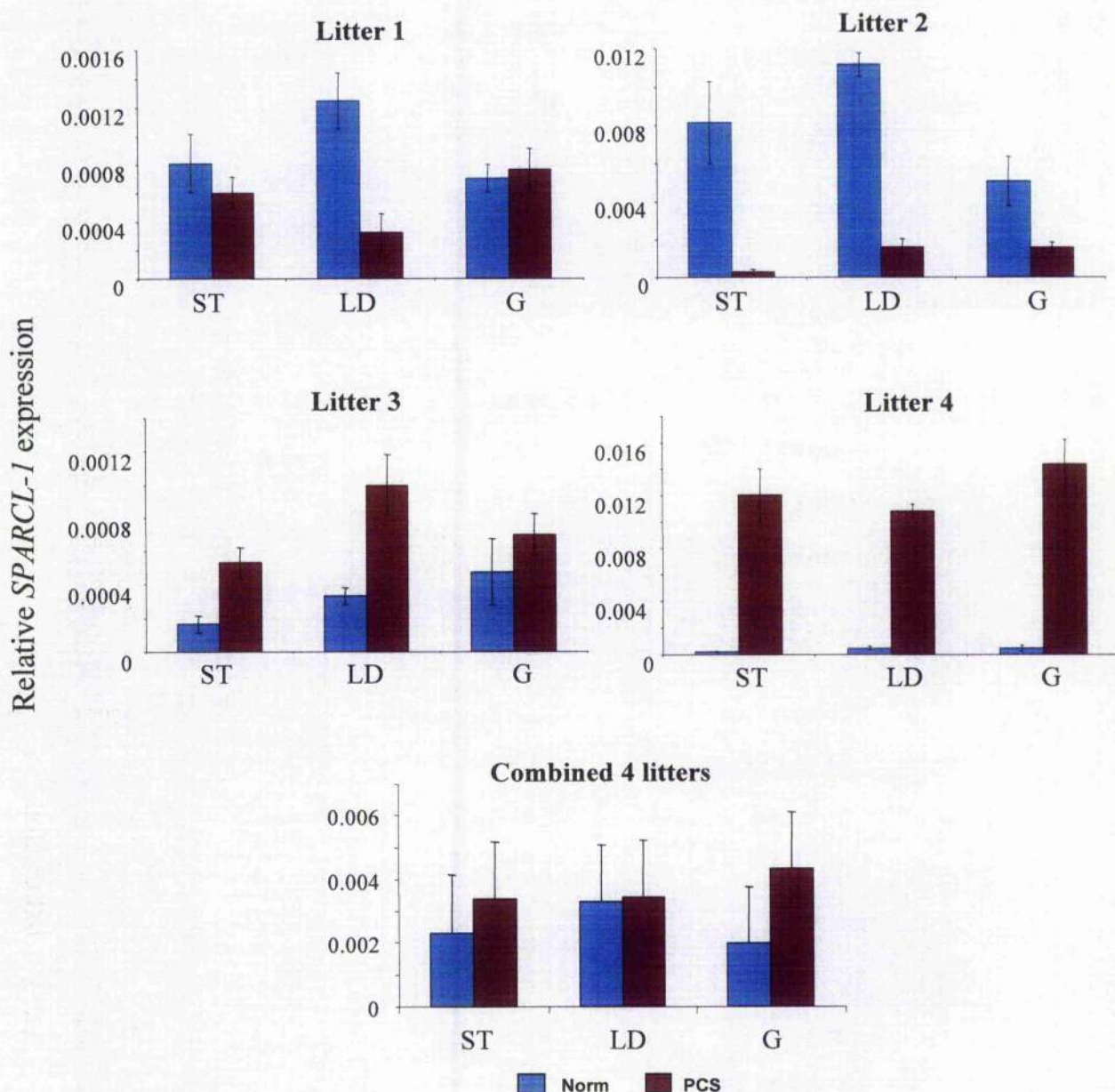


Figure 5.12. Quantitative PCR performed for *SPARCL-1* expression. No significant difference was found between normal and PCS piglets for the combined results of 4 sets of 2-day-old PCS piglets. Results of each litter are expressed as mean \pm standard deviation from triplicate samples within the same experiment. Combined results of 4 sets of PCS piglets were also tested for significance ($*p < 0.05$) in differences between pair-wise combinations of the least square means. Norm= normal; PCS= porcine congenital splayleg.

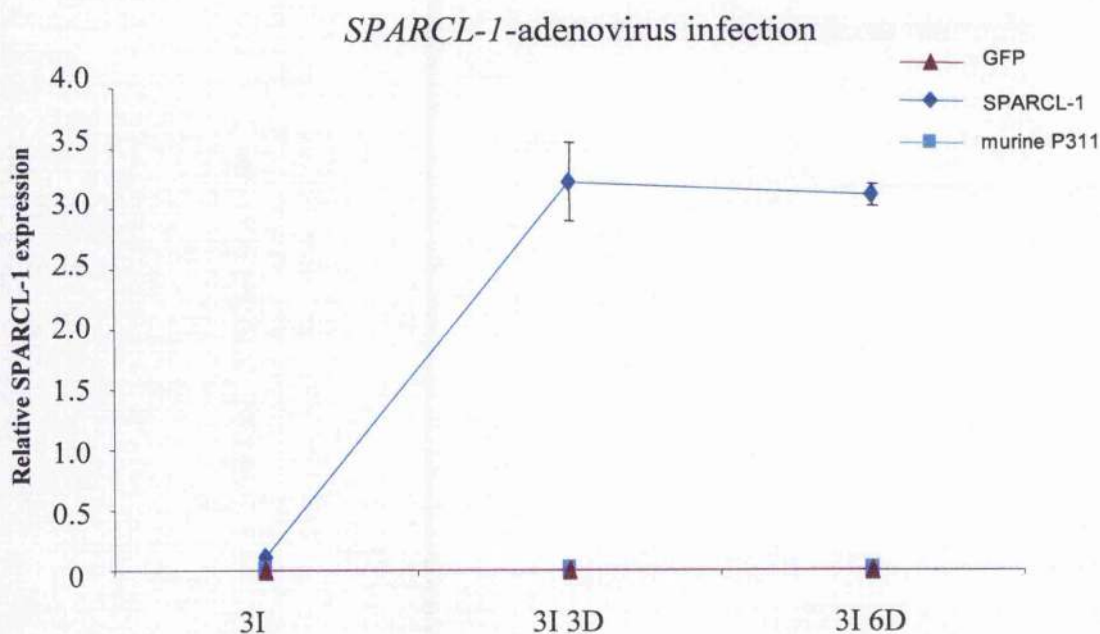


Figure 5.13. Expression interaction between *SPARCL-1* and *P311*. Real-time PCR was performed on cDNAs derived from infected cells over a time course as detailed in Fig. 5.9. No difference of *P311* endogenous expression in *SPARCL-1* over-expressed cells. There are no apparent linkage between *SPARCL-1* and *P311* at RNA level. Results expressed as mean \pm standard deviation from triplicate samples within the same experiment.

5.4. Discussion

A full-length porcine *SPARCL-1* cDNA clone was sequenced and molecularly characterised (Accession. N^o. EF416571). The full-length porcine *SPARCL-1* cDNA was 2.8 kb and the coding sequence was 2.0 kb in length. Although the deduced amino acid sequence of porcine SPARCL-1 is only 76% homologous to human SPARCL-1, the FS domain and EC domains showed 100% and 98.6% similarity respectively, between the 2 species (Fig. 5.5). These two domains are the hall-marks of SPARC family proteins. The FS domain is involved in the inhibition of activin, and thereby inhibits release of follicle stimulating hormone, while EC domain is involved in binding both calcium and collagen (Pottgiesser et al., 1994). The acidic domain of porcine *SPARCL-1* only showed 63.1% similarity to human *SPARCL-1* (Fig. 5.5); it is the most divergent portion among the family of SPARC-like proteins. No direct link of the domains function with skeletal muscles has been reported.

Although *SPARCL-1* was previously highlighted in a PCS paper (Maak et al., 2001), no significant difference in expression between affected and normal piglets was detected (Fig. 5.12). Hence, *SPARCL-1* is unlikely to be linked to PCS. In addition, there is no apparent expression interaction between *SPARCL-1* and *P311* at the RNA level (Fig. 5.13). No SPARCL-1 protein could be detected by Western blotting. Given that cells transfected or infected with *SPARCL-1* showed biological effects of reduced proliferation and reduced muscle gene expression, it was likely that the protein product was translated. Since *SPARCL-1* is a matricellular secreted glycoprotein, protein levels could be higher in culture supernatants. By generating rat anti-SPARCL-1 monoclonal antibodies and the use of immunoprecipitation, SPARCL-1 protein was successfully detected (Brekken et al., 2004). In future, to

improve on SPARCL-1 protein detection, cell culture supernatants could be collected along with cell lysate for detection.

As far as can be determined, there is no information about function of *SPARCL-1* in skeletal muscle. In this study, *SPARCL-1* over-expression in C2C12 skeletal muscle cells led to the reduction in cell proliferation (Fig. 5.10) and down-regulation of MyHC isoforms expression during late differentiation (Fig. 5.11.). *SPARCL-1* is reported as a negative regulator of cell proliferation and cell differentiation when over-expressed in HeLa 3S cells (human uterine cervical cells) (Claeskens et al., 2000). Moreover, smooth muscle cells isolated from SPARC-null mice exhibited a higher rate of proliferation relative to their wild-type counterparts (Bradshaw et al., 1999). Hence, *SPARCL-1* might act as a negative regulator of cell proliferation and cell differentiation in skeletal muscle.

Among the SPARC family members, *SPARCL-1* displays the highest amino acid similarity with *SPARC*, sharing 55.6% identity at FS domain and 61.4% identity at EC domain. Given their structural similarities, *SPARCL-1* could exhibit similar function as *SPARC*, such as the anti-adhesive properties in endothelial cell culture (Girard and Springer, 1996). However, the functions of *SPARC* and *SPARCL-1* could be tissue specific (Framson and Sage, 2004). The expression of *SPARCL-1* endogenous level during myoblast differentiation is unknown, but *SPARC* endogenous expression was reported to be highly up-regulated during differentiation of C2C12 cells (Cho et al., 2000). *SPARC* was suggested to play a role in fusion during myoblast differentiation (Cho et al., 2000). Given that *SPARCL-1* displays high amino acid similarity with *SPARC*, *SPARCL-1* could exhibit similar function to *SPARC*. Endogenous

expression may be required for myoblast differentiation, but over-expression could lead to the down-regulation of muscle genes in late differentiation. Although *SPARCL-1* was not related to PCS, over-expression of this gene demonstrated its important role in regulating skeletal muscle proliferation and differentiation. Clearly, more work is needed to further investigate its potential in skeletal muscle.

Chapter 6

General discussion

The aim of this study is to investigate the cellular and molecular changes in skeletal muscles of PCS. This project is the first to detail the histological, biochemical and molecular changes that take place in muscles of PCS. Results showed that PCS piglets had smaller fibre size and higher fibre density in the *semitendinosus* (ST), *longissimus dorsi* (LD) and *gastrocnemius* (G) muscles. PCS associated atrophy was not accompanied by significant changes in fibre type composition as determined by immunohistochemistry. However, the expression of *MyHC slow*, *MyHC 2x* and *MyHC 2b* gene was significantly reduced, as demonstrated by real-time RT-PCR. *MAFbx*, a marker of muscle atrophy, was highly expressed in all PCS muscles. Conversely, expression of *P311*, a novel 8-kDa protein with a conserved PEST domain, was down-regulated in all PCS muscles tested.

Full-length porcine *P311* (Accession. N^o. EF416570) and *SPARCL-1* (Accession. N^o. EF416571) cDNA clones were sequenced and characterised in this project. The coding sequence for porcine *P311* and *SPARCL-1* cDNA was 0.3 kb and 2.0 kb in length respectively. The deduced amino acid sequence of porcine *P311* and *SPARCL-1* was 87% and 76% homologous to their human counterpart. *P311* over-expression led to raised C2C12 cell proliferation and reduced myotube formation. Consistent with reduced myotube formation, expression of several muscle genes (*MyHC embryonic*, *MyHC 2b*, α -actin and *myf-5*) was down-regulated in late differentiation of *P311*-over-expressed C2C12 cells. In contrast, *SPARCL-1* over-expression led to reduction in C2C12 cell proliferation. No difference in fusion index was found, but *SPARCL-1*-over-expressed C2C12 cells down-regulated *MyHC* isoforms, *Myf-5* and α -actin expression during late differentiation. *SPARCL-1* might act as a negative regulator of cell proliferation and differentiation. *SPARC*

endogenous expression was reported to be highly up-regulated during differentiation of C2C12 cells (Cho et al., 2000). Given that *SPARCL-1* displays high amino acid similarity with *SPARC*, *SPARCL-1* may have similar functions to *SPARC*. Endogenous *SPARCL-1* expression may be required for myoblast differentiation, but its over-expression could lead to the down-regulation of muscle genes in late differentiation.

Stickland and Handel (1986) have showed that there are variations in muscle fibre numbers between piglets. In PCS muscles, reduced *P311* expression could conceivably mediate fibre atrophy through reduced cell proliferation, leading to reduced availability of total myoblast number in the formation of muscle fibres. Moreover, reduced myoblast number could potentially lead to the formation of less muscle fibres, hence myofibre hypoplasia. Future work will require detailed total fibre counting to determine if myofibre hypoplasia is also a feature of PCS muscles. Although *SPARCL-1* was previously highlighted in a PCS paper (Maak et al., 2003), no significant difference in expression between PCS affected and normal piglets was detected. In addition, there is no apparent expression interaction between *SPARCL-1* and *P311*.

Currently, the precise aetiology and pathogenesis of PCS remain unknown, but PCS is believed to be a multifactorial condition which involves environmental and genetic factors. The environmental factors could include sow management, the administration of various drugs and mycotoxins (reviewed in Chapter 1). A combination of history and management evaluation can be used to identify the possible involvement of such factors. In this project, the PCS samples collected did

not show any apparent evidence of strong environmental factors. Proper sow management by the provision of adequate bedding and a dry floor in farrowing crate ruled out the possibility of PCS due to slippery floor. Administration of certain drugs such as glucocorticoids, pyrimethamine and prostaglandin in pregnant sow have been shown to lead to PCS (Jirmanova, 1983; Ohnishi et al., 1989; Bolcskei et al., 1996). None of the drugs were in use on the farm where the PCS affected piglets originated. All pregnant sows in the farm from which the piglets came were on the same diet. Consumption of mycotoxins could be expected to extensively affect all litters in a herd. However, all PCS samples collected were sporadic and isolated cases. Interestingly, all the PCS affected piglets collected for this study were male, which may suggest that males are more susceptible to PCS, which is in line with previous reports (Vogt et al., 1984; Van Der Heyde et al., 1989). The lack of obvious environmental factors in the farm of origin suggests that PCS is connected to genetic factors. The mixture of semen from several boars in artificial insemination hinders the identification of any possible sire involvement. Parental and sibling genotyping could establish the parental linkage of affected individuals.

PCS can be easily identified from the clinical signs, however there are some piglets that may be sub-clinically affected. The sub-clinical condition may not be life threatening as is clinical PCS. Since PCS might be genetically determined, it is useful to detect sub-clinically affected PCS piglets in order to remove them from breeding programmes to reduce the genetic predisposition. Sub-clinical PCS might exhibit similar expression of *MAFbx* and *P311* as clinical PCS. Muscle biopsy of suspected piglets accompanied by real time RT-PCR of *P311* and *MAFbx* could be used to detect the sub-clinical PCS condition, but the diagnostic procedure is costly and

laborious. To explore the potential of *MAFbx* and *P311* as biomarkers in the diagnosis of sub-clinical PCS, more research work is needed. In future, a larger sample size of PCS and normal piglets could be obtained to determine the consistency and repeatability of the expression pattern. Moreover, comparisons between PCS and other myopathies, such as arthrogryposis, could be made in relation to *MAFbx* and *P311* expression. The detection of P311 protein as a potential biomarker is limited by its high lability and short half life. In future, with improved protein preservation and detection methods, P311 and MAFbx proteins could be used in clinical practice as protein markers to distinguish sub-clinically PCS affected piglets from normal piglets. Such an application will be of the greatest value in nucleus herd breeding programmes.

The total number of skeletal muscle fibres (hyperplasia) in pig is virtually fixed before birth (Wigmore and Stickland, 1983). Postnatal muscle growth continues by muscle fibre hypertrophy. This means that any manipulation of muscle fibre number must be undertaken prenatally. In pigs, the primary fibre and secondary fibre formations occur around 30-50 days and 50-90 days of gestation respectively (Wigmore and Stickland, 1983). However, it is impossible to diagnose PCS affected piglets at present merely based on the visualisation of foetuses. PCS affected piglets can only be identified and assessed after birth. Muscle fibre number is an important determinant of postnatal growth. Littermates with higher fibre number tend to outgrow other littermates (Dwyer et al., 1993). At present, it is not certain if PCS-associated fibre atrophy is also accompanied by fibre hypoplasia. Even though 50% of the PCS affected piglets may recover within a week, it may not be economical to attend to affected piglets. PCS affected piglets might not grow as efficiently as the healthy littermates.

Porcine muscle satellite cells could be collected from PCS and normal piglets as an *in vitro* approach in the future. Porcine muscle satellite cells have been successfully isolated to study IGF-1 expression, proliferation and differentiation (Fligger et al., 1998; Mesires and Doumit, 2002). PCS muscle satellite cells may exhibit different gene expression patterns compared with normal muscle satellite cells. It would be interesting to determine the relative expression of *P311* and *MAFbx* in PCS and normal satellite cells over a time-course.

Study on muscle innervation was not done in this project. Previously, smaller size and irregularly distribution of motor endplates were found in PCS muscles compared to normal muscles (Hanzlikova, 1980). In future, it will be interesting to investigate the nerve supply of PCS muscles. Sciatic nerve would be a prime start, since it supplies some of the hindlimb muscles, a region commonly affected in PCS. Morphological, biochemical characteristic and neuromuscular transmission could be measured in both PCS affected and normal piglets to identify possible involvement of neuropathy in PCS (Lindstrom et al., 1976; Somasekhar et al., 1996).

A porcine skeletal muscle cDNA microarray, which comprised 5500 clones from two developmentally distinct cDNA libraries developed at the Molecular Medicine Laboratory (Bai et al., 2003) and several publicly and commercially porcine microarrays (from Ark-Genomics and Affymetrix) are readily available. Such arrays could be used to identify differentially expressed genes that could be involved in PCS. Genes that are up-regulated or down-regulated could be involved in PCS pathogenesis. However, PCS is a multifactorial condition and wide variation in endogenous gene

expression between pigs might occur (Chang et al., 2003). The challenge to any investigator is to identify the correct genes and demonstrate their functional significance in the pathogenesis of PCS.

References

1. Adams GR (2002) Autocrine and/or paracrine insulin-like growth factor-I activity in skeletal muscle. *Clin Orthop Res* 403: 188-196.
2. Adams GR, Haddad F, McCue SA, Bodell PW, Zeng M, Qin L, Qin AX, Baldwin KM (2000) Effects of spaceflight and thyroid deficiency on rat hindlimb development. II. Expression of MHC isoforms. *J Appl Physiol* 88: 904-916.
3. Alliel PM, Perin JP, Jolles P, Bonnet FJ (1993) Testican, a multidomain testicular proteoglycan resembling modulators of cell social behaviour. *Eur J Biochem* 214: 347-350.
4. Andersen JL, Klitgaard H, Saltin B (1994) Myosin heavy chain isoforms in single fibres from m. vastus lateralis of sprinters: influence of training. *Acta Physiol Scand* 151: 135-142.
5. Andersen JL, Mohr T, Biering-Sorensen F, Galbo H, Kjaer M (1996) Myosin heavy chain isoform transformation in single fibres from m. vastus lateralis in spinal cord injured individuals: effects of long-term functional electrical stimulation (FES). *Eur J Phys* 431: 513-518.
6. Antaliova L, Horak V, Matolin S (1996) Ultrastructural demonstration of glucose-6-phosphatase activity and glycogen in skeletal muscles of newborn piglets with the splayleg syndrome. *Reprod Nutr Develop* 36: 205-212.
7. Awede BL, Thissen JP, Lebacqz J (2002) Role of IGF-I and IGFBPs in the changes of mass and phenotype induced in rat soleus muscle by clenbuterol. *Am J Physiol -Endocrinol Metab* 282: E31-E37.
8. Bai Q, McGillivray C, da Costa N, Dornan S, Evans G, Stear MJ, Chang KC (2003) Development of a porcine skeletal muscle cDNA microarray: analysis of differential transcript expression in phenotypically distinct muscles. *BMC Genomics* 4: 8.
9. Balagopal P, Rooyackers OE, Adey DB, Ades PA, Nair KS (1997) Effects of aging on in vivo synthesis of skeletal muscle myosin heavy-chain and sarcoplasmic protein in humans. *Am J Physiol* 273: 790-800.
10. Balagopal P, Schimke JC, Ades P, Adey D, Nair KS (2001) Age effect on transcript levels and synthesis rate of muscle MHC and response to resistance exercise. *Am J Physiol -Endocrinol Metab* 280: 203-208.
11. Baldwin KM, Haddad F (2001) Effects of different activity and inactivity paradigms on myosin heavy chain gene expression in striated muscle. *J Appl Physiol* 90: 345-357.

12. Baldwin KM, Haddad F (2002) Skeletal muscle plasticity: cellular and molecular responses to altered physical activity paradigms. *Am J Phys Med Rehab* 81: 40-51.
13. Bassel-Duby R, Olson EN (2003) Role of calcineurin in striated muscle: development, adaptation, and disease. *Biochem Biophys Res Commun* 311: 1133-1141.
14. Bassuk JA, Birkebak T, Rothmier JD, Clark JM, Bradshaw A, Muchowski PJ, Howe CC, Clark JJ, Sage EH (1999) Disruption of the Sparc locus in mice alters the differentiation of lenticular epithelial cells and leads to cataract formation. *Exp Eye Res* 68: 321-331.
15. Bendik I, Schraml P, Ludwig CU (1998) Characterization of MAST9/Hevin, a SPARC-like protein, that is down-regulated in non-small cell lung cancer. *Cancer Res* 58: 626-629.
16. Birnboim HC, Doly J (1979) A rapid alkaline extraction procedure for screening recombinant plasmid DNA. *Nucl Acids Res* 7: 1513-1523.
17. Bodine SC, Stitt TN, Gonzalez M, Kline WO, Stover GL, Bauerlein R, Zlotchenko E, Scrimgeour A, Lawrence JC, Glass DJ, Yancopoulos GD (2001a) Akt/mTOR pathway is a crucial regulator of skeletal muscle hypertrophy and can prevent muscle atrophy in vivo. *Nat Cell Biol* 3: 1014-1019.
18. Bodine SC, Latres E, Baumhueter S, Lai VKM, Nunez L, Clarke BA, Poueymirou WT, Panaro FJ, Na E, Dharmarajan K, Pan ZQ, Valenzuela DM, DeChiara TM, Stitt TN, Yancopoulos GD, Glass DJ (2001b) Identification of Ubiquitin Ligases Required for Skeletal Muscle Atrophy. *Science* 294: 1704-1708.
19. Bolcskei A, Bilkei G, Biro O, Clavadetscher E, Goos T, Stelzer P, Bilkei H, Wegmuller S (1996) The effect of timing of labor induction on the occurrence of congenital myofibrillar hypoplasia--short clinical report. [German]. *Deut Tierarztl Woch* 103: 21-22.
20. Bollwahn W, Pfeiffer A (1969) Symptomatic treatment of the "straddle-syndrom" in pigs by temporary immobilization of the hind legs. [German]. *Deut Tierarztl Woch* 76: 239-241.
21. Bornstein P (1995) Diversity of function is inherent in matricellular proteins: an appraisal of thrombospondin 1. *J Cell Biol* 130: 503-506.
22. Bradley R, Ward PS, Bailey J (1980) The ultrastructural morphology of the skeletal muscles of normal pigs and pigs with splayleg from birth to one week of age. *J Comp Pathol* 90: 433-446.
23. Bradshaw AD, Francki A, Motamed K, Howe C, Sage EH (1999) Primary mesenchymal cells isolated from SPARC-null mice exhibit altered morphology and rates of proliferation. *Mol Biol Cell* 10: 1569-1579.

24. Brekken RA, Sage EH (2000) SPARC, a matricellular protein: at the crossroads of cell-matrix. *Matrix Biol* 19: 569-580.
25. Brekken RA, Sullivan MM, Workman G, Bradshaw AD, Carbon J, Siadak A, Murri C, Framson PE, Sage EH (2004) Expression and Characterization of Murine Hcvin (SC1), a Member of the SPARC Family of Matricellular Proteins. *J Histochem Cytochem* 52: 735-748.
26. Brooke MH, Kaiser KK (1970) Muscle fiber types: how many and what kind? *Arch Neurol* 23: 369-379.
27. Buller AJ (1965) Mammalian fast and slow skeletal muscle. *Sci Basic Med Annu Rev* 186-201.
28. Caiozzo VJ, Baker MJ, Baldwin KM (1998) Novel transitions in MLIC isoforms: Separate and combined effects of thyroid hormone and mechanical unloading. *J Appl Physiol* 85: 2237-2248.
29. Carroll TJ, Abernethy PJ, Logan PA, Barber M, McEniery MT (1998) Resistance training frequency: strength and myosin heavy chain responses to two and three bouts per week. *Eur J Appl Physiol O* 78: 270-275.
30. Chang DD, Park NH, Denny CT, Nelson SF, Pe M (1998) Characterization of transformation related genes in oral cancer cells. *Oncogene* 16: 1921-1930.
31. Chang KC, da Costa N, Blackley R, Southwood O, Evans G, Plastow G, Wood JD, Richardson RJ (2003) Relationships of myosin heavy chain fibre types to meat quality traits in traditional and modern pigs. *Meat Sci* 64: 93-103.
32. Chikuni K, Muroya S, Nakajima I (2004a) Absence of the functional myosin heavy chain 2b isoform in equine skeletal muscles. *Zool Sci* 21: 589-596.
33. Chikuni K, Muroya S, Nakajima I (2004b) Myosin heavy chain isoforms expressed in bovine skeletal muscles. *Meat Sci* 67: 87-94.
34. Chin ER, Allen DG (1996) The role of elevations in intracellular $[Ca^{2+}]$ in the development of low frequency fatigue in mouse single muscle fibres. *J Physiol* 491: 813-824.
35. Chin ER, Olson EN, Richardson JA, Yang Q, Humphries C, Shelton JM, Wu H, Zhu W, Bassel-Duby R, Williams RS (1998) A calcineurin-dependent transcriptional pathway controls skeletal muscle fiber type. *Genes Dev* 12: 2499-2509.
36. Cho WJ, Kim EJ, Lee SJ, Kim HD, Shin HJ, Lim WK (2000) Involvement of SPARC in in Vitro Differentiation of Skeletal Myoblasts. *Biochem Bioph Res Co* 271: 630-634.
37. Ciccarone V, Chu Y, Schifferli K, Pichet J-P, Hawley-Nelson P, Evans K, Roy L, Bennett S (1999) LipofectamineTM 2000 Reagent for Rapid, Efficient Transfection of Eukaryotic Cells. *Focus* 21: 54-55.

38. Claeskens A, Ongenac N, Neefs JM, Cheyns P, Kaijen P, Cools M, Kutoh E (2000) Hevin is down-regulated in many cancers and is a negative regulator of cell growth and proliferation. *Brit J Cancer* 82: 1123-1130.
39. Comai L, Song Y, Tan C, Bui T (2000) Inhibition of RNA polymerase I transcription in differentiated myeloid leukemia cells by inactivation of selectivity factor 1. *Cell Growth Differ* 11: 63-70.
40. Crabtree GR (2001) Calcium, calcineurin, and the control of transcription. *J Biol Chem* 276: 2313-2316.
41. Cunha TJ (1968) Swine Nutrition and Management. Australian Seminar Series.
42. Cutler RS, Fahy VA, Cronin GM, Spicer EM (2006) Prewaning mortality. In: *Disease of Swine* (Straw BE, Zimmerman JJ, D'Allaire S, Taylor DJ, eds), pp 993-1009. Blackwell Publishing.
43. da Costa N, McGillivray C, Bai Q, Wood JD, Evans G, Chang KC (2004) Restriction of dietary energy and protein induces molecular changes in young porcine skeletal muscles. *J Nutr* 134: 2191-2199.
44. da Costa N, McGillivray C, Chang KC (2003) Postnatal myosin heavy chain isoforms in prenatal porcine skeletal muscles: insights into temporal regulation. *Anat Rec* 273: 731-740.
45. Danieli-Betto D, Betto R, Megighian A, Midrio M, Salviati G, Larsson L (1995) Effects of age on sarcoplasmic reticulum properties and histochemical composition of fast- and slow-twitch rat muscles. *Acta Physiol Scand* 154: 59-64.
46. Delling U, Tureckova J, Lim HW, De Windt LJ, Rotwein P, Molkentin JD (2000) A calcineurin-NFATc3-dependent pathway regulates skeletal muscle differentiation and slow myosin heavy-chain expression. *Mol Cell Biol* 20: 6600-6611.
47. DeMartino GN, Ordway GA (1998) Ubiquitin-proteasome pathway of intracellular protein degradation: implications for muscle atrophy during unloading. *Exercise Sport Sci R* 26: 252.
48. Demirel HA, Powers SK, Naito H, Hughes M, Coombes JS (1999) Exercise-induced alterations in skeletal muscle myosin heavy chain phenotype: dose-response relationship. *J Appl Physiol* 86: 1002-1008.
49. Deng Y, Yao L, Chau L, Ng SS, Peng Y, Liu X, Au WS, Wang J, Li F, Ji S, Han H, Nie X, Li Q, Kung HF, Leung SY, Lin MC (2003) N-Myc downstream-regulated gene 2 (NDRG2) inhibits glioblastoma cell proliferation. *Int J Cancer* 106: 342-347.
50. Denley A, Cosgrove LJ, Booker GW, Wallace JC, Forbes BE (2005) Molecular interactions of the IGF system. *Cytokine Growth F R* 16: 421-439.
51. Dobson KJ (1968) Congenital splayleg of piglets. *Aust Vet J* 44: 26-28.

52. Dobson KJ (1971) Failure of choline and methionine to prevent splayleg in piglets. *Aust Vet J* 47: 587-590.
53. Ducatelle R, Maenhout D, Coussement W, Hoorens JK (1986) Spontaneous and experimental myofibrillar hypoplasia and its relation to splayleg in newborn pigs. *J Comp Pathol* 96: 433-445.
54. Dunn SE, Burns JL, Michel RN (1999) Calcineurin is required for skeletal muscle hypertrophy. *J Biol Chem* 274: 21908-21912.
55. Dwyer CM, Fletcher JM, Stickland NC (1993) Muscle cellularity and postnatal growth in the pig. *J Anim Sci* 71: 3339-3343.
56. Dwyer CM, Stickland NC, Fletcher JM (1994) The influence of maternal nutrition on muscle fiber number development in the porcine fetus and on subsequent postnatal growth. *J Anim Sci* 72: 911-917.
57. Engel J, Taylor W, Paulsson M, Sage H, Hogan B (1987) Calcium binding domains and calcium-induced conformational transition of SPARC/BM-40/osteonectin, an extracellular glycoprotein expressed in mineralized and nonmineralized tissues. *Biochemistry* 26: 6958-6965.
58. Erbay E, Park IH, Nuzzi PD, Schonherr CJ, Chen J (2003) IGF-II transcription in skeletal myogenesis is controlled by mTOR and nutrients. *J Cell Biol* 163: 931-936.
59. Fligger JM, Malven PV, Doumit ME, Merkel RA, Grant AL (1998) Increases in insulin-like growth factor binding protein-2 accompany decreases in proliferation and differentiation when porcine muscle satellite cells undergo multiple passages. *J Anim Sci* 76: 2086-2093.
60. Florini JR, Ewton DZ, Coolican SA (1996) Growth hormone and the insulin-like growth factor system in myogenesis. *Endocr Rev* 17: 481-517.
61. Fluck M, Hoppeler H (2003) Molecular basis of skeletal muscle plasticity--from gene to form and function. *Rev Physiol Biochem P* 146: 159-216.
62. Framson PE, Sage EH (2004) SPARC and tumor growth: where the seed meets the soil? *J Cell Biochem* 92: 679-690.
63. Freeman WM, Walker SJ, Vrana KE (1999) Quantitative RT-PCR: pitfalls and potential. *Biotechniques* 26(1):112-22, 124-5.
64. Friday BB, Horsley V, Pavlath GK (2000) Calcineurin activity is required for the initiation of skeletal muscle differentiation. *J Cell Biol* 149: 657-665.
65. Ghose R, Shekhtman A, Goger MJ, Ji H, Cowburn D (2001) A novel, specific interaction involving the Csk SH3 domain and its natural ligand. *Nat Struct Biol* 8: 998-1004.

66. Girard JP, Springer TA (1995) Cloning from purified high endothelial venule cells of hevin, a close relative of the antiadhesive extracellular matrix protein SPARC. *Immunity* 2: 113-123.
67. Girard JP, Springer TA (1996) Modulation of endothelial cell adhesion by hevin, an acidic protein associated with high endothelial venules. *J Biol Chem* 271: 4511-4517.
68. Glass DJ (2003) Signalling pathways that mediate skeletal muscle hypertrophy and atrophy. *Nat Cell Biol* 5: 87-90.
69. Glass DJ (2005) Skeletal muscle hypertrophy and atrophy signaling pathways. *Int J Biochem Cell B* 37: 1974-1984.
70. Goldspink G (1996) Muscle growth and muscle function: a molecular biological perspective. *Res Vet Sci* 60: 193-204.
71. Guermah M, Crisanti P, Laugier D, Dezelee P, Bidou L, Pessac B, Calothy G (1991) Transcription of a quail gene expressed in embryonic retinal cells is shut off sharply at hatching. *P Natl Acad Sci USA* 88: 4503-4507.
72. Gyuris J, Golemis E, Chertkov H, Brent R (1993) Cdi1, a human G1 and S phase protein phosphatase that associates with Cdk2. *Cell* 75: 791-803.
73. Haddad F, Qin AX, Zeng M, McCue SA, Baldwin KM (1998) Interaction of hyperthyroidism and hindlimb suspension on skeletal myosin heavy chain expression. *J Appl Physiol* 85: 2227-2236.
74. Handel SE, Stickland NC (1987) The growth and differentiation of porcine skeletal muscle fibre types and the influence of birthweight. *J Ant* 152: 107-119.
75. Hanzlikova V (1980) Histochemical patterns in normal and splaylegged piglet muscle fibers. *Histochemistry* 67: 311-319.
76. Harding JD, Done JT, Darbyshire JH (1966) Congenital tremors in piglets and their relation to swine fever. *Vet Rec* 79: 388-390.
77. Hershko A, Ciechanover A (1998) The ubiquitin system. *Annu Rev Biochem* 67: 425-479.
78. Hill M, Goldspink G (2003) Expression and splicing of the insulin-like growth factor gene in rodent muscle is associated with muscle satellite (stem) cell activation following local tissue damage. *J Physiol* 549: 409-418.
79. Hirschman SZ, Helsenfeld G (1966) Determination of DNA composition and concentration by spectral analysis. *J Mol Biol* 16: 347-358.
80. Hnik P, Vejsada R, Goldspink DF, Kasicki S, Krekule I (1985) Quantitative evaluation of electromyogram activity in rat extensor and flexor muscles immobilized at different lengths. *Exp Neurol* 88: 515-528.

81. Hohenester E, Maurer P, Hohenadl C, Timpl R, Jansonius JN, Engel J (1996) Structure of a novel extracellular Ca(2+)-binding module in BM-40. *Nat Struct Biol* 3: 67-73.
82. Horton MJ, Brandon CA, Morris TJ, Braun TW, Yaw KM, Sciote JJ (2001) Abundant expression of myosin heavy-chain IIB RNA in a subset of human masseter muscle fibres. *Arch Oral Biol* 46: 1039-1050.
83. Innis MA, Gelfand DH (1990) Optimization of PCRs: PCR protocols a guide to methods and applications. (Innis MA, Gelfand DH, Sninsky JJ, White TJ, eds), pp 3-12. Academic Press, Inc., San Diego, Calif.
84. Innis MA, Myambo KB, Gelfand DH, Brow MA (1988) DNA Sequencing with *Thermus aquaticus* DNA Polymerase and Direct Sequencing of Polymerase Chain Reaction-Amplified DNA. *PNAS* 85: 9436-9440.
85. Ishibashi J, Perry RL, Asakura A, Rudnicki MA (2005) MyoD induces myogenic differentiation through cooperation of its NH₂- and COOH-terminal regions. *J Cell Biol* 171: 471-482.
86. Isler SG, Schenk S, Bendik I, Schraml P, Novotna H, Moch H, Sauter G, Ludwig CU (2000) Genomic organization and chromosomal mapping of SPARC-like 1, a gene down regulated in cancers. *Int J Oncol* 521-526.
87. Jirmanova I (1983) The splayleg disease: a form of congenital glucocorticoid myopathy? *Vet Res Commun* 6: 91-101.
88. Johnston IG, Paladino T, Gurd JW, Brown IR (1990) Molecular cloning of SC1: a putative brain extracellular matrix glycoprotein showing partial similarity to osteonectin/BM40/SPARC. *Neuron* 4: 165-176.
89. Kim YI, Lee FN, Choi WS, Lee S, Youn JH (2006) Insulin Regulation of Skeletal Muscle PDK4 mRNA Expression Is Impaired in Acute Insulin-Resistant States. *Diabetes* 55: 2311-2317.
90. Kirk SP, Oldham JM, Jeanplong F, Bass JJ (2003) Insulin-like growth factor-II delays early but enhances late regeneration of skeletal muscle. *J Histochem Cytochem* 51: 1611-1620.
91. Kubis HP, Haller EA, Wetzel P, Gros G (1997) Adult fast myosin pattern and Ca²⁺-induced slow myosin pattern in primary skeletal muscle culture. *Proc Natl Acad Sci U S A* 94: 4205-4210.
92. Laemmli UK (1970) Cleavage of structural proteins during the assembly of the head of bacteriophage T4. *Nature* 227: 680-685.
93. Lane TF, Sage EH (1994) The biology of SPARC, a protein that modulates cell-matrix interactions. *FASEB J* 8: 163-173.
94. Larsson L, Ansved T (1995) Effects of ageing on the motor unit. *Prog Neurobiol* 45: 397-458.

95. Lax T (1971) Hereditary splayleg in pigs. *J Hered* 62: 250-252.
96. Lecker SH, Jagoe RT, Gilbert A, Gomes M, Baracos V, Bailey J, Price SR, Mitch WE, Goldberg AL (2004) Multiple types of skeletal muscle atrophy involve a common program of changes in gene expression. *FASEB J* 18: 39-51.
97. Lexell J, Downham D, Sjöström M (1986) Distribution of different fibre types in human skeletal muscles. Fibre type arrangement in m. vastus lateralis from three groups of healthy men between 15 and 83 years. *J Neurol Sci* 72: 211-222.
98. Lindström JM, Engel AG, Seybold ME, Lennon VA, Lambert EH (1976) Pathological mechanisms in experimental autoimmune myasthenia gravis. II. Passive transfer of experimental autoimmune myasthenia gravis in rats with anti-acetylcholine receptor antibodies. *J Exp Med* 144: 739-753.
99. Lomo OM (1985) Arthrogryposis and associated defects in pigs: indication of simple recessive inheritance. *Acta Vet Scand* 26: 419-422.
100. Lomo T, Westgaard RH, Dahl HA (1974) Contractile properties of muscle: control by pattern of muscle activity in the rat. *P Roy Soc Lond B Bio* 187: 99-103.
101. Lynch GS, Cuffe SA, Plant DR, Gregorevic P (2001) IGF-I treatment improves the functional properties of fast- and slow-twitch skeletal muscles from dystrophic mice. *Neuromus Disord* 11: 260-268.
102. Maak S, Jaesert S, Neumann K, von Lengerken G (2003) Characterization of the porcine CDKN3 gene as a potential candidate for congenital splay leg in piglets. *Genet Sel Evol* 35: 157-165.
103. Maak S, Jaesert S, Neumann K, Yerle M, von Lengerken G (2001) Isolation of expressed sequence tags of skeletal muscle of neonatal healthy and splay leg piglets and mapping by somatic cell hybrid analysis. *Anim Genet* 32: 303-307.
104. Maniatis T, Fritsch EF, Sambrook J (1989) Molecular cloning: a laboratory manual. Cold Spring Harbour Laboratory.
105. Mariani L, McDonough WS, Hoelzinger DB, Beaudry C, Kacsmarek E, Coons SW, Gicse A, Moghaddam M, Seiler RW, Berens ME (2001) Identification and validation of P311 as a glioblastoma invasion gene using laser capture microdissection. *Cancer Res* 61: 4190-4196.
106. Maurer P, Hohenadl C, Hohenester E, Gohring W, Timpl R, Engel J (1995) The C-terminal portion of BM-40 (SPARC/osteonectin) is an autonomously folding and crystallisable domain that binds calcium and collagen IV. *J Mol Biol* 253: 347-357.
107. Maurer P, Mayer U, Bruch M, Jenö P, Mann K, Landwehr R, Engel J, Timpl R (1992) High-affinity and low-affinity calcium binding and stability of the

- multidomain extracellular 40-kDa basement membrane glycoprotein (BM-40/SPARC/osteonectin). *Eur J Biochem* 205: 233-240.
108. Mayer U, Aumailley M, Mann K, Timpl R, Engel J (1991) Calcium-dependent binding of basement membrane protein BM-40 (osteonectin, SPARC) to basement membrane collagen type IV. *Eur J Biochem* 198: 141-150.
 109. McElhinny AS, Kakinuma K, Sorimachi H, Labeit S, Gregorio CC (2002) Muscle-specific RING finger-1 interacts with titin to regulate sarcomeric M-line and thick filament structure and may have nuclear functions via its interaction with glucocorticoid modulatory element binding protein-1. *J Cell Biol* 157: 125-136.
 110. Medhurst AD, Harrison DC, Read SJ, Campbell CA, Robbins MJ, Pangalos MN (2000) The use of TaqMan RT-PCR assays for semiquantitative analysis of gene expression in CNS tissues and disease models. *J Neurosci Meth* 98: 9-20.
 111. Meng X, Lu X, Li Z, Green ED, Massa H, Trask BJ, Morris CA, Keating MT (1998) Complete physical map of the common deletion region in Williams syndrome and identification and characterization of three novel genes. *Hum Genet* 103: 590-599.
 112. Mesires NT, Doumit ME (2002) Satellite cell proliferation and differentiation during postnatal growth of porcine skeletal muscle. *Am J Physiol Cell Physiol* 282: C899-C906.
 113. Michel RN, Dunn SE, Chin ER (2004) Calcineurin and skeletal muscle growth. *P Nutr Soc* 63: 341-349.
 114. Miller JK, Hacking A, Harrison J, Gross VJ (1973) Stillbirths, neonatal mortality and small litters in pigs associated with the ingestion of *Fusarium* toxin by pregnant sows. *Vet Rec* 93: 555-559.
 115. Mitch WE, Goldberg AL (1996) Mechanisms of muscle wasting. The role of the ubiquitin-proteasome pathway. *New Engl J Med* 335: 1897-1905.
 116. Mizutani A, Furukawa T, Adachi Y, Ikehara S, Taketani S (2002) A zinc-finger protein, PLAGL2, induces the expression of a proapoptotic protein Nip3, leading to cellular apoptosis. *J Biol Chem* 277: 15851-15858.
 117. Mortimer DT (1983) Vitamin E/selenium deficiency syndrome in pigs. *Vet Rec* 112: 278-279.
 118. Musarò A, McCullagh K, Paul A, Houghton L, Dobrowolny G, Molinaro M, Barton ER, Sweeney HL, Rosenthal N (2001) Localized Igf-1 transgene expression sustains hypertrophy and regeneration in senescent skeletal muscle. *Nat Genet* 27: 195-200.
 119. Musarò A, Rosenthal N (1999) Maturation of the myogenic program is induced by postmitotic expression of insulin-like growth factor I. *Mol Cell Biol* 19: 3115-3124.

120. Nachlas MM, Tsou KC, De Souza E, Cheng CS, Seligman AM (1957) Cytochemical demonstration of succinic dehydrogenase by the use of a new p-nitrophenyl substituted ditetrazole. *J Histochem Cytochem* 5: 420-436.
121. Nair KS (2005) Aging muscle. *Am J Clin Nutr* 81: 953-963.
122. Noguchi M, Sarin A, Aman MJ, Nakajima H, Shores EW, Henkart PA, Leonard WJ (1997) Functional cleavage of the common cytokine receptor gamma chain (gamma_c) by calpain. *P Natl Acad Sci USA* 94: 11534-11539.
123. Ohnishi M, Kojima N, Kokue E, Hayama T (1989) Experimental induction of splayleg in piglets by pyrimethamine. *Jpn J Vet Sci* 51: 146-150.
124. Olson LD, Prange JF (1968) Spraddle-legged baby pigs. *Vet Med Sm Anim Clin* 63: 714.
125. Paliwal S, Shi J, Dhru U, Zhou Y, Schuger L (2004) P311 binds to the latency associated protein and downregulates the expression of TGF-beta1 and TGF-beta2. *Biochem Biophys Res Commun* 315: 1104-1109.
126. Pallafacchina G, Calabria E, Serrano AL, Kalhovde JM, Schiaffino S (2002) A protein kinase B-dependent and rapamycin-sensitive pathway controls skeletal muscle growth but not fiber type specification. *Proc Natl Acad Sci U S A* 99: 9213-9218.
127. Pan D, Zhe X, Jakkaraju S, Taylor GA, Schuger L (2002) P311 induces a TGF-beta1-independent, nonfibrogenic myofibroblast phenotype. *J Clin Invest* 110: 1349-1358.
128. Parsons SA, Millay DP, Wilkins BJ, Bueno OF, Tsika GL, Neilson JR, Liberatore CM, Yutzey KE, Crabtree GR, Tsika RW, Molkentin JD (2004) Genetic loss of calcineurin blocks mechanical over-load induced skeletal fiber type switching but not hypertrophy. *J Biol Chem* 279: 26192-26200.
129. Parsons SA, Wilkins BJ, Bueno OF, Molkentin JD (2003) Altered skeletal muscle phenotypes in calcineurin Aalpha and Abeta gene-targeted mice. *Mol Cell Biol* 23: 4331-4343.
130. Partlow G, Fisher K, Page P, MacMillan K (1993) Prevalence and types of birth defects in Ontario swine determined by mail survey. *Can J Vet Res* 57: 67-73.
131. Pette D, Staron RS (1990) Cellular and molecular diversities of mammalian skeletal fibers. *Rev Physiol Biochem Pharmacol* 116: 2-76.
132. Pette D, Staron RS (2000) Myosin isoforms, muscle fiber types, and transitions. *Microsc Res Techniq* 50: 500-509.
133. Pette D, Vrbova G (1985) Neural control of phenotypic expression in mammalian muscle fibers. *Muscle Nerve* 8: 676-689.

134. Pette D, Vrbova G (1999) What does chronic electrical stimulation teach us about muscle plasticity?. *Muscle Nerve* 22: 666-677.
135. Pottgiesser J, Maurer P, Mayer U, Nischt R, Mann K, Timpl R, Krieg T, Engel J (1994) Changes in calcium and collagen IV binding caused by mutations in the EF hand and other domains of extracellular matrix protein BM-40 (SPARC, osteonectin). *J Mol Biol* 238: 563-574.
136. Priester WA, Glass AG, Waggoner NS (1970) Congenital defects in domesticated animals: general considerations. *Am J Vet Res* 31: 1871-1879.
137. Rehfeldt C, Kuhn G, Vanselow J, Furbass R, Fiedler I, Nurnberg G, Clelland AK, Stickland NC, Ender K (2001) Maternal treatment with somatotropin during early gestation affects basic events of myogenesis in pigs. *Cell Tissue Res* 306: 429-440.
138. Rommel C, Bodine SC, Clarke BA, Rossman R, Nunez L, Stitt TN, Yancopoulos GD, Glass DJ (2001) Mediation of IGF-1-induced skeletal myotube hypertrophy by PI(3)K/Akt/mTOR and PI(3)K/Akt/GSK3 pathways. *Nat Cell Biol* 3: 1009-1013.
139. Salmons S, Vrbova G (1969) The influence of activity on some contractile characteristics of mammalian fast and slow muscles. *J Physiol* 201: 535-549.
140. Sandholm M, Honkanen-Buzalski T, Rasi V (1979) Prevention of navel bleeding in piglets by preparturient administration of ascorbic acid. *Vet Rec* 104: 337-338.
141. Sandri M, Sandri C, Gilbert A, Skurk C, Calabria E, Picard A, Walsh K, Schiaffino S, Lecker SH, Goldberg AL (2004) Foxo transcription factors induce the atrophy-related ubiquitin ligase atrogin-1 and cause skeletal muscle atrophy. *Cell* 117: 399-412.
142. Sanger F, Nicklen S, Coulson AR (1977) DNA Sequencing with Chain-Terminating Inhibitors. *PNAS* 74: 5463-5467.
143. Schiaffino S, Reggiani C (1994) Myosin isoforms in mammalian skeletal muscle. *J Appl Physiol* 77: 493-501.
144. Schiaffino S, Reggiani C (1996) Molecular diversity of myofibrillar proteins: Gene regulation and functional significance. *Physiol Rev* 76: 371-423.
145. Schraml P, Shipman R, Colombi M, Ludwig CU (1994) Identification of genes differentially expressed in normal lung and non-small cell lung carcinoma tissue. *Cancer Res* 54: 5236-5240.
146. Schulz RA, Yutzey KE (2004) Calcineurin signaling and NFAT activation in cardiovascular and skeletal muscle development. *Dev Biol* 266: 1-16.
147. Semsarian C, Sutrave P, Richmond DR, Graham RM (1999a) Insulin-like growth factor (IGF-1) induces myotube hypertrophy associated with an

increase in anaerobic glycolysis in a clonal skeletal-muscle cell model. *Biochem J* 339: 443-451.

148. Semsarian C, Wu MJ, Ju YK, Marcinek T, Yeoh T, Allen DG, Harvey RP, Graham RM (1999b) Skeletal muscle hypertrophy is mediated by a Ca^{2+} -dependent calcineurin signalling pathway. *Nature* 400: 576-581.
149. Shibanuma M, Mashimo J, Mita A, Kuroki T, Nose K (1993) Cloning from a mouse osteoblastic cell line of a set of transforming-growth-factor-beta 1-regulated genes, one of which seems to encode a follistatin-related polypeptide. *Eur J Biochem* 217: 13-19.
150. Skorjanc D, Traub I, Pette D (1998) Identical responses of fast muscle to sustained activity by low-frequency stimulation in young and aging rats. *J Appl Physiol* 85: 437-441.
151. Soderling JA, Reed MJ, Corsa A, Sage EH (1997) Cloning and expression of murine SC1, a gene product homologous to SPARC. *J Histochem Cytochem* 45: 823-835.
152. Solomon V, Goldberg AL (1996) Importance of the ATP-ubiquitin-proteasome pathway in the degradation of soluble and myofibrillar proteins in rabbit muscle extracts. *J Biol Chem* 271: 26690-26697.
153. Solomon V, Lecker SH, Goldberg AL (1998) The N-end rule pathway catalyzes a major fraction of the protein degradation in skeletal muscle. *J Biol Chem* 273: 25216-25222.
154. Somasekhar T, Nordlander RH, Reiser PJ (1996) Alterations in neuromuscular junction morphology during fast-to-slow transformation of rabbit skeletal muscles. *J Neurocytol* 25: 315-331.
155. Stickland NC, Handel SE (1986) The numbers and types of muscle fibres in large and small breeds of pigs. *J Ant* 147: 181-189.
156. Studler JM, Glowinski J, Levi-Strauss M (1993) An abundant mRNA of the embryonic brain persists at a high level in cerebellum, hippocampus and olfactory bulb during adulthood. *Eur J Neurosci* 5: 614-623.
157. Sutherland H, Salmons S, Ramnarine IR, Capoccia M, Walsh AA, Jarvis JC (2006) Adaptive conditioning of skeletal muscle in a large animal model (*Sus domesticus*). *J Ant* 165-177.
158. Svendsen J, Anderasson B (1980) Perinatal mortality in pigs: influence of housing. *Proceedings of the 6th International Pig Veterinary Society*, S 83.
159. Talmadge RJ (2000) Myosin heavy chain isoform expression following reduced neuromuscular activity: potential regulatory mechanisms. *Muscle Nerve* 23: 661-679.
160. Talmadge RJ, Roy RR, Edgerton VR (1999) Persistence of hybrid fibers in rat soleus after spinal cord transection. *Anat Rec* 255: 188-201.

161. Taylor DJ (2006) Congenital and hereditary conditions. In: Pig diseases (Taylor DJ, ed), pp 327-349. ISBN 0 9506932 6 X.
162. Taylor GA, Hudson E, Resau JH, Vande Woude GF (2000) Regulation of P311 Expression by Met-Hepatocyte Growth Factor/Scatter Factor and the Ubiquitin/Proteasome System. *J Biol Chem* 275: 4215-4219.
163. Termine JD, Kleinman HK, Whitson SW, Conn KM, McGarvey ML, Martin GR (1981) Osteonectin, a bone-specific protein linking mineral to collagen. *Cell* 26: 99-105.
164. Thompson MG, Thom A, Partridge K, Garden K, Campbell GP, Calder G, Palmer RM (1999) Stimulation of myofibrillar protein degradation and expression of mRNA encoding the ubiquitin-proteasome system in C2C12 myotubes by dexamethasone: Effect of the proteasome inhibitor MG-132. *J Cell Physiol* 181: 455-461.
165. Thurley DC, Gilbert FR, Done JT (1967) Congenital splayleg of piglets: myofibrillar hypoplasia. *Vet Rec* 80: 302-304.
166. Tomko M (1993) Influence of parental origin, litter size and sex on the frequency of splayleg in piglets: a case report. *Acta Vet Hung* 41: 329-339.
167. Van Der Heyde H, De Mets JP, Porreye L, Henderickx H, Calus A, Bekacrt H, Buysse F (1989) Influence of season, litter size, parity, gestation length, birth weight, sex and farrowing pen on frequency of congenital splayleg in piglets. *Livest Prod Sci* 21: 143-155.
168. Vander AJ, Sherman J, Luciano DS (2001) Skeletal muscle. In: Human physiology: The mechanism of body function (Widmaier EP, Raff H, Strang H, eds), pp 292-324. McGraw-Hill education.
169. Varshavsky A (1997) The ubiquitin system. *Trends Biochem Sci* 22: 383-387.
170. Vivanco I, Sawyers CL (2002) The phosphatidylinositol 3-Kinase AKT pathway in human cancer. *Nature Rev Cancer* 2: 489-501.
171. Vogt DW, Gipson TA, Akremi B, Dover S, Ellersieck MR (1984) Associations of sire, breed, birth weight, and sex in pigs with congenital splayleg. *Am J Vet Res* 45: 2408-2409.
172. Ward PS, Bradley R (1980) The light microscopical morphology of the skeletal muscles of normal pigs and pigs with splayleg from birth to one week of age. *J Comp Pathol* 90: 421-431.
173. Weiss A, Leinwand LA (1996) The mammalian myosin heavy chain gene family. *Annu Rev Cell Dev Biol* 12: 417-439.
174. Westerblad H, Allen DG (1991) Changes of myoplasmic calcium concentration during fatigue in single mouse muscle fibers. *J Gen Physiol* 98: 615-635.

175. Wigmore PM, Stickland NC (1983) Muscle development in large and small pig fetuses. *J Ant* 137: 235-245.
176. Wijeratne WV, Beaten D, Cuthbertson JC (1974) A field occurrence of congenital meningo-encephalocoele in pigs. *Vet Rec* 95: 81-84.
177. Wilson EM, Hsieh MM, Rotwein P (2003) Autocrine growth factor signaling by insulin-like growth factor-II mediates MyoD-stimulated myocyte maturation. *J Biol Chem* 278: 41109-41113.
178. Yan Q, Sage EH, Hendrickson AE (1998) SPARC is expressed by ganglion cells and astrocytes in bovine retina. *J Histochem Cytochem* 46: 3-10.
179. Yan Q, Sage EH (1999) SPARC, a matricellular glycoprotein with important biological functions. *J Histochem Cytochem* 47: 1495-1506.
180. Yang SY, Goldspink G (2002) Different roles of the IGF-I Ec peptide (MGF) and mature IGF-I in myoblast proliferation and differentiation. *FEBS Lett* 522: 156-160.
181. Zhao L, Leung JK, Yamamoto H, Goswami S, Kheradmand F, Vu TH (2006) Identification of P311 as a potential gene regulating alveolar generation. *Am J Resp Cell Mol* 35: 48-54.